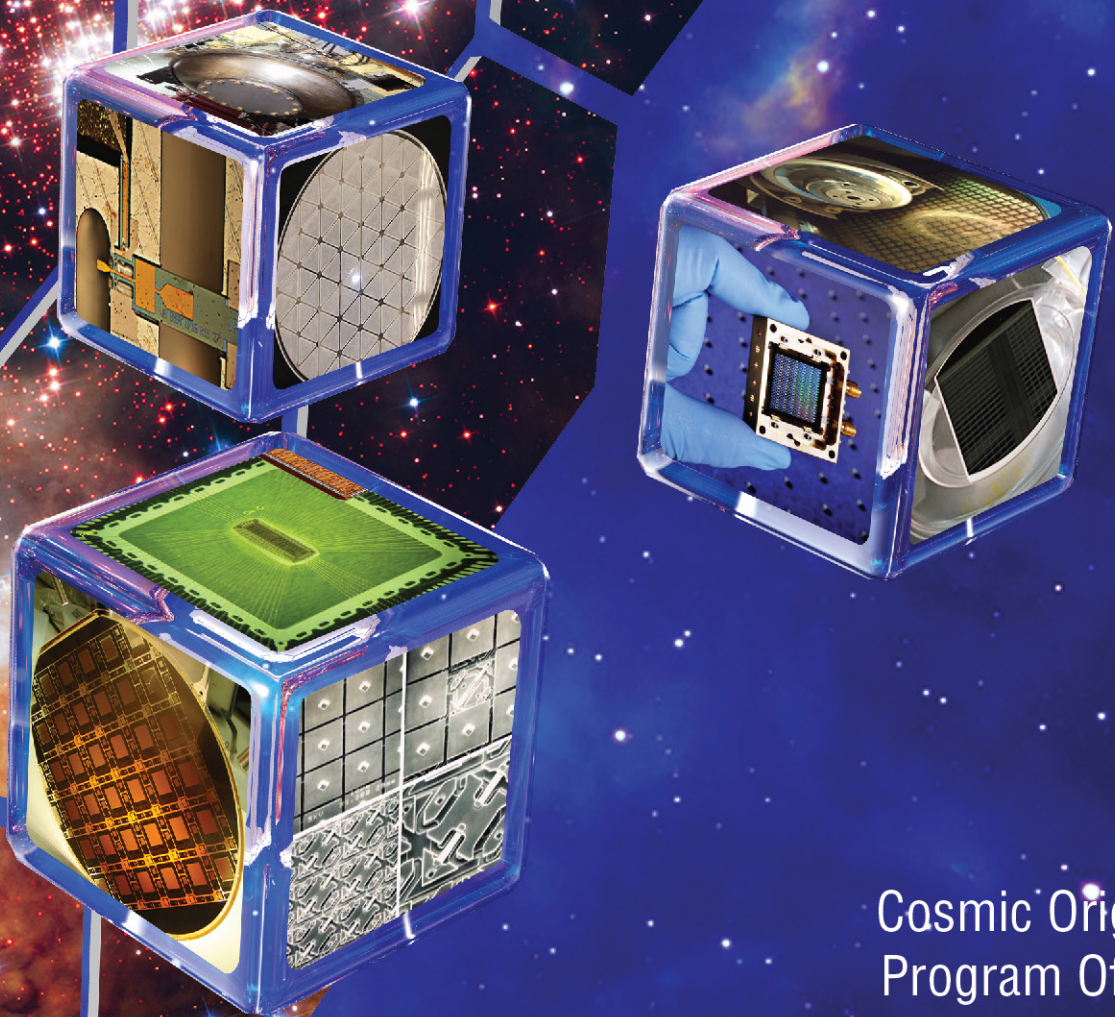




Cosmic Origins Program Annual Technology Report



Cosmic Origins
Program Office
October 2015

This year's cover celebrates the Hubble Space Telescope, showing its 25th-anniversary deep-sky image reflected in a conceptual large-aperture segmented telescope primary mirror. Nine Cosmic Origins Strategic Astrophysics Technology (SAT) project images are set on the faces of three cubes, symbolizing how technological developments serve as building blocks for future missions that will continue to expand our understanding of how the universe came to be.

Table of Contents

Executive Summary	4
1. Science Overview	6
2. Strategic Technology Development Process and Portfolio	9
3. Technology Gaps	14
4. Technology Priorities and Recommendations	41
5. Benefits and Successes Enabled by the COR SAT Program	44
6. Closing Remarks	48
References	49
Appendix A – Technology Development Quad Charts	50
Appendix B – Technology Development Status	59
Appendix C – Training the Future Astrophysics Workforce	140
Appendix D – Acronyms	146

COR 2015 PATR

Executive Summary

What is the Cosmic Origins (COR) Program?

From ancient times, humans have looked up at the night sky and wondered: Are we alone? **How did the universe come to be?** How does the universe work? COR focuses on the second question. Scientists investigating this broad theme seek to understand the origin and evolution of the universe from the Big Bang to the present day, determining how the expanding universe grew into a grand cosmic web of dark matter enmeshed with galaxies and pristine gas, forming, merging, and evolving over time. COR also seeks to understand how stars and planets form from clouds in these galaxies to create the heavy elements that are essential to life – starting with the first generation of stars to seed the universe, and continuing through the birth and eventual death of all subsequent generations of stars. The COR Program’s purview includes the majority of the field known as astronomy, from antiquity to the present.

One surprising recent discovery is that the universe is expanding at an ever-accelerating rate, the first hint of what we now call dark energy, estimated to account for 75% of mass-energy in the universe. Dark matter, so called because we only observe its effects on regular matter, accounts for another 20%, leaving only 5% for regular matter and energy. Scientists now also search for special polarization in the cosmic microwave background to support the notion that in the split-second after the Big Bang, the universe inflated faster than the speed of light! Since this would have been an expansion of space itself, and not energy or matter moving faster than light, the Theory of Relativity would remain intact. The most exciting aspect of this grand enterprise today is that we can finally develop the tools needed for such discoveries.

Why is COR Technology Development Critical?

A 2008 Space Review paper noted that robust technology development and maturation is crucial to reducing flight project schedule and cost over-runs: “...in the mid-1980s, NASA’s budget office found that during the first 30 years of the civil space program, no project enjoyed less than a 40% cost overrun unless it was preceded by an investment in studies and technology of at least 5 to 10% of the actual project budget that eventually occurred” [1]. Such technology maturation program is most efficiently addressed through focused R&D projects, rather than in flight projects, where “marching armies” make the cost of delays unacceptably high. The 2010 Decadal Survey, [*New Worlds, New Horizons in Astronomy and Astrophysics*](#) (NWNH) stressed that “Technology development is the engine powering advances in astronomy and astrophysics... Failure to develop adequately mature technology prior to a program start also leads to cost and schedule overruns” [2].

NASA requires flight projects to demonstrate technology readiness level (TRL) 6* by Preliminary Design Review (PDR) for all technologies they need. However, this can only succeed with a process in place to correctly identify and adequately fund development of relevant “blue sky” technologies to TRL 3†, and then mature them to TRL 5‡ or 6, across the so-called “mid-TRL gap.” This enables robust mission concepts, letting the community focus its strategic planning on proposed missions’ scientific relevance.

What’s in this Report? What’s New?

This fifth Program Annual Technology Report (PATR) summarizes the Program’s technology development activities for fiscal year (FY) 2015. It lists technology gaps identified by the astrophysics community (p. 16), with their priority ranking assigned by the COR Technology Management Board (TMB) (p. 43). Following this year’s prioritization, the Program Office recommends NASA HQ first solicit and fund the following technologies:

* TRL 6: “System/sub-system model or prototype demonstration in a relevant environment.” NPR 7123.1B, Appendix E.

† TRL 3: “Analytical and experimental critical function and/or characteristic proof-of-concept.” NPR 7123.1B, Appendix E.

‡ TRL 5: “Component and/or breadboard validation in relevant environment.” NPR 7123.1B, Appendix E.

- Large-Format, Low-Noise and Ultralow-Noise Far-IR Direct Detectors;
- Band-Shaping and Dichroic Filters for UV/Vis;
- Heterodyne Far-IR Detector Arrays and Related Technologies;
- High-QE, Rad-Hard, Large-Format, Non-Photon-Counting UVOIR Detectors;
- Photon-Counting Large-Format UV Detectors;
- High-Efficiency UV Multi-Object Spectrometers; and
- High-Reflectivity Mirror Coatings for UV/Vis/Near-IR.

These recommendations take into account a set of large mission concepts identified by the Astrophysics Division Director as candidates to be studied to inform the 2020 Decadal Survey. These include three of five “Surveyor” concepts described in the 2013 Astrophysics Roadmap, “[Enduring Quests, Daring Visions](#),” as well as the NWNH-recommended Habitable Exoplanet Imaging Mission. The COR Program Analysis Group (COPAG) and the Program Analysis Groups (PAGs) for the Physics of the Cosmos (PCOS) program, PhysPAG, and Exoplanet Exploration Program (ExEP), ExoPAG, later concurred with this list. The COR Program Office and TMB are ready to respond to technology gaps identified by these studies.

Meanwhile, the Program is pleased to announce four newly awarded COR Strategic Astrophysics Technology (SAT) projects for FY 2016 start (alphabetically, by Principal Investigator, PI):

- “Raising the TRL of 4.7-THz Local Oscillators,” Qing Hu, MIT;
- “Advanced FUV/UV/Visible Photon-Counting Ultralow-Noise Detectors,” Shouleh Nikzad, JPL;
- “Building a Better ALD – Use of Plasma-Enhanced ALD to Construct Efficient Interference Filters for the FUV,” Paul Scowen, Arizona State University (ASU); and
- “Development of Large-Area Photon-Counting UV Detectors,” John Vallergera, UC Berkeley.

Including these, the Astrophysics Division has awarded 15 COR SAT projects to date, funded by COR Supporting Research and Technology (SR&T), and intended to develop telescopes, optics, coatings, and detectors from the Far-IR to the far-ultraviolet (Far-UV), applicable to future strategic COR missions. Eight projects continued from previous years, each reporting significant progress, with several prepared for TRL advancement review. One of these, developing advanced UV-reflective coatings, has now been completed. This PATR reports on the progress, current status, and activities planned for the coming year for the eight projects funded in FY 2015. We thank the PIs of our ongoing projects for their informative progress reports (Appendix A – quad charts, p. 50; Appendix B – development status, p. 59), and welcome our new awardees, two of whom are returning PIs (abstracts at the end of Appendix B).

The following are some examples where Program-funded technologies were infused, or are planned to be infused, into projects and missions, or were deployed at existing facilities:

- Successful on-sky demonstration of kinetic inductance detector (KID) array system at [Caltech Submillimeter Observatory](#) (CSO) (2013);
- TES bolometer detector was selected to support the Stratospheric Observatory for Infrared Astronomy (SOFIA) [High-resolution Airborne Wide-bandwidth Camera](#) (HAWC) instrument (2015 deployment);
- High-efficiency Solid-state Photon-counting Ultraviolet Detector (SPUD) will be flight-tested on the [Faint Intergalactic medium Redshifted Emission Balloon](#) (FIREBall) experiment (2016 launch);
- High-reflectivity UV coatings were used to coat optics for [Ionospheric Connection](#) (ICON) and [Global-scale Observations of the Limb and Disk](#) (GOLD) Explorers (2017 launches); and
- The [Wide-Field Infrared Survey Telescope/Astrophysics Focused Telescope Assets](#) (WFIRST/AFTA) study has adopted the H4RG Near-IR detector to address some of the most enduring questions in astrophysics (mid-2020s launch).

Finally, this PATR introduces a new feature titled “Developing the Future Astrophysics Workforce,” (Appendix C, p. 140). This feature introduces the students and post-doctoral fellows who have worked on and contributed to our SAT projects, gaining the knowledge and experience that will enable them to push the field of astrophysics forward in the coming decades.

1. Science Overview

The goal of the COR Program is to understand the origin and evolution of the universe from the Big Bang to the present day. On the largest scale, COR's broad-reaching science question is to determine how the expanding universe grew into a grand cosmic web of dark matter enmeshed with galaxies and pristine gas, forming, merging, and evolving over time. COR also seeks to understand how stars and planets form from clouds in these galaxies; how stars create the heavy elements essential to life – starting with the first generation of stars to seed the universe, and continuing through the birth and death of stars to today. The majority of the field known as astronomy, from antiquity to the present, falls within the purview of COR.

Background

The Program encompasses multiple scientific missions aimed at meeting Program objectives, each with unique scientific capabilities and goals. The Program was established to integrate those space, suborbital, and ground activities into a cohesive effort that enables each project to build on the technological and scientific legacy of its contemporaries and predecessors. Each project operates independently to achieve its unique set of mission objectives, which contribute to the overall Program objectives.

Current COR missions:

Hubble Space Telescope (HST)

The launch of HST in 1990 began one of NASA's most successful and long-lasting science missions. Over 25 years, HST has relayed over a million observations back to Earth, shedding light on many of the great mysteries of astronomy. HST has helped determine the age of the universe, peer into the hearts of quasars, study galaxies in all stages of evolution, find proto-planetary disks where gas and dust around young stars are birthing grounds for new planets, and provide key evidence for the existence of dark energy.

Spitzer Space Telescope

Spitzer, which recently celebrated the 12th anniversary of its launch, provides sensitive infrared (IR) observations that allow scientists to peer into cosmic regions hidden from optical telescopes, such as dusty stellar nurseries, the centers of galaxies, and still-forming planetary systems. Many of its investigations have focused on objects that emit very little visible light, including brown dwarf stars, extra-solar planets, and giant molecular clouds. Although the primary phase of Spitzer's mission ended in 2009 with the exhaustion of its onboard cryogen, the Spitzer "warm" mission continues valuable work on COR science goals.

Stratospheric Observatory for Infrared Astronomy (SOFIA)

SOFIA is the world's largest airborne observatory, performing imaging and spectroscopy across the IR spectrum. It is operated as a partnership between NASA and the German Aerospace Center (DLR). SOFIA was declared fully operational in May 2014. The SOFIA Program Office and aircraft are based at NASA's Armstrong Flight Research Center (AFRC), with science mission operations based at NASA's Ames Research Center (ARC). SOFIA is managed outside the COR program, but because SOFIA science is well-aligned with COR science, and because SOFIA represents an important platform for maturation of COR technologies that may be applicable to future space missions, certain SOFIA science objectives are considered strategic in relation to the applicable prioritization criteria described in Section 4.

Herschel Space Observatory

The European Space Agency (ESA) Herschel Space Observatory has revealed new information about the earliest, most distant stars and galaxies, as well as those forming and evolving closer to home. NASA contributed significant portions of Herschel's instrumentation, data processing, and science analyses. Herschel was decommissioned in June 2013, but data refinement and analysis will continue until 2017.

COR Development Portfolio 2015

In 2015, the COR Program development portfolio includes:

COR SR&T

The COR Program Office manages the investment of SR&T funds in a variety of avenues to advance COR technology needs. Appendix B details recent progress of projects supported during FY 2015.

Pre-Formulation Mission Study: WFIRST/AFTA

WFIRST is a NASA observatory designed to perform wide-field imaging and slit-less spectroscopic surveys of the Near-IR sky. It was the top-ranked large space mission in NWNH. Because WFIRST survey data will address major COR science questions, such as galaxy evolution, the COR Program supported pre-formulation studies and technology development until late 2013, when they were moved into the WFIRST study. The program continues to follow WFIRST development with specific attention to COR science goals.

James Webb Space Telescope (JWST)

A partnership between NASA and ESA, JWST is the largest science mission under development, and is planned to address important COR science objectives. It will collect Near-IR and mid-IR data allowing investigations of the earliest observable objects in the universe, tracing the evolution of galaxies, and probing obscured star-formation regions in our own and other galaxies. Currently under development, JWST is managed outside the COR Program. However, JWST operations will be managed under the COR Program when the mission transitions to Phase E after launch and commissioning in 2018.

Technology Development

The COR Program is responsible for ensuring that NASA is technologically ready to continue mission developments into the future and to advance the broad scope of COR science goals. Accordingly, the Program Office is charged with overseeing the science of missions in formulation, implementation, and operations, as well as the maturation of technologies in development for these missions.

US astrophysics priorities were last refined in 2010 when the National Research Council (NRC) released the NWNH report. Following the NWNH recommendations, the COR Program has supported focused technology development and mission-concept studies. In NWNH, the NRC placed high value on COR missions relating to Cosmic Dawn (the science theme most closely identifiable with COR). With JWST still in development, the NRC-prioritized recommendations did not include a new specific NASA-led mission that fit solely within COR. However, several of the NWNH recommendations are directly relevant to the COR Program.

- The NWNH report's first priority space recommendation, WFIRST, will address many key COR science goals, such as the formation and evolution of structure and galaxy growth.
- The report gave high priority to technology development in support of a future 4-m UV/Visible-band space telescope.
- The recommendations include a NASA instrument contribution to the Japanese Aerospace Exploration Agency (JAXA) Space Infrared Telescope for Cosmology and Astrophysics (SPICA) mission, if affordable. The Astrophysics Division's [*Astrophysics Implementation Plan*](#) (AIP), released in December 2012 and [*updated in 2014*](#), clarified that the desired contribution would exceed available NASA budgets.
- The report also strongly recommended an augmentation to the Explorers Program that supports astrophysics with rapid, targeted, competed investigations. Explorer missions provide an additional robust way to accomplish COR science: four of the six Medium-Class Explorers (MIDEX)/Small Explorers (SMEX) missions launched in the past 15 years primarily support COR objectives.

Since the COR Program was formulated in 2009 and the NWNH report was released in 2010, fiscal constraints have become significantly more restrictive than anticipated. The Program is committed to managing available funds strategically to foster COR science objectives.

The COR Program is committed to preparing for the next UV/Visible astrophysics mission. NWNH recommends developing technology for a large UV/Visible mission that will continue and extend HST's science accomplishments, through a 4-m-class mission covering wavelengths shorter than HST's key range. However, the COR Program has chosen to consider a broader range of possible future endeavors.

A 2012 Request for Information (RFI) regarding science objectives and requirements for future UV/Visible astrophysics mission(s) led to a September 2012 community workshop based on 34 responses, which are posted on the COR website. A second community workshop in June 2015 continued developing a community consensus on science objectives and technology needs. Further, two independent (non-Program-sponsored) studies considering a future large UV/Visible observatory developed requirements that are likely to help guide the prioritization of COR SR&T technology development needs. Most technology development toward future UV/Visible missions is also expected to benefit the Explorer Program.

In 2012, the Program also studied the feasibility of an instrument contribution to SPICA, then slated for launch around 2022. The Program concluded that based on the readiness level and development risk of possible NASA-provided SPICA instruments, all possible instrument contributions required funding beyond what was available, and could not meet JAXA's schedule constraints. Since then, SPICA has been rescoped and its planned launch significantly delayed, to around 2025. The COR Program is currently working with the Far-IR community to identify alternate ways the US community can address SPICA science goals identified in NWNH. Two Program-sponsored workshops on the future of Far-IR space astrophysics were held in May 2014 and June 2015, to identify the most pressing science questions that can be addressed with Far-IR techniques, to determine technologies needed, and to build community consensus regarding future possible Far-IR astrophysics missions.

SOFIA, which provides a platform for observations across the IR spectrum, with the possibility of frequent instrument upgrades, started Science Cycle 3 at the beginning of 2015. The recently selected upgrade to SOFIA's HAWC will install polarimetric optics and new Far-IR detectors. The new detectors were matured using COR funding in prior years, an example of how COR technology development investment can be handed off to a flight project once the appropriate TRL is reached.

The activity given first priority in NWNH for a future large space mission, WFIRST, is managed by the Exoplanet Exploration Program (ExEP) at the Jet Propulsion Laboratory (JPL), so it is not formally within the COR Program's suite of future missions, but still of great interest for COR science. The WFIRST pre-formulation mission study, using a 2.4-m repurposed telescope termed the AFTA, is working toward a possible new start in 2017. The COR Program, in conjunction with the Cosmic Origins Program Analysis Group (COPAG), is examining how the WFIRST/AFTA mission concept capabilities will address COR science goals. In support of this high-priority mission activity, the COR Program funded detector development through the SAT Program in FY 2013 until the work was moved into the WFIRST study office in FY 2014.

Moving forward, the Astrophysics Division plans to study several mission concepts that would explore the nature of the universe from its earliest moments, in its most extreme conditions, and at the largest scales. The candidate concepts identified by a 2014 white paper from the director of the Astrophysics Division are:

- Far-IR Surveyor;
- Habitable-Exoplanet Imaging Mission;
- UV/Optical/IR Surveyor; and
- X-Ray Surveyor.

The COPAG, PhysPAG, and ExoPAG discussed these and other possible concepts, and in preliminary findings concur that this list identifies the optimal set of large mission concepts to study, make science cases, assess cost and technology needs, and formulate design reference missions to be considered and prioritized by the 2020 Decadal Survey. The PAGs will submit a joint report to the Astrophysics Subcommittee on October 8, recommending which concept studies should be initiated. Note that all three PAGs indicated they assume an L3 gravitational-universe mission study will occur concurrently with these studies. The Program's technology development efforts will be guided by the outcome of these studies.

2. Strategic Technology Development Process and Portfolio

NASA HQ Science Mission Directorate (SMD) Astrophysics Division set up three program offices to manage all aspects of the three focused astrophysics programs: COR, PCOS, and ExEP. The Program Offices shepherd critical technologies toward the goal of implementation into program-relevant flight projects. The offices follow Astrophysics Division guidance, and base their recommendations on science community input, ensuring the most relevant technologies are solicited and developed. The COR Program Office, located at NASA GSFC, serves as HQ's implementation arm on COR Program-related matters. The Astrophysics Division achieves efficiency by having the same staff and physical facilities serve both COR and PCOS Program Offices. The Astrophysics Division funds technology development at all TRLs. Early-stage development ($TRL \leq 3$) and technologies related to non-strategic missions are typically funded by Astrophysics Research and Analysis (APRA). Final maturation ($TRL \geq 6$) is mission-specific and thus handled by flight missions. The SAT program, launched in 2009, funds maturation of technologies across the mid-TRL gap ($3 \leq TRL < 6$).

The COR Technology Development Process

The COR Program Office is charged to develop and administer a technology development and maturation program, moving innovative technologies across the mid-TRL gap to enable strategic COR missions. The Program Office facilitates, manages, and implements the technology policies of the Program. Our goal is to facilitate technology infusion into COR missions, including the crucial phase of transitioning nascent technologies into targeted projects' technology programs during mission formulation. COR SAT projects are funded by the COR SR&T budget. The process for achieving our goal is detailed in the COR technology management plan. Our work is guided by the priorities set forth in the AIP, the Astrophysics Roadmap, and any other current strategic guidance. The AIP describes the Astrophysics Division's planned implementation of space-based prioritized missions and activities identified in NWNH, and considering recent budgetary developments. The Roadmap strives to inspire and challenge the community to pursue the missions and technologies needed over the next three decades to address NWNH-identified science goals.

The process (Fig. 2-1), unchanged from prior years, places at the center of our efforts the science community's inputs through the Decadal Survey process and ongoing identification of technology gaps. The community is encouraged to submit gaps at any time via the COPAG or directly through the COR Program. COPAG, through its science interest groups (SIGs) and science analysis groups (SAGs), reviews gaps submitted before the annual cutoff date, June 1 this year, consolidating, enhancing, and adding to them as needed to create a complete and compelling set of gaps for TMB evaluation. The Program Office charges its TMB annually to evaluate and determine which of the submitted technology developments would meet Program objectives, and prioritize them for further development consideration. The TMB ranks gaps based on Program objectives, strategic ranking of relevant science/missions, benefits and impacts, and urgency. The TMB, a Program-level functional group, thus provides a formal mechanism for input to, and review of, COR technology development activities.

TMB priority recommendations inform Astrophysics Division decisions on which technologies to solicit in the upcoming annual SAT call for proposals, and guide proposal selections. HQ's investment considerations are made within a broader context, and other programmatic factors apparent at the time of selection may affect funding decisions. HQ evaluates resulting technology development proposals, considering overall scientific and technical merit, programmatic relevance, and cost reasonableness given the scope of work. Awardees work to mature their technologies from their initial TRL, normally 3 or 4[§], through TRL 5. PIs report progress and plans to the Program Office periodically, and submit their technologies to TRL advancement review as appropriate. Progress in these projects allows infusion of newly mature technologies into NASA missions and studies, enabling and enhancing their capabilities with acceptable programmatic costs and risks.

[§] TRL 4: "Component and/or breadboard validation in laboratory environment." NPR 7123.1B, Appendix E.

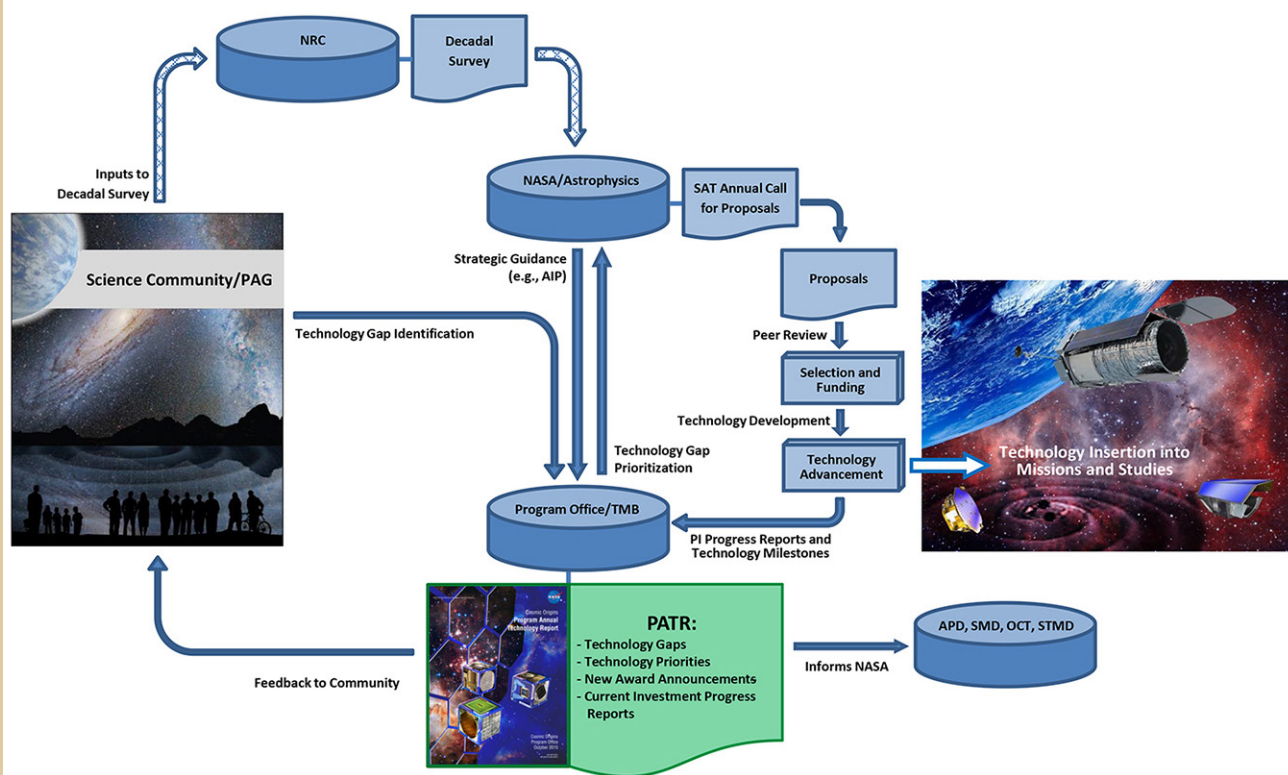


Fig. 2-1. The COR technology development process receives community input on technology gaps, recommends priorities, manages SAT-funded activities, and informs NASA and the science community about progress.

As seen in the graphic, the PATR plays an important role in our technology development process. Through PI reports and quad charts, it describes the status of all strategic COR technologies. It captures technology gaps articulated by the scientific community, and recommends a prioritized list of technologies for future solicitation and funding. The PATR is an open source for the public, academia, industry, and the government to learn about the status of enabling technologies required to fulfill COR science objectives. The report informs NASA organizations, including but not limited to the Astrophysics Division, and updates the community regarding technology development progress, as input for future technology gap submissions. Technological progress and programmatic decisions change the landscape of requirements for COR needs; therefore, the process is repeated annually to ensure continued relevance of priority ranking. Indeed, in any given year, new SAT award decisions are informed by PATRs published over the prior two years, a new SAT solicitation is informed by the prior-year PATR and the current year's TMB report, and the current PATR provides recommendations for next year's SAT.

This technology development and maturation process identifies existing and emerging needs, improves the relevance of COR technology investments, provides the community a voice in the process, and promotes targeted external technology investments by defining needs and identifying NASA as a potential customer for innovative technologies. It also identifies providers of technologies and expertise, the Program PIs, to potential customers and collaborators beyond NASA. This encourages industry and other players to invest in enabling technologies for future missions, and promotes formation of productive collaborations. Beyond involvement in the Decadal Survey process and technology gap submission, the science community is a key stakeholder in Program technology development activities. The community provides feedback and inputs to the technology development process; and participates in COPAG and other committees and workshops, ad-hoc studies, and in technology development by responding to SAT solicitations.

TRL Vetting

As mentioned above, the COR Program Office manages the Program's strategic technology development process. In prior PATRs, we described the overall technology development management effort. With several SAT projects reporting TRL progress, we now expand on our TRL vetting process.

SAT funding helps mature technologies expected to enable and/or significantly enhance future strategic astrophysics missions. These technologies typically enter the SAT program at TRLs 3 or 4, and are intended to progress toward higher TRLs. TRL assertions above a technology's approved entry level are not official until a TRL-vetting TMB concurs with the development team's assessment. When PIs believe their team has demonstrated the required progress, they may request a review to present their case for TRL update. The Program Office then convenes a TMB consisting of Program Office and HQ senior staff and subject matter experts to assess the request and, when warranted, approve the new TRL. The typical forum for such a request is during the PI's end-of-year presentation to the Program Office, but it can be made at any time. Several PIs with projects in the COR portfolio are considering undergoing TRL vetting this coming year.

Why review TRLs?

TRLs are used throughout the agency to help assess the maturity of technologies. The Program Office's charge includes a requirement that it monitor the progress of the Astrophysics Division's investments in technology maturation through SAT projects, relative to the TRL plan and milestones submitted by the PI in the SAT proposal. A key indicator of such progress is TRL advancement as vetted by the Program Office, providing a consistent method of assessing progress across our full portfolio of projects.

What does our vetting mean?

When the Program's TMB approves or vets a new, higher TRL asserted by the PI, it provides an independent assessment and verification that the project has achieved that TRL. The TMB consists of scientists, technologists and systems engineers from the Program, and subject matter experts from the community and Aerospace Corporation, who provide an objective and informed assessment. The primary purpose for issuing this assessment is to inform the Program Office of significant progress in preparing the technology for possible inclusion in strategic missions. It also informs the PI and the science community of the improved state of readiness.

What is expected?

The TRL vetting process is initiated when a PI notifies the Program Office that the milestones necessary for TRL advancement have been met. The PI then presents the progress to a TMB convened by the Program Office, which considers the TRL assertion as guided by TRL definitions in [NASA Systems Engineering Processes and Requirements](#), also known as NASA Procedural Requirements (NPR) 7123.1B. Recognizing that PI teams are busy and must concentrate their efforts on the work of maturing their technology, the Program Office is satisfied to rely on a cogent exposition of the same reports, graphs, and test results the team captures for its own records.

The PI team should prepare a brief but compelling presentation, making the case for the higher TRL. The Program Office has tools to help PIs assess their progress and is available to provide information on the TRL process. Finally, if the project is still ongoing, we recommend the PI present a plan for further TRL advances, if any, allowing the TMB to offer feedback and make recommendations.

What are the benefits for the PI and the Program?

The Program Office's TRL vetting process serves as an opportunity to collect and capture the needed documentary evidence and present it to a group of experts. This can strengthen a potential future TRL case presentation, whether in person or in writing, to flight projects, proposal teams considering adding the technology to their mission, and/or proposal reviewers. Another leveraging opportunity might be in collaboration opportunities. As alluded to above, the TMB can help the PI team fine-tune their plan for future work to achieve the claimed TRL if the current claim was not vetted, or for the next TRL if it was.

Finally, TRLs are NASA's technology development assessment language, and TRL advancement is one of the key success criteria for SAT projects. Our TRL vetting is an objective process, rendering an independent verification of achievement, increasing the credibility of the technology's maturity and its potential for continued funding or infusion into a flight mission.

The COR Technology Development Portfolio as of 2015

For FY 2015, the driving objective is to maintain progress in key enabling technologies for future large UV/Optical/IR (LUVOIR) and Far-IR missions.

There have been 15 COR SAT projects awarded to date. Table 2-1 provides top-level information on the eight that received funding in FY 2015, including where Appendices A and B describe each more fully. Appendix A provides one-page "quad chart" project summaries. Appendix B provides PI reports detailing development status, progress over the past year, and planned near-term development activities. Abstracts for the four recently awarded projects, slated to begin in FY 2016, are at the end of Appendix B. The appendices provide technology overviews and status, not flight implementation details. For additional information, please contact the COR Program Office or the PIs directly. Contact information for each PI appears at the end of his or her report in Appendix B.

Technology Development Title	PI	Institution	Start Year & Duration	Current TRL	Quad Chart & PI Report Location
Ultraviolet Coatings, Materials, and Processes for Advanced Telescope Optics	K. Balasubramanian	JPL	FY13; 3 yrs	3	51, 60
High-Efficiency Detectors in Photon-Counting and Large FPAs for Astrophysics Missions	S. Nikzad	JPL	FY13; 3 yrs	4	52, 70
Development of Digital Micro-mirror Device (DMD) Arrays for use in Future Space Missions	Z. Ninkov	RIT	FY14; 2 yrs	4	53, 81
Enhanced MgF ₂ and LiF Over-Coated Al Mirrors for FUV Space Astronomy	M. Quijada	GSFC	FY12; 3 yrs	4	54, 87
Advanced Mirror Technology Development for Very Large Space Telescopes	P. Stahl	MSFC	FY14; 3 yrs	3	55, 99
Cross-Strip Micro-Channel-Plate Detector Systems for Spaceflight	J. Vallergera	UC Berkeley	FY12; 4 yrs	4	56, 106
A Far-Infrared Heterodyne Array Receiver for CII and OI Mapping	I. Mehdi	JPL	FY14; 3 yrs	4	57, 117
Kinetic Inductance Detector Arrays for Far-IR Astrophysics	J. Zmuidzinas	Caltech	FY13; 3 yrs	3	58, 128

Table 2-1. COR technology development portfolio as of FY 2015 (organized by science topic and PI name).

The Astrophysics Division collaborates with STMD in certain solicitation developments, proposal reviews, and technology co-funding. The Division is open to collaborative efforts when possible, as this allows both to leverage limited funding to advance technologies that meet their respective goals. Such collaborative investments are "win-win-win" opportunities for the Astrophysics Division, STMD, and the PI. The Program looks forward to implementing additional jointly beneficial opportunities in the future.

Strategic Astrophysics Technology Selection for FY 2016 Start

The COR Program funds SAT projects to advance the maturation of key technologies to make feasible their implementation in future space-flight missions. The Program focuses on advancing those technologies most critical for substantive near-term progress on strategic priorities. Three technology areas were called out in the 2014 COR SAT solicitation as being of particular interest for the Program: next-generation detectors from the extreme UV to Far-IR; optical coatings, gratings, and filters; and precision large optics.

The COR SAT proposals selected for FY 2016 start, announced in August 2015, advance four technologies in two of these areas (Table 2-2). Three efforts advance Far-UV/UV/Visible technologies, and one addresses sub-millimeter technology needs.

Technology Development Title	PI	Institution	Duration	Initial TRL	Abstract Location
Raising the TRL of 4.7-THz Local Oscillators	Qing Hu	MIT	3 years	3	136
Advanced FUV/UV/Visible Photon-Counting Ultralow-Noise Detectors	Shouleh Nikzad	JPL	3 years	3	137
Building a Better ALD – Use of Plasma-Enhanced ALD to Construct Efficient Interference Filters for the FUV	Paul Scowen	ASU	3 years	3	138
Development of Large-Area Photon-Counting UV Detectors	John Vallergera	UC Berkeley	2 years	4	139

Table 2-2. COR SAT development starts in FY 2016 (alphabetically by PI).

These new selections were based on the following factors:

- Overall scientific and technical merit;
- Programmatic relevance of the proposed work; and
- Cost reasonableness of the proposed work.

Since these projects have only recently been selected for funding, their status is not presented yet. First-year progress for each will appear in the 2016 COR PATR.

Studies Planned for 2016 – 2019 in Preparation for 2020 Decadal Survey

As mentioned in Section 1, the Astrophysics Division plans to study several mission concepts. These studies will guide efforts to mature technology components, architectures, and make the science cases to be considered and prioritized by the upcoming 2020 Decadal Survey. The candidate mission concepts are as follows (in alphabetical order):

- Far-IR Surveyor;
- Habitable-Exoplanet Imaging Mission;
- UV/Optical/IR Surveyor; and
- X-Ray Surveyor.

Each of these ambitious mission concepts promises breakthrough science results, but implementing them will require us to overcome daunting technology development challenges. The SAT program is certain to play a major role in funding these technology development efforts. We encourage all members of the community to support our efforts to identify the highest priority technology gaps we need to close to make these missions feasible, and continue to submit proposals in response to SAT solicitations. As of this writing, notices of intent to submit for the next SAT round are due January 22, 2016, with proposals due March 18, 2016.

Historic Record of Technology Development for COR (TCOR) Proposals and Awards

The TCOR section of the SAT program (Table 2-3) received 14 proposals in response to the 2010 solicitation, its first year; 24 for 2011; 13 for 2012; none for 2013 as the Program did not solicit SATs that year; and 14 for 2014. Of the first set, three were selected, with five more the following year, three in the third year, and as reported here, four selected in the latest round. This makes the historical selection rate for COR SAT proposals 23%, with the latest round hitting 29% fairly high for technology development solicitations.

Solicitation Year	TCOR Proposals		Proposal Success Ratio
	Submitted	Selected	
2010	14	3	21%
2011	24	5	21%
2012	13	3	23%
2013	Not solicited	N/A	N/A
2014	14	4	29%
Total to Date	65	15	23%

Table 2-3. Number of TCOR SAT proposals and awards.

3. Technology Gaps

Anyone may identify a COR-related technology gap, and submit it to the Program Office directly through the COR website, or via the COPAG. Technology gaps may be submitted throughout the year. However, to allow timely consideration by its TMB, the Program Office sets a deadline for inclusion in the current year's ranking. In 2015, the deadline was set for June 1, allowing the COPAG to review the list for completeness, merge overlapping gaps, and complete and improve entries where the submission did not adequately address the requested information. The final list provided by the COPAG was later assessed and prioritized by the COR TMB.

To maximize the likelihood of high priority ranking, the Program Office encourages submitters to include as much of the information requested as possible. More importantly, the Program Office asks submitters to describe a technology capability gap, not a specific implementation process or methodology. The technology's goals and objectives should be clear and quantified. Additionally, a complete description of the needed capability with specific performance goals based on mission needs is very valuable. Such information serves several important purposes.

1. The TMB is best able to understand and thus correctly assess the identified technology gap.
2. NASA HQ is best able to develop precise technology development proposal calls.
3. The community is clearly informed and best able to match candidate technologies to mission needs.

Aside from submitter information, the technology gap form requests the following information:

- **Technology gap name:** Identifies the gap, and optimally the type of mission filling it would enable.
- **Brief description:** Summarizes the technology gap and associated key performance criteria. In general, well-defined technology gaps receive higher priority than vague ones.
- **Assessment of current state of the art:** Describes the state of the art, allowing the TMB to appreciate the gap between what's available and what's needed.
- **TRL:** Specifies the current TRL(s) of the technology per NPR 7123.1B Appendix E with clear justification. The SAT program funds projects to advance technologies from TRL 3 up through TRL 5, so those already at TRL 6 will likely rank lower unless the existing technology is significantly deficient relative to the needs (see next point).
- **Target goals and objectives:** Details the goals and/or objectives for a candidate technology to fill the described gap. For example, "*The goal is to produce a detector with a sensitivity of X over a wavelength of Y to Z nm.*" Technology gaps with clearly quantified objectives may receive higher priority than those without quantified objectives.
- **Scientific, engineering, and/or programmatic benefits:** Describes the benefits of filling the technology gap. If the need is enabling, this should describe how and why. If the need is enhancing, it should describe, and if possible quantify, the impact. Benefits could be better science, lower resource requirements (e.g., mass, power, etc.), and/or programmatic (e.g., reduced risk, cost, or schedule). For example, "*Material X is 50% stronger than the current state of the art and will enable the optical subsystem for a 2-m telescope to be Y kg lighter.*" Technology gaps with greater potential mission benefits receive higher scores.
- **Application and potential relevant missions:** Technologies enabling or enhancing missions ranked highly by the AIP and/or the Astrophysics Roadmap, or at least by NWNH, will be scored higher. Technologies applicable to a wide range of COR missions, as well as PCOS and/or ExEP missions will rank better.
- **Urgency:** Specifies when the strategic mission enabled or enhanced by the technology is planned to launch. In certain cases where there is a more immediate driving need (e.g., an ESA requirement for achieving TRL 5 or 6 by a certain date to be considered for inclusion in a mission considered strategic by NASA Astrophysics Division), this driving requirement will also be considered. Technology gaps with shorter time windows relative to required development times receive higher priority.

Technology Gaps Submitted to the 2015 TMB

The technology gaps list for 2015 included 17 gaps from the 2014 TMB list, plus 15 new entries and revisions of 2014 gaps submitted by the community, for a total of 32 gaps. To improve the comprehensiveness and quality of the list of gaps prioritized by the TMB, the COPAG Executive Committee (EC) agreed to review the list after the Program Office compiled it. The EC considered the full set of entries, consolidated those with significant overlap, improved the wording on some entries to make them more compelling to the TMB, added entries where appropriate, and recommended removing entries where those were too incomplete or too far outside the charge of the SAT program. At the conclusion of their effort, the EC sent back to the Program Office a list of 28 entries. After further discussion between the COPAG Chair and the Program Office, six more were either removed as too incomplete, or merged into other gaps, leaving a list of 20 gaps for the TMB to assess and prioritize. Of these, nine were the same as in 2014 with at most minor edits, two were combined into one, six were significantly updated, and four new ones were added. Nearly all technologies developed to close these gaps would enable and/or enhance high-priority strategic missions per the AIP, the Astrophysics Roadmap, and/or NWNH. We deeply appreciate the EC's efforts and look forward to continued collaboration in the future. Having the EC review gap entries prior to TMB prioritization serves several important purposes:

- It allows experts in relevant fields to clarify submissions and combine related and overlapping gaps, such that the resulting entries are more compelling and potentially merit higher priority ranking;
- It ensures the final list accurately reflects the community-assessed gaps; and
- It makes the process of generating unique technology gaps more transparent to the community.

The COR TMB reviewed the 20 unique technology gaps in the COPAG's list (Table 3-1), scored, and ranked these gaps, covering a broad range of COR science:

- Improvements in UV, visible band, and near-IR detection, optics, and coatings (7 gaps);
- Far-IR direct and heterodyne detectors and supporting technologies (2 gaps);
- High-performance, affordable LUVOIR telescopes and related technologies, including wavefront sensing and control (6 gaps);
- Far-IR cryogenic telescopes, optics, and interferometry (2 gaps);
- Wide-bandwidth receiving systems (1 gap); and
- High-performance cryo-coolers and sub-Kelvin coolers (2 gaps).

The Program Office continues to solicit and compile technology gap submissions from the community, and as was done this year, will collaborate with the COPAG EC to ensure the gaps ranked by the TMB are unique and compelling.

Table 3-1. Technology Gaps Evaluated by TMB in 2015

Name of Technology	High-QE, rad-hard, large-format, non-photon-counting UVOIR detectors (Previously UV only, but need to update to include Vis/IR to cover HST range of 100 – 2500 nm)
Description	<p>Future NASA UV missions require high quantum efficiency (QE > 70%), large-format (> 2k × 2k pixels), radiation-hard detectors for operation at 90-350 nm or broader for imaging and spectroscopy.</p> <p>Red-leak (longer wavelength) suppression, <i>i.e.</i> visible blind UV detectors, is highly desirable for some applications.</p>
Current State of the Art	<p>Previously flown micro-channel-plate- (MCP) based UV detectors have QE of ~5-20% (wavelength-dependent), require high voltage, and can be difficult to fabricate.</p> <p>Current flight UV-imaging detectors (HST/STIS, HST/COS, FUSE, GALEX) are based on MCP arrays that use CsI and CsTe photocathodes with modest QEs (10-30%).</p> <p>Higher-QE photocathodes (30-80%) using cesiated p-doped GaN have been produced in the lab, but have not yet been integrated into full detector systems.</p> <p>Si-based CCDs have been produced and flown with modest QEs in the near-UV (NUV; 170-300 nm; HST/WFC3).</p> <p>Recent developments with atomic-level control of back-illuminated detector surface (delta doping with molecular beam epitaxy) and anti-reflection coating (atomic layer deposition techniques) have provided high-efficiency UV response (> 50%) for solid state Si detectors (electron-multiplied CCD) but the Si detectors are not visible-blind and require filters. Electron-multiplying CCDs (EMCCDs), electron-bombarded CMOS (EBCMOS) and MCP methods (ceramic and glass) compete for highest QE and largest formats.</p>
Current TRL	3
Performance Goals and Objectives	Routinely produce large-format, high-QE (> 70%), low-noise (< 5 e- root-mean-square, rms), and radiation-hard (operate at L2 for years) UV-sensitive detector arrays that can be used in a variety of Explorer, medium, and strategic missions such as a LUVOIR telescope.
Scientific, Engineering, and/or Programmatic Benefits	High-performance detectors can increase the science impact of missions by ×10-1000, depending on areal coverage and QE.
COR Applications and Potential Relevant Missions	<p>The science impact of cost-constrained, aperture-constrained future missions is dramatically improved by reaching near-perfect detector sensitivity (high QE) and large-format arrays.</p> <p>This is an enhancing technology for a large UV/Visible/Near-IR mission. The 2010 Decadal Survey noted the importance of technology development for a future 4-m-or-greater-class UV/visible mission for spectroscopy and imaging.</p> <p>For example, the Advanced Technology Large-Aperture Space Telescope (ATLAST) mission concept identified a UV imager and UV spectrograph as key instruments.</p> <p>Benefits will also accrue to UV planetary, heliospheric, and Earth missions.</p>
Time to Anticipated Need	<p>As early as possible since mission definition and capabilities are built around detector performance.</p> <p>The goal is to reach TRL 5 by 2019 for consideration in the 2020 Decadal Survey for a large UV/Visible/Near-IR astrophysics mission to start in the 2020s.</p> <p>Significant improvements can be applied quickly in suborbital missions to increase technology readiness for all missions.</p>

Table 3-1. Technology Gaps Evaluated by TMB in 2015 (continued)

Name of Technology	Very-large-format, high-QE, low-noise, radiation-tolerant detectors for the UV/Vis/NIR
Description	<p>Observations in astronomy typically require a combination of large format, high throughput (QE), and low noise to achieve photon- or sky-background-limited sensitivity over the full field of view (FOV) of a telescope or spectrograph.</p> <p>Large-format, high-QE detectors with very low intrinsic read-noise and dark current are essential in the UV, where sky background is low; and in some Vis/NIR applications where high cadence (time-domain studies and some coronagraphic exoplanet searches) or high spectral resolution are needed.</p> <p>Detector arrays need to provide deep full wells and low persistence in high-radiation environments. They also need to be mosaicable in Gpix formats.</p>
Current State of the Art	<p>Current state of the art includes technologies that achieve only a part of the required capability. Flight systems (<i>e.g.</i>, Kepler, Gaia) include moderate-sized focal-plane arrays (~0.1 Gpix) using mosaicked CCDs with modest noise performance (~1-5 e-/pix per read, and dark current of 0.01 e-/s/pix). Alternately, they use individual MCP detectors (<i>e.g.</i>, 4k × 4k pixels, 0.016 Gpix) with low to moderate QE (10-40%), zero read-noise (photon-counting) capability and very low dark current (< 0.000001 e-/pix/s).</p> <p>The current best UV/Vis detector for space astronomy is HST's UVIS CCD, but even it is deficient because of severe charge-transfer inefficiency caused by radiation damage.</p> <p>CCDs and HgCdTe arrays in few-megapixel formats are at TRL > 6. However, CCDs are not radiation-hard. Radiation-hard HgCdTe arrays theoretically have sensitivity through the NUV when the substrate is removed. Scientific use in this wavelength regime hasn't been explored extensively and there is the potential of severe QE degradation or even device damage. In general, hybrid CMOS detectors (including HgCdTe) have higher readout noise than the best CCDs.</p> <p>Estimated current cost is > ~0.1 \$/pixel.</p>
Current TRL	4
Performance Goals and Objectives	<p>Target goals for detector arrays are:</p> <ul style="list-style-type: none"> • Pixel-count 1-4 (0.25-1) Gpix UV/Vis (NIR); • Pixel size 5-10 (10-20) microns UV/Vis (NIR) to achieve diffraction-limited imaging given typical telescope designs; • QE > 0.5 (> 0.9) UV (Vis/NIR); • Read-noise: < 0.1 (< 1) e-/pix/read UV (Vis/NIR); • Dark current: < 0.000003 (< 0.00003) e-/s/pix UV (Vis/NIR) at typ. operating temperatures; • Well-depth: > 2×10⁵ e-; • High ionizing-radiation tolerance; and • Cost < 0.01-0.001 \$/pixel.
Scientific, Engineering, and/or Programmatic Benefits	<p>Detector QE and FOV determine instrument grasp, or etendue, which sets instrument survey power. Higher etendue allows deeper or wider astronomical surveys with space-based telescopes on much shorter timescales. It also enables instrument designs that exploit the telescope aperture size (geometrical area) and full working FOV.</p> <p>Relevant experience with UV, Vis, and/or NIR detectors that simultaneously achieve all these technical goals is essential for maximizing future space observatory science return.</p> <p>These detectors are crosscutting technologies, applicable for astrophysics, planetary, and space sciences. Biological, medical, and security/surveillance applications will also benefit from pushing the limits of sensor technology, particularly for low-light imaging.</p> <p>High-performance detectors can increase the science impact of missions by ×10-1000, depending on areal coverage and QE. Deep full wells with low persistence and radiation tolerance enable transit imaging and spectroscopy at all wavelengths.</p>

COR Applications and Potential Relevant Missions	<p>COR science requires deep multi-wavelength measurements of galaxies and Active Galactic Nuclei (AGN) to study their evolution from the formation of the first stars and black holes to structures observed on all scales in the present-day universe. High priority is given to observations of unseen phenomena such as the cosmic web of intergalactic and circumgalactic gas, resolved light from stellar populations in a representative sample of the universe, UV imagery of early galaxies to improve distance estimates with photometric redshifts, or detailed studies of the stellar evolution process.</p> <p>Potentially relevant missions include the next LUVOIR space telescope, and Probe-class missions that can conduct wide-field surveys. These detectors would greatly benefit Explorer-class missions, enabling them to obtain science currently only available with much larger apertures. They would also greatly increase the science return of small-sat or suborbital experiments that can advance technology while addressing one or more COR science objectives.</p>
Time to Anticipated Need	<p>Detector arrays meeting all target goals specified here (in each major band, UV, Visible, NIR) should be elevated to TRL 6-7 by 2018 or 2019, in time to be incorporated at low risk and high cost confidence in mission designs proposed for the next Decadal Survey.</p> <p>Rapid development and availability of these arrays will enable numerous classes of missions from suborbital, Explorer, Probe, to strategic missions even sooner.</p>

Table 3-1. Technology Gaps Evaluated by TMB in 2015 (continued)

Name of Technology	Photon-counting large-format UV detectors
Description	<p>Future NASA UV missions, particularly those devoted to spectroscopy and high-contrast imaging, require high-QE, low-noise, large-format, photon-counting detectors for operation at 90-350 nm or broader.</p> <p>Red-leak (longer wavelength) suppression is highly desirable for some applications.</p>
Current State of the Art	<p>Previously flown UV detectors obtain ~5-20% QE (wavelength dependent), require high voltage, and can be difficult to fabricate.</p> <p>Silicon-CCD detectors are TRL 4-5.</p> <p>Other technologies (MCP; avalanche photo-diode, APD; Electron-Bombarded CCD, EBCCD; with GaN photocathodes) are TRL 2-4.</p>
Current TRL	2 – 5
Performance Goals and Objectives	<p>The goal is to routinely produce large-format ($> 2k \times 2k$ pixels), high-QE ($> 50\%$), low-noise (< 0.001 e-/pixel/s) UV-sensitive detectors that can be used in a variety of Explorer, medium, and strategic missions for imaging and spectroscopy of the UV sky.</p> <p>Radiation hardness for extended lifetime at L2 orbits is also required.</p> <p>Further enhancement would be to achieve energy-resolving capability.</p>
Scientific, Engineering, and/or Programmatic Benefits	<p>High-performance detectors can increase the science impact of missions by $\times 10$-1000, depending on areal coverage and QE.</p>
COR Applications and Potential Relevant Missions	<p>The science impact of cost-constrained, aperture-constrained future missions is dramatically improved by reaching near-perfect detector performance.</p> <p>The 2010 Decadal Survey noted the importance of technology development for a future 4-m-or-greater-class UV/visible mission for spectroscopy and imaging.</p> <p>Benefits will also accrue to planetary, heliospheric, and Earth missions in the UV band.</p>
Time to Anticipated Need	<p>As early as possible since mission definition and capabilities are built around detector performance.</p> <p>There is a clear plan to achieve this technology. Users have been identified.</p> <p>To support Explorer AOs in the second half of this decade, a focal-plane technology development + flight testing project should be started in 2015 – 2016 (<i>i.e.</i>, immediately). This would allow time for a suborbital mission to fly in 2017 – 2020.</p>

Table 3-1. Technology Gaps Evaluated by TMB in 2015 (continued)

Name of Technology	Photon-counting visible and NIR detector arrays
Description	<p>Future Vis/NIR missions require high-QE, low-noise, fast, photon-counting detector arrays to cover the visible and NIR (400-2500 nm).</p> <p>Important spectroscopic features extend from ozone at 260 nm through at least 2.5 μm.</p> <p>For the NUV through ~ 900 nm, EMCCDs (operated in Geiger mode) are envisioned, though these would benefit from further development. There is currently no photon-counting detector for ultra-low-background astronomy at wavelengths $> \sim 900$ nm, where several important spectral features lie.</p> <p>For high-contrast imaging applications, non-cryo technologies are of particular interest to help mitigate vibration concerns associated with cryo-coolers.</p>
Current State of the Art	<p>EMCCDs with 1 Mpixel have been used to count photons in the visible with greater than 60% QE. Reducing clock-induced charge would be beneficial.</p> <p>HgCdTe arrays in the NIR have been used to count photons at much higher dark-count rates. The state of the art for NIR photon counting is arguably HgCdTe APD arrays. These were pioneered by the defense community for laser communications and laser range-gated imaging. They have also benefitted from substantial NASA investment for LIDAR, but are lower TRL (~ 3).</p> <p>In the last ~ 5 years, several groups including U. Hawaii and the European Southern Observatory have begun working with APD arrays for astronomy, for which the initial application is wavefront sensing. Although promising, we are not aware of any group having achieved the < 0.001 e-/s/pixel dark-current rates required for spectroscopic biomarker detection with coronagraphs. Moreover, there are practical reasons why achieving good impact-ionization gains may be inconsistent with the required ultra-low dark current using existing HgCdTe fabrication technology.</p>
Current TRL	<p>3</p>
Performance Goals and Objectives	<p>QE $> 80\%$ with read-noise $\ll 1$ e- rms and dark current < 0.001 e-/s/pixel. Detector array formats of 4 Mpixel or larger.</p> <p>Wavelength range from 400 to 2500 nm but one detector array does not have to cover the full wavelength range; <i>i.e.</i>, developing separate visible and NIR photon-counting detector arrays is acceptable.</p> <p>Superconducting detectors for UVOIR may be of particular interest.</p> <p>Although superconductors require more cooling than semiconductors, they face no dark-count rate challenge and promise quantum-limited detection with built-in spectral resolution.</p> <p>Arrays of transition-edge sensors (TES) and microwave kinetic inductance detectors (MKID) have already been used at telescopes for UVOIR astronomy. Spectral resolutions of $R \sim 10$ have been achieved, and $R \sim 100$ is feasible. Relevant technologies include TES, kinetic inductance detectors (KID), and superconducting tunnel junctions (STJ).</p> <p>Non-cryogenic solutions are of particular interest for high-contrast imaging applications with a coronagraph to reduce the impact of vibrations associated with cryo-coolers on wavefront error stability.</p>

Scientific, Engineering, and/or Programmatic Benefits	<p>High-performance detectors can increase the science impact of missions by $\times 10$-1000, depending on areal coverage and QE.</p> <p>Photon-counting visible and NIR detector arrays will enable coronagraphic spectroscopy for bio-signature characterization and starlight-suppression wavefront sensing.</p> <p>Superconducting detectors may be especially interesting. Because of the very small superconducting gap (compared to semiconductor band gaps), it is possible to detect and count individual photons with minimal read noise and dark current, though they would need to be optimized for the required spectral resolution. Moreover, by exploiting the energy resolution these technologies offer, it should be possible to achieve spectroscopic resolution $R \geq 70$ in the pixel. These essentially quantum-limited detectors could potentially mitigate cost and complexity associated with spectrograph optics.</p>
COR Applications and Potential Relevant Missions	<p>This is a key technology for a LUVOIR mission. The ATLAST mission concept identified an Exoplanet Imager and Spectrograph (400 - 1800 nm) as key instruments for the mission and these need visible photon-counting detectors for starlight-suppression wavefront sensing and control, and spectroscopy.</p> <p>Future missions with spectroscopic drivers could operate $\sim \times 100$ faster than present. Distant missions (beyond the Zodiacal dust cloud) will observe significantly faster ($> \times 10$) even in imaging applications.</p> <p>This technology can also be used in a wide variety of suborbital, Explorer, Probe, and strategic missions.</p>
Time to Anticipated Need	<p>The goal is to reach TRL 5 by 2019 for consideration in the 2020 Decadal Survey for a LUVOIR astrophysics mission to start in the 2020s.</p> <p>This is a potential game-changing technology that would undoubtedly change the missions that are proposed.</p>

Table 3-1. Technology Gaps Evaluated by TMB in 2015 (continued)

Name of Technology	High-efficiency UV multi-object spectrometers
Description	Future NASA UV missions devoted to spectroscopy require high-throughput (> 50%), multi-object spectrometer (> 100 sources; R~3000 or greater) architectures and components for operation at 100-400 nm or broader band (<i>e.g.</i> , digital micro-mirror device, DMD; advanced diffraction gratings; micro-shutter arrays; fiber-fed spectrographs; and integral-field spectrometers).
Current State of the Art	DMD is at TRL 5, based on European studies for Euclid, and particle-radiation tests at LBL. Micro-shutters for longer wavelengths (> 0.6 microns) are at TRL 6. Low-scatter Echelle gratings are currently at TRL 2.
Current TRL	2 – 6
Performance Goals and Objectives	<p>Routinely produce large-format, high-QE, moderate-resolution systems that can be used in a variety of Explorer, medium, and strategic missions.</p> <p>Key performance criteria for customization, maturation, and characterization of object-selection components (such as DMDs, micro-shutters, or reconfigurable fibers) for UV/Vis/NIR space astronomy include:</p> <ol style="list-style-type: none"> 1. Sensitivity over the spectral interval 0.20-1.7 microns, (0.9-1.8 nm for DMDs). 2. Effective sky background blockage (<i>e.g.</i>, zodiacal light). 3. Low instrumental background (optical scattering, thermal background). <p>Low-scatter Echelle gratings are required for high-resolution far-UV ($\lambda = 90\text{-}180\text{ nm}$) spectroscopy. Performance goals for gratings include scattered light control comparable to the best first-order diffraction grating currently flying (HST-COS), $\sim 10^{-5}$ of peak intensity at $\Delta\lambda = 10\text{ \AA}$ from fiducial wavelength λ_0. In the short term (2014-2016), scattering $< 10^{-3}$ would enable deeper, high-resolution UV spectroscopy than currently available with HST, in an Explorer-class mission.</p>
Scientific, Engineering, and/or Programmatic Benefits	<p>High-performance spectrometers can increase the science impact of missions by orders of magnitude. Space telescopes today can obtain slit spectra of a single object or slit-less spectra of a field, but not slit spectra of multiple objects in a field.</p> <p>A UV/visible slit selector (DMD, micro-shutter array, or multi-fiber) would eliminate confusion and block unwanted background (<i>e.g.</i>, zodiacal light). Better gratings improve contrast and thereby sensitivity.</p> <p>Enabling technology for small, wide-field telescopes appropriate for an Explorer mission.</p>
COR Applications and Potential Relevant Missions	UV/Vis/IR slit selectors are needed for astrophysics, heliospheric, and Earth-science missions.
Time to Anticipated Need	<p>Should come as early as possible since mission definition and capabilities are built around instrument performance.</p> <p>Development for space astronomy is needed in time to respond to an expected announcement of opportunity for an Explorer-class mission in 2015 – 2016.</p>

Table 3-1. Technology Gaps Evaluated by TMB in 2015 (continued)

Name of Technology	Affordable, lightweight, ultra-stable, large-aperture telescopes
Description	<p>Future UV/Vis/NIR telescopes will require ever-larger apertures to answer questions raised by HST, JWST, Planck, and Herschel; and to complement the ≥ 30-m ground-based telescopes coming online in the next decade. Such large UVOIR space telescopes will require:</p> <ol style="list-style-type: none"> 1. 8 m or greater aperture. 2. Diffraction-limited optical quality. 3. UV to NIR wavelength coverage. 4. Picometer-level wavefront error stability to enable starlight suppression for exoplanet science. <p>The extraordinary wavefront stability requirements levied on an observatory by an internal coronagraph necessitate a systems-level approach to the optical telescope assembly (OTA) technology development. Such an approach must include: mirrors, disturbance isolation and damping, metrology, actuators, and thermal control. Underscoring this effort is a critical need for detailed integrated modeling to determine what works and what does not.</p> <p>Investments are needed in mirror systems to prove system performance, thermal and dynamic stability, UV compatibility, low mass, and low cost. These include detailed model-based analysis of mirror system performance, especially addressing dynamic and thermal stability to the levels required for coronagraphy; and mirror system testing at the picometer level to validate the models. Segmented architectures provide a low-cost, low-risk approach that leverages the significant investment made by NASA for JWST. Telescope mirror assemblies require improvements in surface figure error, areal density, areal production rate, and areal cost. Such development will ultimately reduce cost, schedule, and risk by ensuring mirrors can be fabricated quickly, inexpensively, and light enough to enable a range of mission-architecture and launch-vehicle options. New technologies may enable rigid monolithic primary mirrors, or affordable but reliable deployment techniques for segmented apertures to provide increased capabilities.</p>
Current State of the Art	<p>Primary mirror segment technologies have been developed at the needed size (1.2-1.4 m) by NASA and other agencies. ULE glass and SiC-based designs offer alternatives to the Be mirrors used by JWST at lower cost and faster production rates (lightweight 1.3-m Be and SiC mirrors are at TRL 6. Borosilicate glass mirrors are at TRL 5).</p> <p>Thermal control has been demonstrated for figure stability and figure control with actuators. Lightweight ULE segments with alignable edges, offering < 10 nm rms surface figure error (projected), < 5 Å micro-roughness (projected) and < 25 kg/m² total at 1.4 m.</p> <p>SiC mirrors using actuated hybrid mirrors have been demonstrated at 0.5-1.35-m size, < 14 nm rms surface figure error, < 10 Å micro-roughness (projected), and < 25 kg/m² total at 1.4 m.</p> <p>SMEX 40 cm and MidEx 80 cm are affordable with existing technology.</p> <p>Extreme-lightweight Zerodur demonstrated at 1.2 m (TRL 4).</p> <p>Diffractional optics demonstrated at laboratory brass-board level (TRL 3).</p> <p>Frozen-membrane-mirror technology in early stages of development (TRL 3).</p>
Current TRL	3 – 5

Performance Goals and Objectives	<p>Decrease OTA areal density, including primary mirror, its support structure, and mass of additional hardware required to produce an image (<i>e.g.</i>, wavefront control system or chromatic corrector), from current trends of 74 kg/m² (JWST) to OTA areal densities on the order of 10-36 kg/m² or less, surface figure error of 5 to 10 nm rms, and mechanical and thermal wavefront error stability ~10 pm rms per wavefront control step.</p> <p>Telescope fabrication time should be short enough to not be a significant schedule driver, with areal production rates on the order of 30 – 50 m²/year. Similarly, primary development cost should be reduced by half or more from current trends (<i>e.g.</i>, areal cost < \$2 M/m²).</p> <p>A demonstration space-borne OTA using new lightweight mirror technology should be constructed at the 1.5m scale or larger to address both scientific relevance and TRL (<i>e.g.</i>, 1.5+ m primary optic for SMEX with a Pegasus; 3+ m primary optic for a MidEx with a Taurus or Minotaur; 5+ m primary optic for a Probe with an Atlas V or Falcon 9; 3-m primary optic for a balloon-borne payload).</p>
Scientific, Engineering, and/or Programmatic Benefits	<p>Scientific: more collecting area increases sensitivity; larger diameter enables greater angular resolution. Both allow increased and better science for cost- and time-constrained missions addressing key astrophysics questions from cosmic birth to Exo-Earths.</p> <p>Engineering: lower-mass primary allows lighter structure, larger margins; simplified deployment concepts and mechanisms allow larger apertures in smaller launch vehicles.</p> <p>Programmatic: shorter development schedule may remove telescope from critical path and reduce cost. Lighter and cheaper telescope allows greater allocation of mass and money for the science instrument.</p>
COR Applications and Potential Relevant Missions	<p>This is an enabling technology for a LUVOIR mission. The ATLAST mission concept has identified ultra-stable large-aperture mirrors in an active optical system as its second-highest priority technology area for investment after starlight suppression.</p> <p>More generally, the number and cadence of new missions is extremely constrained by available NASA budget. We must maximize the science obtained by those that can be executed. By filling this technology gap, we may achieve MidEx-class science with a SMEX budget and launch vehicle, Probe-class science with a MidEx, and larger-mission science with Probe-class implementation, and reduce risk for future flagship missions by demonstrating key technologies that enable those outlined in the Astrophysics Roadmap.</p>
Time to Anticipated Need	<p>Need a credible path to TRL 5 by 2018 to be considered in the 2020 Decadal Survey.</p> <p>Need to achieve TRL 6 in time for a flagship mission “new start” in 2024.</p> <p>MidEx AO expected in 2018.</p> <p>Decisions about Probe-class missions also in 2017 or 2018.</p> <p>SMEX and additional AOs in subsequent years.</p>

Table 3-1. Technology Gaps Evaluated by TMB in 2015 (continued)

Name of Technology	Thermally stable telescope
Description	Wavefront stability is the most important technical capability that enables 10^{-10} contrast exoplanet science with an internal coronagraph. State of art for internal coronagraphy requires that the telescope must provide a wavefront that is stable at levels less than 10 pm for 10 minutes (stability period ranges from a few minutes to 10s of minutes depending on the brightness of the star being observed and the wavefront-sensing technology being used).
Current State of the Art	No previous space telescope has ever required < 10 pm per 10-min stability. Historically, space telescopes use passive thermal control. JWST's telescope is in a sun-shade shadow. HST's telescope is in a heated tube. While not designed to meet the requirements of a UVOIR exoplanet science mission, JWST is predicted to have a 31 nm rms WFE response to a worst-case thermal slew of 0.22 K and take 14 days to 'passively' achieve < 10 pm per 10 min stability. HST is a cold-biased telescope heated to an ambient temperature. However, it is not a controlled thermal environment. As a result, HST's WFE changes by 10 to 25 nm every 90 min (1–3 nm per 10 min) as it moves in and out of the Earth's shadow.
Current TRL	3
Performance Goals and Objectives	<p>Significant technology development is needed to produce 'stable' isothermal or thermally 'insensitive' telescopes:</p> <ul style="list-style-type: none"> • Thermal design techniques validated by traceable characterization testing of components; • Passive thermal isolation; • Active thermal sense at the < 0.1 K level; and • Active thermal control at the < 10 mK level. <p>To move forward with confidence in designing such a thermal control system (for either monolithic or segmented mirror systems) requires validated thermal performance models.</p> <p>Technology development is required to produce validated models by making traceable components and sub-systems, using the models to make measurable performance predictions, and then quantifying these predictions by testing in a relevant environment.</p>
Scientific, Engineering, and/or Programmatic Benefits	<p>Technology development would enable design and fabrication of a cold-biased telescope placed inside an active thermally controlled environment that heats it to 280 K (above freezing point of water to avoid UV contamination) and responds to solar load as a function of slew/roll to keep the telescope at a constant 280 K.</p> <p>The system should be designed such that if the heaters are turned off, the telescope would stay above a survival temperature of ~250 K.</p>
COR Applications and Potential Relevant Missions	LUVOIR or Hab-Ex
Time to Anticipated Need	<p>Earliest Hab-Ex potential launch date is 2028 to 2032 (depending on how soon it is started).</p> <p>Earliest potential launch date for LUVOIR is 2035 to 2039.</p>

Table 3-1. Technology Gaps Evaluated by TMB in 2015 (continued)

Name of Technology	Affordable monolithic telescope mirror technologies
Description	<p>Capabilities are needed to design and build telescopes for small, cost-capped missions such as Explorers that are larger than those that can currently be proposed with cost credibility and low cost and technical risk.</p> <p>Most telescopes are currently limited more by historical and expected costs than by the size of the launch vehicle payload fairing.</p> <p>New technologies may enable either rigid and monolithic mirrors, or affordable but reliable deployment techniques for segmented mirrors. Either approach could provide increased capabilities.</p>
Current State of the Art	<p>Several candidate approaches are in early stages of development:</p> <p>Extreme-lightweight Zerodur has been demonstrated at 1.2-m diameter at TRL 4.</p> <p>Diffraction-membrane optics have been demonstrated at laboratory brass-board at TRL 3.</p> <p>Frozen-membrane mirror technology is in early stages of development, TRL 3.</p>
Current TRL	3 – 4
Performance Goals and Objectives	<p>Enable a 1.5-m primary optic for SMEX with Pegasus, a 3m primary for MIDEX with Taurus or Minotaur, a 3-m primary for balloon-borne payload, a 4-5-m primary for Probe with Atlas V or Falcon 9.</p> <p>Decrease OTA areal density to ~10 kg/m².</p> <p>Shorten development time to take OTA off critical path for most missions.</p>
Scientific, Engineering, and/or Programmatic Benefits	<p>Greater collecting area increases sensitivity. Larger diameter enables greater angular resolution. Both allow increased and better science for lower-cost mission opportunities.</p> <p>Lower mass allows lighter structure, larger margins, and simplified deployment mechanisms.</p> <p>Shorter development schedule may remove telescope from critical path. Lighter and cheaper telescope allows allocation of greater mass and money to the science instruments.</p>
COR Applications and Potential Relevant Missions	<p>The number and cadence of new missions is constrained by the NASA budget. We must maximize the science obtained by those that can be executed.</p> <p>By filling this technology gap we may achieve MIDEX-class science with a SMEX budget and launch vehicle, Probe-class investigations with a MIDEX, and strategic mission science with a Probe implementation.</p> <p>The candidate technologies cited above can be used for UV, visible, and NIR wavelengths.</p>
Time to Anticipated Need	Allow credible descriptions of potential new missions using these technologies to the 2020 Decadal Survey.

Table 3-1. Technology Gaps Evaluated by TMB in 2015 (continued)

Name of Technology	Sensing and control at the nanometer level or better
Description	<p>Diffraction-limited space telescopes require pointing accuracy on the order of $\theta \sim 0.1 \lambda D$.</p> <p>Technologies are required that provide a high degree of thermal and dynamic stability, and wavefront sensing and control (<i>i.e.</i>, very stable materials, actuators with ~ 1 nm step sizes, systems for rigidizing backplane structures, <i>etc.</i>).</p> <p>Techniques to detect relative distances over pm length scale could include capacitive sensing, laser-based trusses, generalized interferometric sensing, or nested combinations of these techniques.</p> <p>Must have a path to spaceflight qualification.</p>
Current State of the Art	<p>Capacitive sensing is used in control of air-gapped etalons to the 10 pm level.</p> <p>Stabilized lasers systems are used with ground-based and space-based interferometers.</p> <p>New techniques utilize dual-laser-frequency methods, laser trusses, and broadband laser interferometry.</p> <p>Sub-10-pm-level sensitivities have been demonstrated in the laboratory with laser systems, with path to space qualification.</p>
Current TRL	3
Performance Goals and Objectives	<p>Measurement sensitivity and stability of 10 pm over one hour, where the long exposure is driven by the integration time to collect sufficient photons to close control loops on active wavefront control.</p> <p>Develop autonomous, closed-loop, onboard wavefront sensing and control with > 100 Giga-floating point operations/s/W and a control bandwidth of 1 per 5 min.</p>
Scientific, Engineering, and/or Programmatic Benefits	<p>Enables NIR/Vis/UV large-diameter telescopes that require active optics and high-stability deformable mirrors (adaptive optics) for observation of faint objects.</p> <p>This will also enable sophisticated coronagraphs that require one part in 10^{10} contrast, as needed for exoplanet spectroscopy, where for a 8-16-m coronagraphic telescope, a system-level wavefront error of order 1 nm is required; wavefront stability of approximately 10 pm/hour; and pointing control of roughly 1 nanoradian.</p>
COR Applications and Potential Relevant Missions	ATLAST, ST2020, LUVOIR, and others to be considered in the upcoming Decadal Survey.
Time to Anticipated Need	Anticipate this should be at TRL 5 or greater by late 2018 – early 2019 to influence the next Decadal Survey and help show plausibility for advanced observatory mission concepts.

Table 3-1. Technology Gaps Evaluated by TMB in 2015 (continued)

Name of Technology	Sensing and control at the picometer level
Description	<p>Diffraction-limited space telescopes require pointing accuracy on the order of $\theta \sim 0.1 \lambda/D$.</p> <p>Technologies are required that provide a high degree of thermal and dynamic stability, and wavefront sensing and control (<i>i.e.</i>, very stable materials, actuators with ~ 1 nm step sizes, systems for rigidizing backplane structures, <i>etc.</i>).</p> <p>Techniques to detect relative distances over pm length scale could include capacitive sensing, laser-based trusses, generalized interferometric sensing, or nested combinations of these techniques. Must have a path to spaceflight qualification.</p> <p>High-speed, pm-scale metrology is required for ground testing and to validate linearity assumptions used in integrated modeling.</p>
Current State of the Art	<p>Capacitive sensing is used in control of air-gapped etalons to the 10 pm level.</p> <p>Stabilized-laser systems are used with ground-based and space-based interferometers.</p> <p>New techniques utilize dual-laser-frequency methods, laser trusses, and broadband laser interferometry.</p> <p>Sub-10 pm level sensitivities have been demonstrated in the laboratory with laser systems, with path to space qualification.</p> <p>High-speed interferometry has achieved nm-level measurements at 2.5 KHz in the lab.</p>
Current TRL	<p>3</p>
Performance Goals and Objectives	<p>Measurement sensitivity and stability of 10 pm per wavefront control step, where the step-time is driven by the integration time to collect sufficient photons to close control loops on active wavefront control.</p> <p>Develop autonomous, closed-loop, onboard wavefront sensing and control with > 100 Giga-floating point operations/s/W and a control bandwidth of 1 per 5 min.</p> <p>Develop high-speed pm-level metrology for ground-based testing in air to anchor integrated modeling assumptions.</p>
Scientific, Engineering, and/or Programmatic Benefits	<p>Enables UV/Vis/NIR large-diameter telescopes that require active optics and high-stability deformable mirrors (adaptive optics) for observation of faint objects.</p> <p>This will also enable sophisticated coronagraphs that require one part in 10^{10} contrast, as needed for exoplanet spectroscopy, where for a 8-16-m coronagraphic telescope, a system-level wavefront error of order 1 nm is required; wavefront stability of ~ 10 pm/wavefront control step; and pointing control of roughly 1 nanoradian.</p> <p>Enables ground-based metrology and validates integrated modeling techniques at pm level.</p>
COR Applications and Potential Relevant Missions	<p>ATLAST, ST2020, LUVOIR, Habitable-Exoplanet imager and others to be considered in the upcoming Decadal Survey.</p>
Time to Anticipated Need	<p>Need a credible path to TRL 5 by 2018 to be considered for the 2020 Decadal Survey.</p> <p>Need TRL 6 in time for a flagship mission “new start” in 2024.</p>

Table 3-1. Technology Gaps Evaluated by TMB in 2015 (continued)

Name of Technology	Disturbance isolation
Description	<p>Assuming high-contrast exoplanet science is performed by an internal coronagraph capable of achieving 10^{-10} raw contrast, the top-level requirement for wavefront stability is currently understood to be 10's of pm rms per wavefront control step. The control frequency is currently unknown and largely depends on the coronagraph architecture, observing strategy, and brightness of the host star. As this is still an open question, there is a desire to make the observatory as stable as possible to accommodate the possibility of a very slow wavefront control system.</p> <p>Dynamic stability is enabled by a tiered approach of active and passive vibration isolation, as well as stiffer structures. Improvements in reaction wheel damping and isolation help reduce vibrations generated in the spacecraft side of the observatory. Non-contact active isolation schemes physically separate the payload from the spacecraft, preventing the transmission of dynamic disturbances to the sensitive optical systems.</p>
Current State of the Art	<p>Passive isolation on JWST achieves 80 dB attenuation at frequencies > 40 Hz.</p> <p>Non-contact isolation systems have been modeled at 70 dB attenuation with 6-degree-of-freedom low-order active pointing.</p>
Current TRL	4 – 5
Performance Goals and Objectives	<p>140 dB attenuation at frequencies > 20 Hz between spacecraft reaction wheels and telescope.</p> <p>Demonstration of required isolation including power and data transmission across the bus-payload interface. Investigate other potential isolation techniques that may be combined to meet the dynamic stability requirements to reduce overall system risk.</p>
Scientific, Engineering, and/or Programmatic Benefits	<p>Wavefront stability is a key technological challenge to achieving high-contrast imaging via internal coronagraph.</p> <p>Jitter and pointing stability is critical. Vibration isolation between disturbance source and the telescope will enable pm-level wavefront stability for high-contrast imaging.</p>
COR Applications and Potential Relevant Missions	ATLAST/LUVOIR and/or a Habitable Exoplanet Imaging mission will benefit from improved vibration isolation.
Time to Anticipated Need	<p>The goal is to reach TRL 5 by 2019 for consideration in the 2020 Decadal Survey for a LUVOIR astrophysics mission to start in the 2020s.</p> <p>This is a potential game-changing technology that would undoubtedly change the missions that are proposed.</p>

Table 3-1. Technology Gaps Evaluated by TMB in 2015 (continued)

Name of Technology	Band-shaping and dichroic filters for the UV/Vis
Description	<p>Bandpass filters are employed throughout astronomy, and efficient transmissive designs are now quite standard in the Vis/NIR. To facilitate accommodation in standard instrument designs, there is a pressing need for high-efficiency UV-transmitting bandpass filters.</p> <p>Because some classes of UV detectors have significant visible light sensitivity, UV-transmitting “red-blocking” filters are also of high value.</p> <p>Finally, UV/Vis/NIR dichroic filters are useful in creating multiple channels in an instrument, allowing simultaneous observation using band-optimized instrumentation and detectors over the widest possible FOV.</p>
Current State of the Art	<p>Current state of the art includes UV-transmission filters with efficiencies of < 10-20% below 180 nm and < 50% for 180-280 nm.</p> <p>Red-blocking “Woods filters” with low efficiency (< 10-15%) and lifetime issues have been employed for solar-blind imaging.</p> <p>Dichroic filters have been designed for the UV, for example the far-ultraviolet (FUV)/NUV split in the GALEX instrument, but efficiency in each channel (50/80%) and effective bandwidth in each channel (< 50 nm) is limited at current state of the art.</p>
Current TRL	4
Performance Goals and Objectives	<ul style="list-style-type: none"> • Filter transmittance in UV for R~5 bandpass filter: > 50% (FUV), > 80% (NUV); • Red-blocking transmittance: > 50-75% (UV), < 0.0001%-0.01% Vis-NIR; • Dichroic: Mid-UV Split: R (FUV) > 0.8, T (NUV) > 0.9; • Bandwidth: FUV (100 nm), NUV (100-200 nm); • Minimum wavelength: 100-105 nm; and • Dichroic: UV/Vis Split: R (UV) > 0.9, T (Vis) > 0.9.
Scientific, Engineering, and/or Programmatic Benefits	<p>High efficiency and low noise resulting from out-of-band rejection, and multi-channel instruments using dichroics allow deep astronomical surveys to be conducted with space-based telescopes on much shorter, feasible timescales, and enables instrument designs that exploit the aperture size (geometrical area) and full working FOV of the telescope.</p> <p>Relevant experience with UV, Vis, and/or NIR filters and dichroics that achieve the technical goals set forth above is essential for maximizing the return of future space observatories. This technology is crosscutting, with applications across astrophysics, planetary, and space sciences. Commercial applications similarly benefit from high throughput and band-rejection.</p>
COR Applications and Potential Relevant Missions	<p>COR science requires deep multi-wavelength measurements of galaxies and AGN to study their evolution from the formation of the first stars and black holes to structures observed on all scales in the present-day universe.</p> <p>High priority for observations of unseen phenomena such as the cosmic web of intergalactic and circumgalactic gas and resolved light from stellar populations in a representative sample of the universe.</p> <p>Potentially relevant missions include a LUVOIR space telescope, Explorer and Probe-class missions that can conduct wide-field surveys, and small-sat experiments that can advance technology while addressing one or more COR science objectives.</p>
Time to Anticipated Need	<p>Ideally, filters and dichroics meeting target goals specified above will have been advanced to TRL 6-7 by the end of this decade (2018 – 2019), in time to be incorporated at low risk and high cost confidence in mission designs proposed for the next Decadal Survey.</p>

Table 3-1. Technology Gaps Evaluated by TMB in 2015 (continued)

Name of Technology	High-reflectivity mirror coatings for UV/Vis/NIR
Description	<p>High-reflectivity, highly uniform mirror coatings with low polarization are required to deliver high throughput UV observations and support high-contrast imaging via starlight suppression. High-reflectivity coatings would allow multiple reflections without throughput penalty in the UV, and provide very wide bandpasses.</p> <p>For a UVOIR flagship telescope, a single reflective coating that has excellent reflectivity and wavefront over the UV/Vis/NIR bandpass would directly increase the science return of the mission.</p> <p>Exoplanet observations drive the requirements for reflectance uniformity and control of polarization effects that might compromise the performance of a coronagraph. This capability includes:</p> <ol style="list-style-type: none"> 1. High reflectance broadband mirrors for the UV/Vis/NIR. 2. Access to the FUV (90-120 nm) spectrum, with minimal impact to sensitivity and wavefront in Vis and NIR. 3. Ultra-high reflectance for multi-mirror instruments with high degrees of multiplexing (Integral Field Units, IFUs; or MOS), particularly in the UV and FUV. 4. Safe, effective, reliable, last-minute or in-flight mirror-cleaning technologies.
Current State of the Art	<p>The best current lab coatings provide > 90% reflectivity for wavelengths 300-2500 nm and longer, ~85% reflectivity for 120-300 nm, and < 50% for 90-120 nm. Current coatings can provide 2% uniformity at wavelengths greater than 120 nm. Conventional technologies such as chemical vapor deposition with precision controls have been developed for producing high-performance mirror coatings on large-diameter substrates.</p> <p>New coating technologies such as atomic layer deposition (ALD) have potential to produce higher performance, but have only been applied to small optical components (< 0.5m).</p> <p>Existing approaches for mirror cleaning (<i>e.g.</i>, CO₂ snow, or electrostatic wands with AC excitation), do not remove molecular contamination. Promising methods (<i>e.g.</i>, electron or ion beams) could clean off molecular layers as well as dust on substrates.</p>
Current TRL	3
Performance Goals and Objectives	<ol style="list-style-type: none"> 1. Develop coatings with excellent UV and FUV efficiency, particularly in the 90 to 2500 nm range (> 90% for as much as possible of this spectral range). 1a. Also develop coatings with excellent UV and acceptable IR efficiency. 2. Develop high-uniformity coatings (< 1%), over a large spectral range (90-2500 nm), with low polarization (< 1%) for wavelengths 200-1800 nm, for high-contrast imaging. 3. Develop techniques to apply these coatings to large optics (0.5-4+ m) as well as to smaller instrument optical elements. 4. Evaluate durability of these high-performance coatings for mission lifetimes > 10 years. 5. Develop techniques for last-minute ground or in-flight cleaning technology to remove molecular coatings as well as dust.
Scientific, Engineering, and/or Programmatic Benefits	<p>High coating reflectivity in UV makes possible high-performance optical systems that can be highly multi-passed, significantly increasing potential impact of future missions.</p> <p>Wideband coatings could enable a combined UV to IR mission with very broad scientific potential from general astrophysics to exoplanet imaging and spectroscopy.</p> <p>The availability of effective, safe, last-minute ground-based cleaning technologies, or in-flight cleaning technologies, could reduce the high cost of keeping equipment clean for a decade in clean rooms. Mirror-cleaning technology could simplify mirror processing before launch and reduce schedule (cost) and mitigate the risks of re-coating. Post-launch cleaning would improve on-orbit performance and could extend mission life.</p>

COR Applications and Potential Relevant Missions	<p>NWNH noted the importance of technology development for a future ≥ 4-m class UV/visible mission for spectroscopy and imaging. This technology would also support the next generation of UV missions, including Explorers, medium-size Probe missions, and large (> 4-m apertures) future UV/Vis/IR telescopes, and is key for NASA's next large UVOIR mission.</p> <p>All future missions with optics, particularly missions with an important FUV or UV component, will benefit from improved coatings.</p> <p>Benefits will also accrue to planetary, heliospheric, and Earth missions utilizing the UV band.</p>
Time to Anticipated Need	<p>The technology needs to have a credible path to TRL 5 by 2019, if a large UVOIR astrophysics mission, starting in the 2020s is to receive favorable consideration in the 2020 Astrophysics Decadal Survey.</p> <p>Alternatively, availability of this technology at TRL 6 by 2018 would enable a strong UV or FUV Explorer to be selected late this decade. Starting technology work in 2016 would support flight-testing on a suborbital mission to fly in 2017 – 2020.</p> <p>Mirror cleaning would be immediately useful for missions already in development.</p>

Table 3-1. Technology Gaps Evaluated by TMB in 2015 (continued)

Name of Technology	Large-format, low-noise and ultralow noise far-infrared (FIR) direct detectors
Description	<p>Future FIR missions require large-format detectors optimized for the very low FIR backgrounds present in space.</p> <p>Arrays containing thousands of pixels are needed to take full advantage of spectral information content.</p> <p>Arrays containing tens of thousands of pixels are needed to take full advantage of the focal plane available on a large, cryogenic telescope.</p> <p>Detector sensitivity is required to achieve background-limited performance, using direct (incoherent) detectors to avoid quantum-limited sensitivity.</p>
Current State of the Art	<p>Single detectors are at TRL ~5, but demonstrated array architectures are lagging at TRL ~3.</p> <p>Sensitive, fast detectors (TES bolometers, and MKIDs in small arrays) are at TRL 3 for application in an interferometric mission.</p>
Current TRL	3
Performance Goals and Objectives	<p>Detector format of at least 16×16 with high fill factor and sensitivities (noise-equivalent powers) of 10^{-19} W/$\sqrt{\text{Hz}}$ are needed for photometry.</p> <p>Detector sensitivities with noise-equivalent powers of $\approx 3 \times 10^{-21}$ W/$\sqrt{\text{Hz}}$ are needed for spectroscopy, arrayable in a close-packed configuration in at least one direction.</p> <p>Fast detector time constant (~ 200 μsec) is needed for Fourier-transform spectroscopy.</p>
Scientific, Engineering, and/or Programmatic Benefits	<p>Sensitivity reduces observing times from many hours to a few minutes ($\approx 100\times$ faster), while array format increases areal coverage by $\times 10$-100. Overall mapping speed can increase by factors of thousands.</p> <p>Sensitivity enables measurement of low-surface-brightness debris disks and proto-galaxies with an interferometer.</p>
COR Applications and Potential Relevant Missions	<p>FIR detector technology is an enabling aspect of all future FIR mission concepts, and is essential for future progress. This technology can improve science capability at a fixed cost much more rapidly than larger telescope sizes. This development serves Astrophysics almost exclusively (with some impact on planetary and Earth studies).</p>
Time to Anticipated Need	<p>Should come as early as possible since mission definition and capabilities are built around detector performance.</p> <p>There is a clear plan to achieve this technology. Users have been identified.</p> <p>To support Explorer AOs in the second half of the 2010 – 2020 decade, a focal-plane technology development + flight-testing project should be started in 2015 – 2016. This would allow time for a suborbital mission to fly in 2017 – 2020.</p>

Table 3-1. Technology Gaps Evaluated by TMB in 2015 (continued)

Name of Technology	Heterodyne FIR detector arrays and related technologies
Description	Suborbital and space missions, as well as NASA's SOFIA observatory, could achieve a significant observational capability increase by upgrading from single-pixel coherent (heterodyne) spectrometers to arrays. Heterodyne focal-plane arrays are needed for high-sensitivity, spectrally resolved mapping of interstellar clouds, star-forming regions, and solar system objects including comets. These arrays require mixers with low noise-temperature and wide intermediate frequency (IF) bandwidth, LOs that are tunable but which can be phase-locked, and accompanying system technology including optics and low-cost, low-power digital spectrometers. Specifically, LO sources at frequencies above 2 THz that can generate ≥ 10 mW of power will be essential for large-format heterodyne receiver arrays to observe many spectral lines important for COR (<i>e.g.</i> , HD at 2.7 THz and OI at 4.7 THz). Largely because of the lack of such sources, the only large arrays developed thus far are direct detectors or heterodyne receivers below 1 THz.
Current State of the Art	For SOFIA, only single-pixel receivers have been developed for flight; arrays of 16 pixels are approaching TRL ~4. LOs above 2 THz are at TRL ~2.
Current TRL	2 – 4
Performance Goals and Objectives	Develop broad-tunable-bandwidth array receivers for operation at frequencies of 1-5 THz. Arrays of 10 to 100 pixels are required to build on the discoveries of Herschel and exploit the sub-millimeter/FIR region for astronomy. Should include optics and accompanying system components. For mixers, IF bandwidths of 4 GHz at shorter wavelengths (< 100 microns) are essential to analyze entire galactic spectrum in one observation. For LOs, sources with output power levels ≥ 10 mW at frequencies above 2 THz. For digital spectrometers, 4 GHz bandwidth with > 4000 spectral channels, and < 1 W power per pixel will be necessary for large arrays used in space missions.
Scientific, Engineering, and/or Programmatic Benefits	Ability to observe and map spectral lines (such as OI at 4.774 THz) to study star formation and galactic chemical evolution. Observations of transitions of water are necessary to probe the early phases of planet formation, and to determine the origin of the Earth's oceans. Development of such systems and associated technology will make imaging observations over 10 \times faster. They will also significantly benefit laboratory spectroscopy and biomedical imaging.
COR Applications and Potential Relevant Missions	Needed for future sub-mm/FIR suborbital missions (instruments for SOFIA and balloon missions such as Stratospheric Terahertz Observatory, STO and Galactic/Xtragalactic ULDB Spectroscopic Stratospheric Terahertz Observatory, GUSSTO) and for potential small-sat and Explorer missions beyond Herschel. Solar system studies of planetary atmospheres will directly benefit. For Earth observing, focal-plane arrays will improve coverage speed and provide small spot sizes with reasonably sized antennas.
Time to Anticipated Need	The next round of SOFIA instruments will need to reach TRL 6 by the end of the decade (<i>i.e.</i> , 3-5 years). Potential use in 2020 Decadal FIR Surveyor Mission on slightly longer timescale.

Table 3-1. Technology Gaps Evaluated by TMB in 2015 (continued)

Name of Technology	Wide-bandwidth, high-spectral-dynamic-range receiving system
Description	<p>Receiving systems consisting of an antenna and associated electronics to amplify, filter, and sample the highly redshifted neutral hydrogen signals from Cosmic Dawn, <i>i.e.</i>, at redshifts $z > 10$. The desired signals of interest have amplitudes of milli-Kelvins to potentially a few hundred milli-Kelvin (measured as brightness temperatures), relative to galactic and other foreground emissions at the level of 1000 to 10,000K, implying spectral dynamic ranges of order 1 million or more (60 dB).</p> <p>Further, signals of interest are generated over a wavelength range comparable to their central wavelength.</p> <p>Finally, given signal weakness, the antenna and associated electronics either must not introduce spectral features at levels comparable to those expected from the signals of interest or the spectral behavior of the antenna and associated electronics must be stable and allow sufficient characterization to enable calibration to remove any such spectral features.</p>
Current State of the Art	<p>Notional designs exist for full systems; proof-of-concept subsystems have been demonstrated in laboratory environments, and the individual components likely to be used in a full system have been demonstrated in relevant environments. A demonstration of subsystems and a full system in a relevant environment has not yet been accomplished.</p>
Current TRL	<p>4</p>
Performance Goals and Objectives	<p>The goals of a program to address this gap are two-fold:</p> <ol style="list-style-type: none"> 1. Demonstrate capability to make measurements of sky-averaged highly redshifted neutral hydrogen signals. 2. Demonstrate capability to collect highly redshifted neutral hydrogen signals in a manner allowing later imaging. If the first goal can be met, the technology capability required for the second goal will also be met. <p>A system capable of fulfilling the first goal can be divided into three key sub-systems:</p> <ol style="list-style-type: none"> I. Antenna: Proof-of-concept antennas able to receive signals over at least a 3:1 wavelength range have been constructed; the objective is to construct an antenna with a sufficiently stable frequency response that it changes by only a small amount over range of temperatures expected for a space-based antenna; II. Analog Receiver: The receiver amplifies and, if necessary, filters and conditions for further processing signals collected by the antenna; the receiver must allow characterization at a level sufficient to allow extraction of the cosmological hydrogen signal at a level of 1 part per million of signals received by antenna; designs for such receivers exist; the objective is to construct one in a lab environment, demonstrate its performance, and then construct one for the thermally controlled environment expected for a spacecraft; and III. Digital Spectrometer: The spectrometer converts analog signals to digital and forms them into spectra with sufficient spectral resolution to detect the cosmological hydrogen signal; digital spectrometers with the required performance have been developed in a laboratory environment; the objective is to implement a spectrometer with flight-qualified hardware in the thermally controlled environment expected for a spacecraft.

Scientific, Engineering, and/or Programmatic Benefits	<p>This technology capability would benefit studies of “Cosmic Dawn,” one of the three science objectives for this decade as identified by the NWNH report.</p> <p>Studies of the highly redshifted neutral hydrogen signals will probe the Epoch of Reionization (EoR), NWNH science frontier discovery area, and address the science frontier question “What were the first objects to light up the universe and when did they do it?” from the Origins theme.</p> <p>Studies of highly redshifted neutral hydrogen signals may also be able to probe into the true Dark Ages, before any stars had formed. Such studies would complement COR objectives, and address goals of the PCOS Program.</p>
COR Applications and Potential Relevant Missions	<p>The application is for space- and lunar-based missions designed to find highly redshifted ($z > 10$) signals from neutral hydrogen.</p> <p>Potentially relevant missions described in the Astrophysics Roadmap include a precursor lunar orbiter mission (Introduction to Chapter 6 of the Astrophysics Roadmap) and an eventual Cosmic Dawn Mapper.</p>
Time to Anticipated Need	Two to three years for a precursor lunar orbiter mission.

Table 3-1. Technology Gaps Evaluated by TMB in 2015 (continued)

Name of Technology	Large, cryogenic, FIR telescopes
Description	Large telescopes provide both light-gathering power to see the faintest targets, and spatial resolution to see the most detail and reduce source confusion. To achieve the ultimate sensitivity, their emission must be minimized, which requires these telescopes be operated at temperatures, depending on the application, as low as 4K. Collecting areas on the order of 50 m ² are needed.
Current State of the Art	JWST Be mirror segments may meet requirements now, so TRL 5 with an extremely expensive technology; TRL 3 exists for other materials.
Current TRL	3 – 5
Performance Goals and Objectives	Develop a feasible and affordable approach to producing a 10-m-class telescope with sufficiently high specific stiffness, strength, and low areal density to be launched, while maintaining compatibility with cryogenic cooling and FIR surface quality/figure of ~1 μ m rms.
Scientific, Engineering, and/or Programmatic Benefits	<p>Low-cost, lightweight cryogenic optics are required to enable development of large aperture FIR telescopes in the 2020s.</p> <p>Large apertures are required to provide the spatial resolution and sensitivity needed to follow up on discoveries from the current generation of space telescopes.</p>
COR Applications and Potential Relevant Missions	This is a key enabling technology for any future FIR mission.
Time to Anticipated Need	<p>Should come as early as possible since technology is applicable to small, medium, and large missions.</p> <p>Needed by 2020 for the next large FIR astrophysics mission.</p>

Table 3-1. Technology Gaps Evaluated by TMB in 2015 (continued)

Name of Technology	FIR interferometry
Description	<p>Interferometry in the FIR provides sensitive integral field spectroscopy with sub-arcsec angular resolution and $R \sim 3000$ spectral resolution. It could resolve proto-planetary and debris disks; and measure the spectra of individual high-z galaxies, probing beyond the confusion limits of single-aperture FIR telescopes.</p> <p>A structurally connected interferometer would have these capabilities. Eventually, a formation-flying interferometer would provide Hubble-class angular resolution.</p> <p>Telescopes need to operate at temperatures as low as 4K.</p>
Current State of the Art	Wide-FOV spatio-spectral interferometry has been demonstrated in the lab at visible wavelengths with a test-bed that is functionally and operationally equivalent to a space-based FIR interferometer.
Current TRL	4
Performance Goals and Objectives	Develop a feasible and affordable (Probe-class) approach to produce a 40-m-class interferometer capable of launch and operation, in which a single science instrument provides both dense coverage of the u - v plane for high-quality, sub-arcsec imaging and Fourier Transform Spectroscopy over the entire spectral range 25-400 microns in an instantaneous FOV > 1 arc minute.
Scientific, Engineering, and/or Programmatic Benefits	40-m-class interferometric baselines are required to provide the spatial resolution needed to follow up on discoveries made with the Spitzer and Herschel space telescopes, and to provide information complementary to that attainable with ALMA and JWST.
COR Applications and Potential Relevant Missions	<p>Wide-field spatio-spectral interferometry is a key enabling technology for a FIR astrophysics mission consistently given high priority by the FIR astrophysics community.</p> <p>Potential applications also exist in NASA's planetary and Earth science programs.</p>
Time to Anticipated Need	<p>Continuation of prototype efforts expected to yield mature technique in time for 2015 balloon flight.</p> <p>To enable credible discussion of a FIR interferometer, recognized as a critical future investment, must reach TRL 6 well in advance of 2020 Decadal Survey (<i>e.g.</i>, by ~2018).</p>

Table 3-1. Technology Gaps Evaluated by TMB in 2015 (continued)

Name of Technology	High-performance, sub-Kelvin coolers
Description	<p>Optics and detectors for FIR, millimeter, and certain X-ray missions require very low temperatures of operation, typically in the tens of milli-Kelvins.</p> <p>Compact, low-power, lightweight coolers suitable for space-flight are needed to provide this cooling.</p> <p>Both evolutionary improvements in conventional cooling technologies (adiabatic demagnetization and dilution refrigerators) and novel cooling architectures are desirable.</p> <p>Novel cooling approaches include optical, microwave, and solid-state techniques.</p>
Current State of the Art	Existing magnetic refrigeration demonstrations and solid-state cooling approach based on quantum tunneling through normal-insulator-superconductor (NIS) junctions are both at TRL 3-4.
Current TRL	3 – 4
Performance Goals and Objectives	<p>A cryo-cooler operating from a base temperature of ~4K and cooling to 30 mK with a continuous heat lift of 5 μW at 50 mK and 1 μW at 30 mK is required for several mission concepts.</p> <p>Features such as compactness, low power, low vibration, intermediate cooling, and other impact-reducing design aspects are desired.</p>
Scientific, Engineering, and/or Programmatic Benefits	<p>Sub-Kelvin cryo-coolers are required to achieve astrophysical photon background-limited sensitivity in the FIR and high-resolution sensitive X-ray microcalorimetry.</p> <p>Techniques to lower cooling costs and improve reliability will aid the emergence of powerful scientific missions in the FIR and X-ray.</p>
COR Applications and Potential Relevant Missions	<p>This technology is a key enabling technology for any future FIR mission.</p> <p>Sensors operating near 100 mK are envisioned for future missions for X-ray astrophysics, measurements of the CMB, and FIR imaging and spectroscopy.</p> <p>Applicable to missions of all classes (balloons, Explorers, Probes, and flagship observatories).</p>
Time to Anticipated Need	<p>Beneficial to undertake soon, to take advantage of existing development momentum, to allow time for system integration and cryo-thermal system performance verification, and enable balloon and Explorer applications in advance of the 2020 Decadal Survey.</p> <p>To support an Explorer AO in the second half of this decade, a focal-plane technology development + flight-testing project should be started in 2015 – 2016. This would allow time for a suborbital mission to fly in 2017 – 2020.</p>

Table 3-1. Technology Gaps Evaluated by TMB in 2015 (continued)

Name of Technology	Advanced cryo-coolers
Description	Cryo-coolers are required for achieving very low temperatures (<i>e.g.</i> , ~4K) for detectors and/or optics for COR missions. Eliminating the need for expendable materials (cryogenics) will increase achievable lifetime and reduce system mass and volume. Improvements are needed in terms of flyability and performance, especially low power consumption and low vibration levels.
Current State of the Art	<p>Cryo-coolers capable of ultralow temperatures (< 0.1 K) based on magnetic refrigeration and quantum tunneling through normal-insulator-superconductor junctions have been demonstrated. For several-Kelvin temperature designs, the current state of the art includes pulse-tube, Stirling, and Joule-Thomson coolers which are at high TRL but are expensive, and do not yet have good enough performance. An example is the development of 6K cooler system for MIRI, which was extremely problematic, slow, and costly.</p> <p>Coolers are largely custom developments (<i>e.g.</i>, Planck, Herschel), and while successful, this is a major deterrent to small and medium missions as well as to more ambitious missions using cooled telescopes.</p> <p>TRL for FIR interferometric mission application is 4.</p>
Current TRL	3 – 4
Performance Goals and Objectives	<p>Several mission concepts require sustaining temperatures of a few Kelvin, with continuous heat-lift levels of a few dozen to ~200 mW at temperatures ranging from 4 K to 18 K. Other concepts could benefit from greater heat lifts at somewhat higher temperatures. All this needs to be accomplished with < 200 W input power. Such coolers need to be compact, and impose only low levels of vibration on the spacecraft.</p> <p>Large FIR telescopes are likely to pose more stringent requirements, if a cryo-cooler is used to cool the primary mirror.</p> <p>In some applications, a sub-Kelvin cooler will be implemented, and an advanced few-Kelvin cryo-cooler able to maintain the sub-Kelvin cooler's hot zone at a steady (<i>e.g.</i>) 4 K will be very beneficial.</p>
Scientific, Engineering, and/or Programmatic Benefits	<p>Cryo-coolers able to operate near 4 K, cooling detectors and optics directly, as well as serving as a backing stage for ultralow temperature (sub-Kelvin) coolers will enable large FIR telescopes, as well as ultra-low-noise operation of cryogenic detectors for other bands.</p> <p>Increased heat lift, lower mass, lower volume, increased operational lifetime, and reduced cost will enable such missions to fly extended durations without wasting critical resources on cooling.</p> <p>Large-capacity cryo-coolers are required to achieve astrophysical photon-background-limited sensitivity in the FIR and meet sensitivity requirements to achieve the science goals for future FIR telescopes or interferometers.</p>
COR Applications and Potential Relevant Missions	This technology is a key enabling technology for any future FIR mission. It is applicable to missions of all classes, including balloons, Explorers, Probes, and Flagship observatories. For example, it would improve performance of ST02 long/ultra-long duration balloon, SOFIA instruments, and a FIR Surveyor (Roadmap), but other Explorer missions would also be very positively impacted.
Time to Anticipated Need	<p>No FIR missions are called out by NWNH. Thus the timeline for this need is driven by possible Explorer and suborbital missions.</p> <p>Developing and implementing new cryo-coolers in such missions would enable consideration of a large FIR mission in the 2020 Decadal Survey.</p> <p>The earliest possible missions would start with the upcoming MIDEX call in FY 2017. Immediate funding would take advantage of current development momentum, allowing time for system integration and cryo-thermal system performance verification. Tests on balloons could start anytime.</p>

4. Technology Priorities and Recommendations

Background

As part of its annual technology prioritization process, the Program Office convened a TMB to prioritize the technology gaps submitted. The TMB followed an agreed-upon set of evaluation criteria, resulting in the priorities shown below. TMB membership included senior staff from NASA HQ Astrophysics Division, the Program Office, STMD, and the Aerospace Corporation. For 2015, the TMB used a prioritization approach similar to that used in prior years, with a streamlined set of four criteria. These included strategic alignment, benefits and impacts, applicability, and urgency.

- **Strategic alignment:** How well does the technology align with COR science and/or programmatic priorities of the AIP or current programmatic assessment (*e.g.*, the Astrophysics Roadmap)?
- **Benefits and impacts:** How much impact does the technology have on applicable missions? To what degree does it enable and/or enhance achievable science objectives, reduce cost, and/or reduce mission risks?
- **Scope of applicability:** How crosscutting is the technology? How many Astrophysics programs and/or mission concepts would it benefit?
- **Urgency:** When are the enabled/enhanced missions' launches anticipated and/or by when do other schedule drivers require progress?

The TMB assigned weighting factors, reflecting the relative importance placed on each criterion. Each technology gap received a score of 0 to 4 for each criterion. The scores were multiplied by their respective weights, and the products were summed. Some technologies could be scored based on several missions or mission classes. In such cases, the TMB scored each scenario independently, assigning the highest overall score (*e.g.*, a gap might receive an overall score of 91 for a highly aligned mission, but only 75 for a less-aligned class of missions, in which case it would be assigned the higher score). Table 4-1 details the criteria descriptions, weighting factors, and TMB scoring guidelines.

This process provides a rigorous, transparent ranking of technology gaps based on the Program's goals, community scientific rankings of relevant missions, Astrophysics Division priorities as outlined in the AIP and Roadmap, and the external programmatic environment. Since the SAT program is intended to promote development and maturation of technologies relevant to missions and concepts identified as strategic, the strategic alignment criterion is driven by the AIP, which is in turn based on NWNH. The AIP details highly ranked science missions and technology development, which for COR include Far-IR and UV/Optical/IR observatories; and prioritizes those based on current budget realities. This year, the TMB also considered the five potential "Surveyor" missions envisioned by the Astrophysics Roadmap, as well as the Habitable Exoplanet Imaging Mission recommended by the NWNH, several of which will be studied as concept missions in preparation for the 2020 Decadal Survey.

Cosmic Origins Program Annual Technology Report

Criterion	Weight	Max Score	Max Weighted Score	General Description/ Question	4	3	2	1	0
Strategic Alignment	10	4	40	How well does the technology align with COR programmatic priorities of the AIP or current programmatic assessment (e.g., Astrophysics Roadmap)?	Applicable COR mission concept receives highest AIP consideration	Applicable COR mission concept receives medium AIP consideration, or is envisioned as a "Surveyor" in the Roadmap	Applicable COR mission concept receives low AIP consideration	Applicable COR mission concept not considered in the AIP but was positively addressed in NWNH	Not considered by the AIP, Roadmap, or NWNH for COR
Benefits and Impacts	8	4	32	How much impact does the technology have on applicable mission(s)? To what degree does the technology enable and/or enhance achievable science objectives, reduce cost, and/or reduce mission risks?	Critical and key enabling technology; required to meet mission concept objectives; without this technology, applicable missions would not launch	Highly desirable; not mission-critical, but provides major benefits in enhanced science capability, reduced critical resources need, and/or reduced mission risks; without it, missions may launch, but science or implementation would be compromised	Desirable; not required for mission success, but offers significant science or implementation benefits; if technology is available, would almost certainly be implemented in missions	Minor science impact or implementation improvements; if technology is available would be considered for implementation in missions	No science impact or implementation improvement; even if available, technology would not be implemented in missions
Scope of Applicability	3	4	12	How cross-cutting is the technology? How many Astrophysics programs and/or mission concepts could it benefit?	Applies widely to COR mission concepts and both PCOS and ExEP mission concepts	Applies widely to COR mission concepts and either PCOS or ExEP mission concepts	Applies widely to COR mission concepts	Applies to a single COR mission concept	No known applicable COR mission concept
Urgency	4	4	16	When are launches and/or other schedule drivers of missions enhanced or enabled by this technology anticipated?	Launch anticipated in next 5-9 years (2020-2024) or other schedule driver requires progress in 3-4 years (2018-2019)	Launch anticipated in next 10-14 years (2025-2029) or other schedule driver requires progress in 5-9 years (2020-2024)	Launch anticipated in next 15-19 years (2030-2034)	Launch anticipated in next 20-24 years (2035-2039)	Launch anticipated in 25 or more years (2040 or later)

Table 4-1. Clear, strategic criteria provide a rigorous, transparent process for prioritizing technology gaps.

Prioritization Results

As mentioned above, in 2015, the COR TMB received and scored 20 technology gaps per the criteria described in Table 4-1. Reviewing the scores, the TMB binned the technology gaps into three groups based on a number of factors, including primarily a natural grouping of overall scores. The groups were as follows (entries within a group are numbered for convenience, but are ranked equally):

Priority 1: Technologies the TMB determined to be of the highest interest to the COR Program. Filling these gaps would provide key enabling technologies for the highest-priority strategic COR missions including a Far-IR Surveyor and a LUVOIR Surveyor. The TMB recommends SAT calls and award decisions address these technology gaps first.

1. Large-Format, Low-Noise and Ultralow-Noise Far-IR Direct Detectors.
2. Band-Shaping and Dichroic Filters for UV/Vis.
3. Heterodyne Far-IR Detector Arrays and Related Technologies.
4. High-QE, Rad-Hard, Large-Format, Non-Photon-Counting UVOIR Detectors.
5. Photon-Counting Large-Format UV Detectors.
6. High-Efficiency UV Multi-Object Spectrometers.
7. High-Reflectivity Mirror Coatings for UV/Vis/Near-IR.

Priority 2: Technologies the TMB believes would be critical, highly desirable, or desirable for a variety of strategic missions. The TMB recommends that should sufficient funding be available, SAT calls and award decisions address closing these technology gaps as well.

1. Affordable, Lightweight, Ultra-Stable, Large-Aperture Telescopes.
2. Large, Cryogenic Far-IR Telescopes.
3. Sensing and Control at the Nanometer Level or Better.
4. Advanced Cryo-Coolers.
5. Thermally Stable Telescope.
6. Disturbance Isolation.
7. Far-IR Interferometry.
8. High-Performance Sub-Kelvin Coolers.

Priority 3: Technologies the TMB deemed supportive of COR objectives, but scoring lower than Priority 1 and 2 technology gaps.

1. Affordable Monolithic Telescope Mirror Technologies.
2. Photon-Counting Visible and Near-IR Detector Arrays.
3. Very-Large-Format, High-QE, Low-Noise, Radiation-Tolerant Detectors for the UV/Vis/Near-IR.
4. Wide-Bandwidth, High-Spectral-Dynamic-Range Receiving System.
5. Sensing and Control at the Picometer Level.

From 2011 through 2015, nearly all gaps achieving Priority 1 maintained that rank or changed by one level due to minor shifts in how priority scores break up naturally into groups. Also, funded projects have addressed high-priority gaps, mostly Priority 1, and occasionally Priority 2. For example, six of seven of the 2015 Priority 1 gaps have already been addressed by SAT projects, as have one of the eight Priority 2 gaps and one of the five Priority 3 gaps, which was Priority 2 in 2014. Over the years, certain high-urgency Priority 1 gaps were funded directly or via a funded flight project or study, rather than by SAT grants.

5. Benefits and Successes Enabled by the COR SAT Program

Benefits Enabled by COR SATs

The main benefit of the SAT program is in maturing technologies across the mid-TRL gap, so they can be infused into strategic COR missions and/or enable international collaboration on projects relevant to Program goals. Where appropriate, newly matured technologies are also likely to be implemented in flight missions. These may well extend beyond the COR Program, to PCOS, ExEP, and even outside the Astrophysics Division.

As reported by Perez *et al.* [3], TCOR-funded projects have provided significant positive outcomes. One example, mentioned above, is a COR SAT-supported development of new H4RG near-IR (0.7-2.0 μm) detectors, which were later adopted by WFIRST/AFTA. Current progress indicates the technology can meet the required performance levels for this mission. Another SAT project developed and matured advanced UV-reflective coatings, leading to the PI being invited to implement those for Explorer missions ICON and GOLD. Yet another SAT project has advanced high-efficiency, photon-counting CCD detectors, which were implemented into the FIREBall long-duration balloon mission, and Guide and Focus CCDs for Wafer-Scale Imager for Prime (WaSP) instrument at Palomar and for Caltech Optical Observatory's Zwicky Transient Facility.

Beyond supporting technology maturation, selection for SAT funding offers additional benefits to PIs, research groups, institutions, and the community. During the preparation of this PATR, the Program Office surveyed current PIs about additional benefits resulting from their SAT funding.

Four of eight PIs reported they were able to leverage SAT funding to generate matching internal research and development funding; fellowships (*e.g.*, NASA Postdoctoral Program, NPP; NASA Earth and Space Science Fellowship, NESSF; Millikan Prize; and National Science Foundation, NSF, fellowship); contributed labor, parts, and/or infrastructure funding; industry contracts; and/or funded parallel efforts on related projects. All eight PIs hired students and post-doctoral fellows to assist their technology development work (on average, more than four per project), helping train the next generation of researchers and technologists needed to support future missions. Three of those later converted to full-time employment status within their respective organization, and another took a civil service position at NASA's Langley Research Center, proving that the Program is helping train and shape the future astrophysics work force. Several PIs went on to successfully propose additional technology development projects through the SAT and APRA programs, including two of the four new COR SATs selected for FY 2016 start.

Early this year, the Program presented a poster of all then-current PCOS and COR technology development projects at the January 2015 American Astronomical Society (AAS) meeting in Seattle (Fig. 5-1), displaying the breadth of scope of our SAT investment, and explaining the Programs' technology development process.

Involving Students and Postdocs in SAT Projects

The COR SAT projects have involved dozens of students and postdocs, helping train the future astrophysics workforce (see Appendix C for details). As can be seen in the following quotes, the Program is making a deep impact on these future technologists, and through them promotes astrophysics missions over many decades to come.



The Broad Impacts of the SAT Program

Figure 5-2 depicts the geographic breadth of SAT program (both COR and PCOS) impacts, showing the locations of our PI institutions, their collaborators and partners, and the universities and colleges where the students and post-doctoral fellows involved in SAT projects attend school and work.

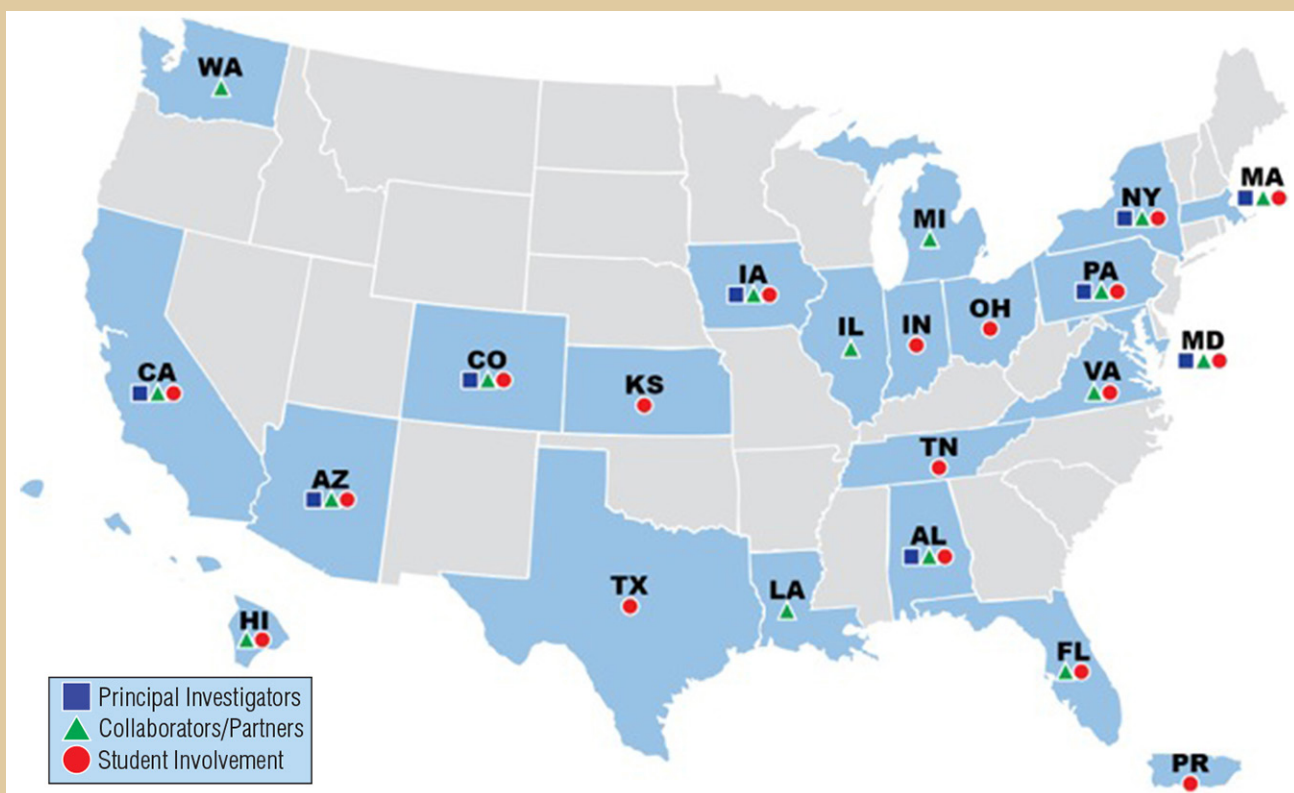


Fig. 5-2. SAT Program Impacts Map. The Program supports research efforts of PIs and collaborators/partners, and develops our future astrophysics workforce through student involvement (locations shown for both COR and PCOS Programs).

6. Closing Remarks

This 2015 COR PATR serves as a snapshot of the dynamic state of technology development managed by the Program Office and provides future directions for technology planning and maturation. As we complete another year of COR technology development activities, we see many positive developments.


Our technology development portfolio is growing, and continues to deliver significant advancements. All funded technologies are maturing toward higher TRLs, with several providing direct benefits to flight missions. New SAT awards slated to start in FY 2016 will fund four additional technologies supporting future Far-UV, UV, visible, and sub-millimeter missions. COR SAT investments are also generating benefits beyond direct advancement of strategic technologies. This includes leveraging internal and external (including non-NASA) funding; contributed materials, parts, and facility/equipment usage; hiring students and postdocs, thereby training our future astrophysics workforce; and generating research collaborations and industry partnerships, in support of COR science goals.

Our established and streamlined technology gap prioritization process continues to adhere to strategic guidance based on the AIP, NWNH, and now the Astrophysics Roadmap “Surveyor” concepts, with the TMB assigning the most significant weight in technology gap prioritization to strategic alignment. As a result, Astrophysics Division continues to fund projects addressing technology gaps identified by the TMB as having the highest priority. The latest set of highest-priority TMB-recommendations submitted to the Astrophysics Division include Far-IR direct and heterodyne detectors, UVOIR and UV detectors, UV multi-object spectrometers, UV/Vis filters, and UV/Vis/Near-IR coatings.

To continue and support the ever-evolving technology needs of the COR community, we continue to interact with the broad scientific community through the COPAG, through various workshops, via public outreach activities, and at public scientific conferences. These activities identify and incorporate the astrophysics community’s ideas about new science, current technology progress, and new needs for technology in an open and proven process. Each year, we incorporate new lessons learned and make appropriate improvements to our process.

We would like to thank the COR scientific community, the PIs and their teams, and the COPAG for their efforts and inputs that make this annual report current and meaningful. We welcome continued feedback and inputs from the community in developing next year’s PATR, which should be sent to [Thai Pham](#) at the Program Office. For more information about the Program and its activities, or to provide your feedback and inputs, please visit the [COR website](#).

References

- 
- [1] J. Mankins, “*The critical role of advanced technology investments in preventing spaceflight program cost overrun*”, The Space Review, December 1, 2008. Available at www.thespacereview.com/article/1262/1. Accessed May 2014.
 - [2] National Research Council, “*New Worlds, New Horizons in Astronomy and Astrophysics*,” Washington, DC: The National Academies Press, 2010. Available at www.nap.edu/catalog.php?record_id=12951. Accessed May 2014.
 - [3] M. Perez, B. Pham, and P. Lawson, “*Technology maturation process: The NASA strategic astrophysics technology (SAT) program*,” Proc. SPIE, Montreal, June 2014.

Appendix A

Technology Development Quad Charts

UV/Vis/IR



K. 'Bala' Balasubramanian – “Ultraviolet Coatings, Materials, and Processes for Advanced Telescope Optics” 51



Shouleh Nikzad – “High-Efficiency Detectors in Photon-Counting and Large Focal-Plane Arrays for Astrophysics Missions”. 52



Zoran Ninkov – “Deployment of DMD Arrays for Use in Future Space Missions” 53



Manuel Quijada – “Enhanced MgF_2 and LiF Over-Coated Al Mirrors for FUV Space Astronomy” 54



H. Philip Stahl – “Advanced UVOR Mirror Technology Development for Very Large Space Telescopes”. 55



John Vallergera – “Cross-Strip MCP Detector Systems for Spaceflight” 56

Far-IR



Imran Mehdi – “A Far-Infrared Heterodyne Array Receiver for CII and OI Mapping” 57

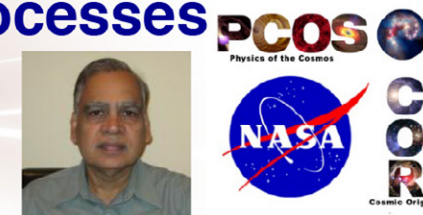


Jonas Zmuidzinas – “Kinetic Inductance Detector Arrays for Far-IR Astrophysics” 58

For more information, see full status reports starting on page 59

Ultraviolet Coatings, Materials, and Processes for Advanced Telescope Optics

PI: K. 'Bala' Balasubramanian / JPL



Objectives and Key Challenges:

- Development of UV coatings with high reflectivity (>90-95%), high uniformity (<1-0.1%), and wide bandpasses (~100 nm to 300-1000 nm) is a major technical challenge; this project aims to address this key challenge and develop feasible technical solutions
- Materials and process technology are the main challenges; improvements in existing technology base and significant innovations in coating technology such as Atomic Layer Deposition (ALD) will be developed

Significance of Work:

- This is a key requirement for future Cosmic Origins and Exo-Planets missions

Approach:

- Develop a set of experimental data with MgF_2 , AlF_3 , and LiF-protected Al mirrors in the wavelength range 100-1000 nm for a comprehensive base of measurements, enabling full-scale developments with chosen materials and processes
- Study enhanced coating processes including ALD
- Improve characterization and measurement techniques

Key Collaborators:

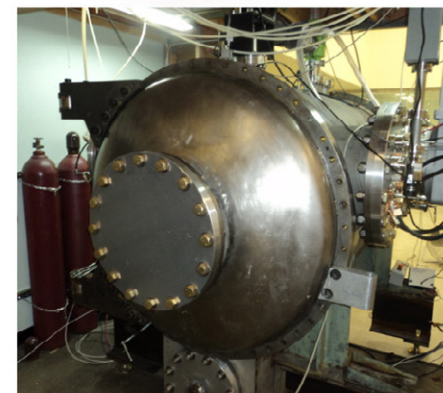
- Stuart Shaklan, Nasrat Raouf, John Hennessey, and Shouleh Nikzad (JPL)
- Paul Scowen (ASU)
- Manuel Quijada (GSFC)

Current Funded Period of Performance:

Jan 2013 – Dec 2015



ALD chamber at JPL



1.2-m coating chamber at Zecoat Corp.

Recent Accomplishments:

- ✓ Upgraded coating chamber with sources, temperature controllers, and other monitors to produce various coatings
- ✓ Upgraded measurement tools at JPL and GSFC
- ✓ Produced and tested coatings with MgF_2 , AlF_3 , and LiF
- ✓ Fabricated several iterations of bi-layer protective coatings
- ✓ Developed ALD coating processes for MgF_2 and AlF_3 at JPL

Next Milestones:

- Enhancements to conventional coating techniques
- Further improve ALD and other enhanced coating processes for protected and enhanced aluminum mirror coatings (2015)
- Produce and characterize test coupons representing 1m-class mirror (June – Sep 2015)

Application:

- Future astrophysics and exoplanet missions intended to capture key spectral features from far-UV to near-IR

$TRL_{In} = 3$ $TRL_{Current} = 3$ $TRL_{Target} = 5$

High-Efficiency Detectors in Photon-Counting and Large Focal-Plane Arrays for Astrophysics Missions

PI: Shouleh Nikzad / JPL



Objective and Key Challenges:

- Atomic-level control of back-illuminated detector surfaces and detector/AR coating interfaces to produce high-efficiency detectors with stable response and unique performance advantages in the challenging UV and FUV spectral range

Significance of Work:

- High-efficiency, high-stability imaging arrays developed under this SAT task are an efficient and cost-effective way to populate UV/Optical focal planes for the large aperture UV/O telescope recommended by the 2010 Decadal Survey and for spectroscopic missions

Approach:

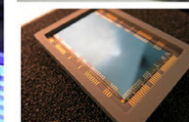
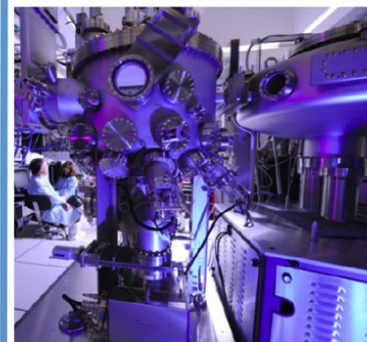
- Develop and produce 2-megapixel, AR-coated, delta-doped, electron-multiplying CCDs (EMCCDs) using JPL's 8-inch capacity silicon molecular beam epitaxy (MBE) for delta doping and atomic layer deposition (ALD) for AR coating
- Perform system-level on-sky evaluation (broadband p-channel arrays) to validate performance over a wide range of signal levels
- Validate in FIREBall suborbital balloon flight

Key Collaborators:

- Chris Martin (Caltech)
- David Schiminovich (Columbia University)
- Paul Scowen (Arizona State University)
- Michael Hoenk (JPL)

Current Funded Period of Performance:

Jan 2013 – Dec 2015



JPL facility and 2-megapixel device before and after packaging

Recent Accomplishments:

- ✓ Produced and tested multiple UV photon-counting, 2-megapixel
- ✓ FIREBall and demonstrated on 2-megapixel arrays
- ✓ Measured ~80% QE at FIREBall peak with very low dark current
- ✓ Produced large-format arrays for broadband detection for on-sky observation; demonstrated good performance at Mount Bigelow

Next Milestones:

- Characterize FIREBall AR-coated 2-megapixel arrays for noise especially dark current with low noise system (FY 2015 Q4)
- Select FIREBall detector from pool of processed devices and deliver to Caltech and the spectrograph team
- Further evaluate performance in astrophysics- and mission-relevant environments (FY 2016 Q1, FY 2016 Q3), Mount Bigelow 61" (Nov 2015), and FIREBall (FY 2016 Q3)

Applications:

- Large aperture UV/Optical telescope
- Explorers
- Spectroscopy missions
- UV/Optical imaging

TRL_{In} = 4 TRL_{Current} = 4 TRL_{Target} = 5

Development of DMD Arrays for Use in Future Space Missions

PI: Zoran Ninkov / Rochester Institute of Technology



Objectives and Key Challenges :

- A technology is needed that allows selection of targets in a field of view that can be put into an imaging spectrometer for use in remote sensing and astronomy
- We are looking to modify and develop COTS Digital Micro-mirror Devices (DMD) for this application

Significance of Work :

- Existing DMDs need to have their commercial windows replaced with windows appropriate for the scientific application desired
- The radiation hardness and scattering properties of the DMDs need to be investigated

Approach:

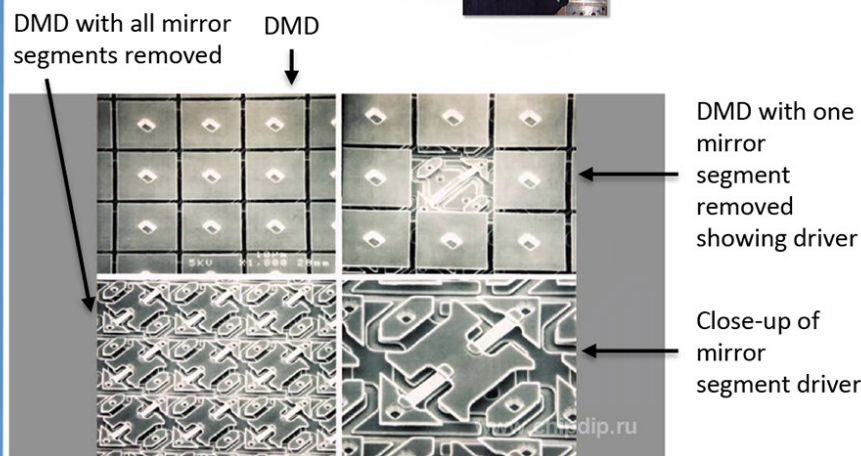
- Use available 0.7 XGA DMDs to develop window-removal procedures and then replace delivered window with a hermetically sealed UV transmissive one (magnesium fluoride or HEM sapphire)
- Test and evaluate such devices and Cinema DMDs (2048 x 1080)

Key Collaborators:

- Sally Heap, Manuel Quijada (NASA/GSFC)
- Massimo Robberto (STScI)
- Alan Raisanen (RIT)

Current Funded Period of Performance:

May 2014 – May 2016



Recent Accomplishments:

- ✓ 0.7 XGA DMDs ordered and delivered (Dec 2014)
- ✓ MgF_2 and HEM Sapphire windows delivered (Jun 2015)
- ✓ DMDs de-lidded at RIT and characterized at GSFC (Jun 2015)

Next Milestones

- XGA DMDs with Sapphire & MgF_2 windows delivery (Sep 2015)
- Cinema DMDs and electronics delivery (Sep 2015)
- Heavy Ion testing at Texas A&M (Aug 2015)
- Scattered-light and contrast measurements (Dec 2015)

Applications:

- Any hyper-spectral imaging mission
- Galaxy Evolution Spectroscopic Explorer

$TRL_{In} = 4$ $TRL_{Current} = 4$ $TRL_{Target} = 5$

Enhanced MgF_2 and LiF Over-Coated Al Mirrors for FUV Space Astronomy

PI: Manuel A. Quijada / GSFC Code 551



Objectives and Key Challenges:

- Develop high-reflectivity coatings to increase system throughput, particularly in the far-UV (FUV) spectral range
- Study other dielectric fluoride coatings and other deposition technologies, such as Ion Beam Sputtering (IBS), expected to produce the nearest-to-ideal-morphology optical-thin-film coatings and thus low scatter

Significance of Work:

- High reflectivity (> 90-95%) in the 90 to 250 nm range will enhance throughput in UV telescopes
- Scaling coatings up to large diameter (1+ m) mirror substrates will enable large-aperture UV and/or UVOIR missions

Approach:

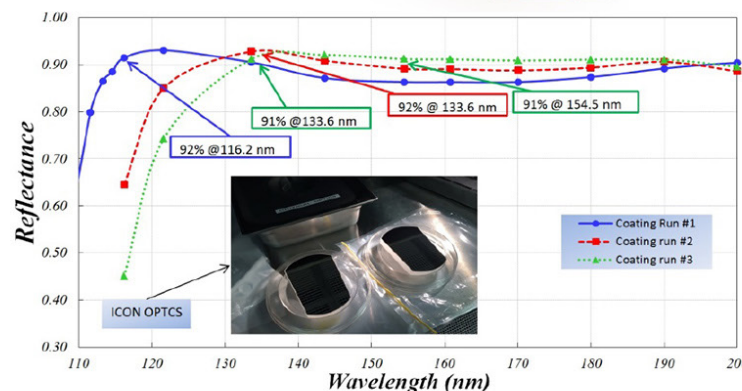
- Retrofit a 2-m coating chamber with heaters/thermal shroud to perform Physical Vapor Depositions at high temperatures (200-300 C) to further improve performance of Al mirrors protected with either MgF_2 or LiF overcoats.
- Optimize deposition process of lanthanide trifluorides as high-index materials that when paired with either MgF_2 or LiF will enhance reflectance of Al mirrors at Lyman-alpha
- Establish the IBS coating process to optimize deposition of MgF_2 and LiF with extremely low absorptions at FUV wavelengths

Key Collaborators:

- Javier del Hoyo, Steve Rice, and Felix Threat (GSFC Code 551)
- Jeff Kruk and Charles Bowers (GSFC Code 665)

Latest Funded Period of Performance:

Oct 2011 – Sep 2014



Data from various test runs to produce coatings with over 90% reflectance for ICON spectral range

Recent Accomplishments:

- ✓ Performed end-to-end testing of the three-step Physical Vapor Deposition (PVD) coating process in 2-m chamber to enable 1+ m class mirrors with either Al+ MgF_2 or Al+LiF coatings for FUV applications
- ✓ Completed characterization of lanthanide trifluorides (GdF_3 and LuF_3) to pair them with low-index MgF_2 layers to produce narrow-band dielectric reflectors at FUV wavelengths
- ✓ Produced mirrors with reflectance over 90% in FUV for ICON and GOLD projects

Application:

- Application of these enhanced mirror coating technology will enable FUV missions to investigate the formation and history of planets, stars, galaxies, and cosmic structure; and how the elements of life in the universe arose

$TRL_{In} = 3$ $TRL_{PI-Asserted} = 4$ $TRL_{Target} = 4$

Advanced UVOIR Mirror Technology Development for Very Large Space Telescopes

PI: H. Philip Stahl / MSFC



Objectives and Key Challenges:

- Advance TRL of key technology challenges for the primary mirror of future large-aperture Cosmic Origins UVOIR space telescopes
- Include monolithic and segmented optics design paths
- Conduct prototype development, testing, and modeling
- Trace metrics to science mission error budget

Significance of Work:

- Deep-core manufacturing method enables 4-m class mirrors with a 20-30% lower cost and risk
- Design tools increase speed and reduce cost of trade studies
- Integrated modeling tools enable better definition of system and component engineering specifications



Rounding the glass face plate

Approach:

- Science-driven systems engineering
- Mature technologies required to enable highest priority science and result in high-performance, low-cost, low-risk system
- Provide options to science community by developing technology enabling both monolithic- and segmented-aperture telescopes
- Mature technology in support of 2020 Decadal process

Key Collaborators:

- Dr. Scott Smith, Ron Eng, and Mike Effinger (MSFC)
- Bill Arnold (AI Solutions)
- Gary Mosier (GSFC)
- Dr. Marc Postman (STScI)
- Olivier Guyon (U of Arizona)
- Stuart Shaklan and John Krist (JPL)
- Al Ferland, Gary Matthews, and Rob Eggerman (Harris)

Current Funded Period of Performance:

Sep 2011 – Sep 2016

Recent Accomplishments:

- ✓ Finalized 1.5-m design, traceable to 4 m, using A-Basis strength data
- ✓ Fabricated 1.5-m mirror face/back plates
- ✓ Characterized 40-cm deep core with X-ray computed tomography
- ✓ Received approval for Arnold Mirror Modeler code distribution
- ✓ Developed thermal MTF modeling methodology
- ✓ TRL Board Assessment

Next Milestones:

- Publish recent results
- Fabricate and assemble 1.5-m mirror substrate

Applications:

- Flagship optical missions
- Explorer-type optical missions
- Department of Defense and commercial observations

$TRL_{In} = 3$ $TRL_{Current} = 3$ $TRL_{Target} = 4$

Cross-Strip MCP Detector Systems for Spaceflight

PI: John Vallergera / UC Berkeley



Objective and Key Challenges:

- Cross strip (XS) MCP photon-counting UV detectors have achieved high spatial resolution (12 μm) at low gain (500k) and high input flux (MHz) using lab electronics and decades-old ASICs; we plan to develop new ASICs ("GRAPH") that improve this performance, including amplifiers and ADCs in a low-volume, low-mass, and low-power package, crucial for spaceflight and demonstrate its performance to TRL 6

Significance of Work:

- A new ASIC with amplifiers 5 \times faster, yet with similar noise characteristics as existing amplifier ASIC, GHz analog sampling, a low-power ADC per channel, and FPGA control of ASICs will allow enhanced performance in a package suited to spaceflight

Approach:

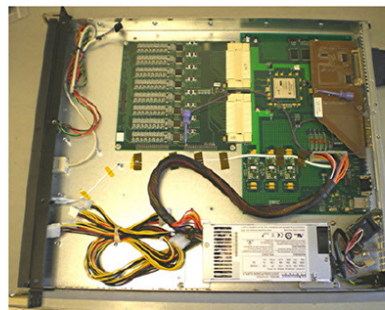
- We will develop the ASIC in stages, by designing the four major subsystems (amplifier, GHz analog sampler, ADC, and output multiplexer) using sophisticated simulation tools for CMOS processes
- Small test runs of the more intricate and untested designs can be performed through shared access of CMOS foundry services to mitigate risk
- We plan two runs of the full-up GRAPH design (CSA preamp and "HalfGRAPH"); in parallel, we will design and construct an FPGA readout circuit for the ASIC as well as a 50mm XS MCP detector that can be qualified for flight use

Key Collaborators:

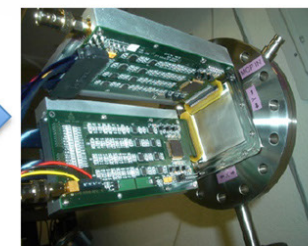
- Prof. Gary Varner (U. Hawaii)
- Dr. Oswald Siegmund (UC Berkeley)

Current Funded Period of Performance:

May 2012 – Apr 2016



Existing 19" rack-mounted XS electronics



Two small, low-mass, low-power ASIC and FPGA boards qualified for flight

Recent Accomplishments:

- ✓ 50-mm detector design and fabrication complete
- ✓ Confirmed detector performance with PXS electronics
- ✓ Designed, fabricated, and tested first half-GRAPH1 ASIC
- ✓ Designed and fabricated half-Graph ver2
- ✓ Successful thermal test of detector (-30°C to +55°C)
- ✓ Successful Vibration test of detector (14.1 g_{rms})
- ✓ Submission of Charge Amp ASIC ver. 2 to foundry

Next Milestones:

- ASIC integration with control FPGA boards (Fall 2015)
- Environmental tests of Detector + ASICs (Dec 2015)

Applications:

- High-performance UV (1-300 nm) detector for astrophysics, planetary, solar, heliospheric, or aeronomy missions
- Particle or time-of-flight detector for space physics missions
- Neutron radiography/tomography for materials science

$TRL_{\text{In}} = 4$ $TRL_{\text{Current}} = 4$ $TRL_{\text{Target}} = 6$

A Far-Infrared Heterodyne Array Receiver for CII and OI Mapping

PI: Imran Mehdi / JPL



Objectives & Key Challenges:

- Proposed work will advance the TRL of Far-IR heterodyne array receivers so that they can be deployed on airborne platforms such as SOFIA or future suborbital and space missions
- We will develop a 16-pixel heterodyne receiver system to cover both the C+ and the O+ lines.

Significance of Work:

- Heterodyne technology is necessary to answer fundamental questions such as: How do stars form? How do circumstellar disks evolve and form planetary systems? What controls the mass-energy-chemical cycles within galaxies?

Approach:

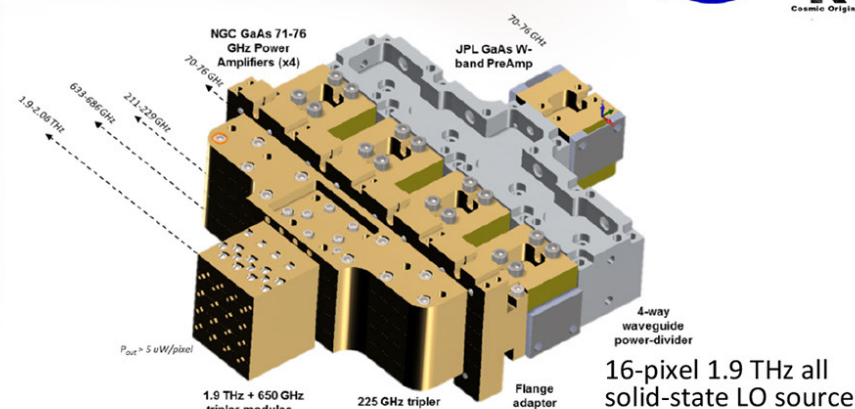
- Use JPL-developed membrane diode process to construct tunable sources in the 1.9 - 2.06 THz range
- Use novel, waveguide-based, active-device, power-combining schemes to enhance power at these frequencies
- Design and build compact, silicon, micro-machined housing for HEB mixer chips
- Use CMOS technology for back-ends/synthesizer
- Characterize and test multi-pixel receivers to validate stability and field performance

Key Collaborators:

- Paul Goldsmith (Science Lead), Jon Kawamura, Jose Siles, Choonsup Lee, and Goutam Chattopadhyay (JPL)
- Frank Chang (UCLA)
- Sander Weinreb (Caltech)

Current Funded Period of Performance:

Oct 2013 – Sep 2016



Recent Accomplishments:

- ✓ Completed system architecture design and interface controls
- ✓ Designed mixer devices
- ✓ Designed multiplier devices
- ✓ Fabricated mixer devices
- ✓ Fabricated multiplier devices
- ✓ Demonstrated 4 pixel LO source at 1.9 THz
- ✓ Demonstrated 4-pixel receiver at 1.9 THz

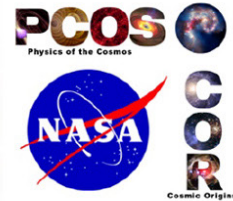
Next Milestones:

- Assemble 4-pixel receiver with CMOS back-end
- Characterize receiver sensitivity and stability
- Design 16-pixel receiver components
- Fabricate 16-pixel receiver components
- Assemble and test 16-pixel receiver

TRL_{In} = 4 TRL_{Current} = 4 TRL_{Target} = 5

Kinetic Inductance Detector Arrays for Far-IR Astrophysics

PI: Jonas Zmuidzinas / Caltech



Objectives and Key Challenges:

- Half of the electromagnetic energy emitted since the big bang lies in the far-IR. Large-format far-IR imaging arrays are needed to study galaxy formation and evolution, and star formation in our galaxy and nearby galaxies. Polarization-sensitive arrays can provide critical information on the role of magnetic fields.
- We will develop and demonstrate far-IR arrays for these applications.

Significance of Work:

- Far-IR arrays are in high demand but are difficult to fabricate, and therefore expensive and in short supply; our solution is to use titanium nitride (TiN) and aluminum absorber-coupled, frequency-multiplexed kinetic inductance detectors.

Approach:

- Raise the TRL of these detectors so investigators may confidently propose them for a variety of instruments:
 - Ground telescope demo, 350 μm , $3 \times 10^{-16} \text{ W Hz}^{-1/2}$
 - Lab demo for space, 90 μm , $5 \times 10^{-19} \text{ W Hz}^{-1/2}$

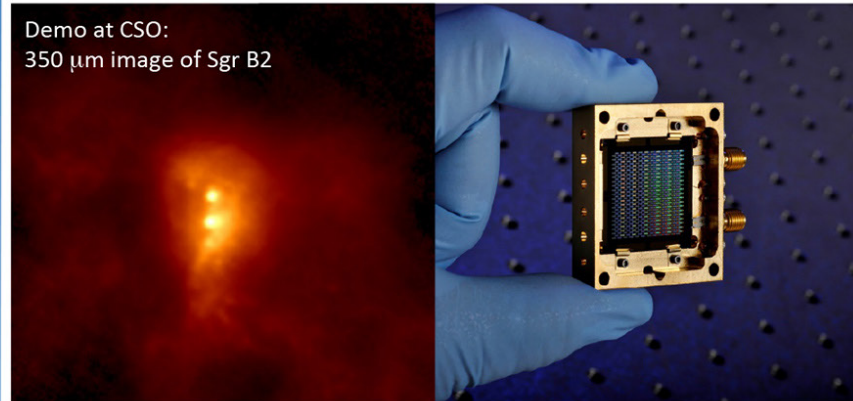
Key Collaborators:

- Goutam Chattopadhyay, Peter Day, Darren Dowell, and Rick Leduc (JPL)
- Chris McKenney (JPL/NIST)
- Pradeep Bhupathi, Matt Hollister, and Attila Kovacs (Caltech)

Current Funded Period of Performance:

Mar 2013 – Feb 2016

Demo at CSO:
350 μm image of Sgr B2



Recent Accomplishments:

- ✓ Successful 350 and 850 μm demos on telescope (350 μm image above)
- ✓ Photon-noise-limited 350 μm lens-coupled arrays
- ✓ Low-cost, high-yield multiplexing of 500-pixel arrays
- ✓ Process improvement (high yield) in aluminum KID for space-background operation
- ✓ Demonstration of new chirped readout technique at telescope

Next Milestone:

- Optical tests of space-sensitivity arrays (through end of project)

Applications:

- Future space missions, *e.g.*, Far IR Surveyor
- Suborbital projects: SOFIA instruments and balloon payloads
- Cameras and spectrometers for ground-based telescopes
- CMB arrays, now under development at Columbia University

$TRL_{In} = 3$ $TRL_{Current} = 3$ $TRL_{Target} = 4$

Appendix B

Technology Development Status

UV/Vis/IR



K. 'Bala' Balasubramanian – “Ultraviolet Coatings, Materials, and Processes for Advanced Telescope Optics” 60



Shouleh Nikzad – “High-Efficiency Detectors in Photon-Counting and Large Focal-Plane Arrays for Astrophysics Missions”. 70



Zoran Ninkov – “Deployment of DMD Arrays for Use in Future Space Missions” 81



Manuel Quijada – “Enhanced MgF_2 and LiF Over-Coated Al Mirrors for FUV Space Astronomy” 87



H. Philip Stahl – “Advanced UVOR Mirror Technology Development for Very Large Space Telescopes”. 99

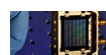


John Vallergera – “Cross-Strip MCP Detector Systems for Spaceflight” 106

Far-IR



Imran Mehdi – “A Far-Infrared Heterodyne Array Receiver for CII and OI Mapping” 117



Jonas Zmuidzinas – “Kinetic Inductance Detector Arrays for Far-IR Astrophysics” 128

Abstracts of SAT Projects Starting in 2016

Qing Hu – “Raising the Technology Readiness Level of 4.7-THz Local Oscillators” 136

Shouleh Nikzad – “Advanced FUV/UV/Visible Photon-Counting and Ultralow-Noise Detectors” 137

Paul Scowen – “Building a Better ALD – Use of Plasma-Enhanced ALD to Construct Efficient Interference Filters for the FUV” 138

John Vallergera – “Development of Large-Area (100 mm \times 100 mm) Photon-Counting UV Detectors” 139

Ultraviolet Coatings, Materials, and Processes for Advanced Telescope Optics

Prepared by: K. 'Bala' Balasubramanian (PI; JPL/Caltech); John Hennessy, Nasrat Raouf, Shouleh Nikzad, and Stuart Shaklan (JPL/Caltech); Paul Scowen (Arizona State University); and Manuel Quijada (NASA/GSFC)

Summary

Development of high-reflectivity coatings, particularly for the ultraviolet (UV) part of the spectrum, is considered a technology challenge requiring significant materials research and process development. Our primary objectives address the need to develop new and improved coating technologies for advanced telescope optics as identified by the NASA Cosmic Origins (COR) program.

A successful pathway to achieve the objectives, namely to develop durable mirror coatings that will provide high reflectance over the extended spectral band in the Far-UV (FUV) to near-infrared (NIR), requires the best choice of materials and processes after a careful experimental study of potential candidates. Void-free thin films of absorption-free materials are required to protect and maintain high reflectivity and durability of aluminum mirrors in laboratory and pre-launch environments. A precisely controllable and scalable deposition process is also required to produce such coatings on large telescope mirrors.

During the first year of our three-year project commencing in 2013, we investigated the applicability of common materials and known processes, and identified promising candidates [1-3]. MgF_2 , LiF , and AlF_3 stand out as the most promising materials for protective coatings while GdF_3 , LaF_3 , and LuF_2 are other potential materials to be considered. We produced coatings of some of these materials using a conventional vacuum deposition process, and measured their basic properties. Our initial results were reported in a poster paper presented at the American Astronomical Society (AAS) meeting in Baltimore, MD [4]. Preliminary results with coating experiments on Al mirrors protected with MgF_2 and AlF_3 were also reported in our report in the 2014 COR Program Annual Technology Report (PATR).

Over the past year, we conducted several coating experiments with conventional coating techniques as well as Atomic Layer Deposition (ALD) to produce thin MgF_2 and AlF_3 protective coatings. With the 1.2-m coating chamber at our sub-contract vendor, Zecoat Corp. of Torrance, CA, we produced a number of samples with chosen recipes as detailed below. Similarly, several samples of newly developed ALD protective coatings on Al were produced at JPL. A Perkin Elmer UV/Vis spectrophotometer at JPL and an ACTON FUV spectrophotometer at the NASA Goddard Space Flight Center (GSFC) were employed to measure the reflectance properties of these samples. A spectroscopic ellipsometer was also employed at JPL to characterize the films. Theoretical model fits of measured characteristics were analyzed. Key advances were made this year on the ALD front with successful process development for MgF_2 and AlF_3 coatings at faster rates and lower temperatures. Further process development for protected Al coatings with these chosen materials is in progress. A paper [5] on the most recent ALD results was presented at the ALD conference in Portland, OR on June 29, 2015.

Background

It has been recognized that in the Mid-UV to Far-UV wavelengths ($90 < \lambda < 300 \text{ nm}$), it is possible to detect and measure important astrophysical processes, which can shed light on the physical conditions of many environments of interest. For example, in the local interstellar medium (LISM) all but two (Ca II H and K lines) of the key diagnostic of resonance lines are in the UV [6]. In addition to the fruitful science areas that UV spectroscopy has contributed since the early 1970s, France *et al.* [7] have emphasized the role of UV photons in the photo-dissociation and photochemistry of H_2O and CO_2 in terrestrial planet atmospheres, which can influence their atmospheric chemistry, and subsequently the

habitability of Earth-like planets. However, only limited spectroscopic data are available for exoplanets and their host stars, especially in the case of M-type stars. Similarly, new areas of scientific interest are the detection and characterization of the hot gas between galaxies and the role of the intergalactic medium (IGM) in galaxy evolution [8].

The 2011 COR PATR (Technology Needs, Table 7, Item 8.1.3., page 43, Oct 2011) [9] defined the primary goal that we have adopted for this project: “*Development of UV coatings with high reflectivity (> 90-95%), high uniformity (< 1-0.1%), and wide bandpasses (~100 nm to 300-1000 nm).*” More recently, the Advanced Technology Large-Aperture Space Telescope (ATLAST) technology team assessed and stressed the technology development for maturing mirror coatings for the Far-UV spectral range [10]. A comprehensive summary of the Far-UV science requirements (a Science Traceability Matrix, STM) was compiled by Paul Scowen [11], a Co-I on our project. Table 1 lists some of the important spectral lines in the FUV region for general astrophysics. High reflectivity coatings covering the 100-300 nm spectral range are considered important for studying intergalactic matter. The COR Program Analysis Group (COPAG) assessed the degree of difficulty to achieving this as very high. This is indeed very challenging. “*The COPAG is considering a future large UVOIR [UV/Optical/Infrared] mission for general astrophysics that would also perform exoplanet imaging and characterization. Some technologies may be specifically required to make these two missions compatible, for example telescope coatings.*” [12, see p. 5].

Objectives and Milestones

The main objectives of the three-year project were: a) to explore materials and processes to produce protective coatings for Al mirrors providing high reflectivity over a wide spectral range from the Far-UV to NIR, and b) to demonstrate fabrication of durable mirror coatings with chosen processes on distributed coupons representing a meter-class mirror. Conventional coating processes and advanced ALD processes are pursued and investigated to achieve these goals. During the reporting period, from June 2014 to May 2015, the primary objectives were:

1. Fabricate and test coatings of Al protected by MgF_2 , AlF_3 , and LiF deposited by conventional coating processes after producing single-layer fluoride coatings to establish a baseline performance of these coatings over the full spectrum.
2. Produce Al mirror samples with bi-layer protective overcoats with MgF_2 , LiF, and AlF_3 , the promising candidates chosen from previous experiments.
3. Optimize ALD process for absorption-free thin MgF_2 coatings, and conduct experiments with MgF_2 -protected Al mirrors.
4. Optimize ALD process for absorption-free thin AlF_3 coatings, and conduct experiments with AlF_3 -protected Al mirrors.
5. Measure time-dependent changes in the reflectance characteristics of these mirror samples.
6. Develop and perform environmental tests (humidity and thermal cycling) to establish protection of Al and its reflectivity, particularly in the Far-UV. Measure Reflectance, R, before and after environmental tests, and characterize the surface microscopically (extended to Year 3 due to reprioritization of objectives); this task is set for the latter half of 2015 with optimized coatings that demonstrate better long-term stability.

The major objectives listed above are adopted from our original proposal and reprioritized to start on the most promising ALD process development early on.

Wavelength (nm)	Species	Significance	Bodies of Interest
68.1, 69.4	Na IX	Coronal-gas ($> 10^6$ K) diagnostic (density, ionization state, <i>etc.</i>)	Intergalactic medium, quasi-stellar object (QSO) sight lines
77.0	Ne VIII	Warm-hot-gas ($5 \times 10^5 - 10^6$ K) diagnostic (density, ionization state, <i>etc.</i>)	Intergalactic medium, QSO sight lines
99.1, 175.0	N III	Gas-temperature diagnostic	Stellar-atmosphere abundances
102.6	H, Ly- β	Lyman Series H recombination line	Plasma diagnostics for ionized gas in astrophysical contexts
103.2, 103.8	O VI	Recombination-line doublet	Diagnostic for presence of coronal gas and the boundaries between such gas and cooler gas envelopes or media
108.5, 164.0	He II	Balmer line for He	Stellar-atmosphere diagnostic used to trace flares and coronal-mass ejections (CMEs)
117.5	C III	Gas-electron-density diagnostic	Stellar atmospheres and stellar winds
120.6	Si III	Optically thin emission line of silicon	Used as a diagnostic line sensitive to time-variability in emitted or ionizing flux
121.6	H, Ly- α	Lyman Series H recombination line	Plasma diagnostics for ionized gas in astrophysical contexts – especially used for cosmological targets such as reionization-era galaxies and stars
123.8, 124.3	N V	Gas-emission diagnostic	Used to study extended stellar coronae
133.5	C II	Absorption line for ionized carbon	Used as a diagnostic and tracer for stellar chromospheres and planetary atmospheres
139.4, 140.3	Si IV	Emission line of silicon	Used to perform diagnostics of stellar coronae including density, temperature, and abundance
140.7	O IV	Gas-density-sensitive doublet	Used to study upper chromospheres in stars
148.8	N IV	Gas diagnostic line – sensitive in particular to electron collision strengths	Used to study stellar coronae and changes in their emission and bulk motion
154.8, 155.1	C IV	Gas-density-sensitive doublet	Used to diagnose most ionized-gas phases including stellar atmospheres and nebulae
166.3	O III	Gas-temperature- and density-sensitive diagnostic	Used to diagnose nebula gas emission
175.0	N III	Gas-temperature-sensitive diagnostic	Used for stellar-plasma observations and diagnosis
189.5	Si III	Gas-density-sensitive diagnostic	Used to study astrophysical plasmas
190.9	O III	Gas-temperature- and density-sensitive diagnostic	Used to diagnose nebula gas emission
232.6	C II	Absorption line for ionized carbon	Used as a diagnostic and tracer for stellar chromospheres and planetary atmospheres
233.6	Si II	Gas-density-sensitive diagnostic	Magnetic-field diagnostic in stellar atmospheres; density diagnostic in stellar chromospheres

Table 1. Significant diagnostic spectral lines in the UV (50-250 nm) (Courtesy: Paul Scowen)

Progress and Accomplishments

Single-layer coatings of applicable transparent protective materials by conventional deposition process

Single-layer coatings of MgF_2 , LiF , AlF_3 , LaF_3 , Na_3AlF_6 , and GdF_3 were produced initially with conventional coating processes in a 1.2-m chamber fitted with resistive sources, electron gun, ion gun, heater lamps, liquid nitrogen (LN) traps, cryo-pumps, residual-gas analyzers, and computer controls, at pressures in the range of 2×10^{-7} to 1×10^{-6} Torr and temperatures in the range of 20° to 200°C . Figure 1 shows the coating chamber employed for this purpose. A sample transport with masking mechanism was installed in the chamber. This enabled multiple coatings on different samples without breaking vacuum. An FUV optical monitoring system was also installed in the system to measure reflected signal from the growing film during deposition and post-deposition under varying total pressure, water vapor and oxygen content, *etc.*, for diagnostic purposes.

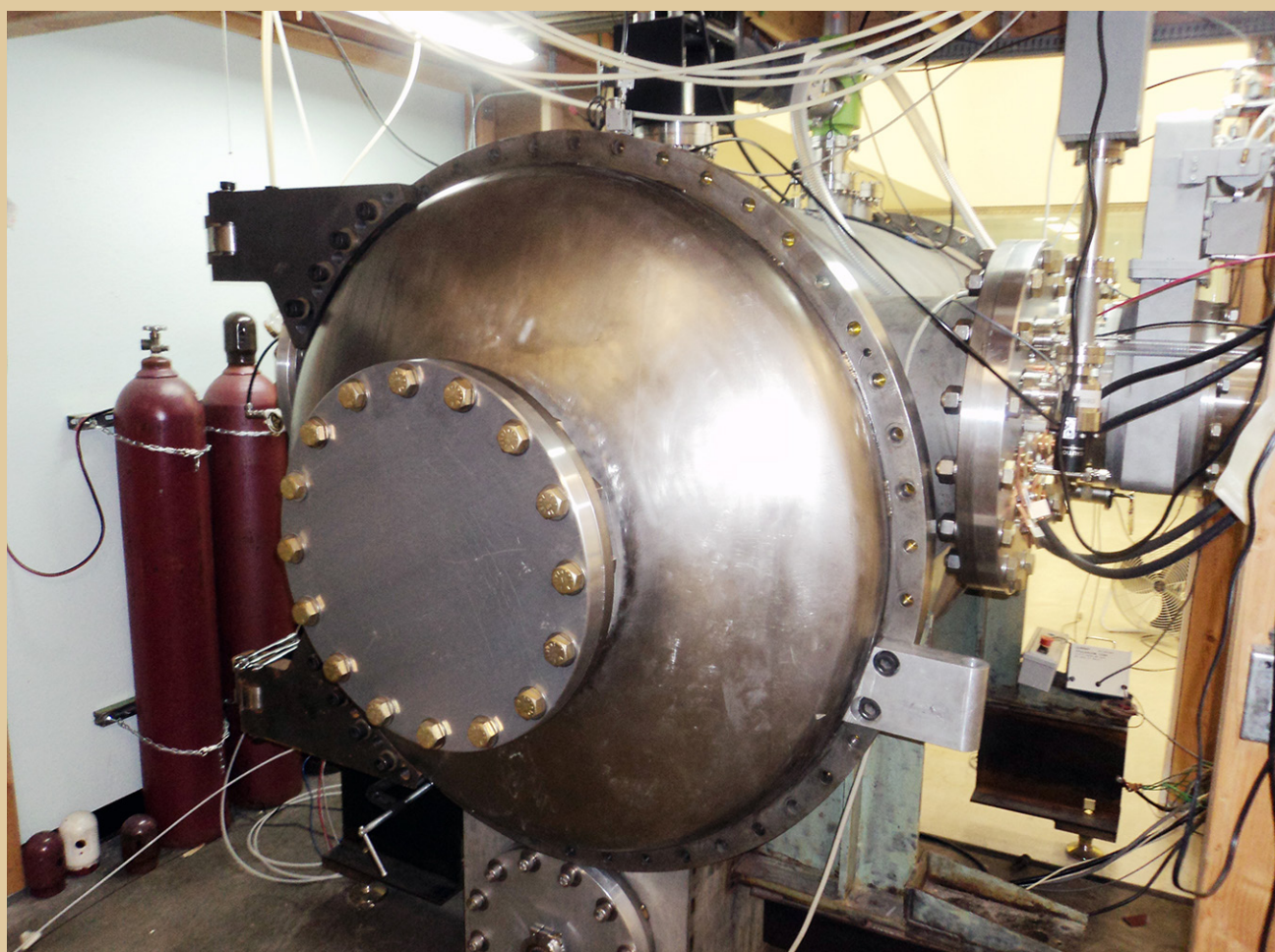


Fig. 1. A 1.2-m coating chamber fitted with process controllers, thickness monitor, and gas analyzer (courtesy: Zecoat Corp).

MgF_2 , LiF , and AlF_3 are considered the most promising coatings based on their UV transparency, as evidenced by results from these initial experiments. Other materials, particularly high-index fluorides, could be employed in other multilayer devices such as filters and beam splitters. Several coatings were prepared on fused silica and silicon substrates. Spectral performance characteristics of these coatings were measured with a state-of-the-art UV/Vis spectrophotometer (PerkinElmer Lambda 1050) as well as with an ACTON FUV spectrometer.

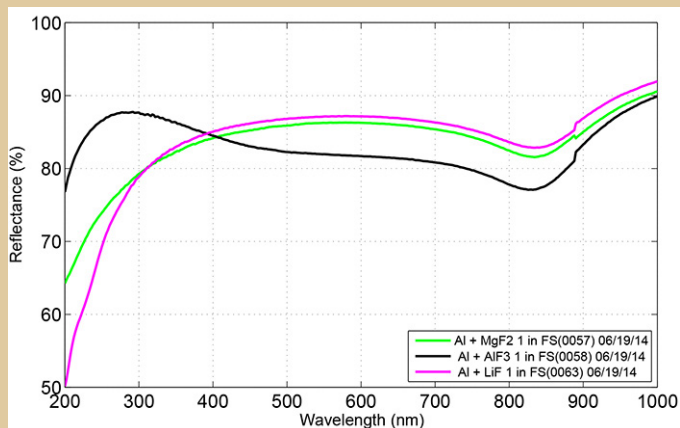


Fig. 2. Reflectance of single-layer-protected Al mirror samples on fused silica (FS) substrates. Measurements in the 200 to 1000 nm range after about eight months from the date of fabrication.

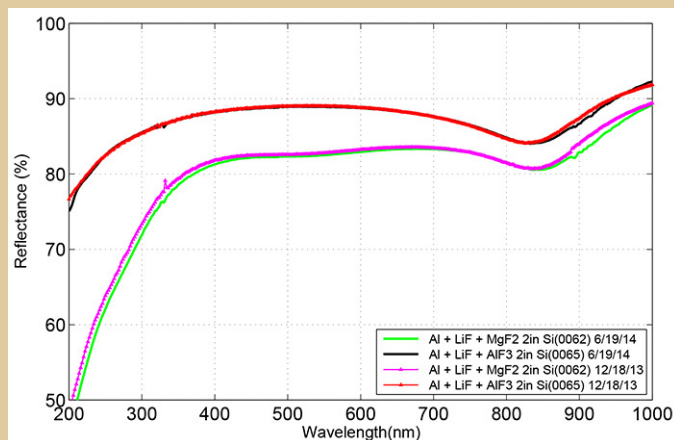


Fig. 3. Reflectivity of Al+LiF mirror samples with MgF_2 and AlF_3 protective layers. Measured six months after fabrication, these samples show little degradation.

Protected Al mirror coatings

MgF_2 , AlF_3 , and LiF single-layer- and bi-layer-protected Al mirror samples were produced in 2014 with a conventional deposition process in the chamber described above. Figure 2 shows the reflectance of three samples over the 200 to 1000 nm spectral range. These experimental data indicate a preference for AlF_3 as protective layer. Similarly, Fig. 3 shows the reflectance of bi-layer-protected Al mirror samples from initial experimental runs in the same chamber. These samples remained in the lab in a dry-nitrogen flow-box except during measurements involving a few days of exposure to normal lab environment with ~30 to 50% humidity. Figure 4 shows the spectral reflectance performance of a bi-layer-protected ($\text{LiF}+\text{AlF}_3$) Al mirror sample for FUV to NIR, measured over a period of 14 months after fabrication. The data show excellent stability. While UV to NIR (200 to 1000 nm) reflectance measurements were done at JPL, FUV (50 to 200 nm) measurements with an ACTON FUV spectrophotometer were done at GSFC under the guidance of Dr. Manuel Quijada. These samples were produced using conventional deposition techniques. Optimization and enhancement of reflectance in the 100 to 200 nm range is a subject of further experimental investigation of process conditions and layer structures. In this context, research done at GSFC has been reported [13, 14] at an SPIE conference and at the AAS meeting in Baltimore, MD. ALD deposition of such coatings is now in progress at JPL.

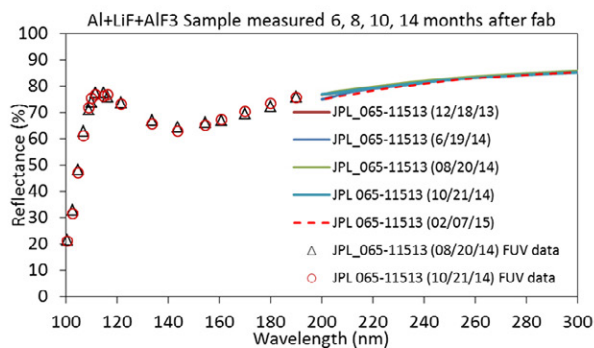
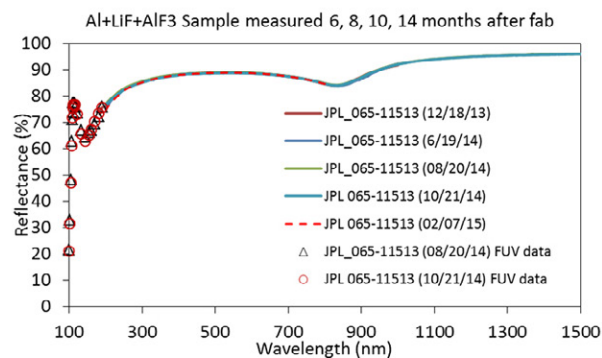


Fig. 4. Measured reflectance of a bi-layer-protected Al mirror sample measured 6, 8, 10, and 14 months after fabrication showing excellent stability. Left: Results across the FUV to NIR spectral range. Right: Expanded view showing details of reflectance in the FUV spectral range.

With further refinement of process controls in the conventional coating chamber, we prepared new samples of MgF_2 - and AlF_3 -protected mirrors with Al and LiF layers. FUV measurements of such tri-layer samples indicate a reflectance greater than 75% achievable at 110 nm and greater than 50% at 100 nm (Fig. 5). Further optimization of coating thicknesses and process parameters is expected to enhance FUV reflectance up to 90%. To enable such experiments, the required upgrades are being carried out on the coating chamber, including adding pumps and controllers.

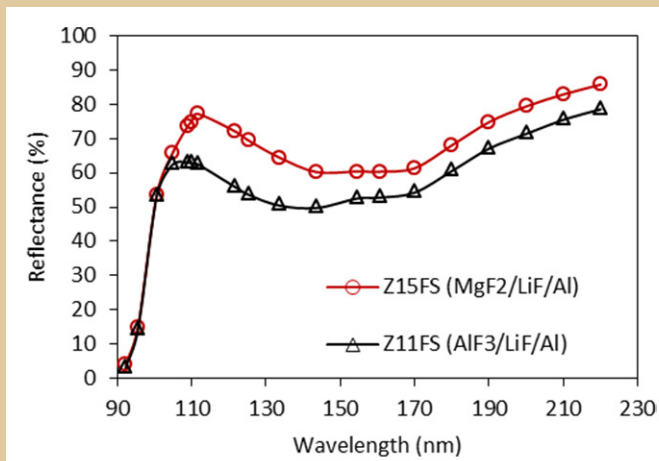


Fig. 5. FUV reflectance of tri-layer mirrors.

Atomic Layer Deposition

ALD processes are under development at JPL to produce MgF_2 and AlF_3 protective coatings for high-reflectivity mirrors using an Oxford OpAl showerhead-style ALD reactor and a Beneq ALD system (Fig. 6).



Fig. 6. ALD systems at JPL. Left: Oxford OpAl showerhead-style ALD reactor with gas feedthroughs and process controls enabling AlF_3 and MgF_2 coatings development. Right: Beneq ALD deposition system.

ALD films were deposited using bis(ethylcyclopentadienyl) magnesium ($\text{Mg}(\text{EtCp})_2$) and trimethylaluminum (TMA) as the metal-containing precursors and anhydrous hydrogen fluoride (HF) as the fluorine-containing precursor in our Oxford reactor. Although metal fluorides are not common ALD materials, there have been several previous reports of their deposition using metal fluorides such as TaF_5 or TiF_4 as the fluorine-containing source [15, 16]. This tends to result in residual metal contamination which degrades the absorption properties in the FUV and results in a process which can only be performed at substrate temperatures greater than 250°C . As a result of this high deposition temperature, the fluoride films deposited with this method tend to crystallize readily, resulting in significant surface morphology which is undesirable for many optical applications. In contrast, the JPL-developed ALD process using HF results in fluorides with lower residual contamination that can also be deposited at low temperature, resulting in smoother, denser films. Future Atomic Force Microscopy (AFM) studies will investigate the surface roughness of these materials as a function of process conditions more precisely.

As part of this effort, MgF_2 and AlF_3 were deposited at substrate temperatures ranging from 100°C to 250°C . Film thickness and refractive index were measured by spectroscopic ellipsometry and monitored as a function of process conditions such as process purge times and substrate temperature. Recent reports on the same JPL ALD materials have also shown good optical performance at wavelengths down to 90 nm [5, 17].

Typical ALD conditions involve heating the $\text{Mg}(\text{EtCP})_2$ precursor, which is then bubbled with Ar into the process chamber with exposure times of approximately 1 s. TMA and HF are delivered by vapor draw at room temperature with shorter exposure times of 15-30 ms. The chamber is purged with Ar between each half-cycle exposure in the ALD process, to ensure saturated, self-limiting deposition. We have demonstrated both MgF_2 and AlF_3 with thickness uniformities better than 1% over six inches in diameter. Initial X-ray Photoelectron Spectroscopy (XPS) measurements suggest the films are approximately stoichiometric and future studies will investigate how material composition changes as a function of process conditions.

A key goal in the development of an ALD process is to optimize the process at acceptably low temperature, *i.e.*, to be below 100°C , in order to enable large mirror coatings in high vacuum. Our recent experiments indicate that this is achievable in the near term for the relevant fluorides.

Reflectance degradation of Al with an oxide formation

To assess the nature and progression of oxide formation on fresh Al coating, we conducted a series of control experiments with Al coatings of different thicknesses deposited at different rates at a high vacuum of $\sim 2 \times 10^{-9}$ Torr in an ultra-high vacuum (UHV) chamber at JPL. Figure 7 shows the measured (symbols) and modelled (lines) performance of an unprotected Al mirror in the wavelength range from 190 to 290 nm over a period of about 1500 minutes after deposition. A single nm of oxide formation is estimated to be sufficient to degrade the reflectance as shown. Figure 8 shows the measured FUV reflectance of an unprotected Al mirror and its model fit with an oxide formation at different thicknesses. These measurements and simulations show that an oxide layer of less than 2 nm thickness affects the FUV reflectance dramatically.

Unprotected and protected samples with ALD coatings were also fabricated and measured within about 20 minutes and thereafter for several days to assess the nature of degradation and the effectiveness of a thin protective layer. Figure 9 shows the drop in reflectance over time at wavelengths from 190 to 240 nm as measured by a UV/Vis spectrophotometer. Careful study indicates that the drop is significant in the

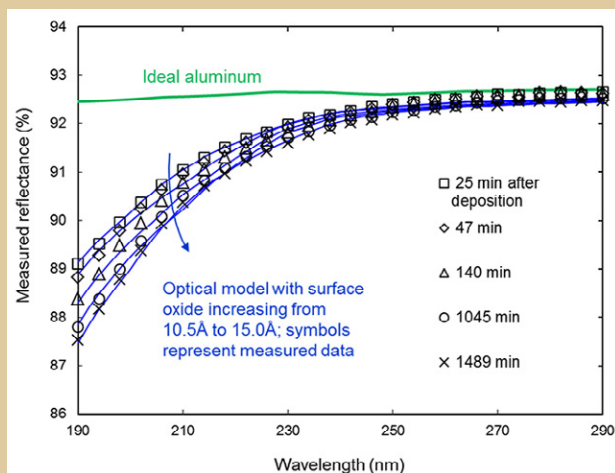


Fig. 7. Oxidation-induced near-UV reflectance reduction of Al mirror samples; model fits match a progressive increase of oxide formation.

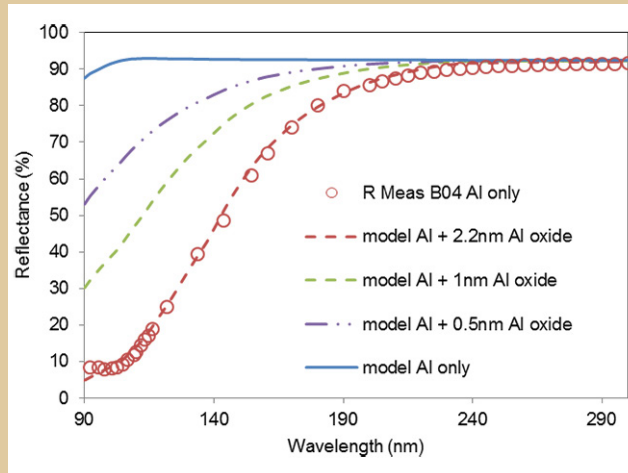


Fig. 8. Unprotected Al reflectance (ideal) and modelled with a thin oxide layer matched measured characteristics in the FUV spectral range.

first two hours and especially within the first few minutes. Encouragingly, as Fig. 10 shows, a very thin protective layer of AlF_3 preserves the reflectance adequately in laboratory conditions. This ensures a pathway to enhance and preserve the FUV reflectance of Al below 120 nm with an appropriate thin protective layer. Rate of deposition of the Al layer is a critical parameter that affects the reflectance as well as its stability over time. Samples were fabricated at different rates at high vacuum. While further experiments are in progress, initial measurements indicate that a rate of about $20\text{\AA}/\text{s}$ is favorable for obtaining better reflectance in the FUV due to denser microstructure and lower oxidation in the bulk of the layer compared to lower rate samples.

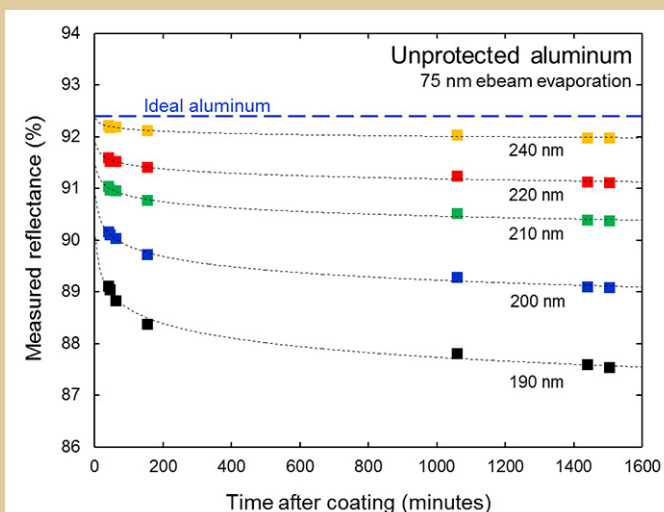


Fig. 9. Unprotected aluminum degradation over time (sample L1). Shorter wavelengths (below 190 nm) would suffer greater degradation, not captured in the above measurements.

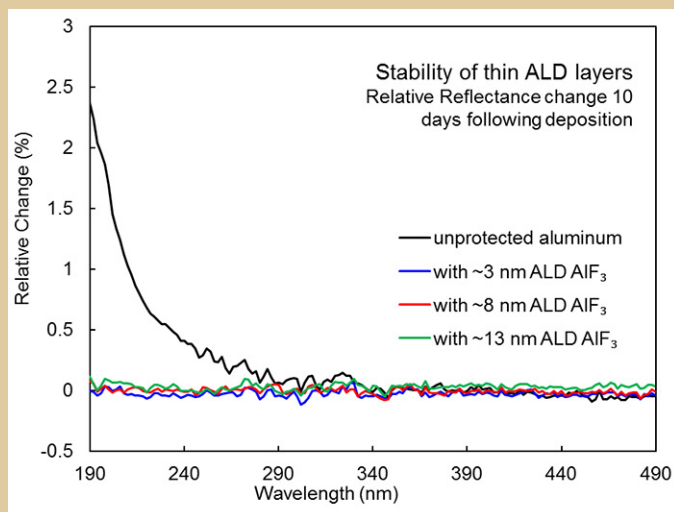


Fig. 10. Stability of Al mirror (sample K series) coated with thin AlF_3 layer using ALD; Even 3 nm of AlF_3 provides adequate protection against reflectance drop.

Protected Al mirrors

A series of AlF_3 -coated Al mirror samples were prepared with different thicknesses of the protective fluoride coated using the ALD process. The UV reflectance of four of these samples was measured over several days. Figure 11 shows the stability or change in reflectance from immediately after fabrication to more than six days after fabrication. Figure 12 shows the FUV reflectance of the samples measured after several days. Model fits indicate a smaller level of oxide formation in the Al layer when thicker protective coating is applied. This is primarily due to the delay in transferring the Al coated sample from the UHV chamber to the ALD reactor for applying the protective fluoride layer. More samples made recently with reduced delay and different process conditions are being measured and characterized now.

Path Forward

In the remaining part of the third year, we will focus on optimizing deposition parameters of the ALD process and prepare samples of protected aluminum mirrors for reflectivity measurements. With conventional deposition techniques, we plan to prepare MgF_2 -, AlF_3 -, and LiF -protected Al mirror samples with optimum deposition rate in better than 10^{-7} Torr vacuum in a large chamber. Samples will be subjected to environmental tests with particular attention to FUV performance. Finally, we plan to coat a set of samples in the large chamber representing a meter-class mirror for uniformity and performance tests, thus advancing the technology development efforts towards the program objectives.

Acknowledgements

The research reported here is performed at the Jet Propulsion Laboratory, California Institute of Technology under a grant from the NASA Cosmic Origins Program.

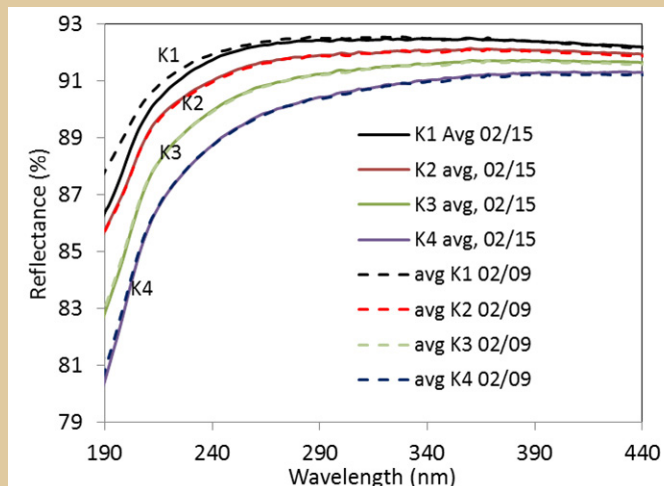


Fig. 11. Aging performance of AlF_3 -protected Al samples compared with unprotected sample K1. K2 with ~ 3 nm AlF_3 and K3 with ~ 8 nm AlF_3 show no degradation over six days after fabrication. The initial drop from 92% to 86% at 190 nm as seen above is due to the oxidation of the bulk of the Al layer as a surface layer of Al_2O_3 formed during and immediately after deposition. Preventing this initial drop is the key challenge.

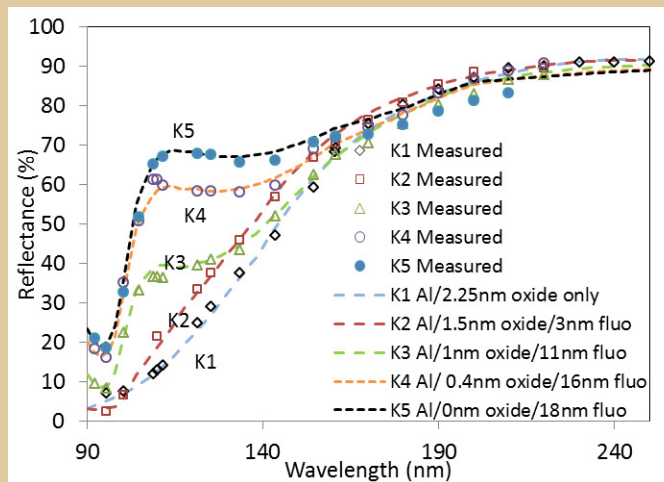


Fig. 12. Model fits (dotted lines) and measured (symbols) FUV reflectance of unprotected (sample K1) and AlF_3 -protected samples (K2 to K5). Formation of an oxide layer before the application of a protective AlF_3 layer is matched by models showing that the oxide formation is arrested by the fluoride layer, though not yet adequately. This is primarily due to the few-minute delay in transferring the sample from the UHV chamber to the next ALD reactor for fluoride coating.

References

- [1] F. Bridou *et al.*, “Experimental determination of optical constants of MgF_2 and AlF_3 thin films in the vacuum ultraviolet wavelength region (60–124 nm), and its application to optical designs,” *Opt. Communications*, **283**, 1351-1358 (2010)
- [2] Keski-Kuha *et al.*, “Optical coatings and applications for ultraviolet space applications,” (NASA GSFC) ASP Conference Series, vol. **164**, J.A. Morse, et al.; eds. (1999)
- [3] M. Yang, A. Gatto, and N. Kaiser, “Aluminum-enhanced optical coatings for the VUV spectral range,” *Proc. SPIE*, vol. **5963** (2005)
- [4] K. Balasubramanian *et al.*, “Protective coatings for FUV to NIR advanced telescope mirrors,” AAS 223 Poster paper on the progress presented at the AAS meeting in Baltimore, MD (Jan 2014)
- [5] J. Hennessy *et al.*, “Thin ALD fluoride films to protect and enhance Al mirrors in Far UV,” 15th International Conference on Atomic Layer Deposition, Portland, OR (June 28th – July 1st 2015)
- [6] S. Redfield, “The Local Interstellar Medium,” in ASP Conference Series 352, *New Horizons in Astronomy*, **79**, arXiv:astro-ph/0601117v1 (2006)
- [7] K. France *et al.*, “From Protoplanetary Disks to Extrasolar Planets: Understanding the Life Cycle of Circumstellar Gas with Ultraviolet Spectroscopy,” arXiv:1208.2270 [astro-ph.SR] (2012)
- [8] Shull *et al.*, “The baryon census in a multiphase intergalactic medium: 30% of the baryons may still be missing,” *The Astrophysical Journal*, **759**:23 (2012)
- [9] *Cosmic Origins Program Annual Technology Report and Space Telescope Science Institute Cosmic Origins Program Analysis Group (COPAG) Workshop* (2011)
- [10] Stahle *et al.*, “The Advanced Technology Large-Aperture Space Telescope (ATLAST),” 224th AAS Meeting, Boston (June 4, 2014)
- [11] P. Scowen, in <http://cor.gsfc.nasa.gov/RFI2012/rfi2012-responses.php>
- [12] J. Dalcanton, L. Hillenbrand, K. Sembach, J. Gardner, C. Lillie, P. Goldsmith, D. Leisawitz, and C. Martin (Chair), “COPAG Technology Assessment,” v.1.3 (Nov 10, 2011)
- [13] M. Quijada *et al.*, “Enhanced MgF_2 and LiF Over-coated Al Mirrors for FUV Space Astronomy,” *Proc. SPIE* **8450** (2012)
- [14] M. Quijada *et al.*, “Enhanced Fluoride Over-coated Al Mirrors for FUV Space Astronomy,” Poster paper presented at the AAS meeting in Baltimore, MD (Jan 2014)
- [15] T. Pilvi *et al.*, “Study of a novel ALD process for depositing MgF_2 thin films,” *J. Mater. Chem.*, **17**, 5077 (2007)
- [16] M. Mantymaki *et al.*, “Atomic Layer Deposition of LiF Thin Films from $\text{Li}(\text{thd})$, $\text{Mg}(\text{thd})_2$, and TiF_4 Precursors,” *Chem. Mater.* **25**, 1656 (2013)
- [17] C. Moore *et al.*, “Recent developments and results of new ultraviolet reflective mirror coatings,” presented at SPIE Astronomical Telescopes + Instrumentation, Montreal (2014)

For additional information, contact: K. Balasubramanian, email: kbala@jpl.nasa.gov



High-Efficiency Detectors in Photon-Counting and Large Focal-Plane Arrays for Astrophysics Missions

Prepared by: Shouleh Nikzad (PI; JPL), Chris Martin (Caltech), David Schiminovich (Columbia University), Paul Scowen (ASU), and Michael Hoenk (JPL)

Summary

Future ultraviolet (UV)/optical large-aperture telescopes will require high-quantum-efficiency (QE), low-noise, large-format, space-qualified UV detectors. Future medium-class concepts (Probes) could be furnished with Flagship-class science capabilities if the large shortfalls in detector performance were made up. Recognizing this fact, the NASA Advisory Committee Astrophysics Subcommittee charged the Cosmic Origins Program Analysis Group (COPAG) with assessing technology priorities. The COPAG in its 2012 Technology Assessment judged that UV photon-counting detectors with large formats and low noise were “Mission Enabling” and therefore the highest priority. The Cosmic Origins (COR) Program Annual Technology Report (PATR) reported a similar finding. Because future frontier UV capabilities will exploit high-resolution, wide-field, highly multiplexed imaging spectroscopy, and wide-field high-angular-resolution imaging, the key detector performance requirements are high efficiency, low noise, and large scalable formats. A detector capable of providing a factor of 3-10 improvement in UV efficiency over those in the Hubble Space Telescope (HST) must do so without introducing a commensurate increase in noise.

Our team demonstrated a high-QE, solid-state, UV photon-counting array in small format by applying JPL's back-illumination processes including thinning, delta-doping technology [1-6], and advanced anti-reflection (AR) coatings using atomic layer deposition (ALD) [5, 7] to commercially available Electron-Multiplying Charge-Coupled Devices (EMCCDs) [8, 9]. Using molecular beam epitaxy (MBE) and ALD to achieve atomic-scale control over the device surface and film interfaces, JPL's technology is unique in producing silicon detectors with exceptional stability and world-record QE (50-80%) throughout the UV (Fig. 1) [5, 10]. The performance of this Solid-state Photon-counting Ultraviolet Detector (SPUD) represents a breakthrough in single-photon-counting UV detectors.

In this three-year program, which began mid-January 2013, we will further develop these high efficiency solid-state photon-counting UV detectors and advance the technology through the following steps.

1. Increasing detector format size in response to the requirements of future missions for large pixel count.
2. Characterizing detector noise performance in realistic spectroscopic and imaging applications.
3. On-sky validation over a wide range of flux levels using astrophysical imaging and spectroscopic instruments.
4. Flight-testing the detector on the synergistic balloon experiment Faint Intergalactic medium Redshifted Emission Balloon (FIREBall), flight accommodation and operations already funded by the Astrophysics Research and Analysis (APRA) program during a 2016 launch.

In this effort, we will also be demonstrating the manufacturability, versatility, and reliability of back-illuminated, delta-doped, high-efficiency silicon imagers in photon-counting and other platforms such as devices designed for broadband detection. This latter objective takes advantage of the development over the past three years of high-throughput processes for delta doping using JPL's new 8-inch-wafer-capacity silicon MBE and the associated techniques to produce high-efficiency detectors (Fig. 1).

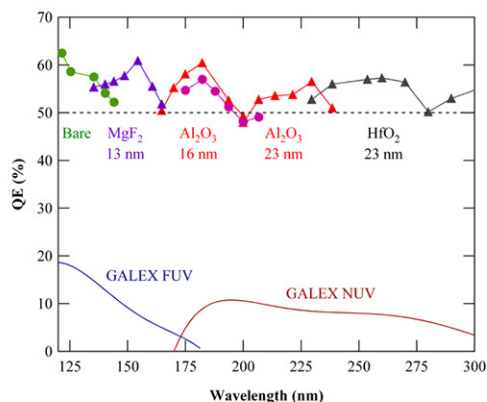
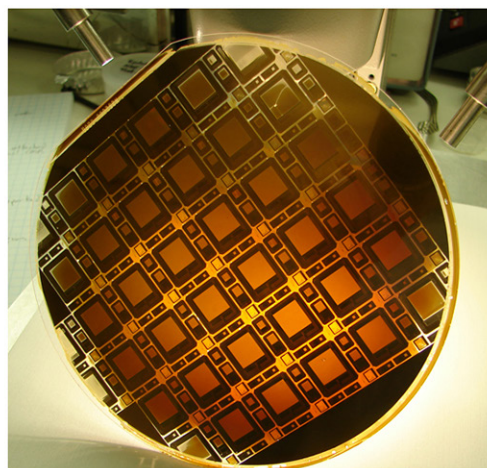
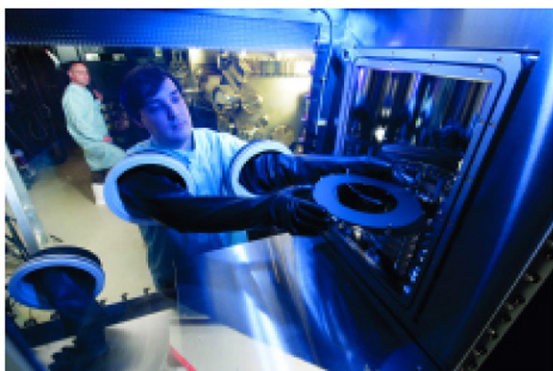


Fig. 1. Top left: JPL facilities with large-wafer capacity for high-throughput delta doping of state-of-the-art CCDs and CMOS imagers. Silicon imagers can be processed in these facilities for back illumination as 150 mm and 200 mm wafers. Right: An 8" wafer with CMOS imagers ready for delta doping. The wafer is thinned using JPL's end-to-end post-fabrication processing facilities. Bottom left: World-record QE achieved by applying this end-to-end processing. The QE of ALD-AR coatings on delta-doped CCDs for 120-300 nm is above 50% for the entire range. All data are obtained for n-channel low-noise $1k \times 1k$ CCDs. Magenta circles are data obtained from delta-doped and AR-coated 0.5-megapixel EMCCDs. QE of Micro-Channel Plate (MCP)-based Galaxy Evolution Explorer (GALEX) detectors are shown for comparison.

This technology maturation plan will create a routine and reliable source for production of high-efficiency and innovative UV/Optical detector arrays for the community. The versatile and robust fabrication techniques presented can have a major impact on future instrument capabilities and scientific discoveries. This development is a team effort with JPL (Drs. Shouleh Nikzad and Michael Hoenk and team), Caltech (Prof. Chris Martin and group), Columbia University (Prof. David Schiminovich and group), and Arizona State University (ASU; Paul Scowen and group). The team's complementary expertise in materials, detectors, instrument building, and observational science allows us the unique capability to carry on the objectives of this effort. By applying the techniques to single-photon-counting platforms and other designs, we demonstrate the versatility of our processes.

In this reporting period, we have produced more 2-megapixel arrays with process fidelity and high performance. In parallel, we calibrated our characterization setup for QE measurements so that our reporting of the QE is cross-calibrated and close to absolute. We evaluated and characterized the QE, dark noise, and uniformity of multiple devices from different batches of processing. The Caltech group made excellent progress in characterizing the engineering-grade single-photon-counting devices and evaluating them for the FIREBall flight requirements. They have shown low dark current in these

measurements and have begun noise characterization of both bare delta-doped 2-megapixel arrays and arrays with narrowband FIREBall coatings. The ASU group completed the modification of their readout system and carried out a successful run using the Mount Bigelow 61" telescope with delta-doped, high-purity p-channel CCDs which are broadband and appropriate for ground-based observation and evaluation of detectors, as well as broadband near-ultraviolet (NUV) to near-infrared (NIR) space-based instruments. A proposal for time at Kitt Peak was submitted to take the broadband delta-doped detector for further on-sky observation. More wafers were processed through our end-to-end post-fabrication processing and delta doping to further establish yield and throughput of our processes.

Background

The 2010 Decadal Survey, *New Worlds, New Horizons in Astronomy and Astrophysics* (NWNH) [11] recommends as a priority path-finding work towards a 4m+ UV/Optical Flagship mission as a successor to the HST. Great emphasis on Explorer missions is also anticipated in this decade.

The COPAG evaluates and recommends technology investments toward a large-aperture UV/Optical telescope, and the Exoplanet Program Analysis Group (ExoPAG) has also embraced this recommendation. In both of these scientific focus areas, high-efficiency, high angular and spectral resolution, and single-photon counting are a priority. Furthermore, these recommendations set as a goal very-large-format (> 100 megapixels), high-QE, UV-sensitive detectors. Frontier astrophysical investigations are necessarily conducted at the limits of resolution, etendue, and sensitivity. The NWNH recommendations reflect the new scientific opportunities enabled by technological breakthroughs in large-scale detector fabrication.

A future 4m+ UV/Optical telescope mission will require significant detector advances beyond HST, GALEX, and Far-Ultraviolet Spectroscopic Explorer (FUSE) detector technologies, particularly in QE, spectral responsivity in the UV, resolution, and pixel count. Our primary performance metric, detector UV QE, represents a dramatic increase (5- to 10-fold) over previous missions (Fig. 1). Dramatically increasing detector efficiency could allow Explorer-class or Probe-class missions to perform what is currently considered Flagship-mission science.

A solid-state detector with high efficiency and photon counting offers scalability and reliability that are necessary and attractive features for reliable, high-performance, and cost-effective instruments. Because of its greatly improved QE, low background, photon-counting ability, and large formats, SPUD will enable high-efficiency, high-resolution UV absorption-line spectroscopy, faint-sky intergalactic medium (IGM) emission spectroscopy, multi-object and imaging UV spectroscopy, and efficient wide-field UV/Optical imaging, at the Explorer, Probe, and Flagship scale. SPUD optimized for visible light would enable integral field spectroscopy required for exoplanet characterization, which must be photon-counting because of the low background in space for diffraction-limited optical spectroscopy.

The QE and response stability of our SPUD can be applied to practically any silicon imager architecture that might be called for in the next generation of instruments and applications. Our effort is a direct response to the needs of future NASA missions including the NWNH recommendations for a 4m+ UV/Optical telescope and UV detector and coatings technologies. This effort directly responds to the Strategic Astrophysics Technology (SAT) call for high-QE, large-format, photon-counting, and ultralow-noise detectors. The ALD films developed under this effort also advance UV coatings for optics. Because of the dramatic efficiency increase in the detector, HST-class science will be possible with smaller apertures. This effort is likely to have a great impact on future Probe- and Explorer-class missions.

Objectives and Milestones

Table 1 shows the project's milestones and schedule.

Milestone	2013				2014	2015
	Q1	Q2	Q3	Q4		
Demonstrate large-format SPUD and other delta-doped silicon imagers						
Procure wafers of standard larger-format EMCCDs	Δ					
Thin, bond, delta-dope, and AR-coat (iterative)					Δ	
Incorporate sample AR coatings					Δ	
Characterize device functionality and QE (iterative)		Δ			Δ	Δ
Validate by system-level evaluation on-sky and suborbital						
Disseminate devices to partners for evaluation and feedback (iterative)					Δ	
Deploy for on-sky observation, evaluation (two campaigns completed, one remains)						Δ
Deploy for suborbital (funded balloon FIREBall)						Δ
Demonstrate process manufacturability and versatility						
Establish throughput and yield by testing devices produced in multiple wafers (ongoing)						
Demonstrate process on high-purity large-format CCD (n-channel completed, p-channel ongoing)						
Environmental testing						
Noise, QE, with temperature, illumination. Lifetime testing (ongoing)						Δ

Table 1. Project milestones and schedule (in calendar years).

The major objectives are as follows:

- Demonstrate detector in large format, *i.e.*, starting from 0.5-megapixel format to 2-megapixel format (Fig. 2) – Fiscal Year (FY) 2013 Q3-Q4;
- Measure detector QE, noise, and performance for spectroscopic and imaging applications – first results in FY 2014 Q2;
- Advance the manufacturability and reliability of SPUD and, as a byproduct, those of other high-efficiency silicon imagers. Revise the number of wafers to be procured and the associated processing workforce. A reduced number (~5) of wafers of SPUD and other silicon imagers (*e.g.*, full-depletion, delta-doped, and AR-coated wafers) will be processed – iterative, first results in FY 2014 Q4;
- Perform environmental (thermal) tests of the detector – ongoing, first results in FY 2014 Q3;
- Validate on-sky over a wide range of flux levels using astrophysical imaging and spectroscopic instruments – FY 2015/16; and
- Flight-test detector on the synergistic balloon experiment FIREBall – FY 2016.

Progress and Accomplishments

We have made excellent progress on all objectives. The major accomplishments are listed below.

Demonstrate Large-Format Detector

Under this effort, we demonstrated large-format arrays with high UV efficiency. Specifically, 2-megapixel photon-counting devices have been produced as bare delta-doped and AR-coated delta-doped EMCCD arrays. The first wafer and devices were previously reported and are shown in Fig. 2.

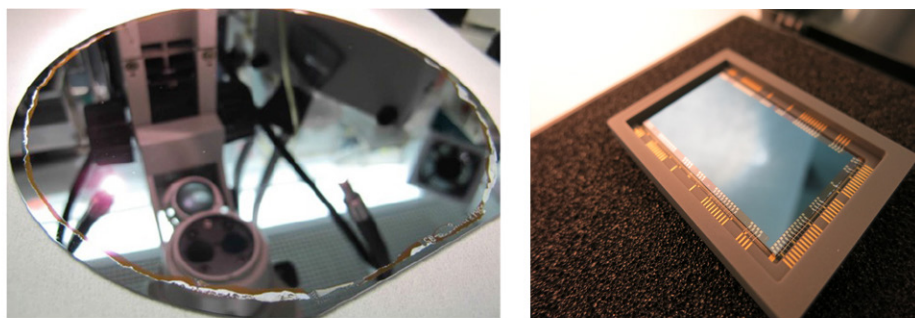


Fig. 2. The first 2-megapixel arrays have been processed. QE measured on this device is not absolute but suggested lower than expected values. As a mitigating step, all process steps including MBE (for delta doping) were reevaluated, and possible contamination sources were removed. Several devices with excellent response have been produced including those shown in Fig. 9.

We applied our end-to-end post-fabrication processes (Fig. 3), including delta doping and advanced AR coatings to silicon arrays of multiple designs (12-megapixel p-channel arrays; 4-megapixel, high-purity, broadband n-channel arrays; standard n-channel arrays; and CMOS arrays) to establish throughput and yield. However, the major focus of this work has been to demonstrate and advance high-efficiency, large-format, photon-counting detectors optimized for UV. Note that the same processes can be tuned for visible-photon-counting detectors. For completeness, we include the end-to-end process flow. We previously reported that we procured wafers from the vendor in the first years. Device wafers were fabricated; and we received, inspected, and prepared these for post-fabrication processing. Processing includes bonding device wafers to “handle” or support wafers prior to thinning. This bonding step allows the wafers to be thinned down to about 8-10 microns. After thinning, wafers are carefully and atomically cleaned in preparation for epitaxial MBE growth. After MBE growth for delta doping, the wafer is patterned, and pads are exposed for wire-bonding. At this point, devices can be coated to optimize for a given spectral range. Devices are packaged as bare delta-doped or are AR-coated prior to packaging.

Multiple devices were processed in the current period as bare baseline (control), for development of AR coatings, and for electro-optical testing. Figure 4 shows a batch of five 2-megapixel devices midway through the process. All devices were functional and all exhibited excellent QE.

AR Coatings Development

Our team has the distinction to be the first to use ALD for detector antireflection coatings [5]. ALD is an atomic-layer by atomic-layer, highly controllable process that can be used to form ultra-thin layers with sharp interfaces that are stoichiometric, uniform, and pinhole-free. These attributes are particularly important in the UV spectral range because the interaction and absorption of photons in this wavelength range takes place in the first few nanometer of the material surface. As such, controlling surfaces and interfaces is particularly important in UV and optical detectors. Combining these ALD coatings with passivation and band-structure engineering of delta doping has created high-efficiency, tailorable response in a variety of detectors. ALD processes were developed for various oxides (Al_2O_3 , SiO_2) as well as fluorides (e.g., MgF_2) on JPL's two ALD systems (Fig. 5). We began our work of developing AR coatings on small (0.5-megapixel) arrays and continued the development on 2-megapixel arrays once they became available.

We design the AR coatings (single and multilayer) using TFCalc™. We then deposit the layers on blank silicon wafers. Extensive reflectivity measurements, in concert with materials analysis on these coated blank wafers (not device wafers), provide us with full calibration of the process. We then transfer the process onto fully fabricated, delta-doped arrays. We chose to focus our AR coating development on

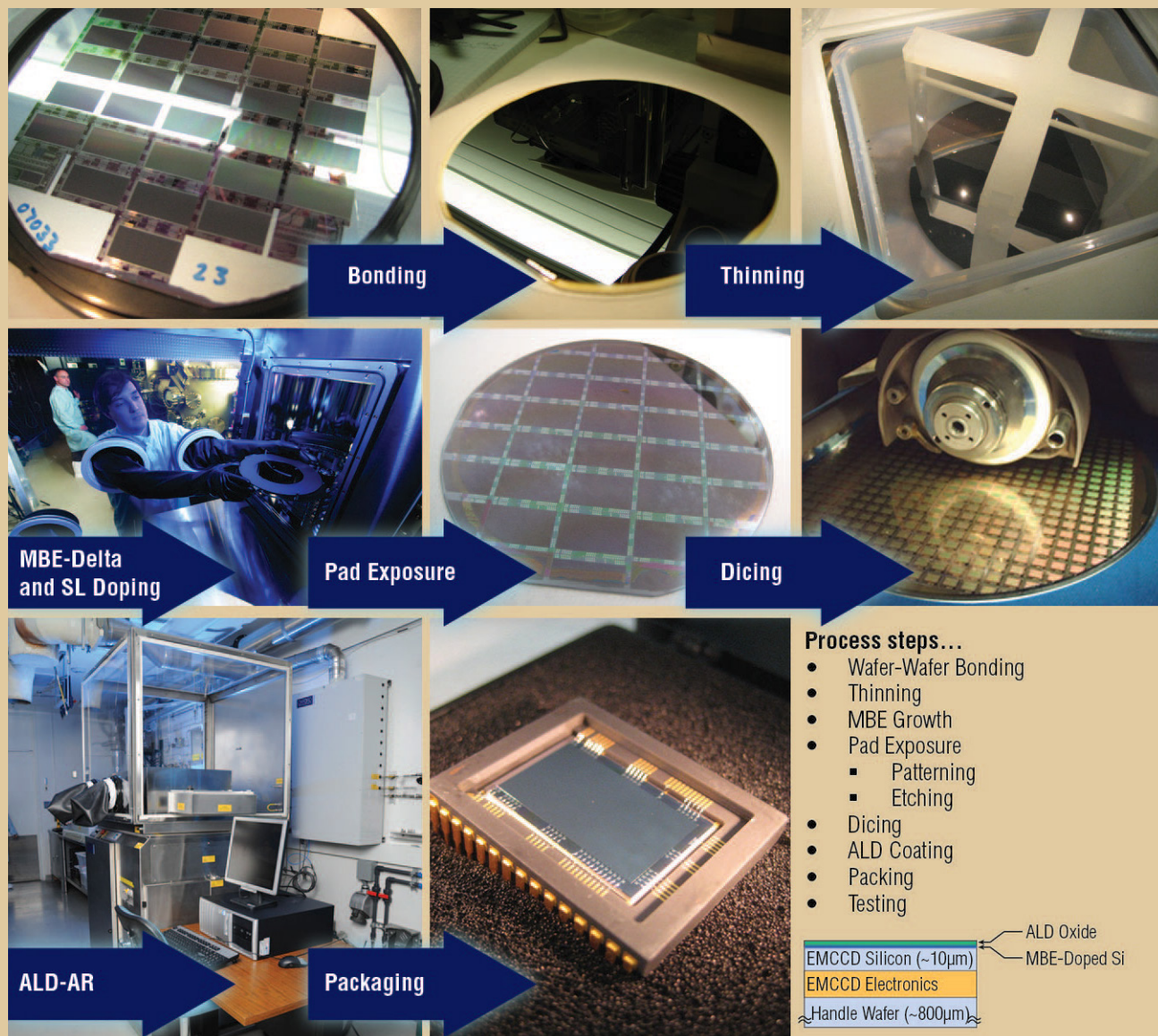


Fig. 3. End-to-end post-fabrication processing for an EMCCD device wafer.

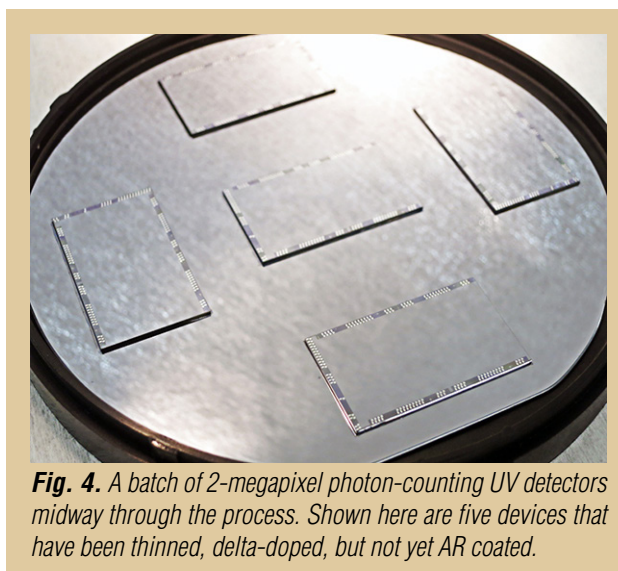


Fig. 4. A batch of 2-megapixel photon-counting UV detectors midway through the process. Shown here are five devices that have been thinned, delta-doped, but not yet AR coated.

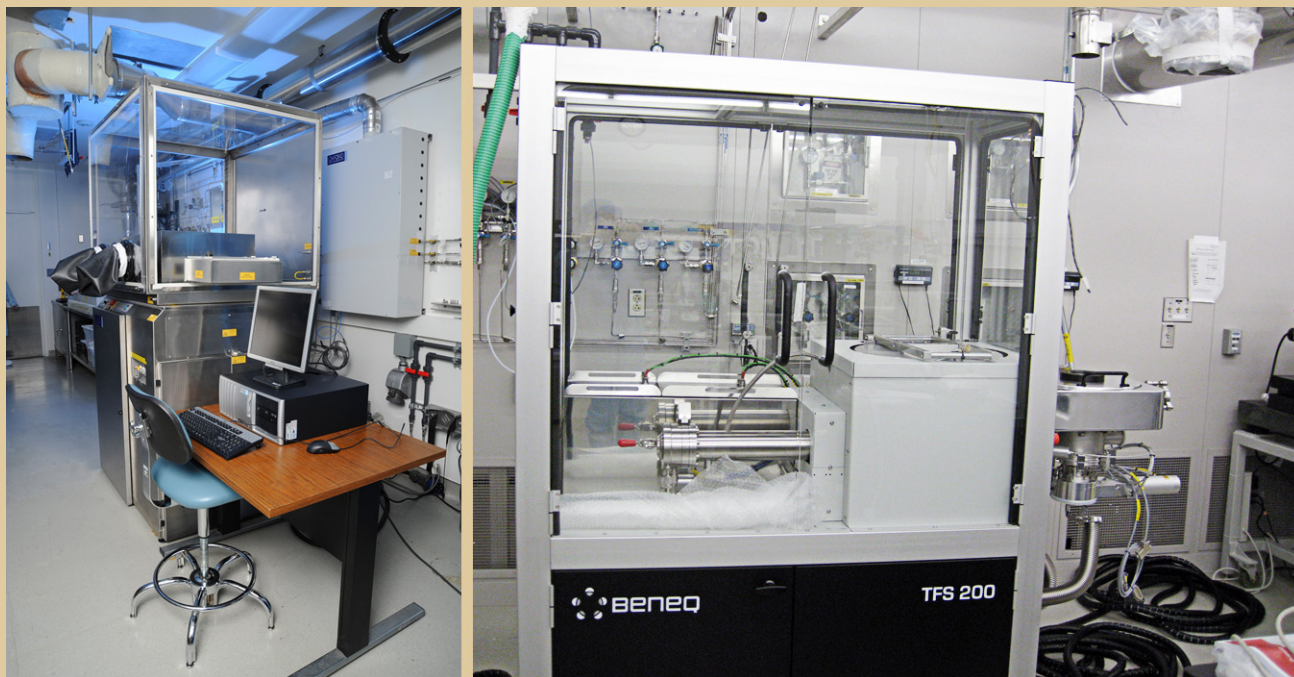


Fig. 5. JPL ALD systems. Both systems can accept samples/wafers up to eight inches in diameter. Most work is done at die level in order to maximize the number of runs on a single die (there are 17 dice of this format on a six-inch wafer).

the FIREBall balloon experiment. With a narrow window in the atmosphere, detector response had to be optimized for 205 nm. A multilayer design provides a narrower peak with high efficiency (Figs. 6 and 7). The more elaborate design that uses more stacks of ALD layers will provide higher efficiency but also a narrower peak. We fabricated multiple 2-megapixel arrays and developed AR-coated (single-layer), delta-doped EMCCDs for basic testing and AR-coating development. The narrower the peak, the more important its positioning becomes. Extensive materials and design work was performed to ensure precise peak positioning.

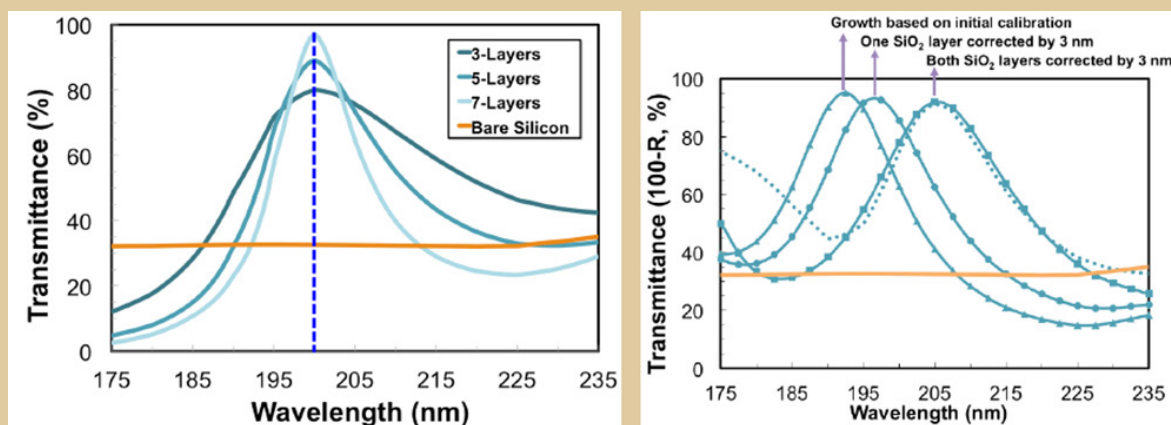


Fig. 6. Left: Predicted transmittance of multilayer double stacks of oxides for the FIREBall experiment range around 200 nm. The narrow peak's position is particularly important. Right: The model shows the underlying reason for the shift in the peak is the variation in SiO_2 thickness. A number of tests were performed which show the nucleation rate of SiO_2 growth on silicon (original rate calibration) was different than on Al_2O_3 (first layer after silicon in the final design). Modeling, followed by experiments that showed the nucleation rate variation, led to correcting the growth parameters and solving the moving peak problem.

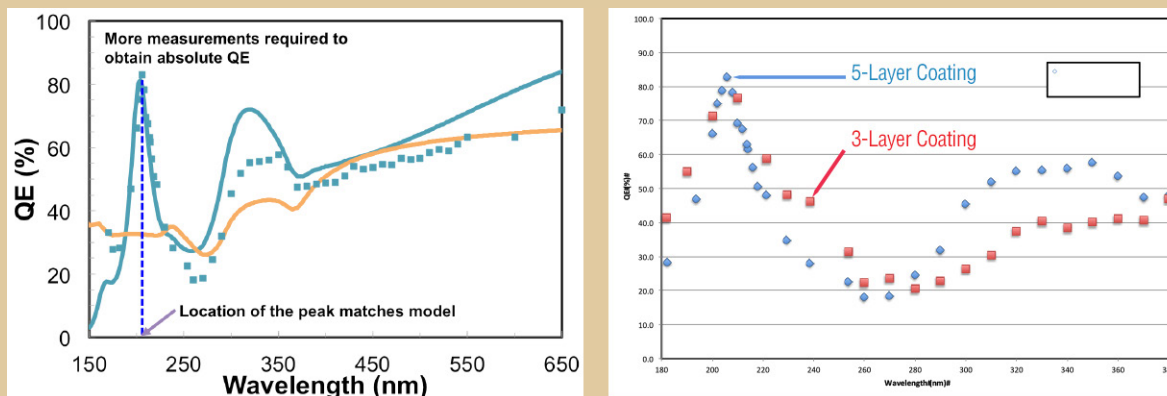


Fig. 7. Left: Design of multilayer double stacks of oxides for FIREBall with QE peaking around 200 nm. This device was produced and characterized to show the precise positioning of the peak. Subsequent measurements showed absolute QE. Right: Results of three- and five-layer coatings demonstrate the peak width and QE of two designs. Both devices are in line for delivery to FIREBall.

Characterizing Device QE, Dark Noise, Noise, and Uniformity

QE, uniformity, and some dark-current measurements are performed at JPL, using two characterization systems. One is equipped with a 1-m monochromator that can be evacuated for Far-UV measurements down to Lyman alpha. The second is equipped with a 0.5-m monochromator, and is suitable for measurements in the 300-1000 nm range. Several wafers with multiple devices were delta-doped and many QE measurements were performed. We use the QE measurement as the first and main feedback to ensure device processing worked as intended. This serves as a methodical and effective process. The same setup is also used to characterize uniformity and perform some dark current measurements. The low-noise setup at Caltech, however, is specifically designed for low-noise, photon-counting measurement.

Excellent results were also obtained at Caltech on dark current and other noise sources. The Caltech group procured a low-noise readout-electronics system (NuVu) controller, and after careful evaluation and characterization of the setup, they prepared for measuring the dark current and read-noise using a high-gain operation mode. The measurements were first performed on an engineering-grade device (Fig. 8). The Caltech readout and dewar system (Fig. 9) are also planned to be used for FIREBall.

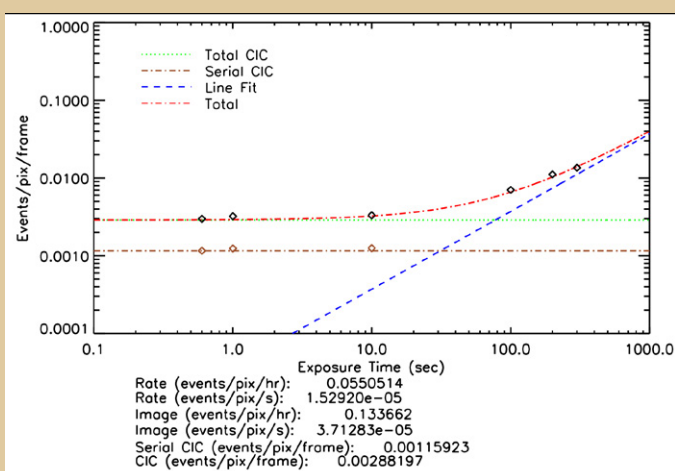


Fig 8. Dark-noise measurements on an engineering-grade device operated with photon-counting gain register showing excellent results (CIC is clock-induced charge).

On-Sky Observations

The ASU team is mainly responsible for obtaining on-sky data from large-format, delta-doped arrays. Time was secured on the Mount Bigelow 61" telescope for these on-sky runs (Fig. 10). For these tests, devices were produced that could cover both short-wavelength atmospheric cutoff as well as silicon-bandgap cutoff. We processed and delta-doped p-channel devices (designed at Lawrence Berkeley National Lab, LBNL, and fabricated at DALSA) for the purpose of broadband ground-based observations. Several multilayer films for broadband coatings were designed. One wafer containing four devices was processed to produce the device for on-sky observations. The wafer was diced and AR coatings were tested on

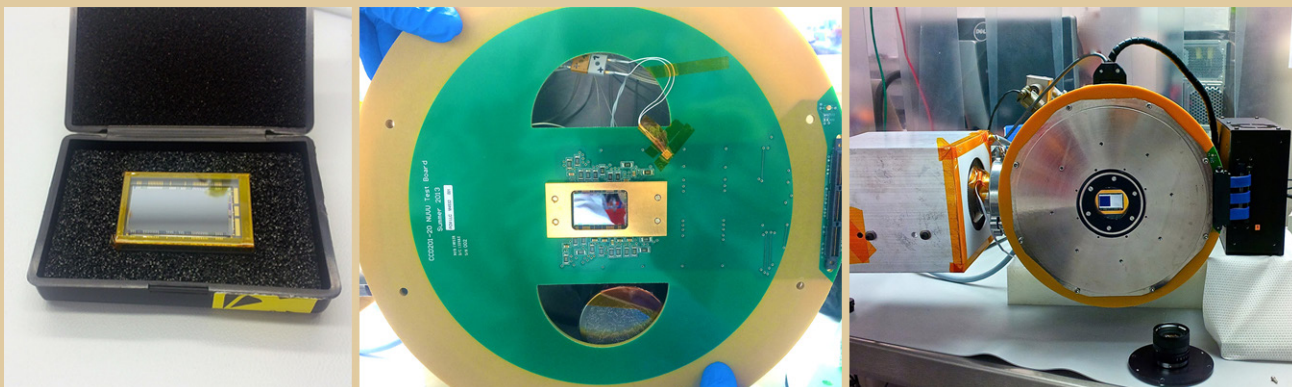


Fig. 9. Left: A delta-doped, photon-counting, 2-megapixel) UV array. Center: The same UV array in a dewar in the Caltech lab. Right: The UV array in the characterization setup for low-noise measurements. This assembly, including the drive/readout electronics, will fly on FIREBall.

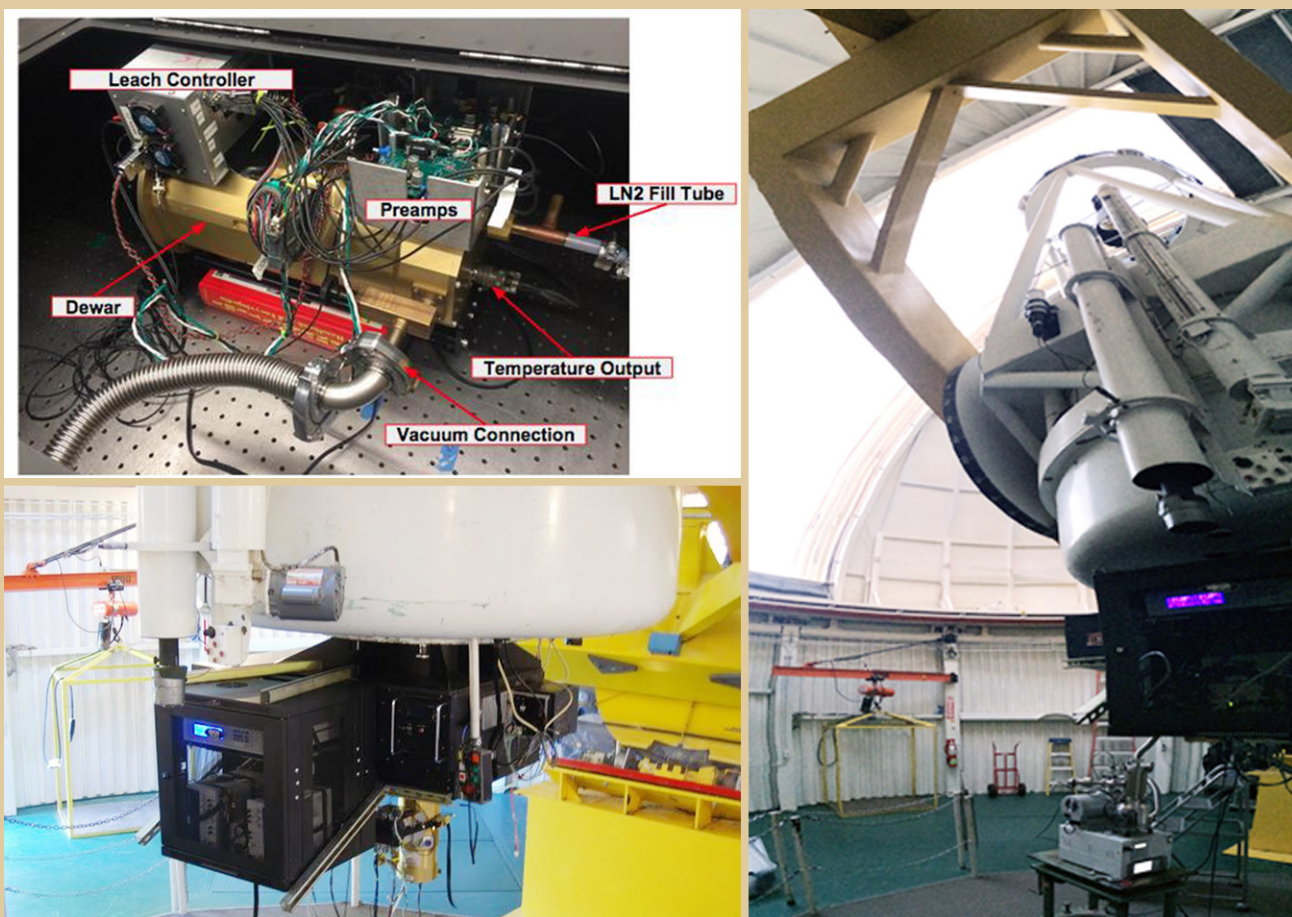


Fig. 10. ASU dewar and setup in the lab (top left), and at Mount Bigelow 61" telescope (bottom left and right).

multiple devices produced from the wafer. One coating was deemed superior. Two 12-megapixel, 10-micron arrays were delta-doped on the same wafer. One bare and one AR (broadband) coated device were delivered to ASU (Fig. 11). The ASU team made two expeditions to the Mount Bigelow 61" telescope. The first run was an engineering exercise, which uncovered mechanical issues and issues related to cooling and readout. The second run, at the end of May 2015, produced highly useful results showing the broadband range of the devices. This second observing run was much more successful because of readout and setup modifications made based on feedback from the first run. Sky images

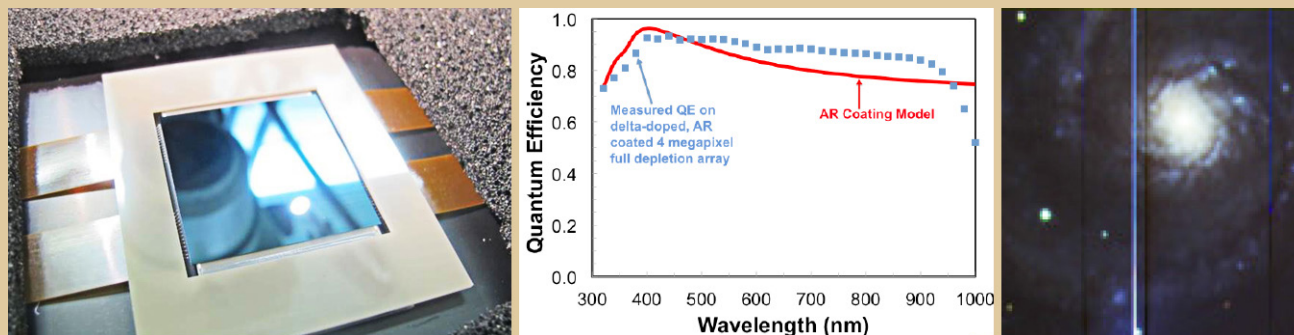


Fig. 11. Left: P-channel LBNL-design, delta-doped, and AR-coated device delivered to ASU by JPL. Center: Measured QE of the device. Right: Sample image taken with this engineering-grade device. Although the second observing run was successful as a whole, the drive electronics behaved differently than it did on the lab bench. More work will be done in the lab to ensure full use of the detector in the next run (Nov 2015).

were obtained, demonstrating detector performance, as well as a series of calibration measurements similar to ones made in the ASU lab using known light sources and a calibrated photodiode.

Other Accomplishments

Leveraging internal funds, delta-doped EMCCDs were tested for total ionization dose up to 60 krad. The devices were tested in a UV spectrometer before and after irradiation, showing excellent performance. Several publications and invited presentations resulted from this work, including:

- J. Hennessy, A. D. Jewell, H. F. Greer, M. C. Lee, and S. Nikzad, “Atomic layer deposition of magnesium fluoride via bis(ethylcyclopentadienyl) magnesium and anhydrous hydrogen fluoride,” *Journal of Vacuum Science and Technology (JVSTA) A* **33** 01A125 (2015). This paper was featured as an “Editor’s Picks” choice on the JVSTA website
- J. Hennessy, A.D. Jewell, M.E. Hoenk, and S. Nikzad, “Metal–dielectric filters for solar–blind silicon ultraviolet detectors,” *Applied Optics* **54** pp. 3507-3512 (2015)
- S. Nikzad *et al.*, “High-Performance Silicon Imaging Arrays for Cosmology, Planetary Sciences, and other Applications,” invited talk and paper in International Electron Devices Meeting (IEDM), San Francisco, CA (December 2014)
- S. Nikzad *et al.*, “High Performance Solid State Detectors for Low Energy Neutral and Charged Particle Detection and EUV Observation,” invited talk at Measurement Techniques in Solar and Space Physics (MTSSP), Boulder, CO (22 April, 2015)
- S. Nikzad, “Seeing the Unseen: The Ultraviolet Universe from Nebulae to Neurons,” special seminar, Rochester Institute of Technology, Center for Imaging Science (14 May 2015)

Our effort has benefited from the work of several graduate students from Caltech, Columbia University, and ASU, whose work on the project forms a major part of their theses. Graduate student and NASA Earth and Space Science Fellow (NESSF) Erika Hamden from Columbia University had some short stays and visits at JPL. She defended her thesis in summer 2014 and joined the Caltech team as a National Science Foundation (NSF) fellow. Rhonda Hilton of ASU joined JPL this summer with support of JPL’s Strategic University Research Partnership (SURP) to gain experience with the detectors and instrumentation. Graduate student Alex Miller is the main ASU graduate student supported by this task and has focused on the on-sky observation. He used knowledge acquired during stays at JPL to modify the ASU test setup to accept detectors under development in this task. Caltech graduate student Nicole Lingner works on the low-noise readout of photon-counting detectors.

Young scientists are a major part of our effort: NASA Postdoctoral Program (NPP) fellow April Jewell and Caltech postdoctoral scholar John Hennessy have been instrumental in developing processes and coatings at JPL, and Gillian Kyne (at Caltech) is making excellent progress on dark-current measurements.

Path Forward

We will process more wafers in order to produce several 2-megapixel arrays. We will evaluate and characterize the QE, dark noise, and uniformity of all these devices and will correlate any process implementation and noise variations in the devices. The Caltech group will complete characterization of the engineering-grade, single-photon-counting devices and evaluate them for the FIREBall flight, and then move on to characterizing both the bare delta-doped, 2-megapixel single-photon-counting arrays and the 2-megapixel, single-photon-counting arrays with narrowband FIREBall coatings. The ASU group will perform more bench-testing to ensure the transition of gain measured in the lab to the observatory. They will conduct another observation run in November at the Mount Bigelow 61" telescope. This run will take the broadband (UV/Optical/NIR) AR-coated, delta-doped detector for on-sky observation to further evaluate it for realistic astrophysics signal levels. In processing more wafers and producing more devices, we will incorporate feedback from these in-depth characterizations to improve processes if needed. As we process multiple wafers, we will demonstrate detector throughput and yield. By applying the techniques to single-photon-counting platforms and other designs, we demonstrate the versatility of our processes.

References

- [1] M.E. Hoenk, P.J. Grunthaner, F.J. Grunthaner, M. Fattahi, H-F. Tseng, and R.W. Terhune, "Growth of a Delta-Doped Silicon Layer by Molecular-Beam Epitaxy on a Charge-Coupled Device for Reflection-Limited Ultraviolet Quantum Efficiency," *Appl. Phys. Lett.*, **61**, 1084 (1992)
- [2] S. Nikzad, M.E. Hoenk, P.J. Grunthaner, R.W. Terhune, F.J. Grunthaner, R. Winzenread, M. Fattahi, and H-F. Tseng, "Delta-doped CCDs: High QE with Long-term Stability at UV and Visible Wavelengths," *Proc. of SPIE*, **2198**, 907 (1994)
- [3] J. Blacksberg, S. Nikzad, M.E. Hoenk, S.E. Holland, and W. Kolbe, "Near-100% Quantum Efficiency of Delta Doped Large-Format UV-NIR Silicon Imagers," *IEEE Trans. on Electron Devices*, **55**, 3402 (2008)
- [4] M.E. Hoenk, T.J. Jones, M.R. Dickie, F. Greer, T.J. Cunningham, E.R. Blazejewski, and S. Nikzad, "Delta-doped back-illuminated CMOS imaging arrays: Progress and prospects," *Proc. of SPIE*, **74190**, 74190-74115 (2009)
- [5] S. Nikzad, M.E. Hoenk, F. Greer, E. Hamden, J. Blacksberg, B. Jacquot, S. Monacos, C. Martin, D. Schiminovich, and P. Morrissey, "Silicon Detector Arrays with Absolute Quantum Efficiency over 50% in the Far Ultraviolet for Single Photon Counting Applications," *Applied Optics*, **51**, 365 (2012)
- [6] S. Nikzad, M.E. Hoenk, P.J. Grunthaner, R.W. Terhune, R. Winzenread, M. Fattahi, H-F. Tseng, and F.J. Grunthaner, "Delta-doped CCDs as Stable, High Sensitivity, High Resolution UV Imaging Arrays," *Proc. of SPIE*, **2217**, 355 (1994)
- [7] E. Hamden, F. Greer, M.E. Hoenk, J. Blacksberg, T.J. Jones, M. Dickie, B. Jacquot, S. Monacos, C. Martin, P. Morrissey, D. Schiminovich, and S. Nikzad, "Antireflection Coatings Designs for use in UV Imagers," *Applied Optics*, **50**, 4180-4188 (2011)
- [8] P. Jarram, P. Pool, R. Bell, D. Burt, S. Bowring, and S. Spencer, "LLLCCD – Low Light Level Imaging without the need for an intensifier," *Proc. SPIE*, **4306**, 178 (2001)
- [9] J. Hyneczek, "Impactron – A New Solid State Image Intensifier," *IEEE Transaction on Electron Devices*, **48** No. 10, 2238-2241 (2001)
- [10] E. Hamden, D. Schiminovich, S. Nikzad, and C. Martin, "UV photon-counting CCD detectors that enable the next generation of UV spectroscopy missions: AR coatings that can achieve 80-90% QE," *Proc. of SPIE*, **8453**, High Energy, Optical, and Infrared Detectors for Astronomy V, 845309 (2012)
- [11] Blandford *et al.*, "New Worlds, New Horizons in Astronomy and Astrophysics," National Academy of Sciences (2010)

For additional information, contact Shouleh Nikzad: Shouleh.Nikzad@jpl.nasa.gov



Development of DMD Arrays for Use in Future Space Missions

Prepared by: Zoran Ninkov (PI; Rochester Institute of Technology, RIT); Sally Heap and Manuel Quijada (NASA/GSFC); Massimo Robberto (STScI); and Alan Raisanen, Dmitry Vorobiev, and Anton Travinsky (RIT)

Summary

This two-year NASA Strategic Astrophysics Technology (SAT) project began in May 2014. The project seeks to investigate the feasibility of using a digital micro-mirror device (DMD) as the slit mask for a multi-object slit spectrograph (MOS) system for a variety of future NASA space missions. In particular, we are investigating a number of key operating parameters for Texas Instruments (TI) commercial-off-the-shelf DMDs including: replacing the borosilicate window with windows transmissive at ultraviolet (UV) and infrared (IR) wavelengths, tolerance to particle-radiation effects, and non-specular scattering properties of the DMDs. The team includes Sally Heap at NASA Goddard Space Flight Center (GSFC), who provides us with insight into the connection between astronomical measurement requirements and our laboratory testing; Massimo Robberto at the Space Telescope Science Institute (STScI), who provides test design guidance and has previous experience with proposed DMD use by the European Space Agency (ESA); Manuel Quijada at GSFC, who provides considerable optics experience and the use of the Carey 5000 Spectrometer at GSFC; and Alan Raisanen at RIT, who provides the necessary microsystems experience to allow for replacement of DMD windows in the RIT cleanroom. Additionally, we have begun collaborating with Jonny Pellish (GSFC Code 561) to proceed with heavy-ion testing of DMDs at Texas A&M and Tim Schwartz (GSFC Code 549) for vibration and shock testing. The project has made significant progress this year including the first window replacement on a TI-delivered DMD array, first measurement of light scattering from the TI DMD, analysis of proton-testing results from the Lawrence Berkeley National Laboratory 88" Cyclotron, development of a plan for heavy-ion testing, and placing an order for a large-format Cinema-class DMD and electronics.

Background

Our ultimate objective is to address two key questions of NASA's Cosmic Origins (COR) Program:

1. How did galaxies evolve from the very first systems to the elliptical and spiral types we observe today?
2. How did super-massive black holes affect the lives of galaxies in which they reside and vice versa?

Ground-based telescopes and the Hubble Space Telescope (HST) have shown us that the Hubble sequence of elliptical and spiral galaxies was in place by redshift $z = 1$. However, what physical processes drove $z > 1$ galaxies to join the Hubble sequence? To understand galaxy evolution, we need to carry out a large spectroscopic survey of the sky with a particular focus on galaxies at redshifts of $z = 1\sim 2$. Experience with the Sloan Digital Sky Survey [1] indicates that a few $\times 10^5$ galaxies need be observed in order to distinguish among the many possible drivers of galaxy evolution (*e.g.*, accretion, mergers, star formation, stellar evolution and feedback, growth of black holes, *etc.*).

A large spectroscopic survey requires an MOS able to record the spectra of hundreds of galaxies in a single exposure. The MOS must have adjustable slits to eliminate confusion with nearby sources and to block out unwanted zodiacal background, which would otherwise swamp the light from these faint galaxies. The MOS should have access to the far ultraviolet (1200-2000 Å) radiation emitted by a $z\sim 1$ galaxy because this spectral region has a rich set of diagnostics of stars, gas, and dust in the galaxy. Access to the blue-red spectral regions (2000-8000 Å) is also essential for determining the precise redshift of a galaxy, its stellar mass, and its elemental abundances; and for characterizing dust extinction. Because the light from a $z\sim 1$ galaxy is redshifted before reaching us, a large spectroscopic survey should be sensitive over the spectral interval 2000-16000 Å.

The Problem: No existing MOS has such a wide spectral range, let alone access to the UV. TI's DMD would make an excellent slit selector for a spectrograph, if it were sensitive in the UV. However, commercial DMD windows block UV light.

Scientific Impact: A UV-transmitting DMD window enables a breakthrough in observational power sufficient to address two key COR science issues. No other telescope, ground- or space-based, present or planned, can accomplish this investigation, because it can't observe all the spectral diagnostics from Ly α (~ 1200 Å) to H α + [N II] (~ 6600 Å) in the same high-redshift galaxy.

Our project intends to investigate the applicability of DMDs to this and other space-based applications by testing the radiation hardness and light-scattering properties of these devices. In addition, our project will look at approaches to replacing the commercially provided windows on DMDs.

The Solution: We therefore propose to optimize the performance of DMDs for the UV region. This requires replacing the DMD window with a UV-transmitting window (> 2000 Å) having an anti-reflection coating on each side, optimized for the UV, optical, and IR. Because the target galaxies are at a redshift of $z \sim 1$, the observed spectrum of a galaxy over 0.2 - 1.6 μm records the light emitted by the galaxy in the spectral range 0.1 - 0.8 μm . This wavelength region contains virtually all the important spectral diagnostics of stars, gas, and dust in the galaxy.

Objectives and Milestones

Table 1 provides the major milestones of this project. Our project started more slowly than expected, principally because it took longer than expected to identify vendors for the needed components (*e.g.*, windows, DMDs) and services (L-1 Standards & Technology). There was also a long delay in getting purchase orders through the GSFC system. Finally, although we received a quote from a US-based distributor to acquire TI Cinema DMDs when we submitted the proposal, it turned out they could not resell those in the USA. The only way to get these DMDs was through TI's European distributor, at a higher-than-budgeted cost. STScI provided the additional funds, but there was a delay in placing the sub-contract and thus the order.

Progress and Accomplishments

For DMD arrays to be suitable for future NASA missions, a number of performance issues must be addressed. This project attempts to investigate these questions, and to improve DMDs to make them more suitable for such instrumentation requirements. The two commercially available DMDs we will be evaluating are the 0.7 XGA 1024×768 13.6-micron pixel pitch and the Cinema 2048×1080 13.6-micron DMD.

Radiation Testing: Proton testing of XGA DMDs was conducted at the Lawrence Berkeley National Laboratory 88" Cyclotron using three different beam energies, specifically 21.0, 34.5, and 40.9 MeV [2]. The DMDs were irradiated in ~ 2 krad increments and tested optically to find any single-event upsets (SEUs) and any optical defects induced in the mirrors. The DMDs remained 100% functional up to a dose of ~ 30 krad. With 100 mils of shielding, this implies the DMDs can withstand a five-year dose at L2 with a $4.5\times$ margin of safety. SEUs were detected in the mirrors at a rate implying that for a 6-krad dose over a six-year mission, a mirror would be upset once every four days on average.

Low Temperature Testing: A modified Infrared Laboratories liquid nitrogen dewar was assembled to house the DMD electronics board for low-temperature testing [3]. The DMD requires many electrical interconnects (~ 200), and routing this many high-speed electrical interconnects through the dewar for the low-temperature experiment was not practical. By mounting the control board in the dewar, only electrical feedthroughs for power, heater, and temperature monitoring needed to be wired through the dewar. A hermetic USB feedthrough was used to control the DMD with an external control computer.

Milestone	Vendor/Work Location	Dates	Comments
Receipt of MgF ₂ windows	Photonics Solutions Group Blue Ridge Optics	Received Apr 2015 Jul 2015	First batch of MgF ₂ windows were warped; a second batch had to be made, resulting in substantial delay
Receipt of Heat Exchanger Method (HEM) Sapphire windows	GT Crystal Systems Blue Ridge Optics	Expected Jul 2015	GT Crystal Systems went into bankruptcy protection in Nov 2014, then emerged; first batch of HEM Sapphire did not meet specifications; second batch looks good
Receipt of Cinema DMDs + drive electronics	VISITECH, Germany	Expected Sep 2015	The final quote for these items was higher than budgeted; supplemental funding from STScI allowed order to proceed
Replacement of TI DMD windows with custom windows by RIT	Semiconductor & Microsystem Fabrication Laboratory, RIT	Apr 2015 (first device with quartz window); further devices expected Aug 2015 and Nov 2015	DMDs with sapphire and MgF ₂ window will be fabricated when windows delivered; also devices with Kapton or Mica window for heavy-ion testing
Replacement of TI DMD windows by commercial vendor	L-1 Standards & Technology	Expected Oct 2015	Awaiting delivery of MgF ₂ and Sapphire windows
Measurement of light scattering from eXtended Graphics Array (XGA) DMD	Carey 5000 at NASA GSFC Code 551	First measurements in Apr and May 2015; final measurements expected Mar 2016	We are developing the testing protocol with devices we have now and will make final tests when final re-windowed DMDs are available
Proton testing of DMD and data analysis	LBNL 88" Cyclotron	Completed 2014	Results published
Heavy-ion testing of DMD and data analysis	Texas A&M Radiation Effects Facility	Scheduled for Aug 11, 2015 Data Analysis expected to complete Apr 2016	We are preparing the test fixtures and software needed to conduct this testing
Testing of Cinema DMDs for scattering properties	Carey 5000 at NASA GSFC Code 551	Awaiting delivery of Cinema DMDs; expected to complete Apr 2016	The fixturing for these tests will need to be modified compared to current tests on the XGA DMD
Vibration and shock testing	NASA GSFC Code 549	To be determined; expected to complete Mar 2016	We have met with GSFC Code 549 and will develop a test plan
Low-temperature testing and analysis	RIT Infrared Laboratory Dewar	Completed 2014	Results published

Table 1. Milestones of this SAT project.

The DMD was cooled from room temperature to ~130 K, with a new set-point established by the Lakeshore controller every 10 K. At each temperature, a series of test patterns were latched in the DMD to test its operation. It was found that DMDs can be latched for at least 30 minutes at low temperature without any hinge memory problems. Repeatedly re-landing the DMDs during cool-down was not required to avoid stiction effects during low-temperature operation.

Scattering Measurements: An experimental spot-scanning apparatus was assembled to measure the scattered light for a 0.7 XGA DMD at the focal plane [4-6]. The illumination conditions at several different wavelengths were similar to that expected in a typical space experiment. Automated data collection was implemented for scattered-light measurement as a function of sub-pixel spot position. The initial devices tested were VGA DMD 640 × 480, which showed contrast ratios close to those expected from modeling. These measurements will be repeated with the next-generation devices now available.

Scattering measurements were obtained using the new Carey 5000 Spectrometer available at GSFC Code 551. A fully adjustable fixture was built at RIT that integrates with the Carey 5000 and enables complete angular-scattering measurements. We are analyzing the scattering measurements made

during several visits to GSFC. Figure 1 below shows results obtained for a 0.95 1080P DMD (1920 × 1080 pixels with 10.8-micron pixels) illuminating with wavelengths ranging from 200 to 700 nm. The specular peak is clearly visible.

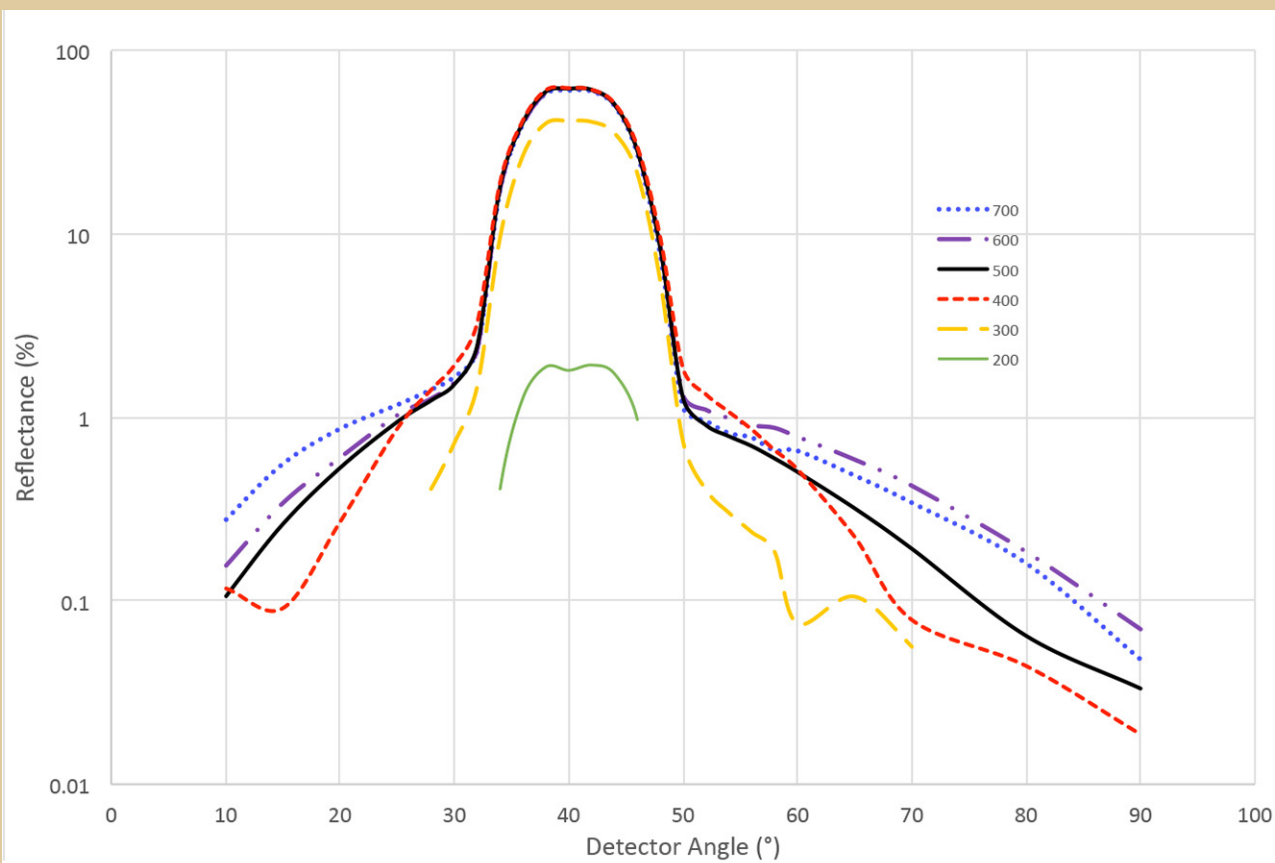


Fig. 1. Reflectance measured as a function of detector angle for a range of illumination wavelengths.

Re-windowing: DMDs involve the use of a Micro-Electro-Mechanical-Systems (MEMS) device that needs to be maintained in a clean environment. TI provides such containment by fusing a borosilicate glass to the Kovar frame, sealing the unit when manufacturing is complete. The borosilicate window limits the usability of this device for our purposes, so this project seeks to replace the window. The principal alternates we plan to use are the following. First, a new, purer form of traditional sapphire called HEM Sapphire. This material, produced by GT Crystal Systems, has excellent transmission properties to wavelengths less than 200 nm, and a co-efficient of thermal expansion matching that of the Kovar metal frame to which it will be attached. The second window to be used is magnesium fluoride, which has higher UV transmission through the wavelength range of interest. Both replacement windows are on order with various vendors, and we await final delivery of the anti-reflection-coated parts. Integration of the windows with the package will be done both by a commercial vendor, L-1 Standards & Technology, and at the RIT [Semiconductor and Microsystems Fabrication Laboratory](#) (SMFL). To this end, we have developed at RIT techniques to remove the existing window (Fig. 2), as well as a fusion method for replacement-window attachment using readily available quartz windows.

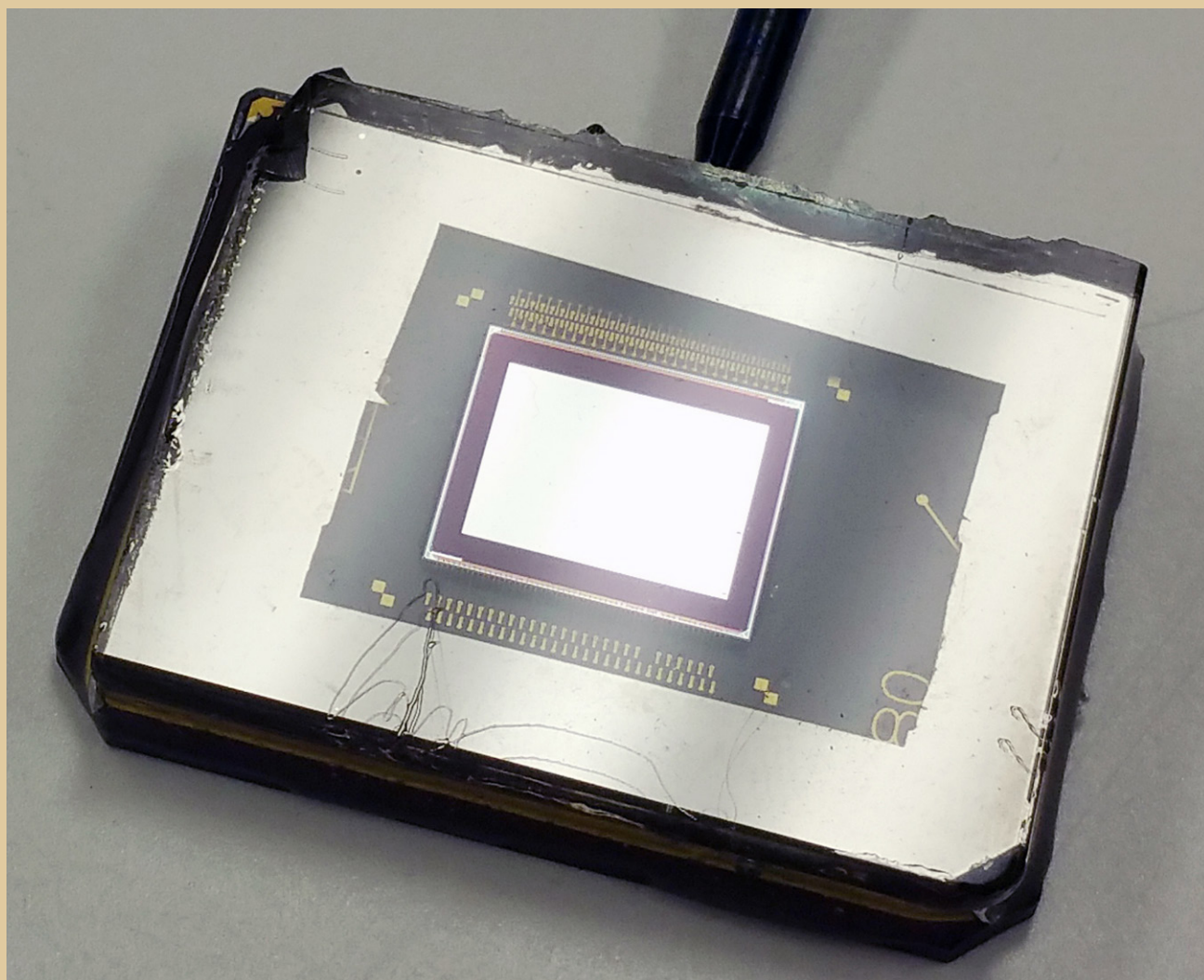


Fig. 2. TI DMD with its borosilicate window removed at RIT.

Path Forward

Much remains to be done in this project, specifically:

1. At the SAT annual presentation made in January 2015, feedback was received that while proton testing was a good start to radiation testing the DMDs, further heavy-ion testing was also needed to evaluate single event effects (SEE). We thus met with Jonny Pellish (GSFC Code 561) and are developing a suitable test plan. We have been granted time at the Texas A&M radiation effects facility starting August 11, 2015 to carry out such tests. It will be challenging to be ready in time, as we need to assemble and test a suitable optical testing setup and software to allow for SEU evaluation after each exposure increment. We also plan to re-window some DMDs with either mica or Kapton windows to permit full heavy-ion-particle energy deposition in the DMD itself, more accurately representing conditions in space. These results will be published.
2. Re-windowing the DMDs needs to be completed, but can only proceed after the much-delayed delivery of the ordered sapphire and magnesium fluoride windows. The actual process of removing and replacing the windows is now sufficiently mature that we can proceed quickly once the windows are available.

3. The fixturing and techniques for obtaining the needed reflectance and scattering measurements have also been developed. Initial scattering measurements on DMDs with borosilicate windows were obtained and analyzed, and will be published. However, further measurements on DMDs with sapphire and magnesium fluoride windows await window delivery. We also plan to measure devices with no window using a temporary, easily removable window. Finally, we will also test the properties of Cinema DMDs after their delivery by VISITECH.
4. We plan to develop, in collaboration with Tim Schwartz (GSFC Code 549), a test plan for DMD vibration and shock testing, for both as-delivered TI devices and re-windowed ones. However, this needs to follow completion of the re-windowing.

References

- [1] Gunn *et al.*, “*The 2.5 m Telescope of the Sloan Digital Sky Survey*,” The Astronomical Journal, Volume **131**, Issue 4, 2332-2359 (2006)
- [2] K. Fourspring, Z. Ninkov, B. Fodness, M. Robberto, S. Heap, and A. Kim, “*Proton radiation testing of digital micromirror devices for space applications*,” Optical Engineering **52** (9):11 091807 doi: 10.1117/1.OE.52.9.091807 (2013)
- [3] K. Fourspring, Z. Ninkov, S. Heap, M. Robberto, and A. Kim, “*Testing of digital micromirror devices for space-based applications*,” Proceedings of the SPIE, Vol **8618**, Emerging Digital Micromirror Device Based Systems and Applications V, id. 86180B (2013)
- [4] K. Fourspring and Z. Ninkov, “*Optical characterization of a micro-grid polarimeter*,” Proceedings of the SPIE Vol **8364**, p 83640M (2012)
- [5] K.D. Fourspring, Z. Ninkov, and J.P. Kerekes, “*Subpixel scatter in digital micromirror devices*,” Proceedings of the SPIE Vol **7596**, Emerging Digital Micromirror Device Based Systems and Applications II (2010)
- [6] K.D. Fourspring, Z. Ninkov, and J.P. Kerekes, “*Scattered light in a DMD based multi-object spectrometer*,” Proceedings of the SPIE Vol **7739**, Modern Technologies in Space- and Ground-Based Telescopes and Instrumentation (2010)

For additional information, contact Zoran Ninkov: ninkov@cis.rit.edu



Enhanced MgF_2 and LiF Over-Coated Al Mirrors for FUV Space Astronomy

Prepared by: Manuel A. Quijada (PI; NASA/GSFC); Javier del Hoyo, Steve Rice, and Felix Threat (NASA/GSFC)

Summary

This project started in Fiscal Year (FY) 2012 with a three-year duration through the end of FY 2014. Since the conclusion of this performance period, we have leveraged resources from other projects that have permitted a continuation of coating activities beyond what was originally proposed. This report will include progress made since the report published in the previous Program Annual Technology Report (PATR), submitted in the summer of 2014.

This project includes three major tasks. The first, to demonstrate the viability of coating medium to moderately large (1-m diameter) mirrors in a large (2-m diameter) chamber to improve the far-ultraviolet (FUV) reflectance of aluminum (Al) mirrors protected with either magnesium fluoride (MgF_2) or lithium fluoride (LiF) over-coats. The gains in FUV reflectance were made possible by employing a three-step Physical Vapor Deposition (PVD) process developed in a smaller coating chamber on substrates of up to 3.5-cm diameter. Application of these high-performing coatings on large primary mirrors of a FUV astronomical telescope will enhance throughput and add flexibility to system design, certain to improve overall performance. The second task was to determine the refractive index (n) and absorption coefficient (k) of gadolinium and lutetium tri-fluoride (GdF_3 and LuF_3 , respectively). These materials are considered high-index options that, when paired with a low-index material such as MgF_2 , could enhance the reflectance of Al mirrors over a narrow bandwidth centered in the range from 110 to 250 nm. A third task was to improve the quality of MgF_2 film depositions by using a two-gas system in a small Ion-Beam Sputtering (IBS) coating system to produce denser films with low scatter.

Among the achievements over the past year, we continued performing end-to-end testing in the 1-m and 2-m coating chambers, and performed numerous runs of the three-step PVD coating process for producing Al test coupons ($2'' \times 2''$), protected with either MgF_2 or LiF films. These efforts produced the highest reflectance ever reported (over 90%) for mirrors in the 116.2 to 150.0 nm spectral range (including Lyman-Alpha at 121.6 nm). These reflectance gains led to our being tasked with coating reflectors of various sizes (26 to 264 mm diameter) for the Ionospheric Connection Explorer (ICON) and Global-scale Observations of the Limb and Disk (GOLD) projects. The goal was to realize reflectance higher than 90% in the wavelength range of interest (133.6 to 154.5 nm) on optics for these Heliophysics Explorer flight missions. We performed dielectric designs by pairing GdF_3 films with the low-index MgF_2 and demonstrated the reflectivity gains obtainable when these dielectric layers are applied on MgF_2 substrates or Al mirrors. We also designed and produced an anti-reflection (AR) coating based on the $\text{GdF}_3/\text{MgF}_2$ pair. This particular AR coating was designed to operate in the visible spectral range (400 to 800 nm) to enhance performance of grism prototypes being considered as part of pre-phase-A studies for the Wide-Field Infrared Survey Telescope (WFIRST) project.

Background

The FUV region (90 to 150 nm) is relevant to many aspects of NASA's Cosmic Origins (COR) Program, particularly the Astrophysics Science Area Objective 2: *"Understand the many phenomena and processes associated with galaxy, stellar, and planetary system formation and evolution from the earliest epochs to today."* Many of the resonance lines for both low-ionization and high-ionization states of common atoms are found largely in this region. Some lines are found at longer wavelengths but often their interpretation requires transitions with different oscillator strengths or different ionization states that are found in the FUV. Furthermore, the electronic ground-state transitions of H_2 are only found below

115 nm. Hydrogen gas is the most abundant molecule in the universe and is the fundamental building block for star and planet formation. The absorption lines of deuterium (D) and the molecule HD are found only in the FUV region as well. Understanding the abundance of D is an important test of Big Bang cosmology and of chemical evolution over cosmic time.

Despite the wealth of information obtainable, astrophysics observations in the FUV have been limited by poor optics coating performance available in this spectral region. It is hard to overstate the importance of producing high-performance reflective coatings, since improved reflectivity in itself would bring enormous throughput gains, amplifying the benefits of more-capable optical systems.

The FUV region from 90 to 115 nm has only been explored by a handful of NASA astronomy missions – Copernicus (also known as Orbiting Astronomical Observatory 3, or OAO-3) in the 1970s, Hopkins Ultraviolet Telescope (HUT), the Orbiting Retrieable Far and Extreme Ultraviolet Spectrometer (ORFEUS) shuttle payloads in the 1990s, and the Far Ultraviolet Spectroscopic Explorer (FUSE) in the 2000s. The FUSE observatory was the most extensive by far, but it was limited by modest effective area (20 cm² below 100 nm to 55 cm² above 102 nm) and a modest spectral resolution ($R \sim 20,000$). The FUSE mission made significant strides in mapping variations in D/H in the galaxy, but due to low reflectance of available coatings, lacked the sensitivity to study D/H in the inter-galactic medium (IGM).

Aluminum is one of the few materials in nature with an intrinsic reflectance that exceeds 90% in the FUV spectral region. However, this metal quickly oxidizes when exposed to oxygen. This oxidation produces a thin aluminum oxide (Al₂O₃) layer that is responsible for the severely degraded reflectance performance (< 10%) that this material exhibits for wavelengths shorter than 150 nm. The most commonly used approach to avoid the formation of this oxide layer on Al, and hence avoid its low FUV performance, is to apply a thin layer of either MgF₂ or LiF. The typical thickness for either of these is approximately a quarter-wave of the design wavelength chosen anywhere between 90 and 150 nm. In addition to protecting against oxidation, these over-coats also produce a dielectric boost in reflectance centered at the chosen design wavelength. Until recently, the reported reflectance values obtained for either Al+MgF₂ or Al+LiF coatings were well short (< 83%) of the theoretical values at Lyman-Alpha (121.6 nm). This poor performance is attributed to the poor quality of the over-coat films achievable with conventional methods. The current project has improved the state of the art by employing a three-step PVD coating process that produces test coupons with a reflectance approaching the theoretical limit (90% to 92%) at 121.6 nm.

Objectives and Milestones

The overall objective of this program was to improve mirror-coating reflectance, particularly in the FUV. This mission-enabling technology specifically addresses the Technology for the Cosmic Origins Program (TCOR) development under the Section 2, titled “*Ultraviolet Coatings*.” Specifically, we addressed:

1. Improved deposition processes for known FUV reflective coatings (e.g., MgF₂ and LiF).
2. Investigation of new coating materials with promising UV performance.
3. Examination of handling processes; contamination control; and safety procedures related to depositing coatings, storing coated optics, and integrating coated optics into flight hardware.

The first objective was to demonstrate or transfer to an existing 2-m PVD chamber at the Goddard Space Flight Center (GSFC) the process for enhancing FUV reflectance of Al mirrors protected with MgF₂ or LiF layers. This process, which consists of reducing absorption in the over-coat layers, was originally implemented in a smaller PVD coating chamber that only allowed coating optics up to a few inches in diameter.

The second objective was to perform a limited material studies, via the PVD process, of the best materials identified in an earlier study [1], which examined a series of lanthanide trifluorides and found potential candidate materials beyond LaF₃. These high-index materials, when paired with a low-index layer (such

as MgF_2) would facilitate the design and fabrication of all-dielectric reflectors and even interference filters for FUV. Our study concentrated on studying the optical properties of GdF_3 and LuF_3 films.

The third and final objective was to develop low-absorption MgF_2 thin-film coatings using a reactive IBS coating process that was expected to produce optical thin film coatings as near as possible to ideal morphology. This reactive process was intended to address the fact the energies involved in the IBS process make it difficult to maintain stoichiometry for certain materials. The stoichiometry deficiency was compensated by flowing a fluorine-containing gas (*e.g.*, Freon) during the deposition process. The objective of this first-phase study was to see if stoichiometric deposits of a candidate material (MgF_2) could be achieved through IBS.

The main milestones reported in the FY 2012 PATR were:

1. Perform additional optimization of MgF_2 and LiF in a small coating chamber (Sep 2012).
2. Perform initial Al+ MgF_2 coatings with a 2-m chamber (Nov 2012).
3. Perform distribution study of Al+ MgF_2 coatings with a 2-m chamber (Dec 2012).
4. Perform initial Al+LiF coatings with a 2-m chamber (Jan 2013).
5. Perform distribution study of Al+LiF coatings with a 2-m chamber (May 2013).
6. Characterize lanthanide trifluoride for FUV application (Nov 2012).
7. Design and fabricate a Lyman-Alpha reflector (Apr 2013).
8. Optimize and characterize MgF_2 films using the IBS process (Nov 2012).
9. Optimize and characterize LiF films using the IBS process (Mar 2013).

Milestone 2 suffered a notable schedule deviation, and was completed in May 2013. This had a ripple effect on completion dates for milestones 3 through 5, caused by a five-month delay in procurement of key hardware (power supply and halogen/quartz heater system) and completion of the thermal shields and installation of the lamp heaters inside the 2-m chamber. It is important to note that these dates were based on the assumption of a two-year program that was due to conclude at the end of FY 2013. Because of this delay, we requested and received a one-year extension. This extension provided ample time for successful completion of the unfinished tasks, which were concluded by the end of FY 2014.

It should be noted that Milestone 8 was reported in the 2013 PATR, where we stated that the MgF_2 films produced with the reactive IBS process were of very poor quality. The problem was traced to the fact that the fluorine contained in the Freon gas was quickly corroding the tungsten filament used in the ion-gun source of our IBS chamber. It was determined that progress could only be achieved with substantial investment in a new coating system, implementing a “filamentless” ion gun. This acquisition exceeded the available budget. Hence, this task and the related Milestone 9 were abandoned.

Progress and Accomplishments

Reflectance of Al+ MgF_2 Mirrors

Figure 1 displays reflectance results for Al+ MgF_2 mirror coatings that are routinely achieved in our 1-m and 2-m coating chambers using the three-step PVD coating process. The procedure starts with applying a 50-nm Al layer with the substrate at ambient temperature. This is followed by an initial 5-nm coating of MgF_2 at ambient temperature on top of the Al to prevent oxidation. The chamber heaters then bring the substrate up to a temperature of 260°C. The remaining MgF_2 deposition (≈ 20 nm for a Lyman-Alpha reflector) is then applied with the substrate at this elevated temperature (earlier studies showed 200°C is the minimum temperature required for good MgF_2 film quality [2]). We have determined the conditions for achieving these results require a very good vacuum (10^{-7} Torr or better) and optimum deposition rates in order to produce MgF_2 layers free of pinholes and with low FUV absorption.

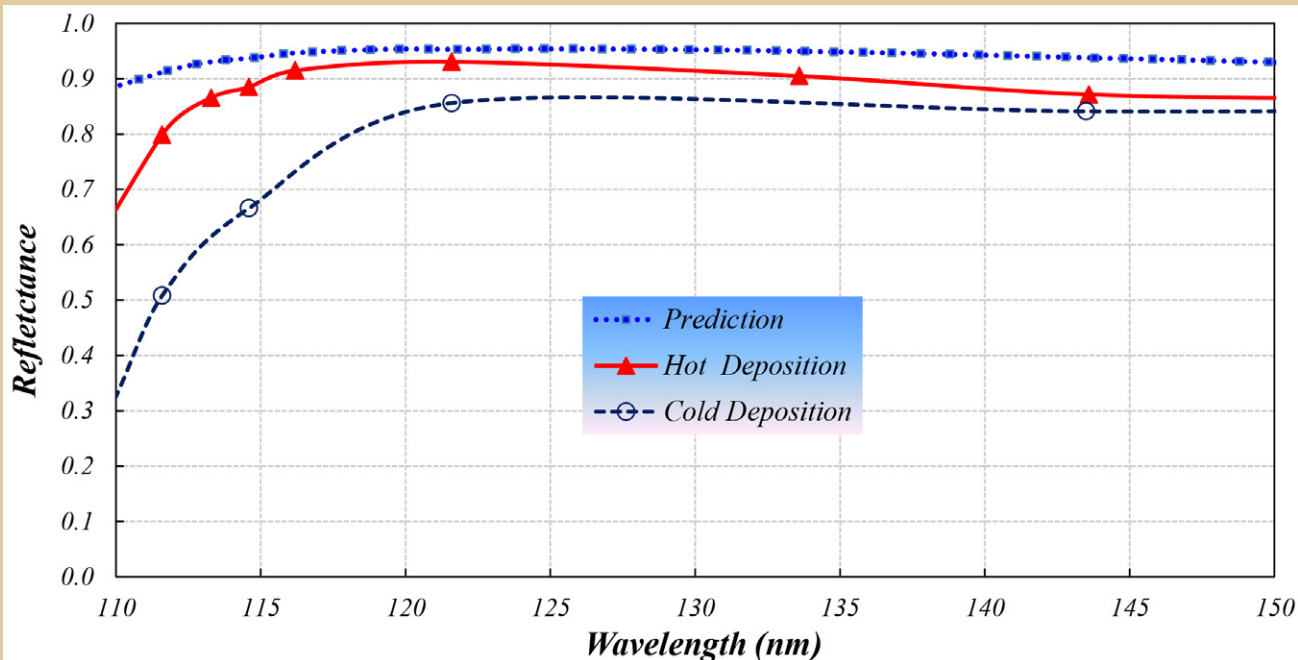


Fig. 1. Predicted and measured FUV reflectance performance of Al+MgF₂ where the MgF₂ was deposited at cold (ambient) and elevated (260°C) temperatures.

The results in Fig. 1 indicate there might be further room for improvement, since we did not reach the theoretical prediction. We also observed slight reflectance suppression in the 135 to 150 nm range. Similar behavior has been reported by others [3] and has been attributed to plasmonic absorption coupled with micro-roughness in the Al layer at those wavelengths.

The results (Fig. 1) indicate that although data obtained on the enhanced process is still below the ideal case, reflectance reached predictions for bare Al at wavelengths close to 121.6 nm (91%). The results also indicate gains in reflectance for the “Hot” deposition are even more dramatic on the short wavelength side, pushing the useful range for this type of mirror coating much closer to the natural cut-off wavelength of bulk MgF₂.

Micro-Roughness of Al+MgF₂ Coatings

We performed a comparative surface study on Al+MgF₂ films prepared under ambient conditions and others where the Al+MgF₂ coatings were produced with the three-step PVD process described above. Measurements were made using an ADE Phase-Shift MicroXAM surface profiler, a phase-sensitive, interferometer-based, non-contact instrument capable of providing highly reproducible surface mapping information at various magnification levels. It consists of an optical microscope with eyepieces and video display of images with a high-resolution camera. Two representative images taken with this instrument are shown in Fig. 2.

The surface roughness parameters derived from images like the ones in Fig. 2 are shown in Table 1. We first noticed the peak-to-valley numbers for the “Ambient” sample are approximately 2-3 times larger than for the one labeled “Hot.” This observation suggests that heating the substrate during the MgF₂ depositions could be providing a more flat surface profile by perhaps relieving the stress of the MgF₂ films. The test mirror that was heated during the MgF₂ deposition had a 30% smaller average root-mean-square (rms) micro-roughness parameter (S_q) that suggests a larger grain size for this sample.

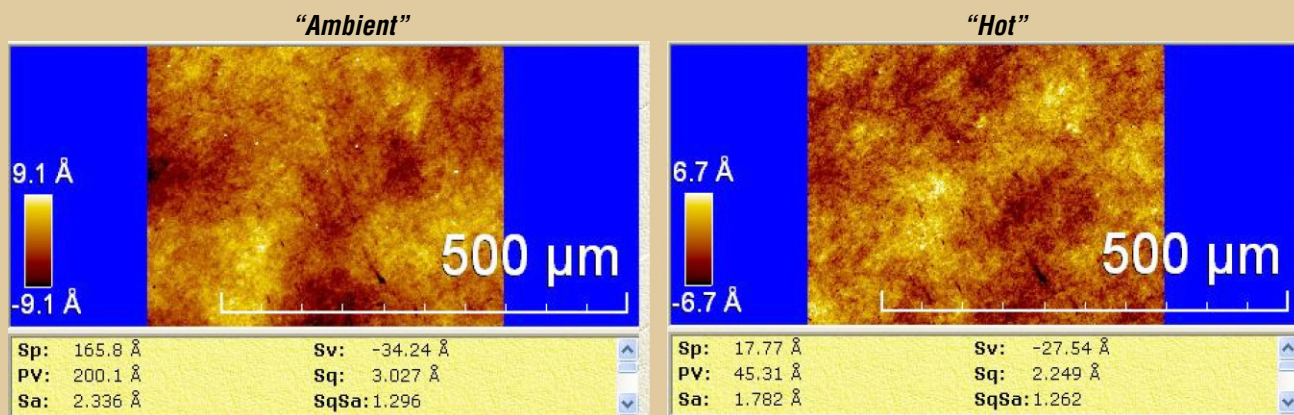


Fig. 2. Maps of a comparative study of micro-roughness of Al+MgF₂ mirror coatings prepared with the “Ambient” and “Hot” processes. The parameters are Sp: height of highest single pixel in the map, PV: difference between the highest peak and lowest valley, Sa: mean absolute deviation of height, Sv: valley height of lowest single pixel in the map, and Sq: Standard deviation of height.

AM2 13 01C	x20 mag/ angstroms	
	PV (Å)	S _q (Å)
Top left	75.58	6.146
Top right	101.2	5.196
Center	128	4.021
Bottom left	200.1	3.027
Bottom right	100	3.282
Average	120.97	4.334

AMCT 13 01A	x20 mag/ angstroms	
	PV (Å)	S _q (Å)
Top left	45.31	2.249
Top right	40.19	2.331
Center	50.96	3.304
Bottom left	44.39	2.923
Bottom right	50.85	3.854
Average	46.34	2.932

Table 1. Micro-roughness (Sq) parameter determined on five locations of Al+MgF₂ slides produced with ambient (left) and hot (right) MgF₂ depositions.

Reflectance of Al+LiF Mirrors

We now turn our attention to Al+LiF coatings following a similar three-step or “hot” process as discussed above. Results are shown in Fig. 3, along with a representative curve from the mirror coating used in the FUSE instrument prior to launch [4]. The coating parameters for the recently prepared Al+LiF sample include an Al layer (43 nm), followed by 8 nm of LiF. The sample was then heated and kept at 250°C during the final LiF layer deposition of 16.4 nm, for a total thickness of 24.4 nm. The data in Fig. 3 show reflectance values greater than 90% in the 110 to 125 nm range. This represents the highest-ever-reported reflectance for Al+LiF coatings in this wavelength range. The FUSE data are still higher below 105 nm when compared to the recently prepared sample. Figure 3 also shows data collected five months later from the same sample. The results suggest a degradation in performance attributed to the hygroscopic nature of LiF, as no special measures were taken to preserve the sample beyond keeping it in a low-relative-humidity (30%) storage box.

We should note the total LiF thickness (24.4 nm) for the recently prepared sample ended up being too large to produce enhancements at wavelengths below 105 nm. The results suggest improvement may be achievable by depositing a thinner LiF layer that would have low FUV absorption, approaching the theoretical limit derived from the optical constants for bulk LiF. This expectation is consistent with the findings of Adriaens and Feuerbacher [5], since the process we are using is analogous to theirs. They found the overcoat layers of both LiF and MgF₂ were significantly improved and reflectivity increased at wavelengths shorter than 130 nm by annealing the deposited films at about 300°C for some 60 hours at a pressure of 10⁻⁷ Torr, using a heater built onto the substrate holder.

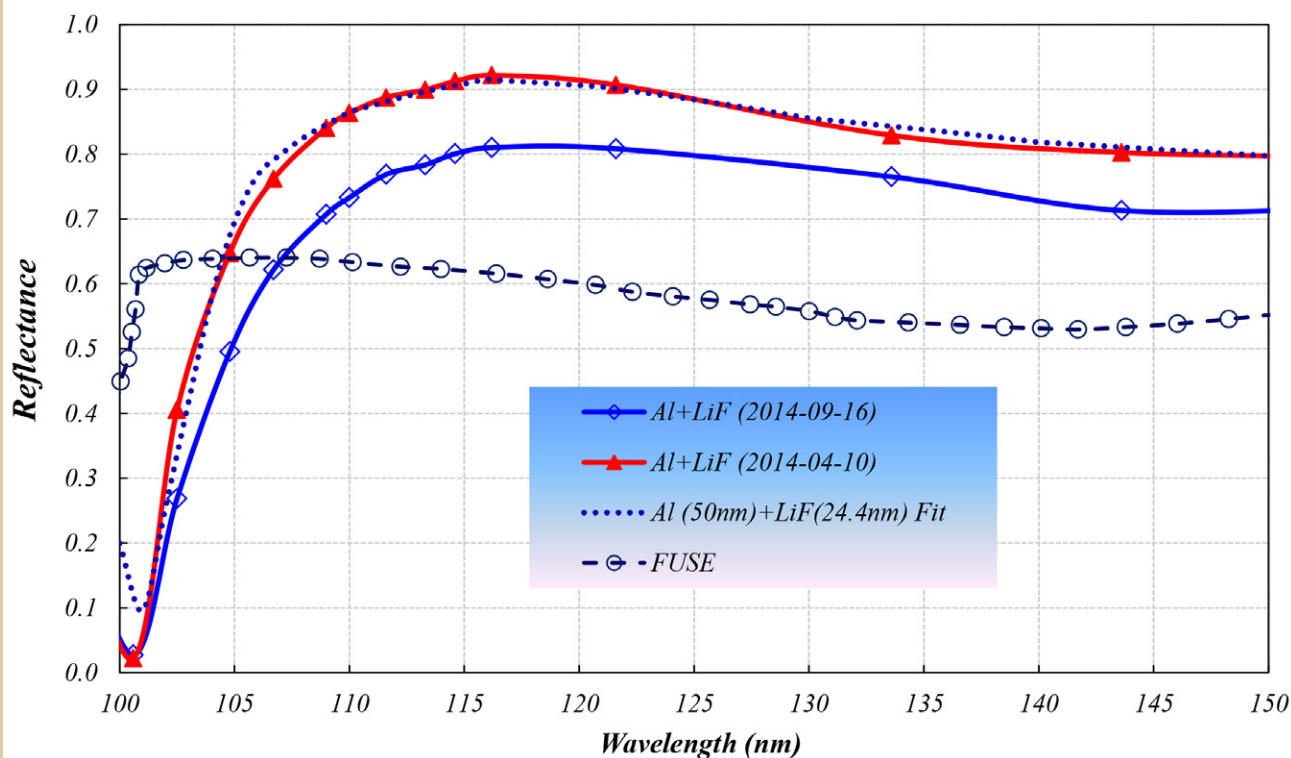


Fig. 3. Reflectance comparison between an Al+LiF coating sample and FUSE primary mirror data. Data for the sample were collected on two occasions, five months apart. The dotted line represents a fit to the 2014-04-10 results.

Refractive Index of GdF_3 and LuF_3 Films

We grew a series of GdF_3 and LuF_3 films on MgF_2 to determine their optical properties (refractive index, n ; and absorption coefficient, k) at FUV wavelengths. The motivation was that an earlier study [1] showed that the n values for both materials are higher than that of MgF_2 in the 250 to 600 nm range, and that their transparency could extend to much lower wavelengths due to their large band-gap energy. These materials may thus be viable alternatives to LaF_3 for use as high-index layers that, when paired with the lower index MgF_2 , will enable production of multilayer coatings that could operate in the FUV range.

The measured transmission ($T(\lambda)$) and reflectance ($R(\lambda)$) for LuF_3 and GdF_3 films grown on MgF_2 substrates provided the basis for determining the optical constants of the LuF_3 and GdF_3 layers. This was done by fitting the data to the Fresnel equations and solving for $n(\lambda)$ and $k(\lambda)$ from the measured $T(\lambda)$ and $R(\lambda)$ values. Since it is not possible to invert these equations directly given that the Fresnel formulae will have multiple roots, *i.e.*, different combinations of $n(\lambda)$ and $k(\lambda)$ will satisfy a given pair of $T(\lambda)$ and $R(\lambda)$ at a given λ , we had to employ root-finding numerical solutions based on the secant and Mueller method [6].

The results of these calculations are shown in Fig. 4, where $k(\lambda)$ is shown for GdF_3 , LuF_3 , and the MgF_2 substrate. The graph clearly shows the onset of absorption for GdF_3 and LuF_3 starts below 130 nm. Therefore, use of either material as a high-index alternative for a dielectric design may only be feasible for wavelengths longer than 130 nm. A final observation is that the $k(\lambda)$ values for MgF_2 remain nearly zero over the range shown in this figure. This is because this material has a lower cut-off wavelength, and the data were derived from measurements on a piece of MgF_2 that has more bulk-like properties than either the GdF_3 or LuF_3 layers.

Figure 5 shows $n(\lambda)$ for GdF_3 and LuF_3 along with results for the MgF_2 substrates. The figure shows the index progressively increases in the 130 to 250 nm range, starting with MgF_2 ($n \approx 1.60$ -1.40) followed by LuF_3 ($n \approx 1.80$ -1.52), and finally GdF_3 ($n \approx 1.95$ -1.60). The combination of the $\text{GdF}_3/\text{MgF}_2$ pair will provide

greater contrast due to their respective refractive index values. This higher refractive index contrast offers a potentially successful dielectric design in the 130 to 250 nm spectral range with fewer layers.

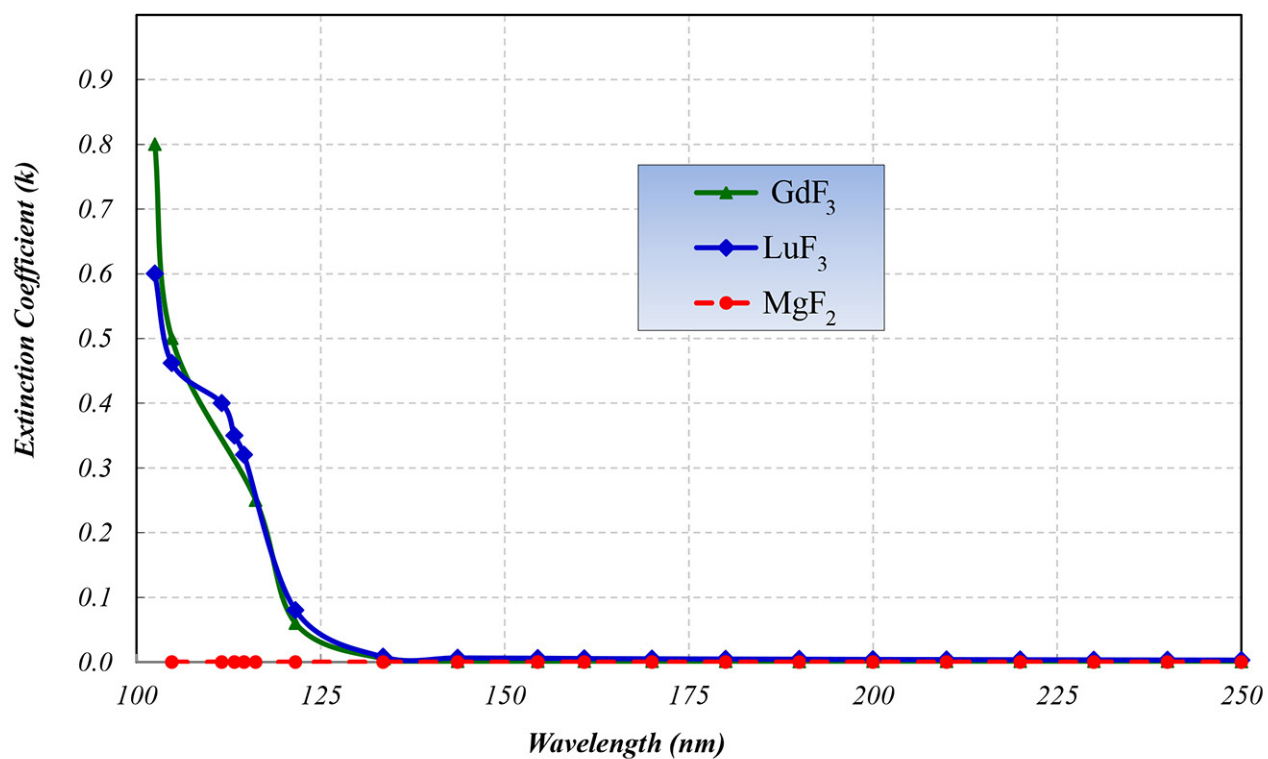


Fig. 4. Extinction coefficient.

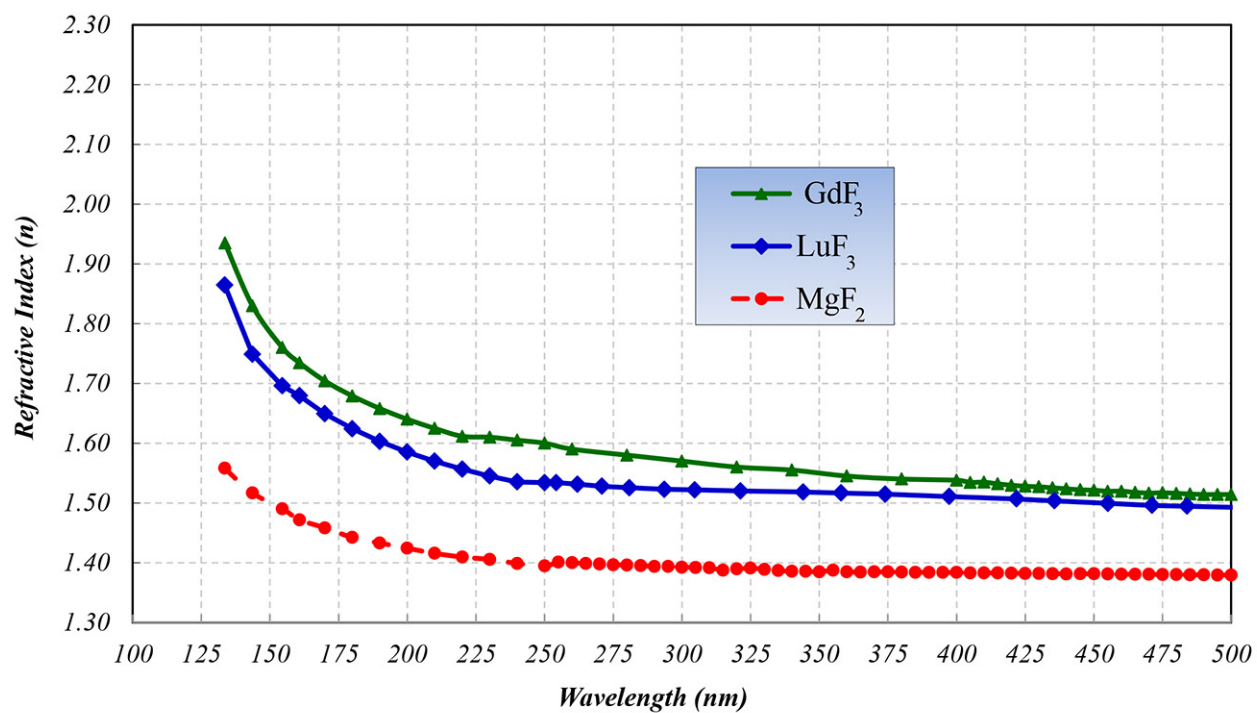


Fig. 5. Refractive index.

Figure 6 shows two reflector models for a dielectric design with 10 $\text{GdF}_3/\text{MgF}_2$ pairs on a MgF_2 substrate (blue curve) and five $\text{GdF}_3/\text{MgF}_2$ pairs on Al (red dot curve). The results show the feasibility of achieving reflectance values greater than 90% at selected wavelengths in the 130 to 160 nm range.

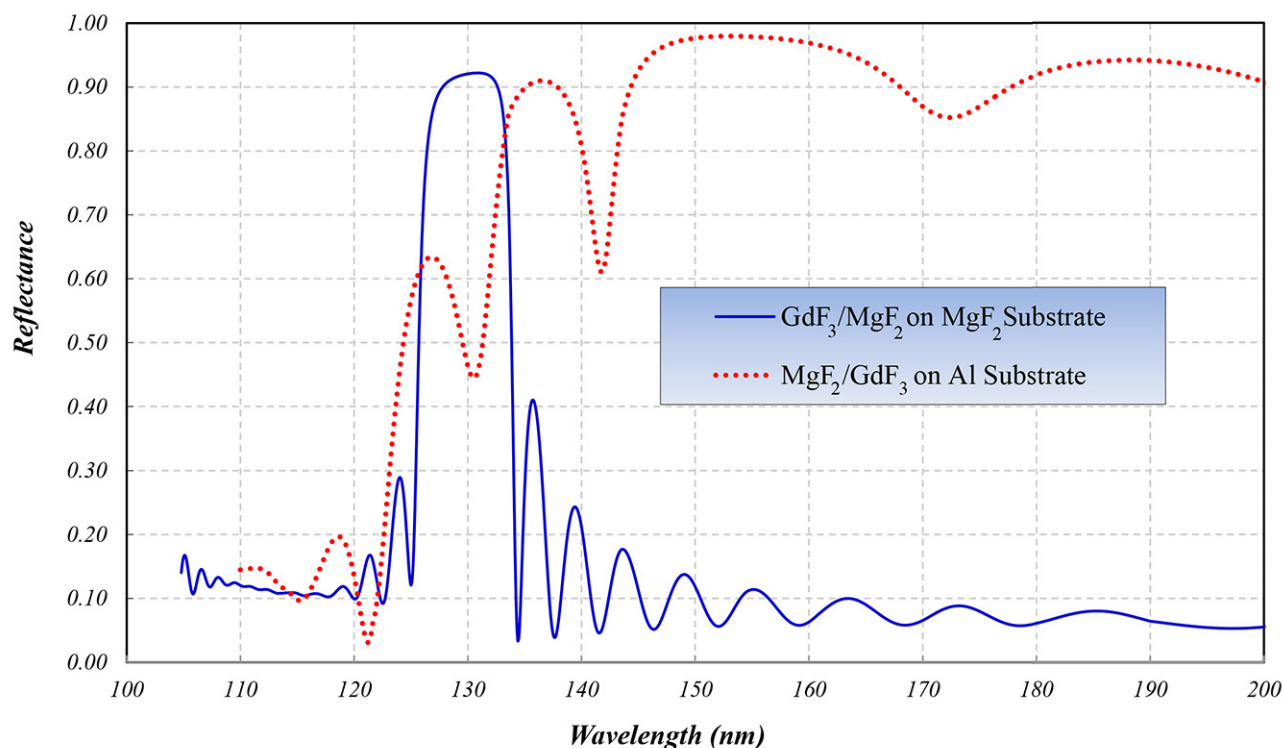


Fig. 6. Reflector design using dielectric stacks of $\text{GdF}_3/\text{MgF}_2$ layer pairs.

WFIRST AR Coating Task

We demonstrated the feasibility of using a high-low pair consisting of a $\text{GdF}_3/\text{MgF}_2$ stack by producing an AR coating design that would operate in the visible range (450 to 800 nm). The design consisted of applying two pairs of $\text{GdF}_3/\text{MgF}_2$ layers (four layers total) on each side of a fused-silica substrate (Corning 7980). This AR coating was also applied on a prototype grism optic (also made out of fused silica) to reduce reflection losses as part of the pre-phase-A activities of the WFIRST project. The results of these coating activities are shown in Fig. 7, where we observe excellent agreement between design and measured reflectance data.

Aluminum Coating with Two-Layer Dielectrics

The reflectance values shown in Fig. 3 for the freshly made Al+LiF sample were fitted with a model that attributed any deviation from an ideal reflectance to absorptions in the LiF layer (light blue dots in Fig. 3). This model allowed determination of the optical absorption in the LiF, which could then be used to predict performance for a thinner layer of LiF applied to the Al layer (Fig. 8).

We notice that when the LiF film thickness is reduced from the nominal 24.4 nm in the actual sample to about 18 nm (blue dash curve), the high-reflectance performance of the Al+LiF mirror is extended down to the LiF cut-off wavelength of about 100 nm. The second (green dot) curve shows the result when the LiF layer is adjusted to 15 nm with a second 5-nm over-coat layer of MgF_2 . This second layer is intended to provide protection to the LiF film from environmental humidity. These results show (in theory) an equally acceptable performance for an Al mirror prescription that includes a dual LiF/ MgF_2 dielectric over-coat.

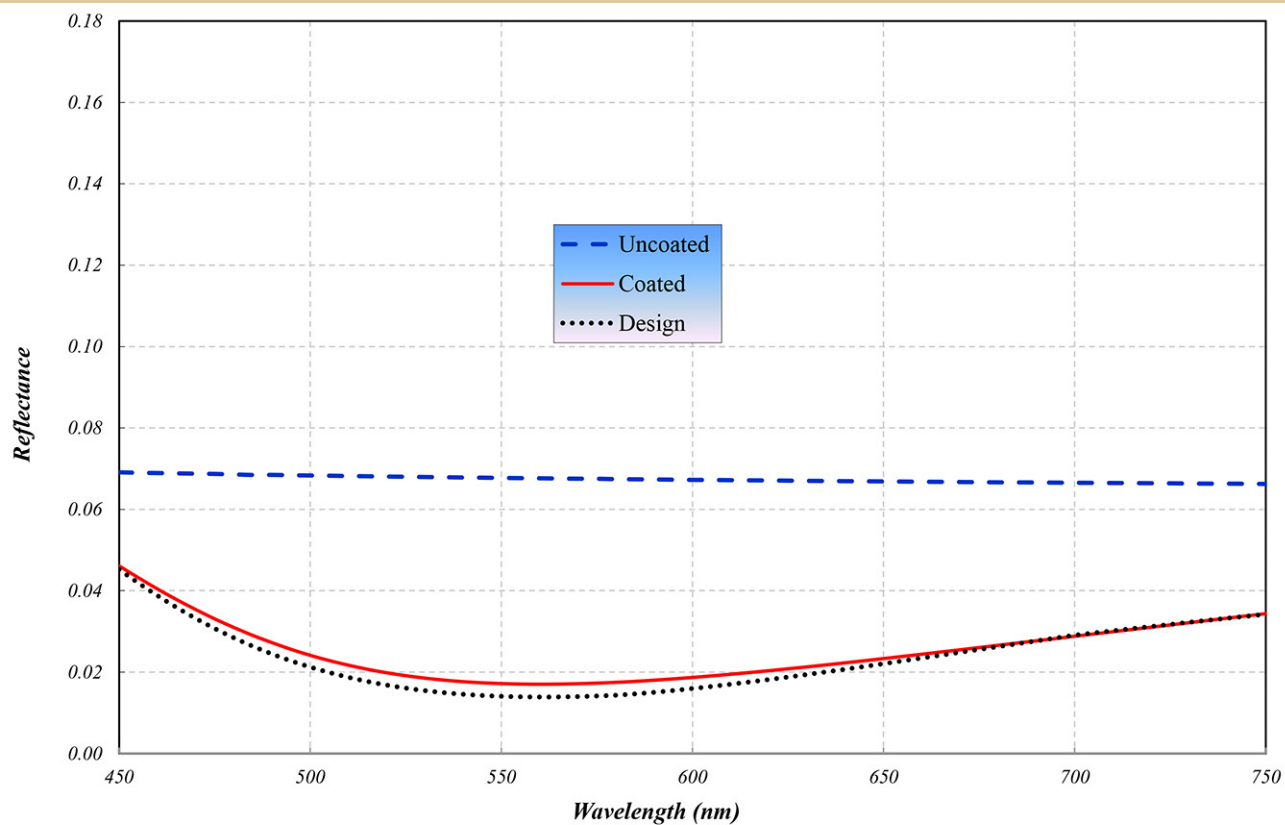


Fig. 7. WFIRST grism AR coating data vs. design performance.

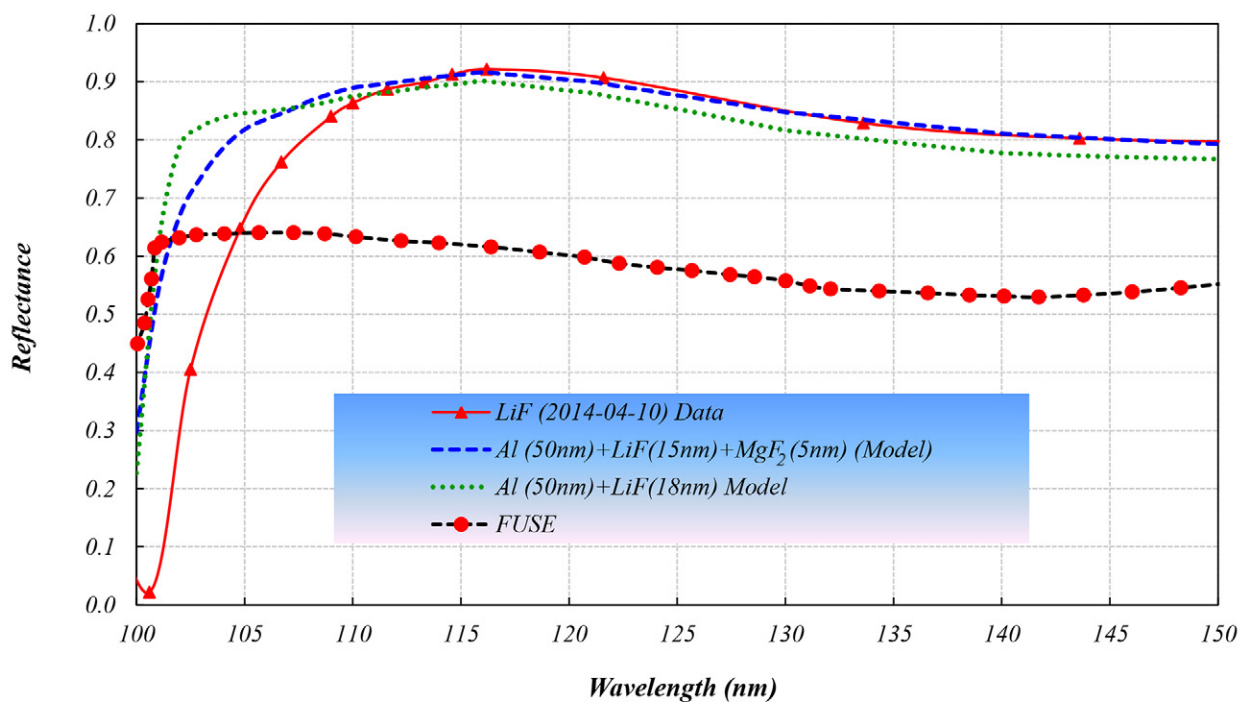


Fig. 8. Modeled reflectance of Al mirror protected with a combination of LiF and MgF₂ over-coats.

Figure 9 shows an assembled two-bowl fixture that allowed us to apply more than one dielectric layer at a time (in addition to Al). We performed a test run with the fixture to determine the performance for an actual mirror done with Al over-protected with a LiF/MgF₂ stack. The results of these coating efforts are shown in Fig. 10. The figure displays the reflectance of a test sample prepared with the following recipe: Al(50 nm)+LiF(13 nm)+MgF₂(6 nm). The measured reflectance should have matched closely the predictions shown by the blue-dotted curve. However, we observe that the results fell short of that prediction. We could not explain the discrepancy other than to mention that this particular sample exhibited unusually high surface micro-roughness in a scan with a surface profiler. This clearly indicates more work needs to be done to determine the reason for high scatter from the LiF/MgF₂ stack. On a positive note, this particular sample appeared to be stable over time, as measurements performed two months later (red-dashed curve) did not show significant changes in reflectance performance, despite the fact that the sample had an LiF over-coat layer, but was stored unprotected in a standard laboratory environment.

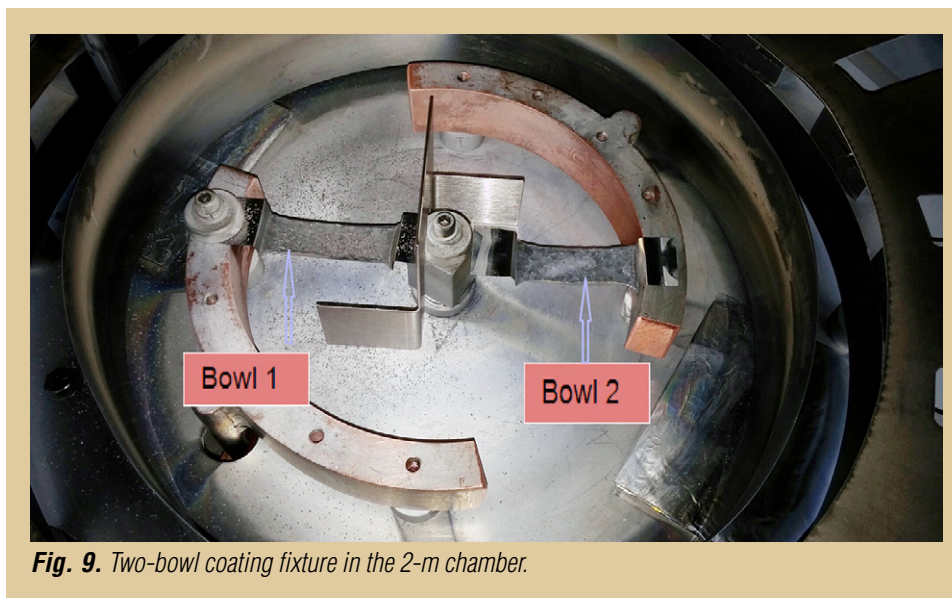


Fig. 9. Two-bowl coating fixture in the 2-m chamber.

ICON/GOLD Coating Tasks

ICON is a NASA Explorer mission selected in April 2013. The ICON instrument (led by a UC Berkeley team) will provide NASA's Heliophysics Division with a powerful new capability to determine conditions in space, modified by weather on the planet, and to understand the way space weather events grow to envelope regions of our planet with dense ionospheric plasma. GOLD is another project (led by a University of Colorado team) approved to move into development (Phase B) in the same Mission of Opportunity as ICON. GOLD's main objective is to map the Earth's thermosphere and ionosphere.

Given our success in producing Al+MgF₂ coatings with better than 90% reflectance at and beyond Lyman-Alpha, we were tasked by ICON and GOLD to coat their optics at the GSFC coating facilities. The tasks include applying Al+MgF₂ reflector coating on a set of 20 different optics including flats, curved mirrors, and gratings. The optics coated ranged in diameter from 26 to 264 mm.

Preparations for these coating tasks included a series of test runs to maximize reflectance at ICON and GOLD's wavelengths of interest (133.6 and 154.5 nm) and to demonstrate the reproducibility of our three-step process. Figure 11 shows reflectance data for three coating runs performed in the summer of 2014. These results demonstrate reflectance values over 91% at the two wavelengths listed above. These high reflectance values will provide the instruments throughput that will enable the two missions' scientific goals. Figure 12 shows the first two ICON aspheric-mirror optics coated successfully, completed in December 2014.

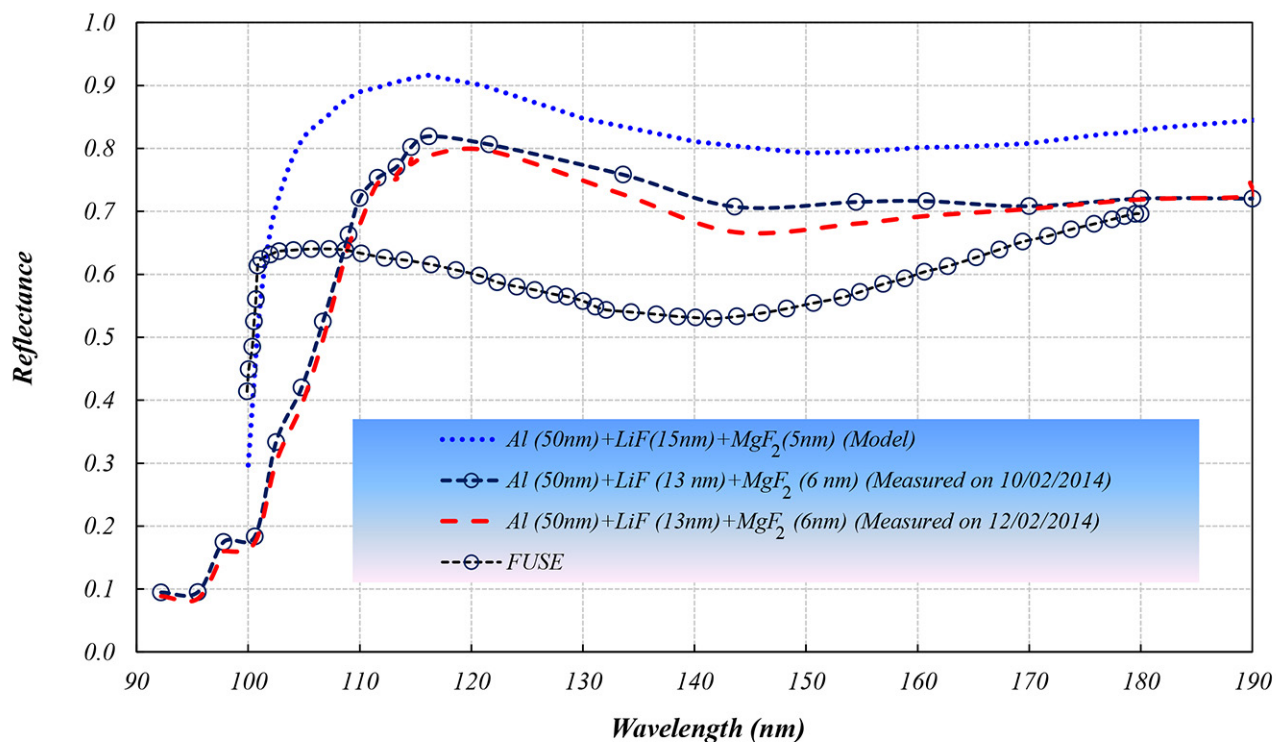


Fig. 10. Reflectance data for Al over-coated with a LiF/MgF₂ dielectric stack.

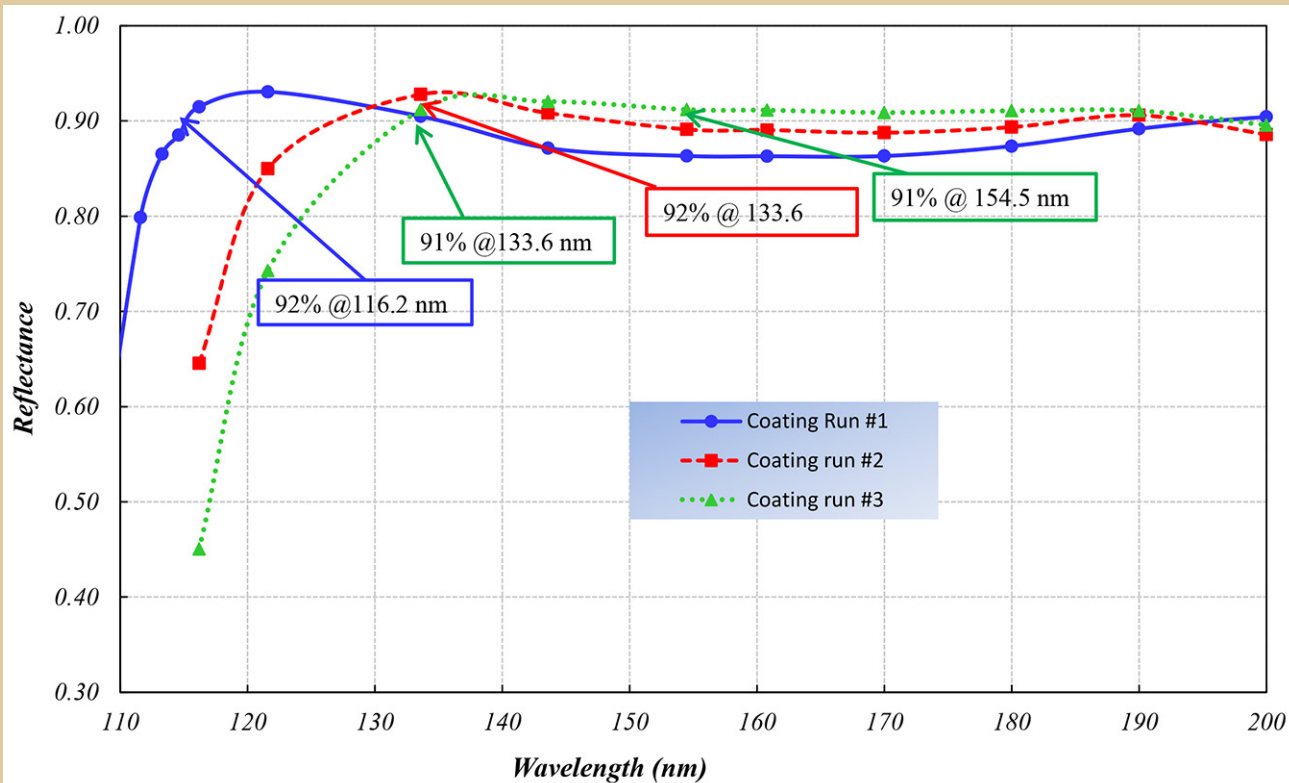


Fig. 11. Reflectance of test runs in preparation for coating the ICON and GOLD optics.

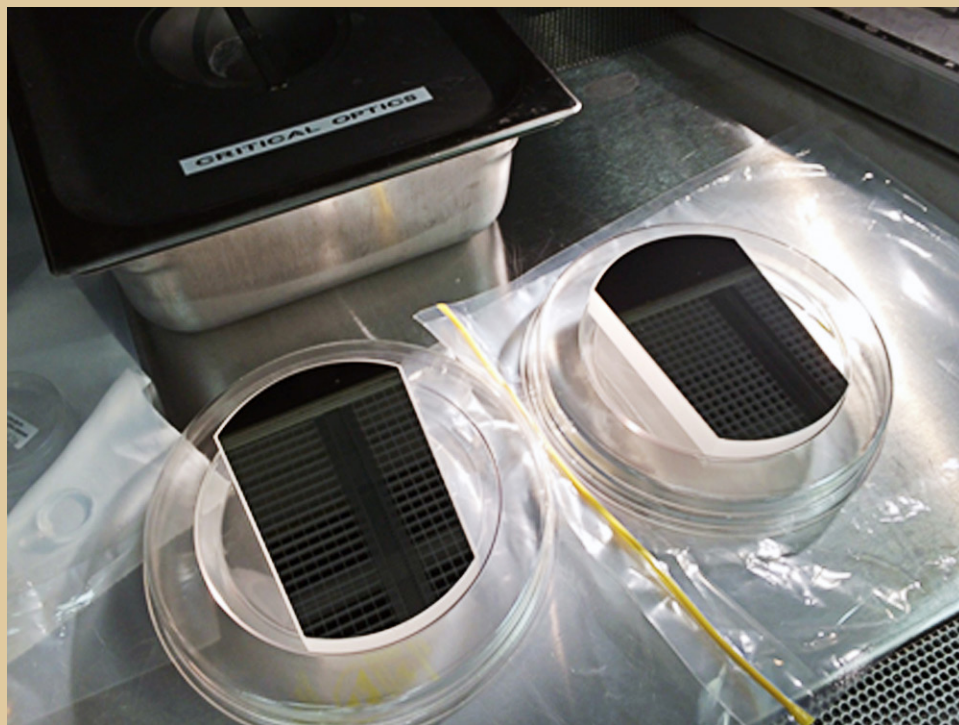


Fig. 12. Two ICON aspheric mirrors after their successful coating run.

References

- [1] L.J. Lingg, J.D. Targove, J.P. Lehan, and H.A. Macleod, "Ion-assisted deposition of lanthanide trifluorides for VUV applications," *Proc. SPIE* **818**, 86-92 (1987)
- [2] M.A. Quijada, S. Rice, and E. Mentzell, "Enhanced MgF_2 and LiF Over-coated Al Mirrors for FUV Space Astronomy," *Proc. SPIE* **8450-78**, 1-10 (2012)
- [3] J.I. Larruquert, J.A. Mendez, and J.A. Aznarez, "Far-UV reflectance of UHV-prepared Al films and its degradation after exposure to O_2 ," *Appl. Optics* **33**, 3518 (1994)
- [4] H.W. Moos, S.R. McCandiss, and J.W. Kruk, "FUSE: Lessons Learned for future FUV missions," *Proc. SPIE* **5488** (2004)
- [5] M.R. Adriaens and B. Feuerbacher, "Improved LiF and MgF_2 over-coated aluminum mirrors for vacuum ultraviolet astronomy," *Appl. Optics* **10**, 77610F (1971)
- [6] W.H. Press, B.P. Flannery, S.A. Teukolsky, and W.T. Vetterling, "Numerical Recipes," Cambridge University Press, New York and Australia (1989)

For additional information, contact Manuel Quijada: manuel.a.quijada@nasa.gov



Advanced UVOIR Mirror Technology Development for Very Large Space Telescopes

Prepared by: H. Philip Stahl, PhD (NASA/MSFC)

Summary

The Advanced Mirror Technology Development (AMTD) project is in Phase 2 of a multiyear effort initiated in Fiscal Year (FY) 2012, to mature toward the next Technology Readiness Level (TRL) six critical technologies required to enable 4-m-or-larger ultraviolet, optical, and infrared (UVOIR) space telescope primary-mirror assemblies for general astrophysics and ultra-high-contrast observations of exoplanets. AMTD's demonstrated deep-core manufacturing method enables 4-m class mirrors with 20-30% lower cost and risk. The design tools we have developed increase speed, resulting in reduced cost of trade studies. In addition, the integrated modeling tools we have developed enable better definition of system and component engineering specifications.

AMTD continues to achieve its goals and milestones. We have done this by assembling an outstanding team with extensive expertise in astrophysics and exoplanet characterization, and in the design/manufacture of monolithic and segmented space telescopes. Our team comes from three NASA centers (Marshall Space Flight Center, MSFC; Jet Propulsion Lab, JPL; and Goddard Space Flight Center, GSFC), academia (Space Telescope Science Institute and University of Arizona) and industry (Harris, formerly Exelis; and A.I. Solutions). We derive engineering specifications for advanced normal-incidence mirror systems needed to make the required science measurements. Then we define and mature solutions to the most important technical challenges in these systems. Our progress was reviewed by the Cosmic Origins (COR) Technology Management Board (TMB). Our results were presented at Mirror Tech Days 2014, and published in proceedings of the 2014 SPIE conference on Space Telescopes and Instrumentation (see publication list at the end of this report). The AMTD team includes the next generation of scientists and engineers in the field. Last year, we had four undergraduate student interns; and Jessica Gersh-Range received her PhD from Cornell University and published two journal papers in the SPIE Journal of Astronomical Telescope and Instrument Systems.

Background

UVOIR measurements provide robust, often unique, diagnostics for investigating astronomical environments and objects. UVOIR observations are responsible for much of our current astrophysics knowledge and will produce as-yet-unimagined, paradigm-shifting discoveries. A new, larger UVOIR telescope is needed to help answer fundamental scientific questions such as:

- Does life exist on nearby Earth-like exoplanets?
- How do galaxies assemble their stellar populations?
- How do galaxies and the intergalactic medium interact?
- How did planets and smaller bodies in our own solar system form and evolve?

According to the 2010 Decadal Survey, New Worlds, New Horizons in Astronomy and Astrophysics (NWNH), an advanced, large-aperture UVOIR telescope is required to enable the next generation of compelling astrophysics and exoplanet science. NWNH also noted present technology is not mature enough to affordably build and launch UVOIR telescopes that are diffraction-limited at visible (or shorter) wavelengths, with apertures larger than 4 m. According to the 2012 NASA Space Technology Roadmaps and Priorities report, the highest priority technology in which NASA should invest to enable "*Objective C: Expand our understanding of Earth and the universe in which we live*," is a new generation of low-cost, stable astronomical telescopes for high-contrast imaging and faint-object spectroscopy to

“Enable discovery of habitable planets, facilitate advances in solar physics, and enable the study of faint structures around bright objects.” Finally, according to the NASA Office of Chief Technologist Science Instruments, Observatory, and Sensor Systems (SIOSS) Technology Assessment Roadmap, technology to enable a future UVOIR or high-contrast exoplanet mission needs to be at TRL 6 by 2018, so a viable flight mission can be proposed to the 2020 Decadal Survey.

Objectives and Milestones

Our long-term objective is to mature technologies to enable large UVOIR space telescopes to TRL 6 by 2018. Because we cannot predict whether monolithic or segmented architectures will be chosen, we are pursuing technologies that can enable both.

Phase 1: advanced technology readiness of six key technologies required to make an integrated primary mirror assembly (PMA) for a large aperture UVOIR space telescope.

- Large-Aperture, Low-Areal Density, High-Stiffness Mirror Substrates;
- Support System;
- Mid/High-Spatial-Frequency Figure Error;
- Segment Edges;
- Segment-to-Segment Gap Phasing; and
- Integrated Model Validation.

Phase 2: continues technology development on three of these key technologies.

- Large-Aperture, Low-Areal-Density, High-Stiffness Mirror Substrates;
- Support System; and
- Integrated Model Validation.

Critical to AMTD's success is our integrated team of scientists, systems engineers, and technologists; and our science-driven systems engineering approach.

Progress and Accomplishments

During FY 2014/15, the advances of AMTD Phase 1 passed review by the COR TMB, and we are progressing in all our Phase 2 technology areas.

Large-Aperture, Low-Areal-Density, High-Stiffness Mirror Substrates

Need: To achieve the ultra-stable mechanical and thermal performance required for high-contrast imaging, both (4-m to 8-m) monolithic and (8-m to 16-m) segmented primary mirrors require larger, thicker, and stiffer substrates for monoliths or very stiff back-structure for segmented mirrors. The system stiffness will have to come from somewhere.

Accomplishment: In FY 2012/13, AMTD partner Harris successfully demonstrated a new five-layer 'stack & fuse' process for fabricating deep-core mirror substrates. It is estimated that this process could reduce the cost to fabricate a 4-m class mirror by ~30%. Using this new process, a 43-cm-diameter 'cut-out' of a 4-m-diameter, 40-cm thick, < 45 kg/m² mirror substrate was fabricated (Fig. 1). This demonstrated the technology can make mirrors with sufficient thickness for a 4-m to 8-m-class mirror.

In FY 2014/15, MSFC performed 3D X-Ray Computed Tomography (CT) measurements of this mirror to quantify the visco-elastic geometric deformations produced during the Low-Temperature Fusing (LTF) and Low-Temperature Slumping (LTS) processes.

In FY 2013/14, Harris tested the core-to-core LTF bond strength using 12 Modulus of Rupture (MOR) test articles (Fig. 2). The Weibull 99% survival value was 30% above the most conservative design allowable value for margin of safety calculations at the core-to-plate LTF bond. The data on the 50 samples ranged from 60% to 250% above this design allowable value.

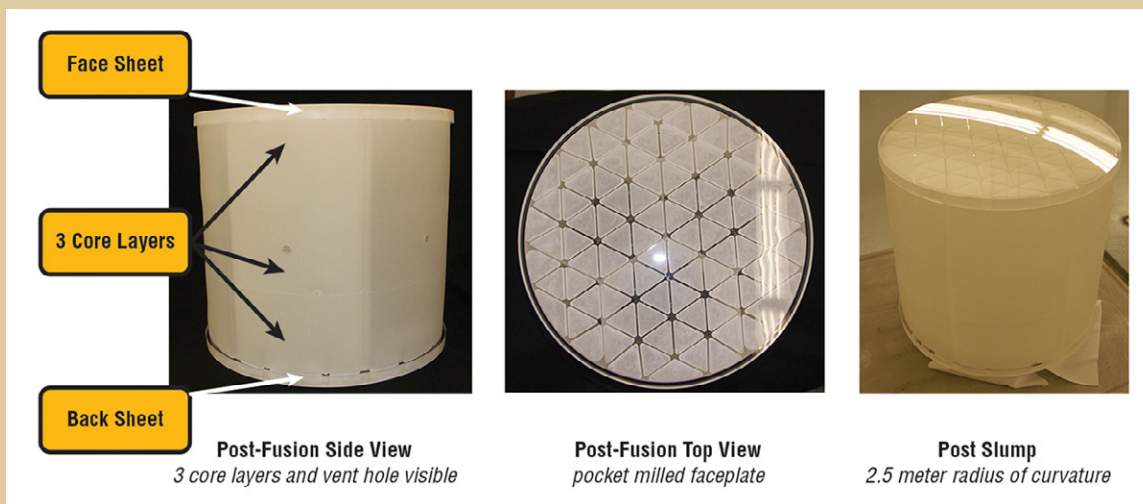


Fig. 1. Deep-core mirror attributes shown at different processing stages.



Fig. 2. MOR test-article fabrication.

In FY 2014/15, Harris performed a more rigorous A-Basis test of the core-to-core LTF bond strength using 60 MOR samples: 30 samples were assembled with nominal alignment and 30 samples were deliberately misaligned. These samples were made in a manner that is more representative of how core-to-core LTF seals are developed compared to the samples tested in FY2014/15. The A-basis Weibull 99% Confidence strength allowable based on 49 of the samples was found to be approximately 50% higher than the strength of core-to-plate LTF bonds.

In FY 2014/15, Harris completed the design of a 1.5-m-diameter, 200-mm-thick mirror (Fig. 3), to be fabricated via deep-core technology. Using the X-ray CT data, the A-Basis strength data, and a non-linear visco-elastic analysis tool, Harris designed a 4-m-class mirror that could be manufactured via the deep-core 'stack & seal' process; then, scaled the mirror to 1.5-m diameter. The primary purpose of this mirror is to demonstrate lateral scalability of the fabrication process. To enable optical and environmental testing, Harris also developed the mount design for the 1.5-m mirror. Currently, Harris is polishing the faceplates. The 18 core elements will be fabricated in September.

Support System

Need: Large-aperture mirrors require large support systems to ensure they survive launch and deploy on-orbit stress-free and undistorted.

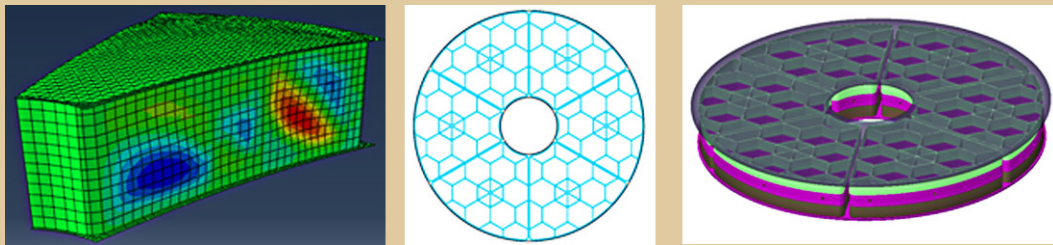


Fig. 3. Final design for 1.5-m mirror.

Accomplishment: We continue to develop our modeling tool in Visual Basic for ANSYS Finite Element Modeling (FEM). This tool allows rapid creation and analysis of detailed mirror designs. The ANSYS models can also be exported into other FEM codes such as Nastran and Abaqus. In FY 2014/15, we studied various mirror support systems integrated to the mirror substrate via kinematic and hexapod mechanisms. We evaluated the stress distribution associated with different support systems (Fig. 4). We continue to use this tool daily to develop point designs for thermal and mechanical analysis. For the duration of our effort, we will continue to refine the tool and optimize candidate point designs. For example, we have evaluated how 95 kg of properly distributed mass can increase the first mode of a 4-m mirror from 50 Hz (725 kg) to 75 Hz (820 kg). We continue to employ undergraduate interns to support these efforts.

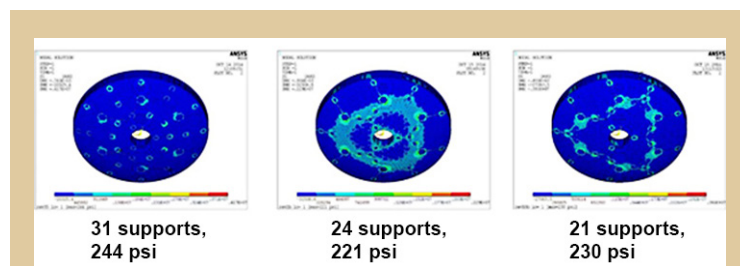


Fig. 4. Different support types demonstrated by mirror modeler.

Segment-to-Segment Gap Phasing

Need: To achieve diffraction-limited performance at a wavelength of 500 nm, the figure error of the primary mirror surface needs to be less than 10 nm root-mean-square (rms). For a segmented mirror, it is necessary to co-phase the mirror segments to better than 5 nm rms. To avoid speckle noise, which can interfere with exoplanet observation, internal coronagraphs require a segment-to-segment

dynamic co-phasing error of under 10 pm rms between Wave Front Sensing and Control (WFSC) updates.

Accomplishment: In FY 2014/15, AMTD science team member Stuart Shaklan performed a preliminary analysis (Fig. 5) which indicated that 1 nm rms of random-segment rigid-body motion can produce unwanted speckles at 10^{-8} to 10^{-7} contrast. To get this speckle noise below 10^{-11} requires random-segment rigid-body motion of about 10 pm. Finally, the time for which the primary mirror must be stable (between WFSC cycles) can vary from a few minutes to many tens of minutes depending on the host star's brightness.

In FY 2013/14, Harris designed, built, and characterized the 'fine' stage of a low-mass, two-stage actuator (Fig. 6), which could be used to co-phase mirror segments to the required tolerance. On other programs, Harris had already developed Force Control Actuators (FCAs) for segment figure correction, which we believe are at TRL 6.

In FY 2014/15, Jessica Gersh-Range published her PhD research, which indicated that connecting segments along their edges with damped-spring interfaces provides potentially significant performance advantages for very large mirrors (Fig. 7). With no edgewise connection, the segments behave independently. With as few as three damped-spring interfaces, the segments start to act as a monolith if the interfaces are sufficiently stiff. Adjusting the spring stiffness tunes the assembly's first mode frequency. Initially, the frequency increases proportionally to the square root of the interface stiffness, but then approaches monolithic performance asymptotically. By adjusting stiffness and damping, a segmented mirror will stabilize faster after a force impulse than a monolithic mirror. A segmented mirror with low-to-intermediate interface stiffness does not propagate disturbance waves, and a segmented mirror with high damping reduces the propagating-wave amplitude quickly.

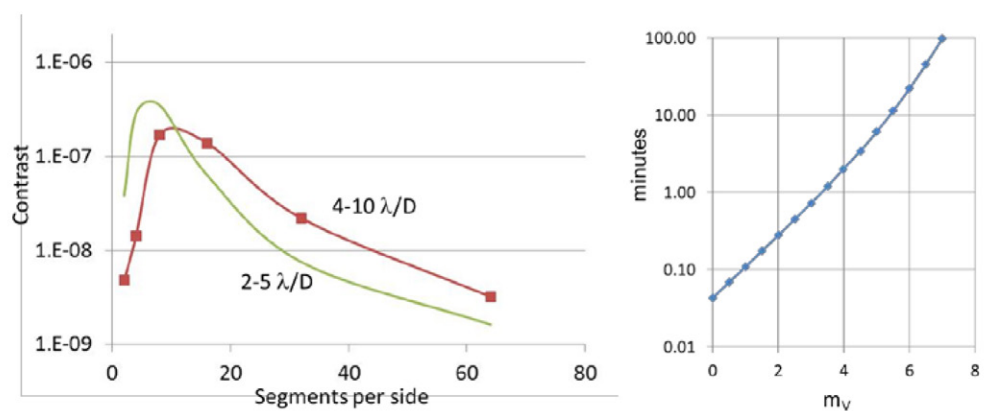
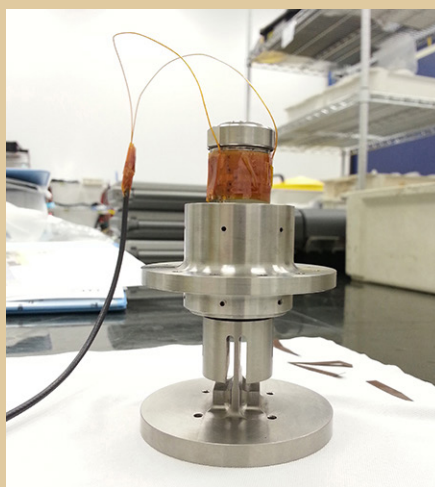


Fig. 5. Left: Primary mirror segment motion stability requirement. Right: Temporal stability period requirement.



Property	Performance
Mass	0.313 Kg
Axial Stiffness	40.9 N/ μ m
Test Range	14.1 μ m
Resolution	6.6 nm (noise-limited result. Expected is 0.8 nm)
Accuracy	1.1 μ m

Fig. 6. Actuator and its performance test results.

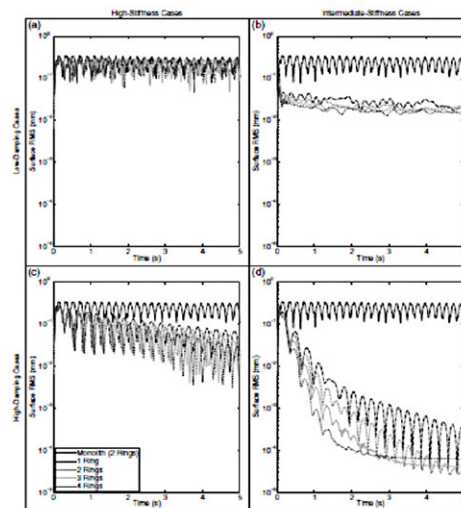
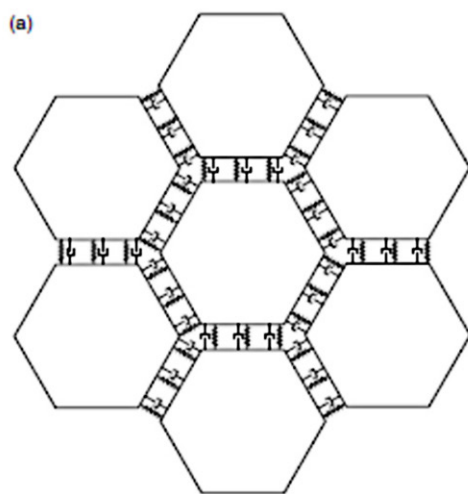


Fig. 7. Left: segmented mirror with edgewise interfaces. Right: dynamic motion vs. stiffness and damping.

Integrated Model Validation

Need: On-orbit performance is driven by mechanical stability (both thermal and dynamic). As future systems become larger, compliance cannot be fully tested; performance verification will rely on results from a combination of sub-scale tests and high-fidelity models. It is necessary to generate and validate as-built models of representative prototype components to predict on-orbit performance for transmitted wavefront, point spread function (PSF), pointing stability, jitter, thermal stability, and vibro-acoustic and launch loads.

Accomplishment: MSFC has developed a new tool methodology for understanding how a primary mirror responds to a dynamic thermal environment (Fig. 8). Any thermal environment can be decomposed into a set of periodic thermal oscillations. These oscillations cause wavefront figure errors on the primary mirror with thermal time constant determined by the mirror's thermal properties (*e.g.*, mass and conductivity). The amplitude of these figure errors depends on the amplitude and period of the input thermal oscillation. For the AMTD 4-m point design, the primary-mirror wavefront error remains below 10 μm for a 50 mK thermal oscillation of period shorter than 70 seconds. This tool can be used to determine thermal boundary and control conditions for passive and active telescope thermal control.

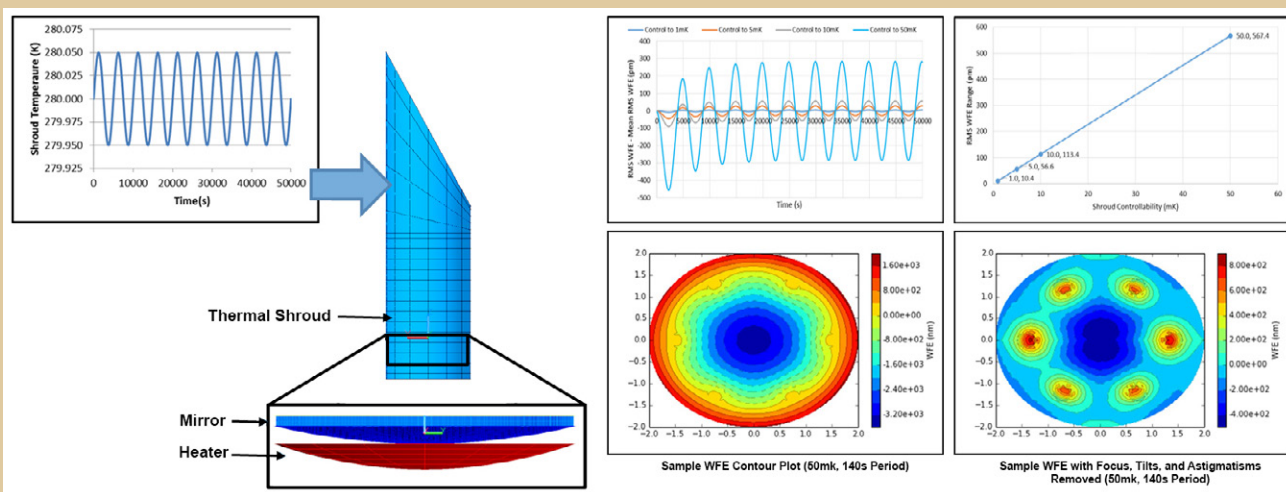


Fig. 8. Thermal modulation transfer function for space telescopes.

Path Forward

AMTD has quantifiable milestones for each key technology. Below is the Phase 2 proposed schedule (Fig. 9). The primary task for FY 2015/16 is to fabricate the 1.5-m Ultra-Low Expansion (ULE[®]) mirror. Thermal characterization of this mirror is scheduled to start in the 3rd quarter of 2016. Unfortunately, Phase 2 was not fully funded, so the modal, vibration, and acoustic tests are not in the baseline plan. We have requested a funding over guide to restore these tasks. Finally, we have not yet executed a contract with Schott to polish and thermally characterize their 1.2-m Zerodur[®] mirror. Otherwise, all tasks are on budget and on schedule.

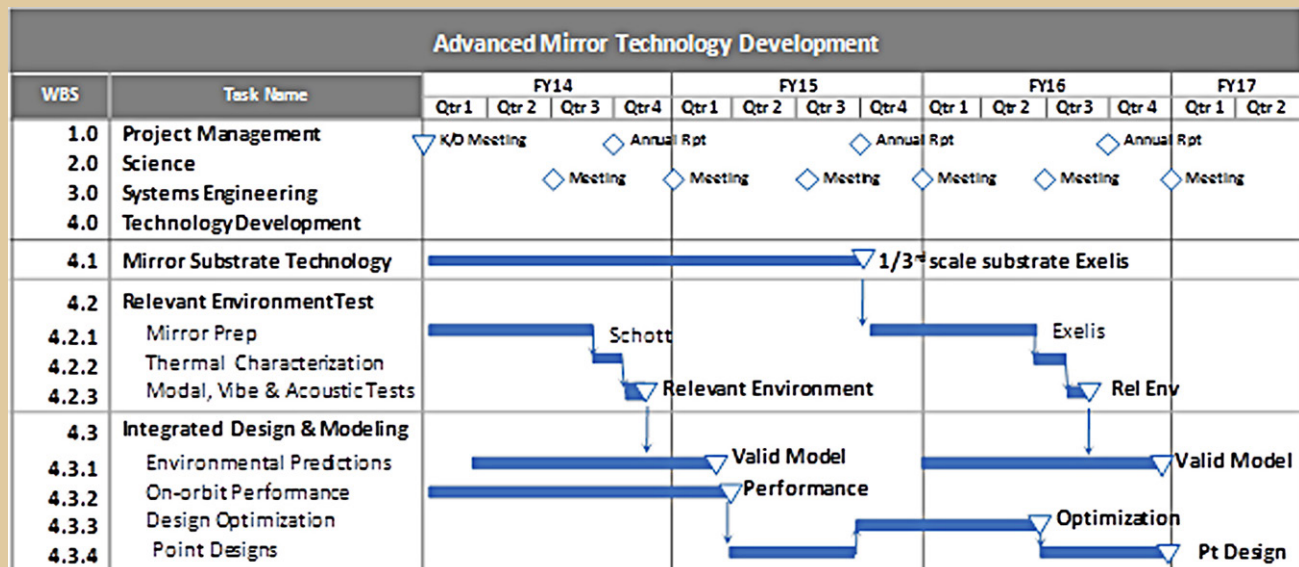


Fig. 9. Proposed AMTD Phase 2 schedule.

AMTD Publications

- [1] H. Philip Stahl *et al.*, "Advanced mirror technology development (AMTD) project: 2.5 year status," Proc. SPIE. **9143**, DOI: 10.1117/12.2054765 (2014)
- [2] H. Philip Stahl *et al.*, "AMTD: update of engineering specifications derived from science requirements for future UVOIR space telescopes," Proc. SPIE. **9143**, DOI: 10.1117/12.2054766 (2014)
- [3] Gary W. Matthews *et al.*, "Development of stacked core technology for the fabrication of deep lightweight UV-quality space mirrors," Proc. SPIE. **9143**, DOI: 10.1117/12.2055284 (2014)
- [4] Jessica Gersh-Range, William R. Arnold Sr., and H. Philip Stahl, "Edgewise connectivity: an approach to improving segmented primary mirror performance," Journal of Astronomical Telescope and Instrument Systems, DOI: 10.1117/1.JATIS.1.1.014002 (2014)
- [5] Jessica Gersh-Range, William R. Arnold Sr., David Lehner, and H. Philip Stahl, "Flux-pinning mechanisms for improving cryogenic segmented mirror performance," Journal of Astronomical Telescope and Instrument Systems, DOI: 10.1117/1.JATIS.1.1.014001 (2014)

For additional information, contact Philip Stahl: h.philip.stahl@nasa.gov



Cross-Strip MCP Detector Systems for Spaceflight

Prepared by: John Vallerga (Space Sciences Laboratory, UC Berkeley)

Summary

Micro-Channel Plate (MCP) detectors have been an essential imaging technology in space-based NASA ultraviolet (UV) missions for decades, and have been used in numerous orbital and interplanetary instruments. The Experimental Astrophysics group at the University of California (UC) Berkeley's Space Sciences Laboratory (SSL) was awarded an Astrophysics Research and Analysis (APRA) grant in 2008 to develop massively parallel cross-strip (XS) readout electronics. These laboratory XS electronics have demonstrated spatial resolutions of 12 μm full-width at half-maximum (FWHM), global output count rates of 2 MHz, and local count rates of 100 kHz; all at gains a factor of ~ 20 lower than existing delay-line readouts [1]. They have even been deployed in biomedical and neutron-imaging labs but are presently too bulky and high-power to be used for space applications, though a current version has been successfully flown on a rocket flight in 2014 [2].

The goal of this Strategic Astrophysics Technology (SAT) program is to raise the Technology Readiness Level (TRL) of this XS technology by:

1. Developing new Application Specific Integrated Circuits (ASICs) that combine optimized faster amplifiers and associated Analog-to-Digital Converters (ADCs) in the same chip(s).
2. Developing a Field Programmable Gate Array (FPGA) circuit that will control and read out groups of these ASICs so that XS anodes of many different formats can be supported.
3. Developing a spaceflight-compatible 50-mm XS detector that can be integrated with these electronics and tested as a system in flight-like environments. This detector design can be used directly in many rocket, satellite, and interplanetary UV instruments, and could be easily adapted to different sizes and shapes to match various mission requirements. Having this detector flight design available will also reduce cost and development risk for future Explorer-class missions. New technological developments in photocathodes (*e.g.*, GaN) or MCPs (*e.g.*, low-background, surface-engineered borosilicate-glass MCPs) could be accommodated into this design as their TRLs increase.

Since the start of our three-year project in April of 2012, we have designed and constructed a 50-mm XS detector with a new low-noise anode, and have demonstrated its excellent performance using our best laboratory electronics. The first versions of our ASICs have been designed, fabricated, and tested; and the second versions are soon (Fall 2015) to be submitted to a foundry for fabrication.

Background

The 2010 Decadal Survey, *New Worlds, New Horizons in Astronomy and Astrophysics* (NWNH), commenting on UV astronomy, noted, “*Key advances could be made with a telescope with a 4-meter-diameter aperture with large field of view and fitted with high-efficiency UV and optical cameras/ spectrographs.*” Further, it recommends to “*invest in essential technologies such as detectors, coatings, and optics, to prepare for a mission to be considered by the 2020 decadal survey.*” Many of the White Paper submissions to the Decadal Survey on UV astrophysics missions require large fields of view (detector formats > 10 cm), high spatial and/or spectral resolution recorded with high efficiency over a large wavelength range [3, 4]. Our SAT program plans to take our successful XS technology that achieves the performance goals above in the laboratory, and raise its TRL by lowering its mass and power and qualifying it for space use.

XS readouts collect the charge exiting from a stack of MCPs with two sets of coarsely spaced and electrically isolated orthogonal conducting strips (Fig. 1). When the charge collected on each strip is measured, a centroid calculation determines the incident location of the incoming event (photon or particle). This requires many identical amplifiers (*e.g.*, 80, 160) whose individual outputs must all be digitized and analyzed. The advantage of this technique over existing and previous MCP readout techniques (wedge and strip, delay-line, intensifiers) is that the anode capacitance per amplifier is lower, resulting in lower noise.

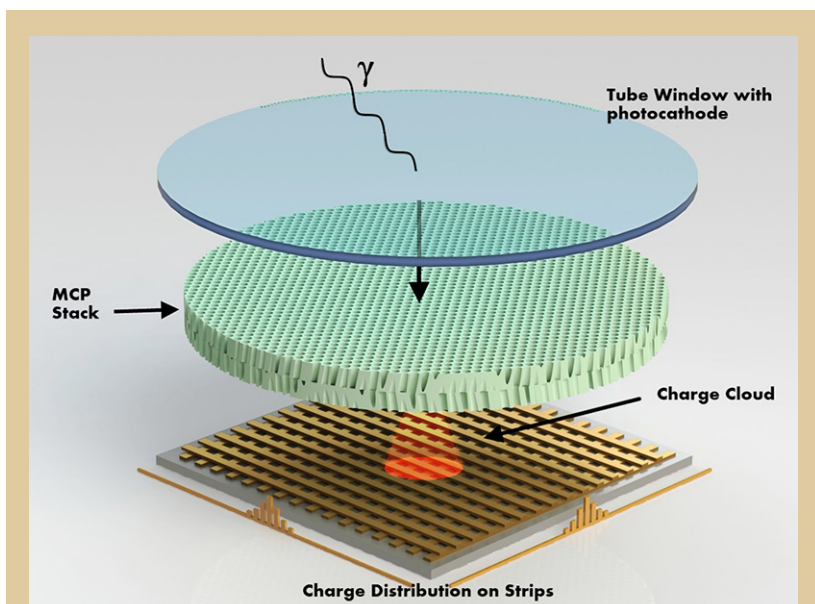


Fig. 1. Schematic of a cross-strip readout behind an MCP stack.

This allows lower MCP gain operation (factors of ~ 20) while still achieving better spatial resolution compared to the delay-line MCP readouts of current space missions [5], thereby increasing the dynamic range of MCP detectors by up to two orders of magnitude. They can also be readily scaled to large ($> 100 \text{ mm} \times 100 \text{ mm}$) or other unique formats (*e.g.*, circular for optical tubes, rectangular for spectrographs, and even curved anodes to match curved MCP focal planes). The XS readout technology is mature enough to be presently used in the field in many laboratory environments producing quality scientific results [6, 7] and is ready for the next step of development – preparing for an orbital or deep-space mission implementation.

Our current XS readout electronics, called the Parallel XS (PXS) electronics, consists of a preamplifier board placed near the MCP anode and a boxed set of electronics containing ADCs and FPGAs. The existing PXS electronics performance presently meets or exceeds ALL of the specifications of the previous flight systems mentioned above. However, the PXS laboratory electronics are too bulky and massive, and use relatively high power and therefore are not currently suitable for a long-term space mission. One important goal of the present effort is to replace the PXS electronics with an ASIC that combines the functionality of the preamp board and the downstream ADCs into one or two low-power, low-mass chip(s). When a set of these chips are combined with an FPGA and XS anode, we expect the performance to exceed the higher-power PXS electronics due to the noise improvement expected for the smaller-scale components.

In addition to the space-flight-appropriate ASIC development, we plan to construct a flight prototype 50-mm XS MCP detector with a XS readout using our new ASICs. The new ASICs and FPGA control electronics will be integrated into a compact package so the performance of the whole detector system can be qualified in space-like environments (*e.g.*, thermal-vacuum tests). This standard detector design will become the baseline XS detector and could be used in many proposed rocket and satellite missions. We note that many UV sounding rocket programs (*e.g.*, at Johns Hopkins University, JHU; and the University of Colorado) currently use MCP detectors. In fact, we expect this detector to be the baseline of many Explorer-class mission proposals in the future. This XS design can also be easily scaled to other useful formats required by specialized instruments. For example, doubling the length of one detector dimension entails adding more strips to the anode and more ASIC chips to read them out, not a redesign of the ASIC.

Objectives and Milestones

1. Design and fabricate an ASIC to amplify and digitize cross-strip signal charges

Developing new ASICs that can overcome the limitations on the front-end of our existing electronics is a major thrust of this proposal. We wish to design and fabricate input ASICs that have the following features:

- An optimized front-end charge-sensitive amplifier (CSA) matched to the anode-strip load capacitance with fast signal rise and fall times to minimize event “collision.”
- Fast ($\sim \text{GHz}$) analog sampling to fully characterize both amplitude and arrival time of the intrinsically fast input charge pulse.

- c. Digital conversion of the analog samples in the ASIC, avoiding complex, bulky, and high-power discrete ADCs downstream.
- d. ASIC self-triggering capabilities to select and transfer only event data across long cables to the FPGA, where the centroiding and timing calculations will take place.

The original proposal called for an ASIC that included a multichannel preamp and an analog sampling and digitization circuit controlled externally by an FPGA. We soon realized that optimization of the analog amplifiers and digital circuits is best done using different fabrication technologies (IBM 130 nm 1.2 V CMOS process, 250 nm for the digital) and noise performance would also improve by not mixing the digital and front-end analog on the same piece of silicon. The original name for the combined ASIC (never built) was Gigasample Recorder of Analog Waveforms from a Photodetector (GRAPH) but after separation of the amplifiers, the sampling digitizer has been named the “HalfGRAPH.”

2. FPGA system to read out HalfGRAPH ASICs

Our proposed parallel XS readout system is not simply comprised of the new ASICs. New board assemblies must be designed, laid out, and constructed to couple these ASICs to our existing XS anodes, minimizing stray load capacitances and incorporating 64 Low Voltage Differential Signaling (LVDS) pairs. These “Digitizer ASIC” boards must send their signals to a new FPGA board that not only has a new input interface, but a new output interface to couple to the high-bandwidth computer interface required for our ultimate event rates.

3. Design of a 50-mm XS MCP detector incorporating new electronics

Migration of our laboratory detectors to a flight-demonstrable scheme can be done in a well-defined way, while allowing for the later incorporation of new developments such as high-efficiency photocathodes (GaN) and novel MCPs (Borosilicate Atomic Layer Deposition, ALD), currently in Astrophysics Research and Analysis (APRA) development. Key issues for the XS MCP detector implementation include a low-mass, robust construction scheme that accommodates the capability for a high-vacuum sealed-tube configuration. Without incurring excessive costs, a reasonable format to accomplish this is ~50 mm. Our expectations are spatial resolution of ~20 μm , background rates $< 0.1 \text{ events cm}^{-2} \text{ sec}^{-1}$, low fixed-pattern noise and long lifetime, ~50% quantum efficiency over much of the Extreme-UV (EUV) – Far-UV (FUV) band, multi-megahertz rate capability with low dead-time, and detector mass of a few hundred grams. The design and construction of brazed body assemblies provides for the best packaging and diversity of applications, so this is one of the core tasks. The overall configuration represents a device compatible with many current sounding rocket experiments, and can be qualified in vibration-thermal-vacuum cycling, *etc.*, in a straightforward manner. It also permits a clear path for use of GaN photocathodes and Borosilicate-ALD MCPs in the future, and is a good stepping-stone for implementation of much-larger-format devices for large optics/missions.

Progress and Accomplishments

Three parallel efforts are expected to come together in the final year of this program – ASIC design and fabrication at the University of Hawaii; FPGA control electronics at UC Berkeley; and 50-mm XS detector design, also at UC Berkeley. Initial versions of the ASICs have been fabricated and tested, as has the 50-mm detector (although using the PXS readout electronics).

ASIC Design

We have so far submitted four ASICs for fabrication and have received three: the 16-channel CSA called “CSA_v2” (Fig. 2) and two versions of the 8-channel HalfGRAPH. The CSA_v2 successfully amplified signal, though with a very high noise value. The HalfGRAPH_ver1 also did not work as expected, because the internal Digital-to-Analog converters (DACs) that bias many of the circuit elements could not be set via the shift register (which did work). We believe we have traced this mistake to the conversion of an existing design to a different design and modeling software (from Tanner to Cadence). We proceeded to redesign the HalfGRAPH (version 2), fixing this error as well as others identified. Therefore, we have no results to present for the HalfGRAPH_ver1. The section below discusses this new design of the HalfGRAPH2 which has been fabricated, packaged, and delivered; and is starting initial testing soon.

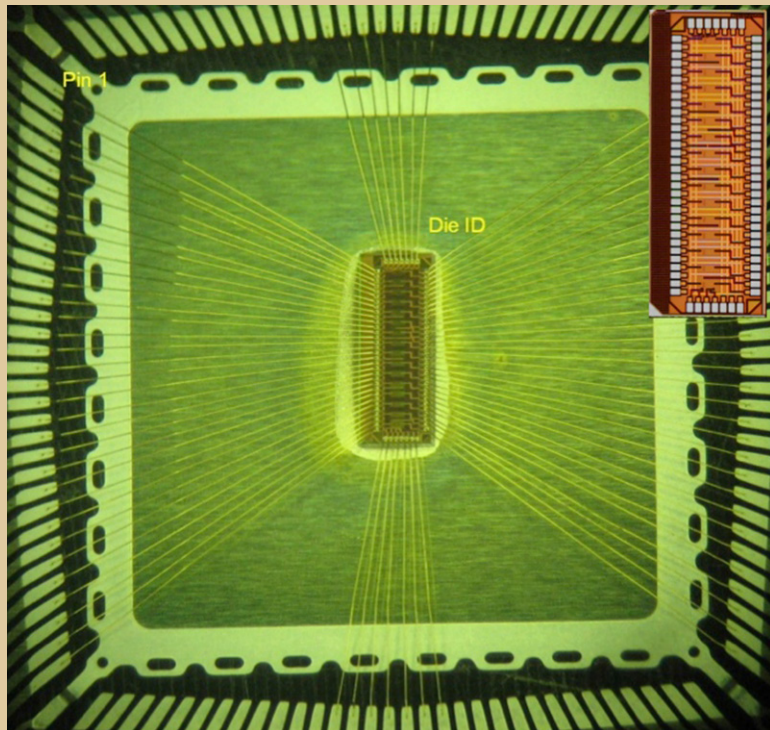


Fig. 2. CSAv2 mounted on 128-pin package with 16 inputs on the left and 16 outputs on the right (inset: die close-up).

rise-time and an ~ 80 ns return to baseline, achieving our timing goals. However, the best noise performance achieved by biasing the circuit was ~ 2300 e^- rms. In terms of gain, the chip exhibits inconsistent behavior from channel to channel. Computer simulations reveal several design flaws that contribute to a suboptimal noise floor. Measuring and modeling the behavior of the CSAv2 has led to important insights on what to redesign for the next version of the amplifier (CSAv3).

CSAv3

In parallel to measurements and simulations, a more basic study investigated better coupling between the stages using circuit analysis tools in the Octave programming language. A transfer function was identified which gave good pulse shaping, with the pulse rise and fall time completed in under 50 ns. The next version of the amplifier, CSAv3, is a complete redesign addressing these issues by resizing the input capacitor, providing a better power-supply-rejection ratio, adding internal DACs for each channel, and improving the basic architecture of the amplifier.

An overall analog schematic for the preamp is shown in Fig. 3. The input CSA is a folded-cascade amplifier with a voltage-controlled feedback resistance to control the return to baseline. It is followed by a standard pole-zero-cancellation (PZC) circuit to return to the baseline faster, and then a shaper circuit with choices of gain and time constants. The signal is then brought to a final buffer amplifier that can drive the downstream HalfGRAPH input. We added the ability to change the signal polarity in case this amplifier is used for other applications (e.g., silicon strip detectors). This circuit was extensively simulated to trade speed for noise and linearity. We expect a noise of 580 e^- rms with an input capacitance of 5 pF. Figure 4 shows our nominal pulse shape for various amplitude inputs with rise times < 20 ns and a return-to-baseline on the order of 75 ns. The final design of CSAv3 was submitted to MOSIS on May 10, and we expect die delivery late July 2015.

HalfGRAPH2

HalfGRAPH2 is a 16-channel, 1 giga-sample-per-second waveform digitizing chip with 12-bit resolution (Fig. 5). It is being designed in the Taiwan Semiconductor Manufacturing Company (TSMC) 0.25 μm CMOS

CSAv2

Our goal for the new preamp was to maintain the noise figure of the existing PreShape32 of ~ 1000 e^- root-mean-square (electrons rms) but to increase the waveform speed, doubling the rise-time to 20 ns and significantly decreasing the time back to baseline to < 100 ns to reduce pileup at high event rates. At an MCP gain of 10^6 , the largest signal expected on a single strip is on the order of 50 fC. We chose the number of channels per die to be 16 to help with the fan-in from the 80 inputs from the 50-mm anode. The amplifier should also be able to drive the input of the HalfGRAPH and the short trace between them.

The resultant die (Fig. 2) was fabricated and bonded in a 128-pin package. Initial results were disappointing, requiring extremely careful biasing to keep the signal stable while minimizing noise. The amplifier demonstrated a 22 ns

Preamplifier Circuit

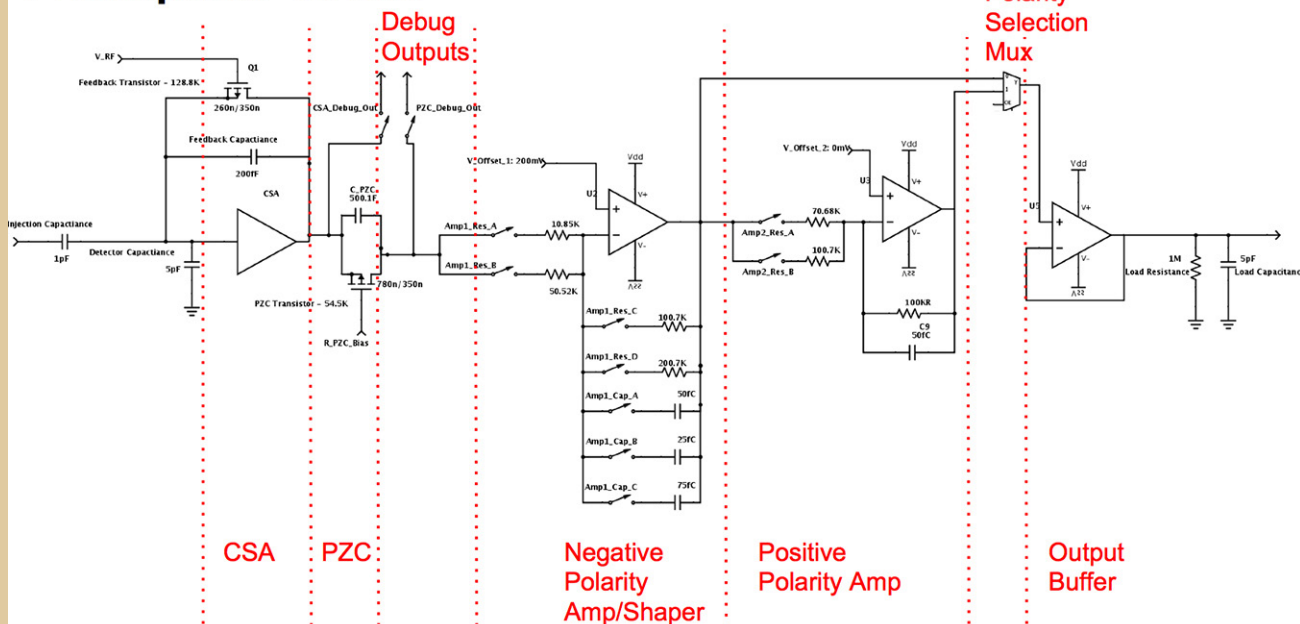


Fig 3. A generalized schematic of the new CSAv3.

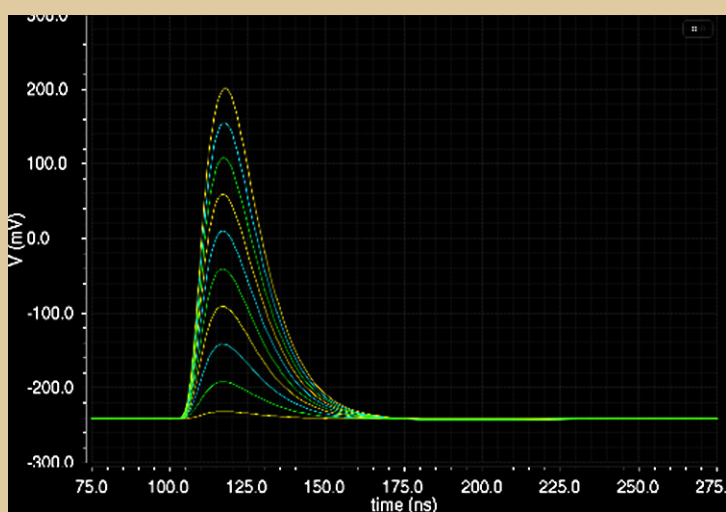


Fig. 4. Simulated output pulses from CSAv3 to various amplitude input charge pulses. Note the 20-ns rise time and a return-to-baseline in 75 ns while retaining a noise value of 580 e^- rms.

technology, using Tanner EDA design and simulation tools. The circuit's heritage is the TeV Array Readout with GSa/s sampling and Event Trigger (TARGET) ASIC used for photomultiplier waveform sampling in a Cherenkov telescope array [8]. Each channel of this digitizer chip has a 2-stage analog storage mechanism. In the first stage, a short sampling array is subdivided into two sample windows each with 32 switched-capacitor storage cells. In the second stage, in a ping-pong fashion, as one sample window is filling, the other is transferred into a larger storage array. This storage array has 8192 cells, organized as two banks of 64 rows of 64 samples each (also called a storage window) for every channel. This results in a continuous sample of 8.192 μ s in length before being overwritten in a circular buffer fashion.

The input analog trigger circuit has four digital output lines that notify a control FPGA of a new event. A trigger pulse is set in place if the measured signal on a channel is higher than a preset threshold. Trigger lines are organized to cover channels 1-4, 5-8, 9-12, and 13-16. This allows finer localization of the strip where the event occurred. The trigger arrival into the FPGA marks the address in the storage array of the samples for that event.

HalfGRAPH2 ASIC

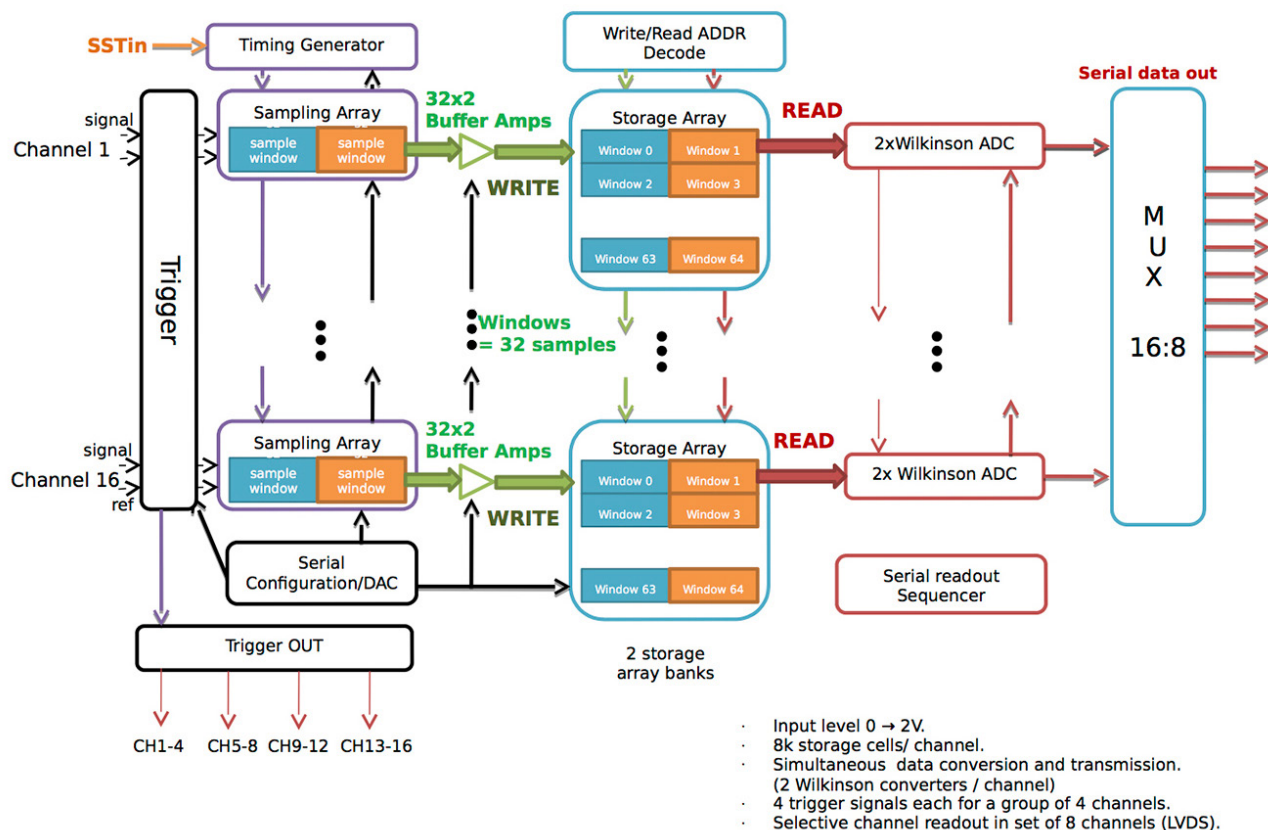


Fig. 5. Functional schematic of the HalfGRAPH2 ASIC design (described in detail in the text).

In order to digitize the acquired signal, each channel uses two banks of 12-bit Wilkinson ADCs. An FPGA selects the storage window to be digitized. Thirty two analog samples in parallel on all 16 channels of the storage window are converted concurrently into digital values using comparators, a voltage ramp, and counting (12-bit counter) with a 500-MHz dual-phase clock until the comparator fires when the ramp exceeds the analog value on the cell. It takes $4.1 \mu\text{s}$ to complete the digitization. At this point, the 32 time samples of 12-bit data are sent out serially over LVDS lines with a 250-MHz clock to the FPGA in $1.5 \mu\text{s}$ ($=12 \times 32 / 250 \text{ MHz}$). This is done for a subset of eight channels in parallel, chosen by the FPGA based on trigger information, allowing the centroid calculation using the properly filtered amplitude derived from the waveform. When the data transfer starts, the next window is digitized by the second Wilkinson converter which takes over the next transmission, saving $1.5 \mu\text{s}$.

Because the FPGA has the address of the events in the storage array, it can prevent overwriting of those cells. Therefore, the throughput of the system is limited by the ADCs' $4.1 \mu\text{s}$ conversion time. The maximum throughput of one channel is 240 kHz, but there is no dead time at rates below this frequency due to the multiple buffering. With five independent ASICs per axis, the event rate that can be supported is 1.2 MHz. The readout rate can be greatly increased by decreasing the bit resolution. For a 10-bit converter, the event rate could reach 5 MHz. Since the event data will be digitally filtered by the FPGA processing, 10 bits will most likely be more than enough to achieve high signal-to-noise ratio.

The 16-to-eight multiplexer allows selection of a group of eight channels out of 16, thus reading out all 16 channels is not necessary. During the operation, a total of eight strips will be transferred per event, allowing the centroid calculation with the properly filtered amplitude derived from the waveform samples. Meanwhile, during data readout, fresh events are stored in the storage array being prepared to read out. This allows multi-hit readout system operation as long as the storage array does not overflow.



Fig. 6. HalfGRAPH2 ASICs in packages.

The HalfGRAPH2 design was submitted to the foundry at the end of 2014, and 750 packaged dies (Fig. 6) were returned mid-May 2015. Special test boards have been designed and are being fabricated, and we expect the first result in July 2015. Scaling from the TARGET designs, we expect the power consumption to be on the order of ~ 10 mW/channel (quiescent), so for 160 channels (X and Y) the total power dissipation is expected to be 1.6 W, but higher for high event rates.

FPGA Controller

It is a bit premature to design the FPGA controller until the ASIC control circuits and output designs are more complete, but initial discussions of the required resources have started. The HalfGRAPH2 will have an LVDS line per channel to meet our throughput requirements, and if we design for 80×80 channels, that would mean 160 LVDS lines running at 250 MHz. Our scheme to avoid this is to use a simple but fast FPGA (*e.g.*, Spartan) to divide by four the number of LVDS lines required, by condensing four 250-MHz lines

into a single GHz LVDS line into the downstream FPGA. These rates are not a problem for current-generation FPGAs, even flight-qualified ones.

50-mm XS Detector

There are two key aspects to our new flight-like 50×50 mm XS detector design. The first is a photolithographic and laser-cut XS anode design made with polyimide. Polyimide's dielectric constant is a factor of three less than alumina ceramic, resulting in lower individual strip capacitance, and therefore lower amplifier noise. The top strip pattern is first etched in the copper, and then a laser ablates the material between the strips. This top layer is then bonded to the bottom strip pattern etched on a much thicker polyimide substrate. The input side of the anode is shown in Fig. 7, installed in the 50-mm XS detector, with the measured strip capacitances matching our design model. Outputs from the 80×80 strips go through a hermetic seal consisting of 2×80 pin connectors sealed with vacuum epoxy (Fig. 8). The other key aspect of our detector is using a Kovar and ceramic brazed body to mount the MCPs over the XS anode. This technique is used in vacuum image tube construction to make a strong, robust, and clean detector that can survive launch stress. Figure 7 shows the brazed body mounted over our XS anode onto a vacuum back-plate with three high voltage (HV) feedthroughs (the MCPs have been removed to show the anode below).

Imaging Results with 50-mm Detector

As the readout ASICs are still under development, we used our existing PXS_II electronics and the 64-channel amplifier boards to read out the central 64×64 strips of this 80×80 XS anode. This corresponds to a central active area of $40 \text{ mm} \times 40 \text{ mm}$. The results below use a stack of two MCPs from Photonis USA with $10\text{-}\mu\text{m}$ pores on $12.5 \mu\text{m}$ centers $53.7 \text{ mm} \times 53.7 \text{ mm}$ and 60:1 L/d ratio ($600 \mu\text{m}$ thick each). We measured the spatial resolution and linearity, and acquired flat fields to measure the UV response uniformity to 183-nm light from a Hg pen-ray lamp.

To measure the spatial resolution, we used a pinhole mask grid mounted directly on the input MCP. The pinholes are $10 \mu\text{m}$ in diameter and spaced 1 mm apart on a square grid (Fig. 9), an excellent method of

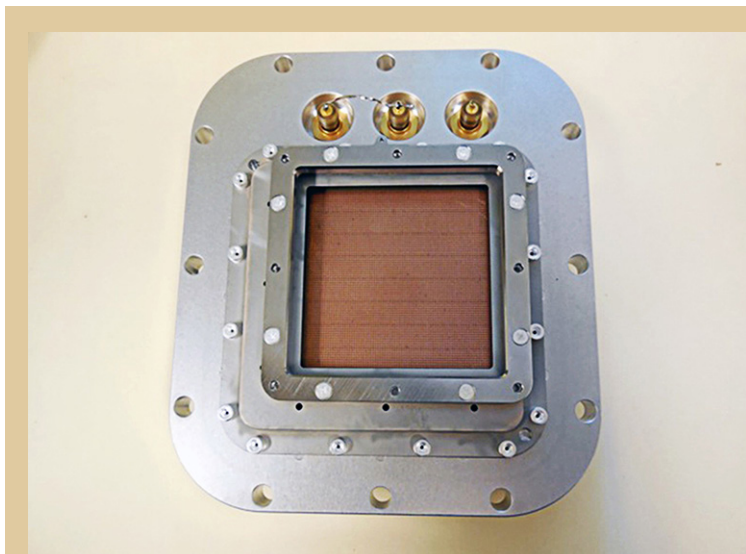


Fig. 7. View of windowless 50-mm XS detector mounted on a vacuum flange with three HV feedthroughs showing the XS anode (MCPs removed).

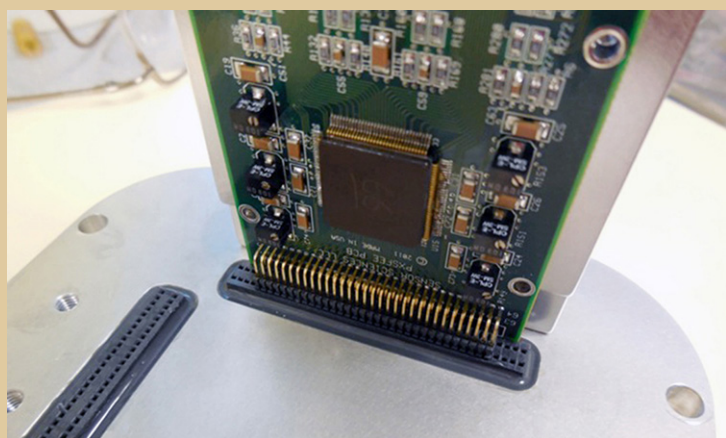


Fig. 8. External side of detector showing 80 contact feedthroughs ($\times 2$) sealed with epoxy and a 64-channel preamp board plugged into one axis.

sampling the Point Spread Function (PSF) across the field of view. To measure the spatial resolution, we had to bin the X, Y event data to 8192×8192 (5- μm pixels) to resolve the PSF. The inset of Fig. 9 shows the X dimension PSF (top strips) of a single pinhole. The average spatial resolutions in the X and Y dimensions were 17.5 μm FWHM and 22 μm FWHM, respectively.

The detector linearity can also be measured with the pinhole mask data, as the pinholes are uniformly spaced at 1 mm. Figure 10 shows the residuals (in μm) to a linear fit to the pixel position of the pinhole vs. pinhole number. The $\pm 15\text{-}\mu\text{m}$ deviation from zero is smaller than the detector spatial resolution measured above, and comparable to the hexagonal 12.5- μm pore spacing. This measurement attests to the accuracy of the photolithographic anode strip regularity.

No detector has a perfectly flat response. For MCP detectors, a uniform input illumination can reveal variations in the MCP sensitivity plus nonlinearities in the X, Y determination of the charge cloud centroid by the anode. To measure response flatness, we collected more than 30 billion counts to achieve 460 counts per 5- μm pixel. Figure 11 is a small, 2.5 mm \times 2.5 mm section of a UV flat field. There is a hint of fixed pattern noise and compressing the data in both dimensions

reveals the presence of a differential nonlinearity at the strip spacing in the Y (bottom) dimension. The effect is at the 3% level peak-to-peak, and can be corrected with a lookup table. We used this flat field to divide another flat field taken the next day (140 counts per 5- μm pixel) and binned to 20- μm pixels. The second flat had only 34% of the counts of the first flat, but the resultant divided image, Fig. 12, shows no fixed pattern and is consistent with Poisson statistics expected from the two images. The inset of Fig. 12 is the histogram of the image pixel values, and has a standard deviation of 2.3%.

Environmental Testing of 50-mm Detector

One of the main goals of this SAT program was to increase the TRL of the 50-mm detector system. Since the new 50-mm detector on its backplate is a new design, we decided to go beyond testing its performance on the bench, and confirm its performance at temperature extremes and its ability to survive the g-forces of standard rocket launches.

The detector and front-end electronics were mounted onto a vacuum housing inside a thermal chamber and cycled from -30°C to $+45^\circ\text{C}$ (Fig. 13). We measured the detector performance between -15°C and $+45^\circ\text{C}$ (allowing the temperature to equilibrate for ~ 1 hour at each test level). At each temperature, we took a deep UV flat field. Because we had a smattering of small dead spots on the detector that acted

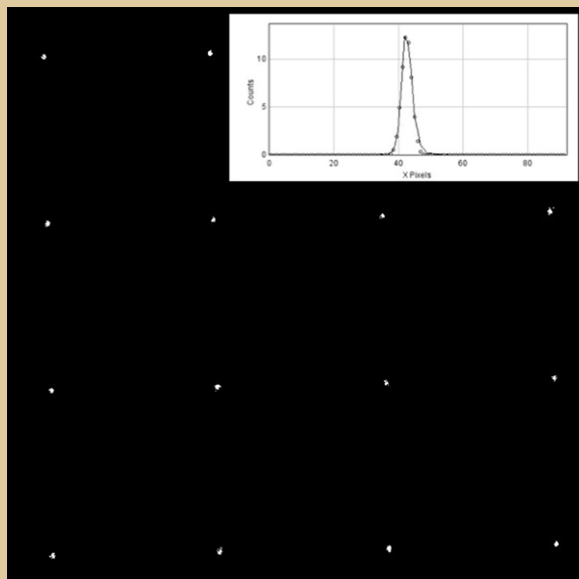


Fig. 9. UV image of pinhole mask of 10- μ m holes on 1-mm square grid. Inset shows the PSF of a single hole with resolution of ~4 pixels FWHM (20 μ m).

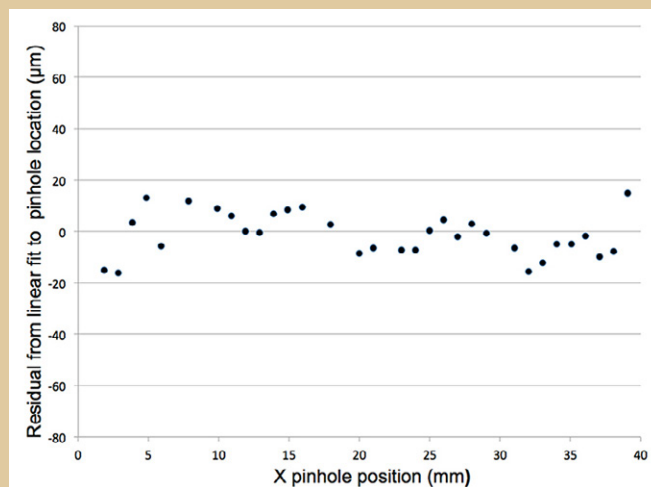


Fig. 10. Residuals to linear fit of derived pinhole position across central 40 mm of the 50-mm XS detector.

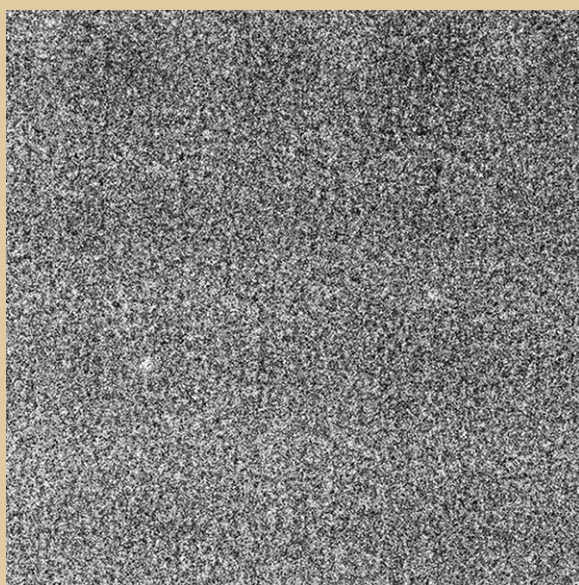


Fig. 11. Small section of very deep (2500 cts/pxl) flat field showing a small but noticeable fixed pattern noise.

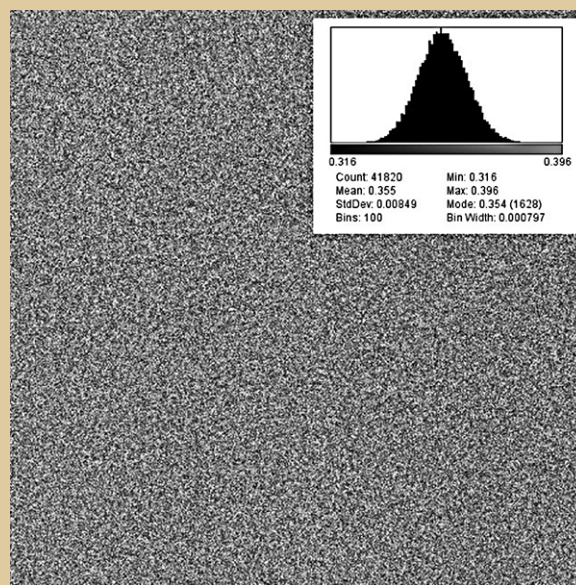


Fig. 12. Same image as Fig 11, but divided by deeper flat field. Residual variation is consistent with the expected Poisson counting statistics (2% standard deviation, inset).

as spatial fiducials, we were able to notice a shift in the image of ~30 microns over a 60°C temperature swing. Since this shift was in the MCP-bias direction, we believe this was due to the electron-cloud kinematics caused by thermally induced MCP gain variation. It speaks to the XS detector's excellent spatial resolution that we can even measure this effect and in all other measures – resolution, background rate, and dynamic range – the detector worked flawlessly.

We also used the SSL vibration table to vibrate the detector (without the electronics) to 14.1g (rms) as recommended in the GSFC General Environmental Verification Standard (GSFC-STD-7000A). Figure 14 shows the detector backplate (air side) on the test fixture and Table 1 shows the vibration spectrum levels we applied to the detector. UV imaging performance was exactly the same before and after vibration, showing this new detector design is ready for flight vibrations.

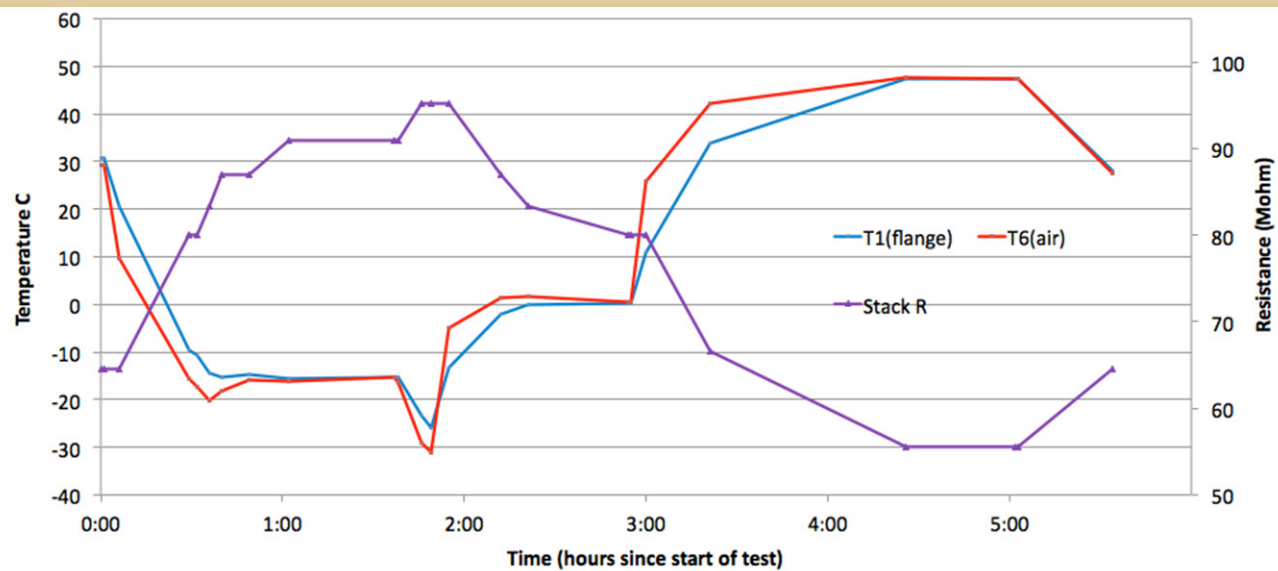


Fig. 13. Detector temperature and MCP resistance during thermal test of XS detector.

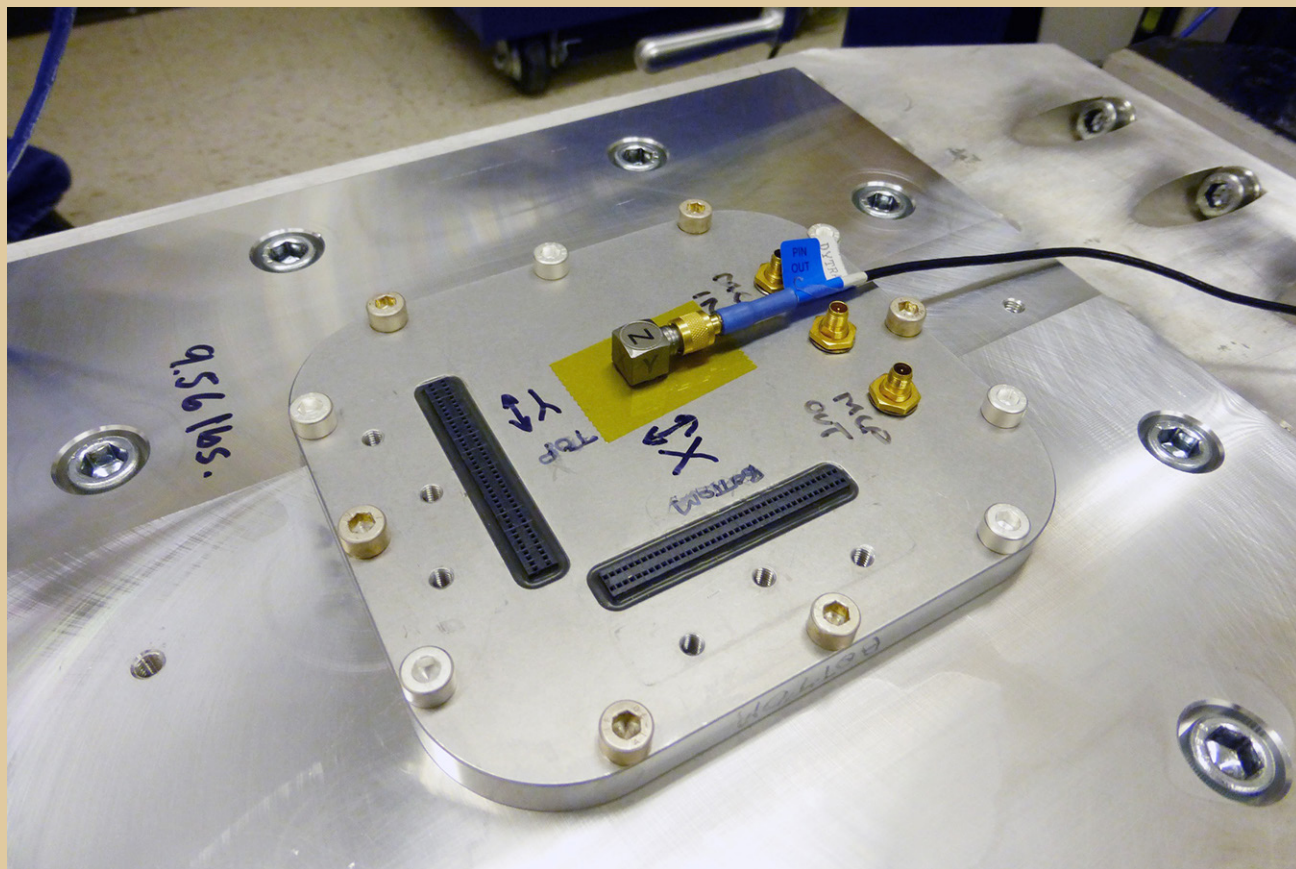


Fig. 14. 50-mm XS detector mounted on vibration table at SSL.

Frequency (Hz)	g^2/Hz	dB/Octave
20	0.026	5.97
50	0.16	0
800	0.16	-5.97
2000	0.026	—

Table 1. Vibration frequency spectrum (14.1g rms).

Path Forward

We expect to begin the detailed electronic testing of the HalfGRAPH2 ASIC on our specialized test board to measure its capability to digitize fast input signals, as well as its power dissipation. The CSAv3 is due to arrive by late August, and we can immediately begin analog testing of its noise, gain, and power characteristics. Once we have confirmed the ASICs' stand-alone performance, we can begin to incorporate them into our FPGA control boards and couple them to the 50-mm XS detector. We will start full performance testing of the 50-mm detector and anode using the new ASIC XS electronics and begin environmental testing, with the goal of finishing by the contract completion date of Feb 2, 2016.

References

- [1] J. Vallergera, R. Raffanti, M. Cooney, H. Cumming, G. Varner, and A. Seljak, "Cross strip anode readouts for large format, photon counting microchannel plate detectors: developing flight qualified prototypes of the detector and electronics," Proc. SPIE, Vol. **9144**, 91443J (2014)
- [2] K. Hoadley, K. France, N. Nell, R. Kane, T.B. Schultz, M. Beasley, J.C. Green, J.R. Kulow, E. Kersgaard, and B.T. Fleming, "The assembly, calibration, and preliminary results from the Colorado high resolution Echelle stellar spectrograph (CHESS)," Proc. SPIE, Vol. **9144** (2014)
- [3] P. Scowen *et al.*, "The Star Formation Observatory (SFO) mission to study cosmic origins," Proc. SPIE, Vol. **7010**, 115 (2008)
- [4] K. Sembach, M. Beasley, M. Blouke, D. Ebbets, J. Green, F. Greer, E. Jenkins, C. Joseph, R. Kimball, J. MacKenty, S. McCandliss, S. Nikzad, W. Oegerle, R. Philbrick, M. Postman, P. Scowen, O. Siegmund, H.P. Stahl, M. Ulmer, J. Vallergera, P. Warren, B. Woodgate, and R. Woodruff, "Technology Investments to Meet the Needs of Astronomy at Ultraviolet Wavelengths in the 21st Century," Astro2010: The Astronomy and Astrophysics Decadal Survey, Technology Development Papers, no. 54 (2009)
- [5] J. Vallergera, R. Raffanti, A. Tremsin, O. Siegmund, J. McPhate, and G. Varner, "Large-format high-spatial-resolution cross-strip readout MCP detectors for UV astronomy," SPIE Vol. **7732** (2010)
- [6] X. Michalet, R.A. Colyer, J. Antelman, O.H.W. Siegmund, A. Tremsin, J.V. Vallergera, and S. Weiss, "Single-quantum-dot imaging with a photon counting camera," Current Pharmaceutical Biotechnology **10** (5), pp. 543-558 (2009)
- [7] F.B. Berendse, R.G. Cruddace, M.P. Kowalski, D.J. Yentis, W.R. Hunter, G.G. Fritz, O. Siegmund, K. Heidemann, R. Lenke, A. Seifert, and T.W. Barbee Jr., "The joint astrophysical plasmadynamic experiment extreme ultraviolet spectrometer: resolving power," SPIE Conference Series, Vol. **6266**, 31 (2006)
- [8] K. Bechtol, S. Funk, A. Okumura, L.L. Ruckman, A. Simons, H. Tajima, J. Vandenbroucke, and G.S. Varner, "TARGET: A multi-channel digitizer chip for very-high-energy gamma-ray telescopes," Astroparticle Physics, **36**, 156-165 (2012)

For additional information, contact John Vallergera: jvv@ssl.berkeley.edu



A Far-Infrared Heterodyne Array Receiver for CII and OI Mapping

Prepared by: Imran Mehdi (PI; JPL, Caltech) and Paul Goldsmith (JPL, Caltech)

Summary

This task was proposed under the 2012 Strategic Astrophysics Technology (SAT) call and was funded in January 2014 for a period of three years. Heterodyne spectroscopic instruments are the only technical possibility for obtaining velocity-resolved spectra in the far-infrared (Far-IR). Building on the Heterodyne Instrument for the Far-Infrared (HIFI) hardware developed by JPL, the focus of this task is to demonstrate a working 16-pixel heterodyne array receiver system. Most components for this system have been demonstrated, but a full 16-pixel system needs to be tested to bring this technology to Technology Readiness Level (TRL) 5. This receiver system enables science beyond HIFI for the next generation of heterodyne instruments on platforms including long-duration and ultra-long-duration balloons, and aircraft observatories such as the Stratospheric Observatory for Infrared Astronomy (SOFIA). GaAs Schottky diode-based high-power multipliers pumped by W-band power amplifier modules, superconducting hot-electron bolometer-based mixers, low-power cryogenic intermediate frequency (IF) amplifiers, and a digital back-end will be integrated and demonstrated in a modularized 16-pixel receiver with TRL 5. The proposed approach will result in a modular architecture for Far-IR array receivers for upcoming suborbital and space-based Cosmic Origins (COR) observing opportunities.

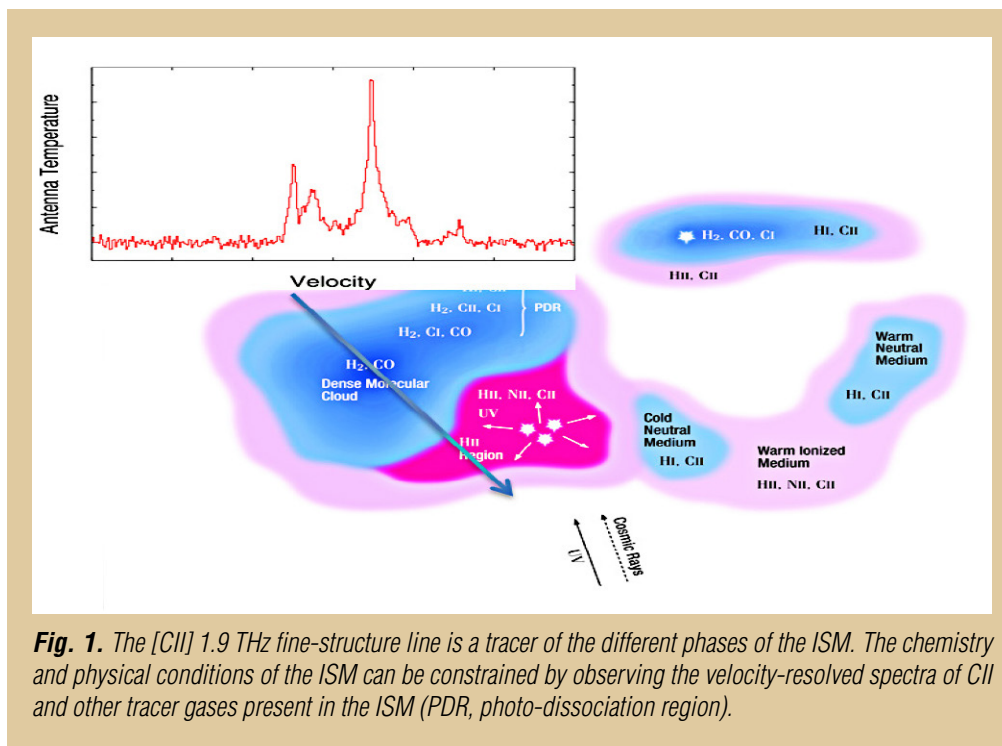
This work is carried out by a team of JPL scientists and technologists, including Imran Mehdi, Paul Goldsmith, Jon Kawamura, Jose Siles, Robert Lin, Choonsup Lee, Bruce Bumble, Adrian Tang, Rod Kim, and Jenna Kloosterman.

Background

The details of the evolution of molecular clouds and the formation of the next generation of stars out of the dust and gas in these dense regions remain mysterious. It is abundantly clear from a large number of Herschel photometric observations with the Photodetector Array Camera and Spectrometer (PACS) and the Spectral and Photometric Imaging Receiver (SPIRE) that the dust is filamentary in nature and that the filaments contain a large number of dense cores [1-4]. Many of these are self-gravitating and likely to form stars, but evidence of star formation is far from universal. What cannot be determined from the photometry is the velocity structure of these filaments, or their relationship to the various phases of the Interstellar Medium (ISM). Photometry cannot trace the processes that lead to the origin of the filaments and the likelihood that stars will form in the cores that form within them [5-8]. Velocity information is required to assess the role of turbulence and gravity in determining the kinematics of the ISM and its evolution into new stars. Not surprisingly, the best tracers of velocity are the strongest available lines – CII and OI, which are complementary in that they trace different regimes of extinction. The molecular tracer CH can be used as a surrogate for H₂, and thus trace the total gas column density. CH has a ground state that interacts strongly with magnetic fields through the Zeeman effect, making it a potential tracer of magnetic fields.

High-spectral-resolution observations will facilitate determination of velocity along the line of sight, allowing the relative motions and states of the ISM to be mapped and correlated with the observed dust structures and evolution of starless and pre-stellar cores. Simultaneous observation of combinations of lines correlated with previous photometric maps allows direct observation of the interactions between ISM phases and the connection of the gas with the dust. High resolution is required to understand the turbulence and dynamics of this interaction, as well as to de-convolve the contributions along the line of sight. Understanding how star formation proceeds in galaxies other than the Milky Way, with different metallicities and at different times in the evolution of the universe, is currently one of the

hottest topics in astronomy. However, understanding these sources will require advanced spectroscopy and better understanding of “prototypical” nearby sources in our own and nearby galaxies. Figure 1 shows heterodyne observations through the Milky Way in CII, HI, and CO, showing how they trace different, but interrelated, regions in the interstellar medium.



Heterodyne array receivers in the Far-IR range will be required to answer questions raised in the 2010 Decadal Survey, New Worlds, New Horizons in Astronomy and Astrophysics (NWNH) [9]. HIFI provided the first glimpse into the universe in this frequency range but had only a single pixel and the mission has now been decommissioned (after using up the cryogen). Technology being developed under this task will allow one to map large areas of the sky instantaneously and provide contextual information that is difficult to patch with single-pixel systems. At the conclusion of this work, we intend to demonstrate a 16-pixel array receiver covering 1.9-2.07 THz with a TRL of 5.

Objectives and Milestones

The main objective of this task is to advance heterodyne array receiver technology from TRL 4 to 5. This will be accomplished by building and characterizing a 16-pixel 1.9 THz array receiver that can enable mapping of the C+ line on platforms such as long-duration balloons and aircraft observatories. The technology is also compatible with flight instruments and can be utilized for future submillimeter-wave instruments for astrophysics. The proposed scheme of the 16-pixel array receiver is shown in Fig. 2 with only a single 1×4 module shown for clarity. The signal from the telescope is combined with the local oscillator (LO) signal via a diplexer, and then fed into the mixer element via a machined feed-horn. This approach provides the flexibility of quasi-optical coupling and redundancy since each mixer is pumped by a dedicated LO chain. The mixer and IF amp are cooled to cryogenic temperature (4 K) to provide higher sensitivity.

The receiver system can be divided into three subsystems, namely,

1. LO subsystem.
2. Mixer and IF amplifier subsystem.
3. Back-end subsystem.

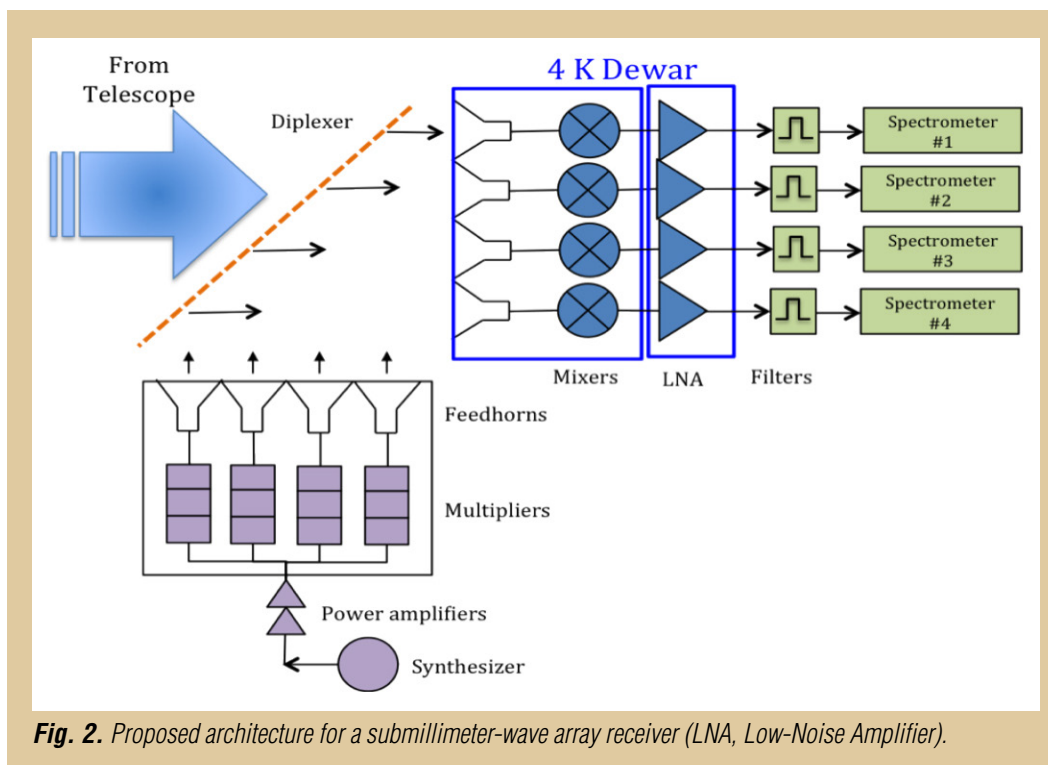


Fig. 2. Proposed architecture for a submillimeter-wave array receiver (LNA, Low-Noise Amplifier).

All three subsystems have been demonstrated in single-pixel systems. The proposed task will bring all three subsystems together to define the ‘relevant environment’ as a functional 16-pixel array receiver. A number of technical problems have to be addressed for building up the array receiver. The architecture of the system, especially the LO subsystem, is critical as all of the LO signals need to be phase-locked. By demonstrating the operation of this 16-pixel receiver system, we will validate it has achieved TRL 5. Further TRL advancement would then require the determination of the relevant environment (balloon, aircraft, space-borne, *etc.*) and environmental tests such as thermal and Radio Frequency (RF) cycling, *etc.*, consistent with the selected platform.

Table 1 lists the major milestones associated with the full three-year development effort. Funding for this task was made available in January 2014 and significant progress has been accomplished, as detailed in the next few sections.

Progress and Accomplishments

LO subsystem

The proposed LO subsystem is shown in Fig. 3. In the last year, significant progress has been made in accomplishing the goal of making a 4-pixel LO subsystem. Since the 16-pixel system will be based on four such modules, this is the first step in demonstrating multi-pixel receivers. A commercially available microwave monolithic integrated circuit (MMIC) has been identified that can be used as the power amplifier. All components for a 4-pixel LO subsystem have been designed and fabricated. Figures 4 – 8 show the completed components for this subsystem along with their measured performance. The first 4-pixel LO module has also been assembled and is shown in Fig. 9. The measured performance from this 4-pixel LO chain is shown in Fig. 15.

Hot Electron Bolometer (HEB) mixer devices

HEB mixers provide one of the most sensitive detectors in this frequency range. The HEB mixers for this task will be packaged in specially fabricated waveguide housings. We believe that by utilizing waveguide-based structures we can provide a more controlled matching environment for the device, thus reducing out-of-band noise. Moreover, the waveguide approach allows us to implement more sophisticated circuit topologies such as balanced mixers, and provides a relatively straight-forward path towards arrays.

Milestone		Completed by	Status
System design			
	System architecture design	March 2014	Completed
	Interface design	June 2014	Completed
	Production of 3-D drawing	August 2014	Completed
Development of high-sensitivity HEB array			
	Design of mixer devices and waveguide housing	July 2014	Completed
	Fabrication of HEB devices	September 2014	Completed
	Fabrication of waveguide housing	October 2014	Completed
	Assembly of 4-pixel mixer array	December 2014	Completed
	Fabrication of optimized HEB mixers	April 2016	
	Fabrication of 16-pixel block	June 2016	
	Assembly and testing of 16-pixel mixers	December 2016	
Development of LO subsystem			
	Design of first-stage tripler	March 2014	Completed
	Design of second-stage tripler	May 2014	Completed
	Procurement of power amps	October 2014	Completed
	Fabrication of multiplier chips	December 2014	Completed
	Fabrication of multiplier blocks	March 2015	Completed
	Assembly of 4-pixel prototype	July 2015	Completed
	Design of 16-pixel module	December 2015	
	Fabrication of 16-pixel block	February 2016	
	Integration of 16-pixel LO subsystem	April 2016	
	Characterization of 16-pixel LO subsystem	May 2016	
Back-end electronics			
	Design of CMOS-based back-end spectrometer	June 2015	Completed
	Prototype assembly with 4-pixel readout	July 2015	Completed
	Spectrometer integration with mixer array	August 2015	In progress
	Detailed characterization of CMOS back-end	December 2015	
System integration and validation			
	Assembly of 4-pixel receiver	September 2015	In progress
	Test and validation of 4-pixel receiver	November 2015	In progress
	Assembly of 16-pixel receiver	September 2016	
	Test and validation of 16-pixel receiver	December 2016	

Table 1. Progress is being made in completing major milestones related to this task.

Since the waveguide block requires very small features (< 25 microns), a novel approach of assembling the waveguide blocks has been developed. The channel for the mixer chip (the most critical part of the design) is formed directly by silicon micro-machining. This small silicon piece is then used in the larger metallic waveguide block. This eliminates the micro-plating step, and results in fairly robust waveguide structures. This approach was validated at 2.7 THz and will be used for the mixers needed under this task. Details of the mixer design and assembly have been presented before. This year, the focus was on packaging a 4-pixel mixer block. This task was successfully accomplished as shown in Fig. 10. The 4-pixel waveguide block is about $10\text{ mm} \times 30\text{ mm}$ with a 4-mm inter-pixel spacing.

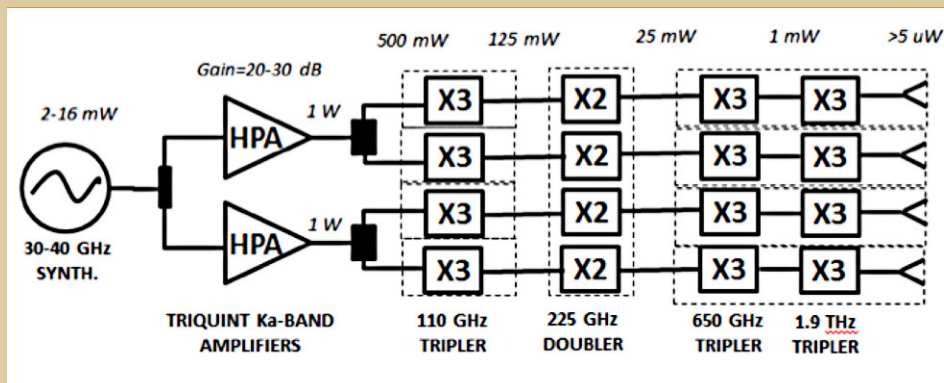


Fig. 3. A modular LO system allows for a compact 16-pixel array receiver.

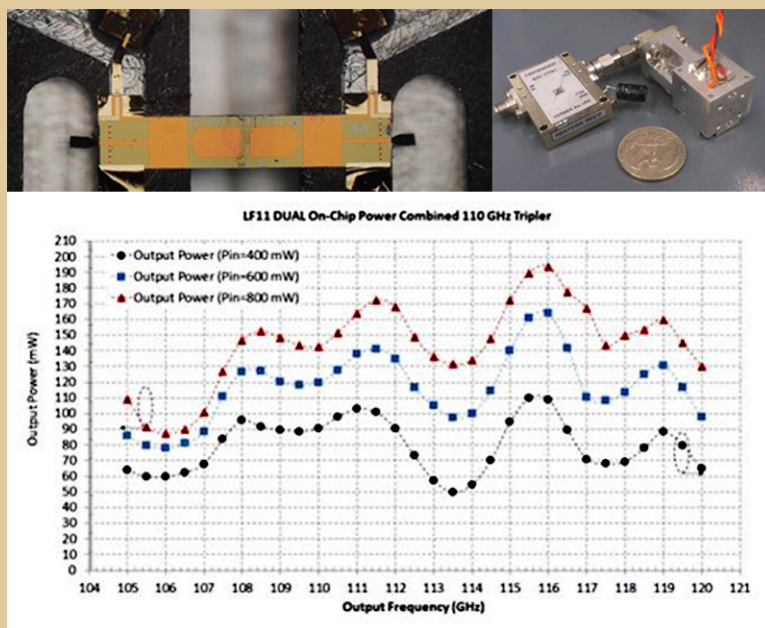


Fig. 4. A high-power 110-GHz tripler has been designed, fabricated, and demonstrated for this task. Top left: Dual-chip tripler packaged in a waveguide cavity. Top right: Power amplifier and waveguide tripler mated together. Bottom: Measured data showing output power from this combination.

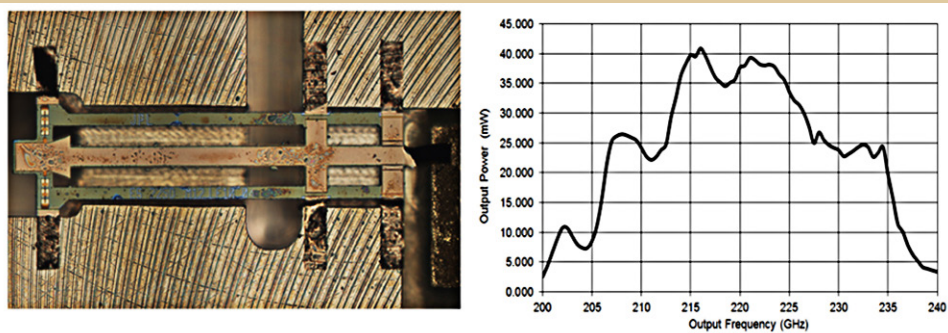


Fig. 5. Performance of the second-stage doubler meets the desired output power and frequency response.

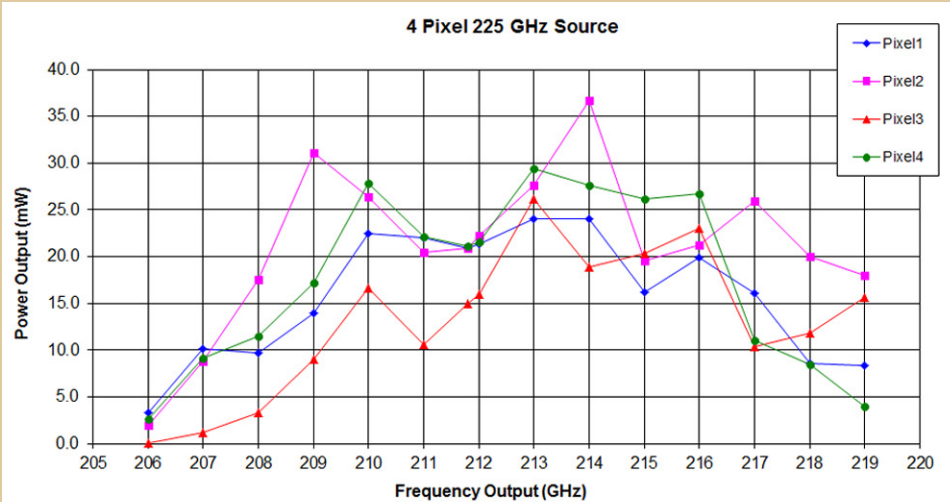


Fig. 6. Measured performance of the four pixels of the 225 GHz doublers. While there is some variability between the four pixels, the output power from each pixel is sufficient to pump the next stage multiplier.

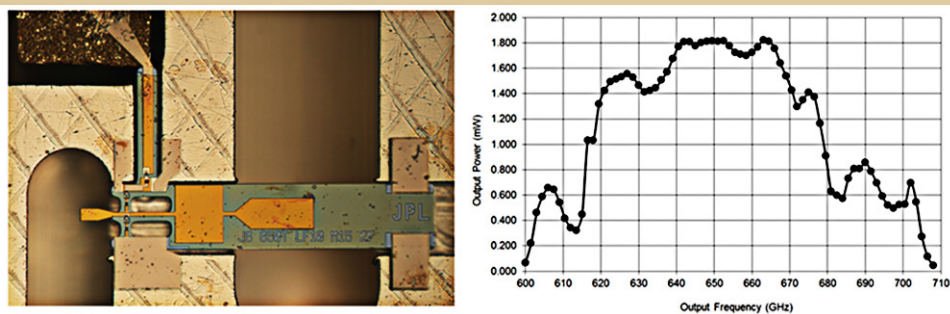


Fig. 7. The third-stage tripler was first mounted and tested in a stand-alone waveguide block. The performance is sufficient to pump the last stage multiplier.

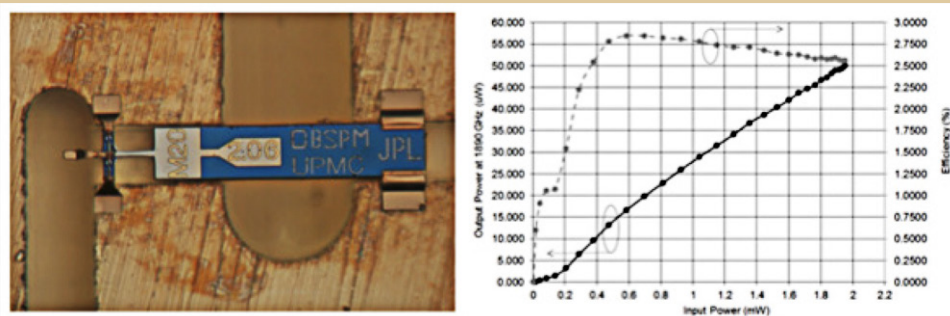


Fig. 8. The final-stage tripler is a biasless design, allowing for simpler implementation of the LO subsystem. These results, measured at room temperature, confirm that sufficient output power is available to pump HEB mixers.

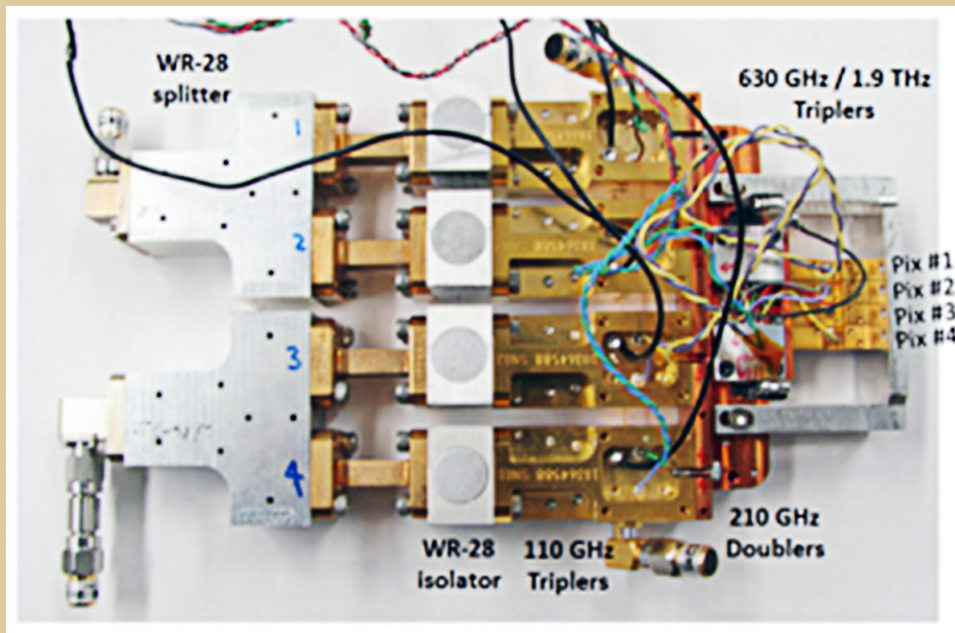


Fig. 9. The 4-pixel LO chain has been assembled. Low-loss isolators are used just before the first multiplication stage to increase subsystem stability.

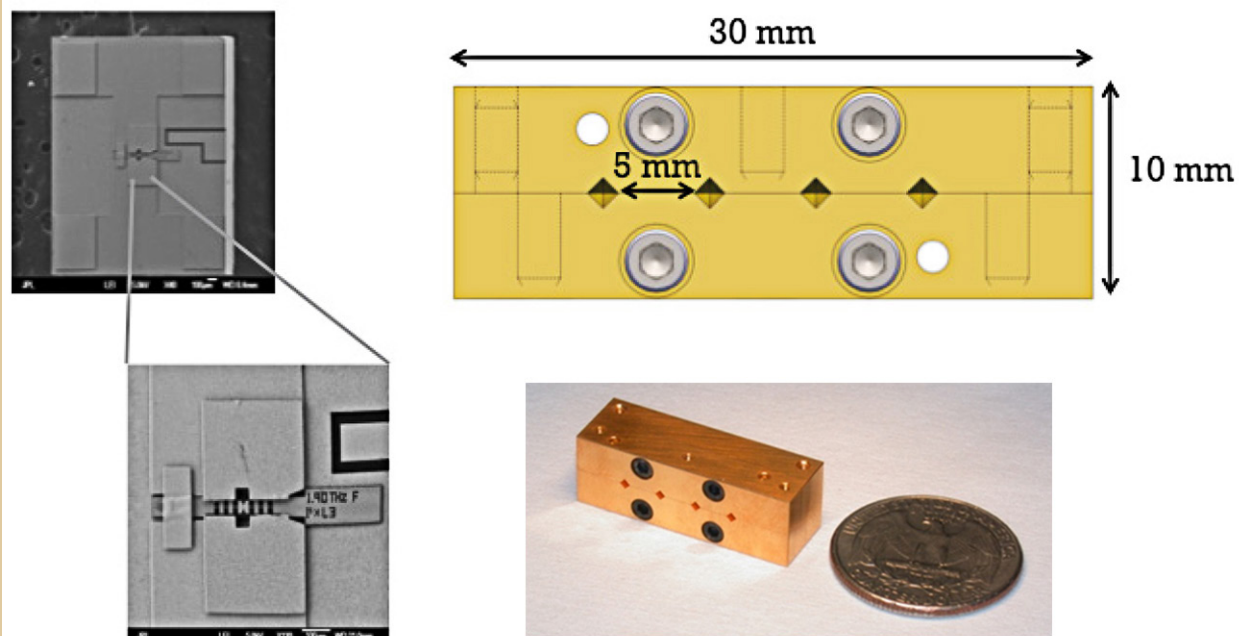


Fig. 10. Top Right: Schematic of completed 4-pixel mixer module. Bottom right: Photo of the 4-pixel mixer module. Top and bottom left: Mixer chip and silicon micro-machined substrate used to mount the mixer chip.

Receiver Back-End (CMOS 4-Channel System-on-Chip Spectrometer Processor)

The system-on-chip (SoC) spectrometer processor module for the 16-pixel sub-millimeter spectrometer is driven by four custom CMOS chips (four pixels per module), previously developed at UCLA. Each chip contains the digitization functions, as well as a Fast Fourier Transform (FFT) processor for spectral computations and averaging/accumulation functions. While the analog-to-digital converter (ADC) offers differential input, it can also be configured for single-ended operation. To reduce overall spectral

processor power, a parallel architecture is employed within the chip, allowing an internal system clock rate at 25% of the input-sampling bandwidth. All functions, including accumulation/observation time and calibration, are controlled through a common control bus that runs to all four channels in parallel. For lab testing, an Atmel 328 microcontroller and USB (universal serial bus) driver are co-located on a printed circuit board (PCB) with the four spectrometer chips. These emulate the Command and Data Handling (C&DH) computer functions of a real spacecraft. Figure 11 shows a simplified block diagram of the 4-pixel spectrometer processor module while Fig. 12 shows the layout of the PCB module with key circuitry identified (left panel) and a microphotograph of the CMOS spectrometer chip with the key circuit blocks identified (right panel).

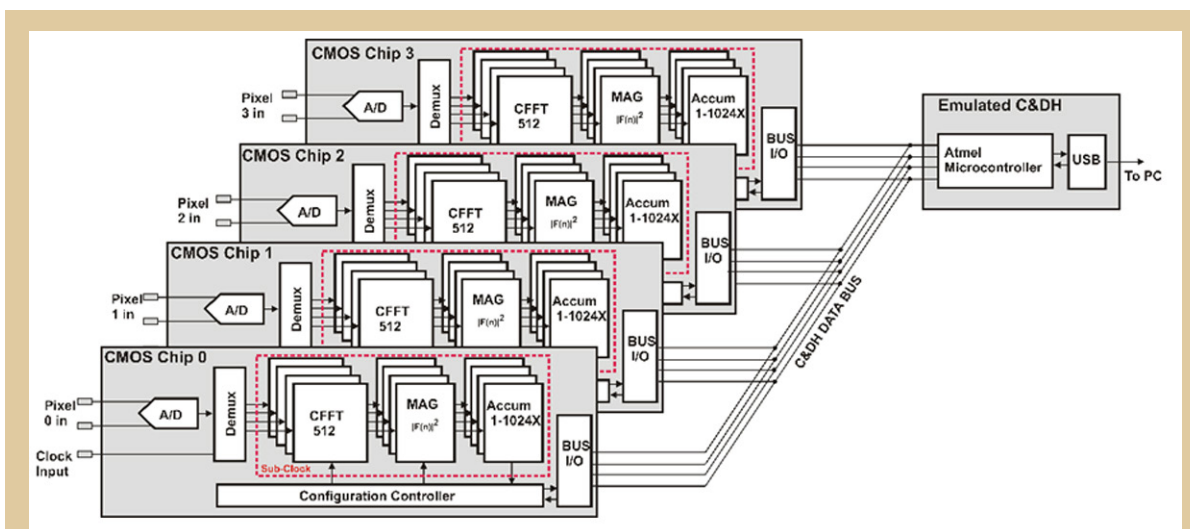


Fig. 11. Block diagram of the 4-pixel back-end spectrometer (A/D, analog to digital; Demux, demultiplexer; CFFT, complex fast Fourier transform; MAG, Magnitude; I/O, input/output).

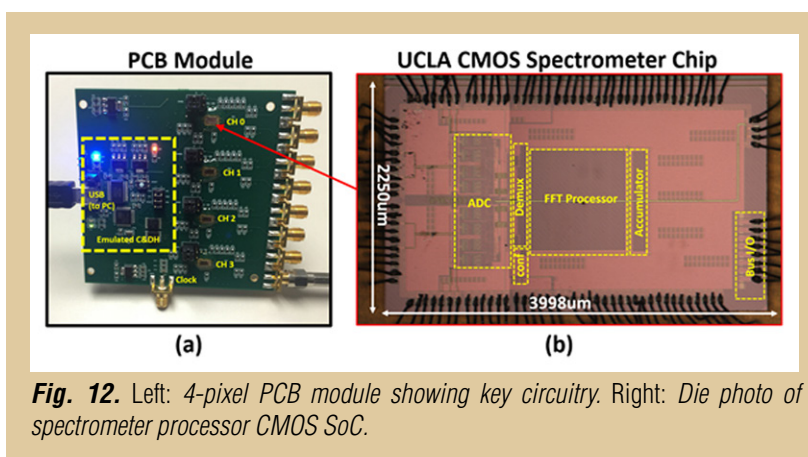


Fig. 12. Left: 4-pixel PCB module showing key circuitry. Right: Die photo of spectrometer processor CMOS SoC.

As an initial test, to ensure all hardware and software drivers are working correctly, each channel was excited using a signal generator capturing the digital outputs in PC software emulating the spacecraft C&DH. Figure 13 shows an example plot with a signal applied at 112.5 MHz (corresponding to spectrometer channel #109). Note that both the strong signal and its harmonics are captured correctly. The entire module consumes 335 mW (83.75 mW per channel) and provides 1 GS/s operation (1 GHz bandwidth with IQ / 500 MHz with Double Side-Band, DSB) with seven physical bits of input resolution.

4-Pixel Receiver Integration and Testing

With the major subsystems of the receiver completed, the receiver integration and characterization work has begun, using an existing cryogenic setup. While minor adjustments for bias and Field of View (FOV) have already been made, the current configuration of the cryostat allows testing of two pixels at a time. The schematic of the receiver testing setup is shown in Fig. 14.

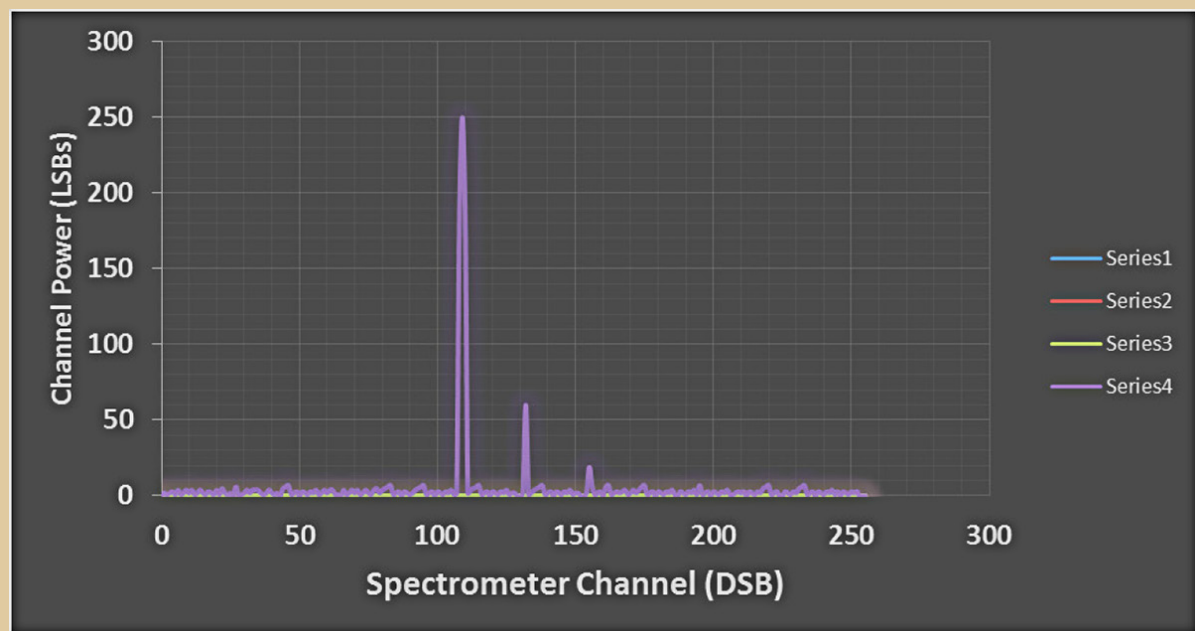


Fig. 13. Initial testing of spectrometer processor showing excitation of the fourth channel with a sine wave from a signal generator.

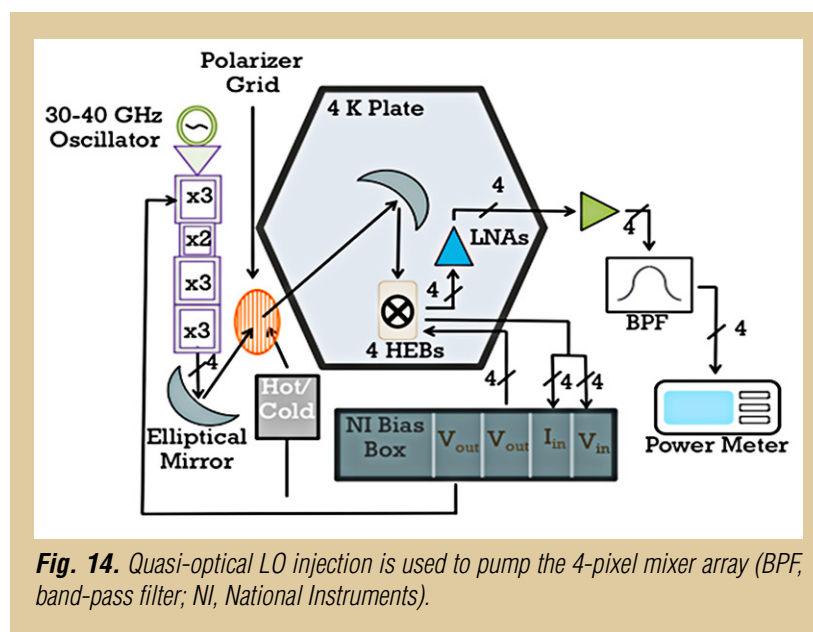


Fig. 14. Quasi-optical LO injection is used to pump the 4-pixel mixer array (BPF, band-pass filter; NI, National Instruments).

The 4-pixel LO chain, described above, was characterized for output power at room temperature, with the measured results shown in Fig. 15. Three of the four pixels work well, producing more than 5 microwatts at 1900 GHz. One of the pixels produces only 3.5 microwatts, which should still be enough to pump a HEB mixer. The best pixel puts out more than 30 microwatts at 1900 GHz.

The lab setup for characterizing the receiver is shown in Fig. 16. The LO signals are focused using an elliptical mirror into the cryostat which holds the mixer block. The LO chain and the mirror can be manipulated to achieve proper alignment. The measured current-voltage (IV) for one of the pixels is shown in Fig. 17. Table 2 summarizes the measured results to date. One of the pixels (with the low LO) also had a malfunctioning HEB mixer. Three of the remaining mixers were characterized successfully.

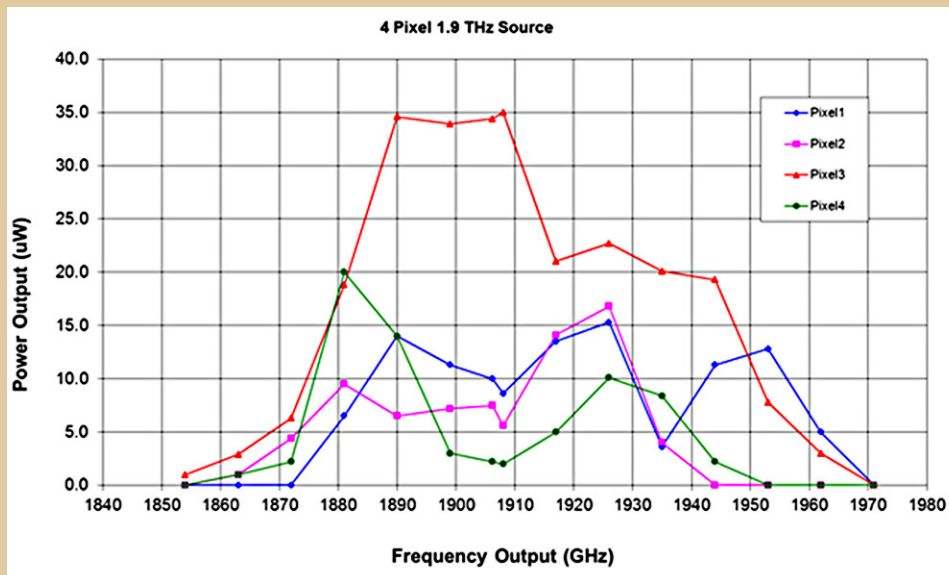


Fig. 15. Three of the four pixels produce more than 5 microwatts at 1900 GHz. All four pixels can be used to demonstrate receiver performance.

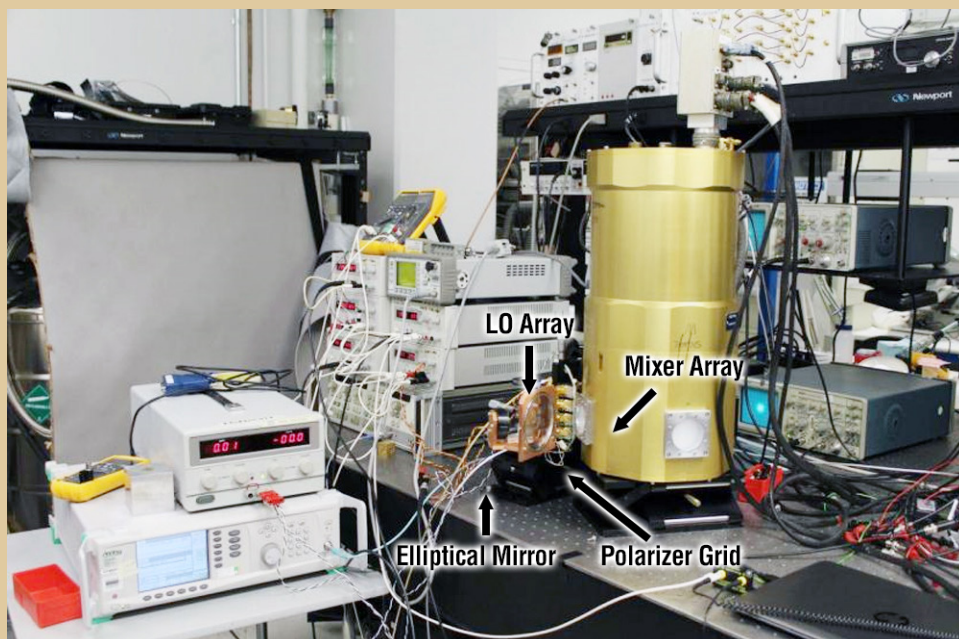


Fig. 16. Lab setup for characterizing the 4-pixel receiver.

Path Forward

Most of the component design work for this task has been completed. A 4-pixel receiver (front-end and CMOS back-end) is currently being assembled and will be characterized thoroughly in the next few months. A 16-pixel system will be demonstrated by the end of the task.

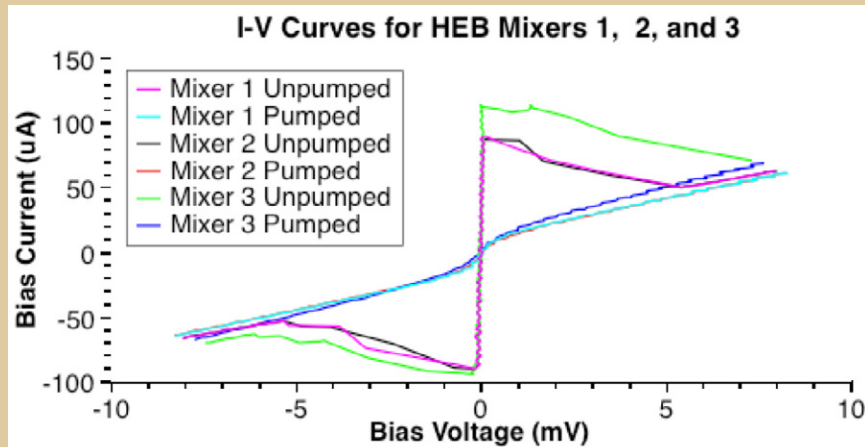


Fig. 17. Measured IV of three pixels with and without LO. Sufficient LO power is available for mixer measurements.

	Ω_{RT}	$I_C (\mu A)$	$V_{BIAS} (mV)$	$I_{BIAS} (\mu A)$	$T_{RX} (K)$
Mixer 1	126	90.2	0.78	13.8	TBD
Mixer 2	114	89.6	0.69	8.6	840
Mixer 3	102	105.4	0.46	11.8	875
Mixer 4	0	N/A	N/A	N/A	N/A

Table 2. Summary of measured mixer performance. Mixer 4 was not operational and Mixer 1 could not be measured in the current test setup.

Acknowledgement

This research was carried out at the Jet Propulsion Laboratory, California Institute of Technology, under a contract with the National Aeronautics and Space Administration.

References

- [1] S. Molinari *et al.*, “Clouds filaments, and protostars: The Herschel Hi-GAL Milky Way,” *Astron. & Astrophys.* **518**, L100 (2010)
- [2] Ph. André *et al.*, “From filamentary clouds to prestellar cores to the stellar IMF: Initial highlights from the Herschel Gould Belt Survey,” *Astron. & Astrophys.* **518**, L102 (2010)
- [3] A. Menshchikov *et al.*, “Filamentary structures and compact objects in the Aquila and Polaris clouds observed by Herschel,” *Astron. & Astrophys.* **518**, L103 (2010)
- [4] V. Konyves *et al.*, “The Aquila prestellar core population revealed by Herschel,” *Astron. & Astrophys.* **518**, L106 (2010)
- [5] P. Padoan, M. Juvela, A.A. Goodman, and A. Nordlund, “The turbulent shock origin of proto-stellar cores,” *Astrophys. J.* **553**, 227 (2001)
- [6] T. Nagai, S.-I. Inutsuka, and S.M. Miyama, “An origin of filamentary structure in molecular clouds,” *Astrophys. J.* **506**, 306 (1998)
- [7] P. Ocvirk, C. Pichon, and R. Teyssier, “Bimodal gas accretion in the Horison-MareNostrum galaxy formation simulation,” *Mon. Not. R. Astron. Soc.* **390**, 1326 (2008)
- [8] F. Nakamura and Z.-Y. Li, “Magnetically regulated star formation in three dimensions: the case of the Taurus molecular cloud complex,” *Astrophys. J.* **687**, 354 (2008)
- [9] “New Worlds, New Horizons in Astronomy and Astrophysics,” Decadal Survey report from the Committee for a Decadal Survey of Astronomy and Astrophysics, National Research Council, ISBN 0-309-15800-1 (2010)



For additional information, contact Imran Mehdi: Imran.mehdi@jpl.nasa.gov

Kinetic Inductance Detector Arrays for Far-IR Astrophysics

Prepared by: Jonas Zmuidzinas (PI; Caltech); Goutam Chattopadhyay, Peter Day, C. Darren Dowell, Rick Leduc, and Chris McKenney (JPL); Pradeep Bhupathi, Matt Hollister, and Attila Kovacs (Caltech)

Summary

This project was initiated in 2013 as a two-year project and extended into a third year (2015) at no additional cost. The project focuses on the development of sensitive detector arrays for far-infrared (Far-IR; $\lambda = 50\text{-}500\ \mu\text{m}$) astrophysics. The detectors must be exquisitely sensitive, capable of measuring power as low as 10^{-16} to 10^{-19} W in a one-second measurement, known as the noise-equivalent power (NEP). Not surprisingly, the detectors operate at very low temperatures, typically in the range 0.1-0.3 K. The evolution of Far-IR detector technology has been very rapid. In the early 1990s, Far-IR instruments typically contained only a few hand-built detectors. The Spectral and Photometric Imaging Receiver (SPIRE) instrument for the Herschel Space Observatory (HSO), developed in the early 2000s, had several hundred detectors. The largest ground-based instruments, Submillimetre Common-User Bolometer Array-2 (SCUBA-2) on the James Clerk Maxwell Telescope (JCMT), and the Atacama Pathfinder EXperiment (APEX) Microwave Kinetic Inductance Detector (A-MKID) camera, now contain 10,000 and 20,000 pixels, respectively. However, Far-IR arrays remain very expensive, difficult to produce and operate, and a significant impediment for future development of the field.

The goal of our project is to develop and demonstrate Far-IR detector arrays using kinetic inductance detectors (KIDs) [1]. The ultimate aim is to provide inexpensive, high-performance, large-format arrays suitable for use on a wide range of platforms including airborne, balloon-borne, and space-borne telescopes. Specific project goals include laboratory demonstrations of arrays targeting the sensitivity and optical power levels appropriate for several of these platforms, along with an end-to-end, full-system demonstration using a ground-based telescope. Ground-based demonstrations of imaging detectors operating at 350 and 850 μm were performed in a succession of observing runs at the Caltech Submillimeter Observatory (CSO) in 2013-2015. The CSO KIDs are made from titanium nitride (TiN), an excellent choice given the relatively high photon background for ground-based and airborne imagers. Aluminum KIDs are likely a better choice for low-background space applications; within the last year, further work on aluminum devices led to process improvements for higher yield, followed by testing with a cryogenic blackbody source. Finally, as part of the system design of KID instruments, a chirped-readout approach achieved “first light” testing at CSO, where it was compared with the more traditional fixed-tone readout.

Background

The universe shines very brightly at Far-IR wavelengths. In fact, about half the photon energy ever produced by stars and galaxies over the history of the universe falls in the Far-IR band. This remarkable fact was originally predicted by Frank Low and Wallace Tucker in 1968, based on a handful of early Far-IR observations of galaxies. It was first demonstrated observationally in 1996 by Jean-Loup Puget and collaborators, working with data collected by the NASA Cosmic Background Explorer (COBE) satellite. To put it differently, there is just as much light in the Far-IR as there is in the visible/Near-Infrared (Near-IR) band. This simple fact alone makes it imperative to study the universe in the Far-IR. Fortunately, the technology to image and survey the universe in this band is now becoming available.

Fundamentally, the large luminosity of the universe in the Far-IR is intimately tied to the process of star formation. Star formation occurs deep inside thick clouds of interstellar dust and gas. The dust provides a shield against radiation that would otherwise heat and ionize the gas, and allows the gas to form

molecules, cool to temperatures below 10 K, and become quite dense. Gravitational collapse of these dense cores then leads to star formation, but the radiation produced by a newly formed star cannot escape its dusty cocoon. Instead, the stellar radiation is absorbed by the surrounding dust and gas, heating this material to temperatures around 50-100 K and causing it to glow brightly in the Far-IR. The Far-IR radiation readily escapes these thick clouds, providing a view of sites of recent star formation, sites that are often entirely invisible in the optical/Near-IR. Such Far-IR studies can be performed locally by imaging sites of star formation in the Milky Way. In addition, the Infrared Astronomical Satellite (IRAS) survey showed that many galaxies are bright in the Far-IR. Indeed, galaxy-galaxy collisions are believed to be a key factor in the evolution of galaxies, and such collisions often trigger giant bursts of star formation that provide a large boost to the Far-IR luminosity. The HSO provides a recent example of the importance of Far-IR observations for studying star formation both near and far, in our galaxy and across cosmic time. Indeed, many of the brightest Far-IR galaxies found by Herschel are undetectable by the Hubble Space Telescope (HST) and the largest ground-based optical telescopes.

The Decadal Survey reports provide a long history of strong support for Far-IR astrophysics, starting with the 1982 Field Report recommendation for the construction of a 10-20 m space-borne Far-IR telescope, known as the Large Deployable Reflector (LDR). As with many Decadal recommendations, this project was never built due to budget issues, but the recommendation did stimulate NASA technology investments and continued support from Decadal panels that ultimately led to NASA's participation in the HSO, launched by the European Space Agency (ESA) in 2009. NASA is once again considering its future in this field: a "Far-Infrared Surveyor" mission was described in the 2013 report chartered by the Astrophysics Division, titled "[*Enduring Quests, Daring Visions: NASA Astrophysics in the Next Three Decades*](#)." Such a mission is now a candidate for study for the 2020 Decadal Survey, and was the topic of a June 2015 NASA workshop held in Pasadena, CA. This workshop again highlighted the abundant scientific opportunities in the Far-IR, as well as the need for large arrays of sensitive detectors to realize these opportunities.

Far-IR detector arrays have evolved rapidly over the past two decades. In the early 1990s, Far-IR detectors were laboriously built, individually, by hand. By circa 2000, several instruments were fielded using lithographically fabricated arrays with a few hundred detectors in which the detectors were read out with individual amplifiers and wiring. The development of superconducting detectors, coupled with the invention of multiplexed readout schemes, propelled the field to its present level of arrays with up to ~1000 pixels. A good example is the ground-based SCUBA-2 instrument, which contains eight array tiles, each with 1280 detectors, for a total of ~ 10^4 pixels. However, the transition-edge sensor (TES)/Superconducting Quantum Interference Device (SQUID) technology used for SCUBA-2, while flexible and adaptable to broad range of requirements, is expensive and difficult to produce. Indeed, detectors now often constitute the largest single budget item for new Far-IR instruments, and impose a bottleneck on future advances. The goal of our project is to show that the simpler, lower-cost KID technology [1, 2] can meet the needs of a similarly broad range of applications, ranging from ground-based to space instruments. KID technology was proposed by our group in 1999 and, with support from NASA, has shown very rapid development over the past decade. However, instrument groups have often been hesitant to adopt the technology due to its lower level of maturity. Our project addresses this issue head-on using full-system, end-to-end demonstrations on a ground-based telescope, as well as laboratory testing to explore a range of sensitivity levels.

Objectives and Milestones

The primary goals of our project are to perform laboratory demonstrations of KID arrays suitable for airborne, balloon, and space platforms; and to perform an end-to-end, full-system demonstration of an instrument on a ground-based telescope. The key performance specifications are shown in Table 1. Our schedule (achieved milestones marked with a check mark) for these tasks is approximately as follows.

- Space – laboratory demonstration:
 - ✓ April 2014 – Design, fabrication, and test effort leading to successful operation of a suitable device in darkness;
 - ✓ Second half of 2014 – Process improvements; and
 - ✓ First half of 2015 – Testing of device with small, known optical load.
- Ground – on-sky demonstration with CSO telescope:
 - ✓ April 2013 – End-to-end system 350- μm demonstration, but with some limitations (single polarization, sensitivity somewhat worse than background limit); and
 - ✓ August 2014 and May 2015 – Additional demonstrations (dual polarization, better sensitivity, on-sky test of chirped readout, 850- μm detection).
- Balloon – laboratory demonstration:
 - ✓ Previous iterations of tested devices designed primarily for ground-based work have satisfied this performance requirement.
- Stratospheric Observatory for Infrared Astronomy (SOFIA) – laboratory demonstration:
 - First half of 2015 – Test of efficiency and sensitivity for $\lambda = 90 \mu\text{m}$ operation (not achieved).

Over the course of the project, our effort focused on the highest and lowest background situations.

Platform	Optical Power	NEP _{phot} (W / Hz ^{1/2})	NEP _{goal} (W / Hz ^{1/2})	TRL goal
Space (90 μm)	0.12 fW	7.3×10^{-19}	5×10^{-19}	3 \rightarrow 4
Balloon (350 μm)	18 pW	1.5×10^{-16}	7×10^{-17}	3 \rightarrow 4
SOFIA (90 μm)	26 pW	3.4×10^{-16}	1.7×10^{-16}	3 \rightarrow 4
Ground (350 μm)	100 pW	6.5×10^{-16}	3.3×10^{-16}	3 \rightarrow 6

Table 1. Performance specifications for Far-IR continuum detectors relevant to this project.

Progress and Accomplishments

Titanium nitride KIDs targeting NEP $\approx 10^{-16}$ W/Hz^{1/2}

The first on-sky testing of JPL-produced Far-IR ($\lambda = 350 \mu\text{m}$) KIDs was performed in April 2013, four months after the start of our project. These detectors were made from TiN, which has convenient properties for the Far-IR [3]. Overall, this end-to-end system demonstration at CSO was very successful, and images of astrophysical sources were obtained with quality equivalent to those produced by facility Far-IR imagers. However, the detector design had not been optimized prior to the observing run, resulting in a sensitivity penalty of roughly 10 \times relative to the photon-background limit achieved by the CSO's 350- μm facility camera, the Submillimeter High-Angular Resolution Camera (SHARC) II.

In the following year (May 2013 – July 2014), work on higher background (NEP $\approx 10^{-16}$ W/Hz^{1/2}) detectors focused on design and implementation of dual-polarization response (Fig. 1), introduction of a micro-lens array to the detector package for radiation concentration, and tuning of the Ti vs. N ratio and hence critical superconducting temperature to achieve best sensitivity. Further improvements were made to the method of coupling the KIDs to the readout line, and to the fabrication process. Three methods for silicon micro-lens array fabrication were pursued – laser machining by commercial source (Veldlaser), gradient-index lenses designed and micro-machined by our own team, and anisotropic etching using a mask of hemispherical photo-resist bumps. A Parylene film applied by a commercial vendor is used for anti-reflection coating. The laser-machined and gradient-index lenses have been tested optically with the KID arrays and shown to work well in concentrating the radiation and improving responsivity.

As a result of detector design improvements, the TiN detectors are background-limited at 350 μm for 100 K to 300 K loads in the lab. An array of 488 such detectors with the Veldlaser micro-lenses was brought to CSO for testing and system demonstration in August 2014. The instrument showed a substantial ($\sim 3\times$) sensitivity improvement relative to the April 2013 run, but did not yet match the performance achieved with SHARC II.

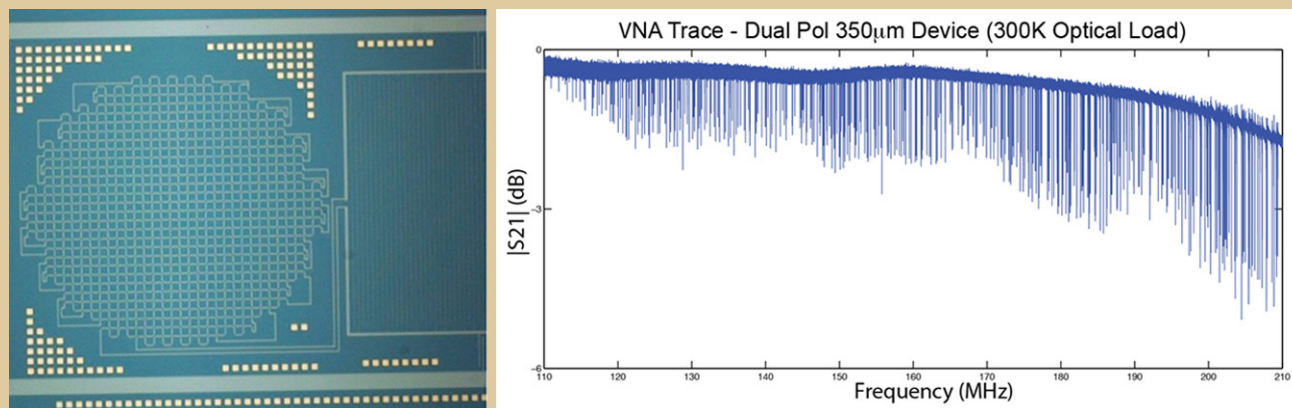


Fig. 1. Left: Micrograph of single detector (TiN KID) in an array tested on the CSO telescope in August 2014. The square grid with circular boundary at left is the photosensitive inductive element of the 540- μm -diameter KID, appropriate for a micro-lens-coupled device operating at 350 μm . Right: Vector Network Analyzer “sweep” of frequency range occupied by the KIDs, showing absorbed power at the resonance of each of the ~ 500 detectors.

A subsequent (September 2014 – April 2015) intensive testing campaign in the laboratory indicated an inadequate baffling of stray light, a problem that had also been encountered during the development of SHARC II. The optical filtering was modified to more closely match the scheme adopted for SHARC II, and laboratory testing of this revised scheme indicated a substantial sensitivity improvement, about what was needed to close the remaining gap relative to SHARC II. The instrument was brought to the CSO for a third time in May 2015 for testing. Although the instrument was installed and operated successfully, the weather was not favorable and the 350- μm atmospheric opacity was too high during the run to allow useful observing. It was thus impossible to adequately evaluate the sensitivity of the instrument. Unfortunately, the impending closure of the CSO will prevent us from making any further progress in this direction.

Since reaching a background-limited full-system sensitivity at 350 μm for the CSO ground-based instrument was considered our project’s top priority, and given the challenges faced in reaching that goal, we focused our efforts on that task rather than attempting additional demonstrations of detectors suitable for balloon instruments at 350 μm or SOFIA instruments at 90 μm .

Aluminum KIDs targeting $\text{NEP} \approx 10^{-18} \text{ W/Hz}^{1/2}$

While TiN KIDs cover a broad wavelength range for detectors operating with $> \text{pW}$ background power, aluminum KIDs are more appropriate for $\sim \text{fW}$ backgrounds. In general, the volume of a KID optimized for NEP scales with background power [4]. At the small volume needed for space backgrounds, the much lower resistance of aluminum in the IR makes it easier to satisfy the condition for efficient radiation absorption for a device with convenient surface area.

Our work on Al KIDs for the Far-IR began in the first year of this project. We fabricated KID arrays (Fig. 2) using aluminum absorbers with an absorber line-width of 150 nm on a 15- μm pitch and a volume of 38 μm^3 . The 20-nm-thick aluminum has a per square resistance of 1 ohm, resulting in an effective absorber resistance of 100 ohms, appropriate for matching to radiation through silicon.

We have two lithographic tools we can use to achieve these 150-nm wide lines, the Canon FPA3000-EX6 5 \times deep ultraviolet projection lithography stepper, and the JEOL JBX-9300 FS electron-beam lithography system. The e-beam tool can easily achieve these dimensions, but the patterns are serially written and the process is slow and costly. The stepper exposes in a parallel fashion one field at a time and is faster, but is limited in resolution and depth of focus, requiring significant lithographic optimization to achieve these dimensions. We have produced KIDs using both approaches.

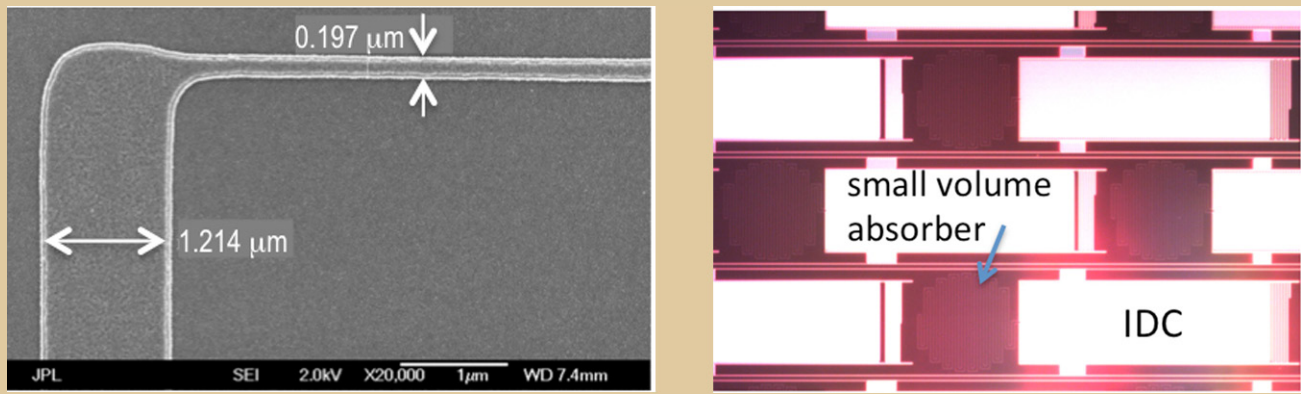


Fig. 2. Left: Micrograph showing a section of the small-volume Al absorber. Lines as narrow as 150 nm were fabricated using the deep UV stepper lithography system at JPL's Micro-devices Laboratory. Narrower lines were fabricated using e-beam lithography. Right: A section of an array of aluminum KIDs with 150-nm line-width. The pixel design is similar to the TiN design shown in Fig. 1; the major difference is a much smaller area-filling factor for the aluminum absorber, due to the much lower resistivity of aluminum vs. TiN.

Array sensitivity (Fig. 3) was estimated using thermal calibration. In this method, the array base temperature is swept, and the frequency response to the thermally generated quasi-particle population is measured to derive the response to input optical power. In order to convert from optical power to quasi-particle density changes, the recombination time needs to be known. However, this is not straightforward to infer from response time measurements when the resonance frequency is in the ~ 300 MHz range, because the resonator response time is normally slower than the quasi-particle recombination time. To estimate detector sensitivity, we have assumed a recombination time of 1 ms, which has been previously measured for aluminum. The derived sensitivity of $\sim 2 \times 10^{-19}$ W/Hz $^{1/2}$ (Fig. 3) is very encouraging.

One possible disadvantage of the use of aluminum detectors is that aluminum is a relatively soft material and thin films can degrade in air over extended periods of time. The yield of the arrays was found to be lower than desired, due to damage to the thin absorber lines in a mechanical cleaning step performed after the aluminum etch. To improve yield and durability, we investigated arrays made of aluminum with a thin (~ 10 nm) protective TiN layer deposited on top. The bilayer is patterned in a single step. The electrical properties of the bilayer are dominated by the aluminum due to its higher conductivity and lower kinetic inductance. Arrays made with bilayer have shown a very high (95%) yield. A typical transmission spectrum is shown in Fig. 4.

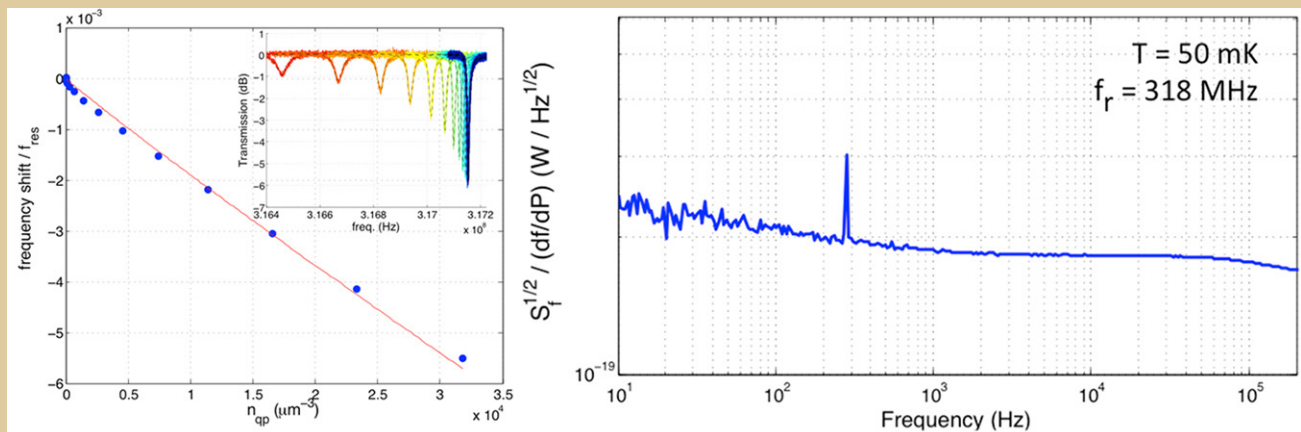


Fig. 3. Left: Calibration of detector sensitivity using thermal measurements. The resonance frequency is measured vs. bath temperature (inset). The response of the detector to absorbed power is inferred from the measured frequency shift vs. thermal quasi-particle density. Right: Measured frequency noise spectrum expressed in NEP units using the thermal response data and assuming a quasi-particle lifetime of 1 ms.

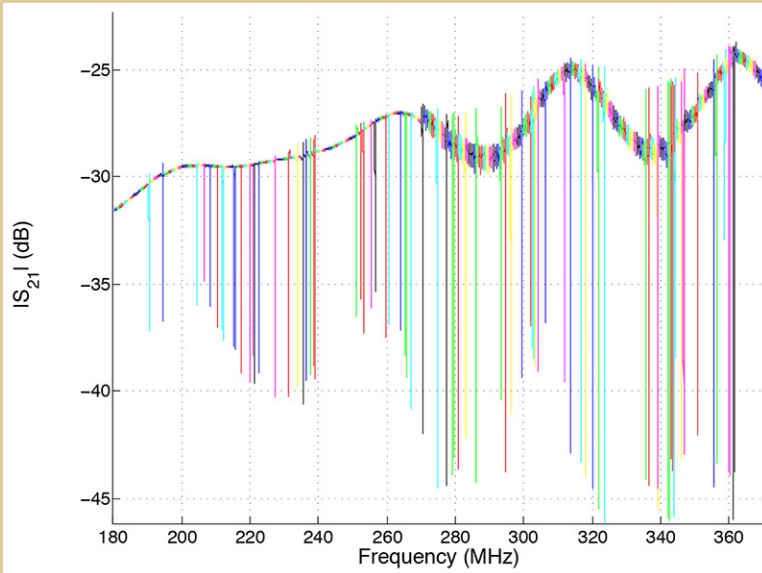


Fig. 4. Transmission of an Al/TiN bilayer array with 150-nm absorber line-width.

The bilayer arrays were tested optically using a blackbody source internal to the cryostat. The detector response and noise were measured to derive an optical NEP. The noise spectra, expressed in NEP units, are shown in Fig. 5 (left) for various blackbody temperatures. The increase in noise with blackbody temperature and the shape of the curves suggest that the detectors are photon-noise-limited over the range of powers corresponding to the higher of the blackbody temperatures studied ($T_{\text{load}} \geq 16\text{K}$). Figure 5 (right) compares the measured and expected noise as a function of optical power. The measurement and photon-noise prediction agree for optical power greater than about 1 pW.

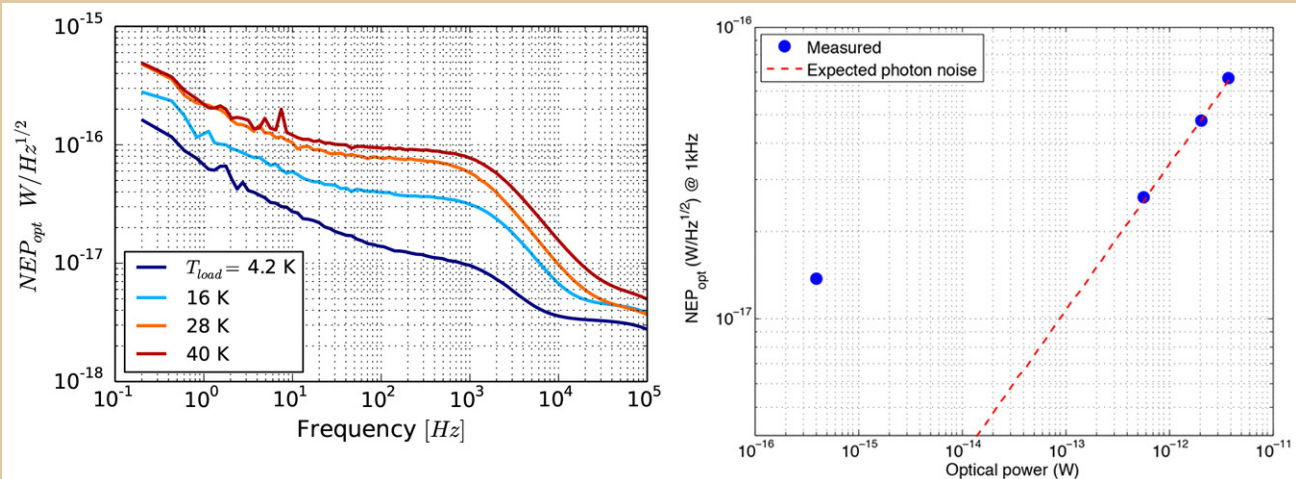


Fig. 5. Left: Noise spectra of an Al/TiN bilayer detector for various blackbody temperatures. The noise is expressed in NEP units by dividing by the measured responsivity. Right: Measured vs. expected noise as a function of optical power.

The NEP of about $10^{-17} \text{ W/Hz}^{1/2}$ measured with the blackbody at 4.2 K falls short of the expectation for these detectors and of the sensitivity calculated by assuming a 1 ms quasi-particle lifetime. We believe that the sensitivity is degraded because the detector responsivity is limited by a much shorter lifetime, which may be due to several effects. First, the T_c of the bilayer was measured to be 1.9 K, which is considerably higher than for pure aluminum. Measurements of a range of superconducting materials have found that the maximum lifetime varies with T_c , approximately as T_c^{-3} . Second, we believe that an excess quasi-particle population may be present due to the leakage of pair-breaking radiation into the detector housing, which decreases the lifetime due to self-recombination. Third, it is possible that the presence of the TiN over-layer causes a reduction in the quasi-particle lifetime compared to that of clean aluminum.

Future work will concentrate on investigating and increasing the quasi-particle lifetimes. The lifetimes may be measured directly using IR photon pulses. The critical temperature, T_c of the TiN over-layer is tunable by adjusting the stoichiometry, which suggests that it should be possible to produce a bilayer T_c closer to 1.2 K, corresponding to bulk aluminum. We are also constructing better light-tight enclosures

for reducing background radiation in the test bed. Finally, we have developed and proposed new detector concepts that promise to combine the ease of fabrication associated with TiN films and the high responsivity associated with clean aluminum films (see below).

Chirped readout for KIDs

In a traditional KID readout, each of the resonances is excited with a fixed tone, and the time-variable amplitude and/or phase shift of the tone due to changes in incident radiation is recorded. This works well in many instruments, and is the primary readout technique for our CSO demonstration camera. However, the fixed-tone readout loses sensitivity when the resonances shift in frequency by half a line-width or more. A chirped readout addresses this issue; the entire frequency band containing the resonances is excited using a broadband, short-duration chirped pulse, which allows resonant frequencies to be excited and read out even if they move significantly in frequency. In detail, the radio-frequency chirped pulse is applied to the input line. Then, during a “listening” period, the output signal consisting of a superposition of the ring-down signals from all the resonators is digitized and Fourier-transformed, and the resonators that are ringing due to the chirp excitation are identified and stored. This chirping and identification can be done at kHz rates.

We have been developing a chirp readout using a PC-based system containing a commercial Analog-to-Digital and Digital-to-Analog Converters (ADC/DAC) board and a Graphics Processing Unit (GPU) board. This system achieved “first light” at CSO (albeit in poor weather) with the KID demonstration camera in May 2015 (Fig. 6). During these tests, we successfully read out all detectors in the 350- μm KID array in the 125-250 MHz range, at up to 3.6 kHz readout rate. The system showed low $1/f$ noise (Fig. 6), and the performance compared favorably with the fixed-tone readout. For the majority of detectors, the sensitivity was essentially the same for both readouts; for each of the remaining detectors, the loss of sensitivity is understood as insufficient readout power (resulting in amplifier-dominated noise) or excessive readout power (resulting in a distorted and less-responsive resonance). These observations led us to develop a new signal processing scheme that does not suffer distortion or loss of performance at high power, and which will therefore provide considerable margin in the power level of the chirp pulse, making it possible to read out the entire array with full sensitivity. Given the advantages and recent demonstration of the chirp readout, it will be an important part of our KID-based systems going forward.

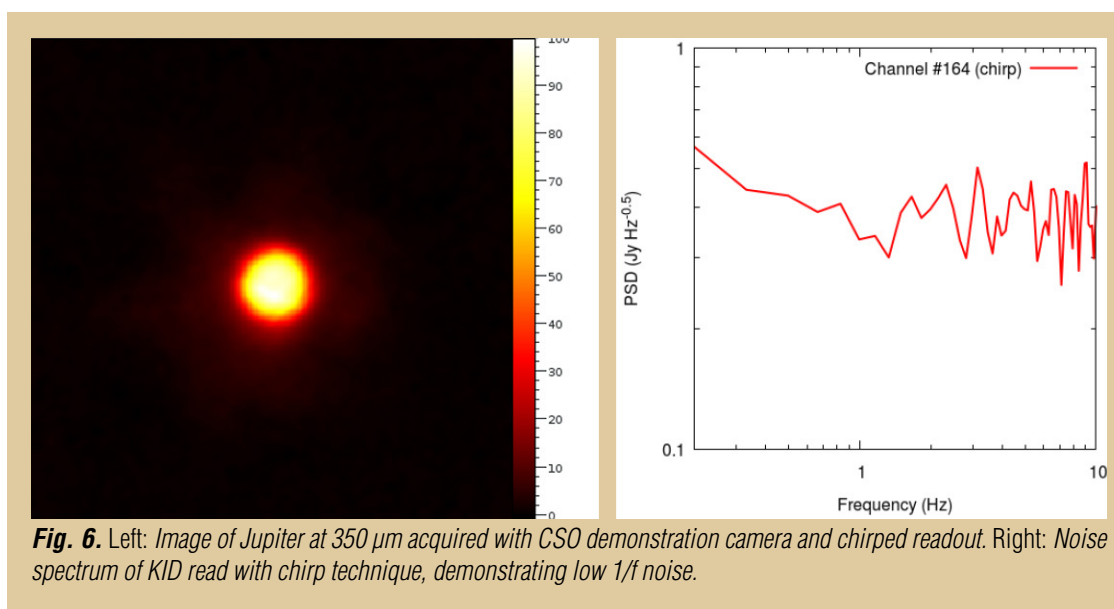


Fig. 6. Left: Image of Jupiter at 350 μm acquired with CSO demonstration camera and chirped readout. Right: Noise spectrum of KID read with chirp technique, demonstrating low $1/f$ noise.

Path Forward

Our two-year project, extended into a third year, is now nearly completed. Although we have accomplished a significant fraction of our original goals, there is considerable work left to do in the future. Instrument testing at the CSO has given us high confidence that KID arrays are very strong contenders for use in future Far-IR space astrophysics missions. Although the closing of the CSO will prevent us from continuing our instrument tests at 350 μm , we will seek out new opportunities for ground-based testing in the future.

From our perspective, the major outstanding issue is a demonstration that a low NEP in the $10^{-19} \text{ W/Hz}^{1/2}$ range can be achieved in an array that combines low readout frequency (100-200 MHz), high yield, and high optical efficiency. An aluminum-based array remains a possibility, though our experience indicates that the tall poles will be related to the intertwined issues of fabrication yield and material quality. We have instead identified a promising new direction that combines the fabrication and optical efficiency advantages of TiN detectors with the sensitivity advantage of high quality, clean aluminum films; this concept is the subject of a 2015 proposal submitted to the NASA Astrophysics Research and Analysis (APRA) program.

References

- [1] P.K. Day, H.G. LeDuc, B.A. Mazin, A. Vayonakis, and J. Zmuidzinas, “A broadband superconducting detector suitable for use in large arrays,” *Nature* **425**, no. 6960, 817-821 (2003)
- [2] S.P. Doyle, P. Mauskopf, J. Naylon, A. Porch, and C. Duncombe, “Lumped element kinetic inductance detectors,” *Journal of Low Temperature Physics* **151**, no. 1-2, 530-536 (2008)
- [3] H.G. LeDuc, B. Bumble, P.K. Day, B.H. Eom, J. Gao, S. Golwala, B.A. Mazin, *et al.*, “Titanium nitride films for ultrasensitive microresonator detectors,” *Applied Physics Letters* **97**, no. 10, 102509-102509 (2010)
- [4] J. Zmuidzinas, “Superconducting microresonators: Physics and applications,” *Annu. Rev. Condens. Matter Phys.* **3**, no. 1, 169-214 (2012)

For additional information, contact Jonas Zmuidzinas: jonas@caltech.edu



Raising the Technology Readiness Level of 4.7-THz Local Oscillators

By Qing Hu (MIT)

The 63- μm (4.744 THz) [OI] fine-structure line is the dominant cooling line of warm, dense, neutral atomic gas. Because of its great intensity in high UV photodissociation regions (PDRs) and shocks, the [OI] 63- μm line is superior in probing regions of massive star formation and the centers of galaxies. It is a unique probe of PDRs, shock waves from stellar winds/jets, supernova explosions, and cloud-cloud collisions. These radiative and mechanical interactions shape the interstellar medium of galaxies and drives galactic evolution. The size scale of the interactions can excite [OI] emission over many parsecs. Moreover, the emission regions are often complex, with multiple energetic sources processing the environment. Spectrally resolved observations of the [OI] line with a heterodyne receiver array will allow users to disentangle this convoluted interaction and permit the study of the energy balance, physical conditions, morphology, and dynamics of these extended regions. In this way, such a receiver array will provide new, unique insights into the interrelationship of stars and gas in a wide range of galactic and extragalactic environments.

Despite the great potential, however, astrophysical observation of the OI line has rarely been performed because the frequency (4.744 THz) is beyond the reach of most of the implemented local oscillators (LOs) in sensitive heterodyne receivers involving cryogenic mixers. In this proposed three-year project, we plan to raise the Technology Readiness Level (TRL) of THz Quantum-Cascade Lasers (QCLs) for LO applications to 5 or beyond, so that we will bridge this mid-TRL gap between a promising and enabling technology and a mission-ready component. Such a development will significantly reduce the risk of several proposed suborbital projects such as GUSSTO (The Gal/Xgal U/LDB Spectroscopic/Stratospheric THz Observatory), which is a long-duration balloon flight. The proposed system includes a nine-element heterodyne receiver array for the 4.744-THz OI line. Those heterodyne receiver arrays will require a large LO power level in a good beam pattern. Specifically, by the end of the proposed project, we will develop single-mode Distributed Feedback (DFB) lasers with frequency to be within 10 GHz of the target 4.744-THz line, continuous-wave (cw) output power of ~ 5 mW with a wall-plug power efficiency of $\sim 0.5\%$ at an operating temperature of ~ 40 K, and beam patterns narrower than 10\AA at 10 K.

This proposed project mainly addresses NASA's Strategic Subgoal 3D: "*Discover the origin, structure, evolution, and destiny of the universe, and search for Earth-like planets.*" It also addresses NASA's Strategic Subgoal 3A: "*Study planet Earth from space to advance scientific understanding and meet societal needs;*" and NASA's Strategic Subgoal 3C: "*Advance scientific knowledge of the origin and history of the solar system, the potential for life elsewhere, and the hazards and resources present as humans explore space.*"

For additional information, contact Qing Hu: qhu@mit.edu

Advanced FUV/UV/Visible Photon-Counting and Ultralow-Noise Detectors

By Shouleh Nikzad (JPL)

We will develop detectors with high efficiency and photon-counting capability in the UV/Optical/NIR by combining our bandstructure engineering and high-efficiency detection techniques with both CMOS imagers with in-pixel gain as well as electron-multiplying CCDs and compare the performance in terms of noise, efficiency, uniformity, and environmental (radiation and thermal cycling) stability. We will build on our molecular beam epitaxy (MBE) and atomic layer deposition (ALD)-based techniques for integrated coatings; further develop and advance the Technology Readiness Level (TRL) of silicon arrays with high efficiency in the spectral range < 200 nm; and finally, advance the TRL of high-inband-efficiency and high out-of-band-rejection coatings by integrating these coatings with high-TRL CCD detectors, and measuring the quantum efficiency and rejection ratio. This effort directly addresses the need for detectors as stated in the Strategic Astrophysics Technology (SAT) call.

For additional information, contact Shouleh Nikzad: Shouleh.Nikzad@jpl.nasa.gov

Building a Better ALD – Use of Plasma-Enhanced ALD to Construct Efficient Interference Filters for the FUV

By Paul Scowen (ASU)

Over the past few years the advent of atomic layer deposition (ALD) technology has opened new capabilities to the field of coating deposition for use in optical elements. At the same time, there have been major advances in both optical designs and detector technologies that can provide orders-of-magnitude improvement in throughput in the far-ultraviolet (FUV) and near-ultraviolet (NUV) passbands. Recent review work has shown that a veritable revolution is about to happen in astronomical diagnostic work for targets ranging from protostellar and protoplanetary systems, to the intergalactic medium that feeds gas supplies for galactic star formation, to the most distant of objects in the early universe. These diagnostics are rooted in access to a forest of emission and absorption lines in the ultraviolet (UV), and all that prevents this advance is the lack of throughput in such systems, even in space-based conditions. We propose to use a range of materials to implement stable optical layers suitable for protective overcoats with high UV reflectivity and unprecedented uniformity, and use that capability to leverage innovative ultraviolet/optical filter construction to enable the type of science described above. The materials we will use include aluminum oxide and hafnium oxide (as an intermediary step for development only) and progressing to a range of fluoride-based compounds (for production). These materials will be deposited in a multilayer format over a metal base to produce a stable construct. Specifically, we will employ the use of PEALD (plasma-enhanced atomic layer deposition) methods for the deposition and construction of reflective layers that can be used to construct unprecedented filter designs for use in the ultraviolet. Our designs indicate that by using PEALD, we can further reduce adsorption and scattering in the optical films as a result of the lower concentration of impurities and increased control over the stoichiometry to produce vastly superior quality and performance over comparable traditional thermal ALD techniques currently being developed by other NASA-funded groups.

For additional information, contact Paul Scowen: paul.scowen@asu.edu

Development of Large-Area (100 mm × 100 mm) Photon-Counting UV Detectors

By John Vallergera (UC Berkeley)

Microchannel Plate (MCP) detectors have been an essential imaging technology in space based NASA UV missions for decades and have been used in numerous orbital and interplanetary instruments. The reasons for this are many: they have high QE in the extreme and far ultraviolet; they are photon-counting with high spatial and temporal resolution; they are available in various large, adaptable formats, even curved; readout electronics can be compact, low mass and low power; they do not require cryogenics; and they are quite radiation-hard. However, as with any detector technology, they have had their limitations: lower QE in the near UV, MCPs with fixed pattern noise; and limited lifetime and dynamic range as a result of high-gain operation. The first of these limitations is being addressed by an Astrophysics Research and Analysis (APRA) grant on GaN photocathodes and the second has been largely ameliorated by new MCP fabrication techniques by industry. We have addressed the remaining issues with our cross-strip (XS) anode readout technology. We are currently near the end of our Strategic Astrophysics Technology (SAT) program where we were funded to increase the Technology Readiness Level (TRL) of XS readout electronics by converting our bulky and high-power laboratory designs into application-specific integrated circuits (ASICs) that are lower-power and lower-mass. We also developed a standard 50 mm × 50 mm XS MCP detector that was tested in flight-like environments (thermal-vacuum and vibration). We now have in hand the higher TRL 50-mm detector and the ASICs to read it out. The goal of this SAT proposal is to now scale the 50 mm × 50 mm detector to 100 mm × 100 mm XS detector using these ASICs and scaling the detector mechanical structure and anode by a factor of two (four in area) in an aggressive two-year program. The basic ASIC design will not change, except that we will migrate the 250-nm CMOS technology to a more modern 130-nm CMOS technology that is known to be faster and more radiation resistant. With this new effort we will have an adaptable prototype 100-mm detector qualified for flight-like environments.

Cross-strip readouts collect the charge exiting from a stack of MCPs with two sets of coarsely spaced and electrically isolated orthogonal conducting strips. When the charge collected on each strip is measured, a centroid calculation determines the incident location of the incoming event (photon or particle). This requires many identical amplifiers (*e.g.*, 160, 320) whose individual outputs must all be digitized and analyzed. The advantage this technique has over existing and previous MCP readout techniques (wedge and strip, delay line, intensifiers) is that the anode capacitance per amplifier is lower, resulting in a higher Signal-to-Noise Ratio (SNR). This allows lower-gain operation (factors of ~20) while still achieving better spatial resolution. Furthermore, lower-gain operation of the MCPs increases both their lifetime and the local counting-rate capability.

We plan to scale this 50-mm XS technology up to 100 mm × 100 mm and raise it to TRL 6 from TRL 4 by proposing to: (1) Test the sensitivity of the new ASICs to high radiation doses and migrate them to a more robust 130-nm CMOS technology; and (2) Develop a spaceflight compatible 100 mm × 100 mm XS detector that integrates with these electronics and can be tested as a system in flight-like environments while maintaining the imaging performance achieved with the smaller detector (< 20 Å μm FWHM spatial resolution, spatial linearity of < 10 Å/μm, count rates > 2 MHz, 10% deadtime, *etc.*). This detector design can be used directly in many rocket, satellite, and interplanetary UV instruments and could be easily adapted to different sizes and shapes to match various mission requirements. Having this detector flight design available will also reduce cost and development risk for future Explorer-class missions. New technological developments in photocathodes (*e.g.*, GaN) or MCPs (*e.g.*, low background, surface-engineered borosilicate glass MCPs) would be able to be accommodated into this design as their TRLs increase.

For additional information, contact John Vallergera: jvv@ssl.berkeley.edu

Appendix C

Developing the Future Astrophysics Workforce

Strategic Astrophysics Technology (SAT) projects mature technologies that enable the strategic astrophysics missions of the next decade or two. Student involvement may offer a minor strength in assessing individual proposals. However, without a trained astrophysics workforce, we will be unable to deploy new technologies into groundbreaking missions. Some of the students and postdocs participating in current SAT projects may become Principal Investigators (PIs) in their own right in 10-30 years, developing technologies for missions 50 years into the future. This demonstrates the SAT program's far-reaching impact, in that directly or indirectly, it enables the astrophysics missions of the next half century. Below we introduce some of the many students and postdocs whose work supported our current portfolio of Cosmic Origins (COR) SAT projects. We would be surprised if we don't meet them again at conferences, and as PIs, technologists, and researchers supporting flight missions enabled by the technologies they worked on early in their careers.



Ryan Bevan

Undergraduate student, Mechanical Engineering, University of Alabama (UA), Huntsville.

PI: H. Philip Stahl

"I was an undergraduate Mechanical Engineering student at UA Huntsville when I began working at MSFC as an intern. I worked with the Advanced Mirror Technology Development (AMTD) team to help develop a user-friendly, high-precision mirror modeling design tool in an effort to significantly reduce engineering time when modeling large-aperture mirrors (≥ 4 m). I also had the opportunity to witness a live test at the X-Ray and Cryogenic Facility (XRCF), where we tested a 40-cm deep-core mirror. I was able to assist this test by developing a thermal prediction model, based on the model outputted from the Arnold Lightweight Mirror Modeler Tool that accurately depicted the expected thermal and mechanical behaviors as witnessed during the testing phase of this project.

"Moreover, the experience and knowledge obtained from this experience were invaluable. Since my internship at NASA, I have pursued my Master's Degree in Aerospace Engineering at the University of Southern California (USC). Upon completion of my graduate degree, I hope to continue making significant contributions within the astrophysics community.

"Lastly, I would like to thank Dr. Philip Stahl, Bill Arnold and the rest of the AMTD team for challenging me and enabling me to learn and grow both professionally and academically."



Harley Cumming

Graduate student, Electrical Engineering, University of Hawai'i at Manoa (UH)

PI: John Vallergera

"I am a graduate student at the University of Hawai'i at Manoa, working towards my Master's in Electrical Engineering. I began working with Space Sciences Laboratory (SSL) while pursuing my undergraduate degree at UH in 2012. My thesis is on the design of a charge sensitive amplifier, called the CSAv3, which was developed in collaboration with the SSL for the readout of an ultraviolet (UV) Micro-Channel Plate (MCP) detector. This project has been a very enjoyable and educational experience, wherein I learned a great deal about readout electronics and detectors, and gained analog circuit design and VLSI (Very-Large-Scale Integration) design experience."



Javier del Hoyo

Graduate student, Optical Science, University of Arizona; graduated with MSc fall 2013; now civil servant at GSFC Code 551, supporting coating work on Ionospheric Connection (ICON) Explorer optical elements.

PI: Manuel Quijada

"I worked as a NASA Pathways student during the performance period for this SAT grant, working towards my master's degree in optical science at the University of Arizona. I assisted in the effort of modifying the 2-m ultra-high-vacuum chamber to support the deposition of hot resistive heated thermal evaporation at 250°C. After completing my degree requirements, I converted to a full-time civil servant as an optical engineer in the thin-films coatings laboratory at GSFC Code 551. During my service, I developed a deposition process to limit the absorption and scatter while increasing the optical properties (e.g., reflectance and transmittance) of a magnesium fluoride thin film at the far-ultraviolet (FUV) spectral range (i.e., 121.6-200 nm)."



Matthew Fitzgerald

Undergraduate student, Mechanical Engineering, University of Tennessee, Martin

Using Arnold Lightweight Mirror Modeler tool, evaluated candidate primary 4-m and 8-m mirror substrate and assembly designs for mass, thickness and first mode frequency. Published presentation at Technology Days 2012.

PI: H. Philip Stahl

"I spent the summer after my undergraduate studies working with Dr. Stahl on the design of UV/Optical/Near-IR monolithic telescope mirrors. For much of the internship, I assisted in the development of the Arnold Lightweight Mirror Modeler tool and later used the completed modeler to evaluate primary 4-m and 8-m mirror substrate and assembly designs for their mass, thickness, and first mode frequencies. This

work was later presented at Technology Days 2012 and was a part of the efforts that received NASA's Group Achievement Honor Award in 2015.

"I am grateful for the opportunity of having worked with Dr. Stahl on something with such an impact on the optics community. The lessons learned and experience gained have proved invaluable in both my graduate studies and in my career as an engineer."



Jessica Gersh-Range

Graduate student, Mechanical Engineering, Cornell University

PI: H. Philip Stahl

"For part of my doctoral research, I developed a segmented mirror architecture that can perform comparably to or better than a monolith, with a modular design enabling on-orbit assembly and scalability. I also developed and tested a mechanism that, when used with this architecture, increases the stiffness, and particularly the damping, of a cryogenic segmented mirror. This research was partially funded by a NASA Graduate Student Researchers Program fellowship, and I presented the project at the 2011 SPIE Optics+Photonics Conference. I also wrote two articles that appeared in the new Journal of Astronomical Telescopes, Instruments, and Systems. Working at MSFC was an incredible experience, and I learned a great deal from collaborating with researchers, engineers, and opticians working on the next generation of space telescopes. I look forward to

continuing to use the skills I gained to solve design, control, and operations challenges faced by current or planned telescope missions."



Erika Hamden

Started as a NASA Earth and Space Science Fellow (NESSF) while a graduate student at Columbia University, and is now a postdoctoral fellow (Millikan Prize and NSF) at Caltech.

PI: Shouleh Nikzad

"As a graduate student funded by a Space Grant and then NESSF fellowship, I worked in Shouleh Nikzad's group at JPL, designing and testing anti-reflection coatings for use on delta-doped detectors. From my first visit to JPL, I had a fantastic experience. It was my first time working in a real lab and I can still remember my excitement when driving into the gates on my first day. Dr. Nikzad provided a welcoming environment where I felt immediately comfortable and able to learn. The work itself was interesting and exciting and even as just a graduate student, I was able to make significant contributions to the project. Dr. Nikzad provided a level of mentoring and guidance which inspired me to continue working on the project over many years,

through both successes and difficulties. The ultimate success of our detector work and my lab experience working at JPL meant that a lot of doors were opened to me as I explored job possibilities at the end of graduate school. It also taught me to never accept current technology as good enough – detectors can be made better, coatings can be made better, telescopes can be made better.

"Being able to work closely with Dr. Nikzad and others at JPL has been an incredible experience, and was an important part of my decision to move to Pasadena for a postdoctoral position. Now as a postdoc, funded by an National Science Foundation (NSF) Astronomy and Astrophysics Postdoctoral Fellowship and the R.A. & G.B. Millikan Prize Postdoctoral Fellow in Experimental Physics at Caltech, I am still learning a tremendous amount from Dr. Nikzad about how to conduct long-term research, developing relationships with vendors and other scientists, and managing and inspiring a group of researchers to work towards an incredible result.

"Looking back on my relatively short career thus far in Astrophysics, I know my experiences at JPL and working with the scientists at NASA have been incredibly valuable. They set me on the path I'm on today and I'm extremely grateful for the opportunities I've had. I can only hope that, in the future, I'll be able to have as profound an effect on someone's life as Dr. Nikzad and JPL have had on mine."



Matthew Pugh

Undergraduate student, Mathematics, University of Alabama; later graduated with MS in Operations Management from University of Alabama; currently Industrial Engineer at Michelin North America

PI: H. Philip Stahl

Evaluated costs of selected Space Launch System components using three cost estimating software programs; examined the effects of safety and reliability on costs.

"My involvement with NASA on this project was a truly thrilling experience. With the exodus of the Space Shuttle, it was exciting to be a part of the project to create the launch vehicle of the future. To play just a small part in this achievement is a feat I will treasure for the rest of my life."



Andrej Seljak, PhD

Postdoc, University of Hawai'i at Manoa

PI: John Vallerger

"IDLab at UH and Space Sciences Laboratory collaborate on the development of flight-ready application specific integrated circuits (ASICs), designed to read out position-sensitive UV detectors. A readout system for such a detector is composed of charge-sensitive amplifiers and signal digitizers. Both chips are being designed to enable single-photon counting at very high count rates, thus representing the current state-of-the-art technology. The outcome of the design and development will be presented in November in two posters at the IEEE/NSS 2015 conference in San Diego. My post-doc stay at UH, working on the SAT project, is a very valuable experience which enhanced my knowledge and expertise in the design of ASICs, readout systems for space applications, and project management."



Vihtori Virta

Graduate student, University of Hawai'i at Manoa

PI: John Vallergera

"For part of my graduate coursework, I worked in collaboration with the SSL, wherein I helped design an ASIC, the Charge Sensitive Amplifier CSAv3. My focus in this design was to help develop the pad ring for the ASIC. As part of my studies, I had to learn the design tools, research input protection schemes, and generally experience the ASIC design process. During the journey I gained a lot of knowledge and experience about ASIC design, which will benefit my future work with ASICs."



Dmitry Vorobiev

PhD student, Astrophysical Sciences and Technology, RIT

PI: Zoran Ninkov

"Working on the space qualification of Digital Micro-mirror Devices (DMDs) and the development of a DMD-based multi-object spectrometer has been challenging, but extremely rewarding. My main responsibilities include the design and implementation of testing procedures to measure the optical characteristics of the DMD (such as its reflectance and scattering properties) and its performance in a radiation environment. It is extremely satisfying to carry out a measurement from the design phase through data collection, and then analyze the data to answer a question about the DMD's performance. I really appreciate the level of autonomy I am allowed and, at the same time, the support offered by the rest of the team."

"Although this is a great training opportunity for me, I am mostly motivated by the desire to determine the suitability of DMDs for a variety of astronomical applications. These devices can be the core of a large number of useful and efficient instruments, which cannot be built using conventional techniques. It is very rewarding, as a scientist, to know that my effort on this project will produce results which will be useful for instrument designers (including myself) in the future."

Beyond those featured above in their own words, many more students and postdocs participate in current SAT projects, or participated in the past, each making his or her unique contribution while gaining valuable research and development knowledge and experience.

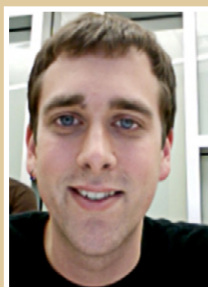


Michael Ayala

Undergraduate student, Electrical Engineering, Cal State, Los Angeles; graduated June 2015

PI: K. 'Bala' Balasubramanian

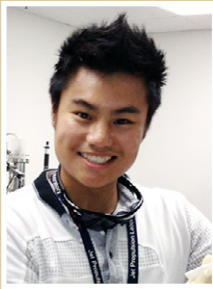
Divided his time between various projects at JPL; for this SAT, measured transmission and reflection properties of films and mirror coatings with spectrophotometers; and wrote Matlab code to analyze and plot the data as needed.



Mike Caldwell

Graduate student, MS in Mechanical, Manufacturing and Electromechanical Technology, RIT

PI: Zoran Ninkov



Sam Cheng

Undergraduate student, Electrical Engineering, Cal Poly, Ponom; then graduate student, Electrical Engineering, USC

PI: Shouleh Nikzad

Joined group in parallel to undergrad and graduate studies.



Dr. April Jewell

A chemist with a BS from George Washington University and PhD from Tufts University.

PI: Shouleh Nikzad

NASA Postdoctoral Program (NPP) Fellow, 2012 until converted to full-time JPL position in early 2015.



John Hennessy

Received BSc from the Cooper Union, and MS and PhD from MIT, all in Electrical Engineering.

PI: Shouleh Nikzad

Joined Advanced Detectors, Systems, and Nanoscience at JPL as a Caltech postdoctoral scholar in 2012, and was converted to staff scientist/engineer in early 2015.



Gillian Kyne

Postdoctoral scholar at Caltech supported in part by Keck Institute for Space Studies (KISS); PhD from NUI Galway.

PI: Shouleh Nikzad

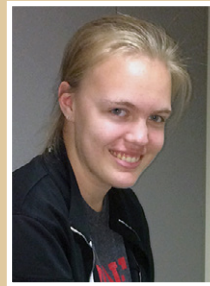


James Holt

Undergraduate student, Mechanical Engineering, University of Texas at El Paso

PI: H. Philip Stahl

Provided user testing of the Arnold Lightweight Mirror Modeler to help identify and fix software bugs. Also used ANSYS Mechanical to perform a trade study determining the ideal geometry and suspension system parameters for a 4-m space telescope mirror using three different mirror materials.



Lauren Morehouse

Undergraduate student, Material Science, Cornell University

PI: Zoran Ninkov

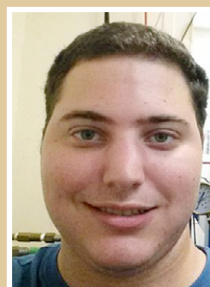


Ruben Jaca

PI: H. Philip Stahl

Modeled 8-m lightweight primary mirror for large space telescopes to identify how its internal stress varies with respect to its stiffness using the Arnold Lightweight Mirror Modeler. Also used an ANSYS mechanical

model to conduct modal analysis.



Brian Newman

Undergraduate student, Mechanical Engineering, Florida State University

PI: H. Philip Stahl

Designed and fabricated a Delrin damping test apparatus. Tested correlated magnets for damping and compared to previous results from test using an aluminum test fixture.



Kimberly Kolb

Recent PhD from RIT. NESSF Fellow.

PI: Shouleh Nikzad

Made measurements with delta-doped electron-multiplying CCDs (EMCCDs), and performed extensive modeling of EMCCDs for single-photon-counting detectors.



Anton Travinsky

PhD student, Center for Imaging Science, RIT

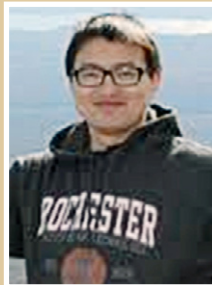
PI: Zoran Ninkov



Nicole Lingner

Graduate student at Caltech working on PhD in astrophysics.

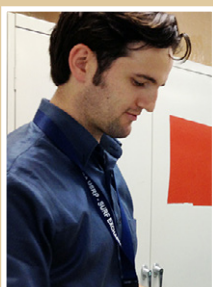
PI: Shouleh Nikzad



Gefei Yang

Graduate student, Imaging Science, RIT

PI: Zoran Ninkov



Alex Miller

Graduate student, Arizona State University (ASU)

PI: Shouleh Nikzad

Works on characterizing high-performance, high-quantum-efficiency broadband (UV/Near-IR), delta-doped, p-channel arrays for on-sky

observation and sounding-rocket experiments.

Appendix D - Acronyms

A

AAS	American Astronomical Society
A/D	Analog to Digital
ADC	Analog-to-Digital Converter
AFM	Atomic Force Microscopy
AFRC	Armstrong Flight Research Center
AFTA	Astrophysics Focused Telescope Assets
AGN	Active Galactic Nuclei
AIP	Astrophysics Implementation Plan
ALD	Atomic Layer Deposition
ALMA	Atacama Large Millimeter/submillimeter Array
A-MKID	Atacama Pathfinder EXperiment (APEX) Microwave Kinetic Inductance Detector
AMTD	Advanced Mirror Technology Development
AO	Announcement of Opportunity
APD	Avalanche Photo Diode
APEX	Atacama Pathfinder EXperiment
APRA	Astrophysics Research and Analysis
AR	Anti-Reflection
ARC	Ames Research Center
ASIC	Application-Specific Integrated Circuit
Astro.	PSU Department of Astronomy and Astrophysics
ASU	Arizona State University
ATLAST	Advanced Technology Large-Aperture Space Telescope

B

BPF	Band-Pass Filter
-----	------------------

C

CCD	Charge-Coupled Device
C&DH	Command and Data Handling
CFFT	Complex Fast Fourier Transform
CHESS	Colorado High Resolution Echelle Stellar Spectrograph
CIC	Clock-Induced Charge
CME	Coronal-Mass Ejection
CMOS	Complementary Metal-Oxide Semiconductor
COBE	Cosmic Background Explorer
COPAG	Cosmic Origins Program Analysis Group
COR	Cosmic Origins
COS	Cosmic-Origins Spectrograph
COTS	Commercial off the Shelf
CSA	Charge-Sensitive Amplifier
CSO	Caltech Submillimeter Observatory
CT	Computed Tomography
cw	continuous wave

D

DAC	Digital-to-Analog Converter
Demux	Demultiplexer
DFB	Distributed Feedback
DLR	Forschungszentrum der Bundesrepublik Deutschland für Luft- und Raumfahrt (German Aerospace Research Center)
DMD	Digital Micro-mirror Device
DSB	Double-Side Band

E

EBCCD Electron-Bombarded CCD
 EBCMOS Electron-Bombarded CMOS
 EC Executive Committee
 EMCCD Electron-Multiplying Charge-Coupled Device
 EoR Epoch of Reionization
 ESA European Space Agency
 EUV Extreme-Ultraviolet
 ExEP Exoplanet Exploration Program
 ExoPAG Exoplanet Program Analysis Group

F

Far-IR Far-Infrared
 Far-UV Far-Ultraviolet
 FCA Force Control Actuators
 FEM Finite Element Model
 FFT Fast Fourier Transform
 FIREBall Faint Intergalactic medium Redshifted Emission Balloon
 FOV Field of View
 FPGA Field Programmable Gate Array
 FS Fused Silica
 FUSE Far-Ultraviolet Spectroscopic Explorer
 FUV Far Ultraviolet
 FWHM Full-Width at Half-Maximum
 FY Fiscal Year

G

GALEX Galaxy Evolution Explorer
 GMOX Gemini Multi-Object eXtra-wide-band Spectrograph
 GOLD Global-scale Observations of the Limb and Disk
 GPix Giga-Pixel (10^9 pixels)
 GPU Graphics Processing Unit
 GRAPH Gigasample Recorder of Analog waveforms from a PHotodetector
 GSFC Goddard Space Flight Center
 GUSSTO Galactic/Xtragalactic ULDB Spectroscopic Stratospheric Terahertz Observatory

H

HAWC High-resolution Airborne Wide-bandwidth Camera
 HEB Hot Electron Bolometer
 HEM Heat Exchanger Method
 HIFI Heterodyne Instrument for the Far Infrared
 HQ Headquarters
 HSO Herschel Space Observatory
 HST Hubble Space Telescope
 HUT Hopkins Ultraviolet Telescope
 HV High Voltage

I

IBS Ion-Beam Sputtering
 ICON Ionospheric Connection Explorer
 IEDM International Electron Devices Meeting
 IEEE Institute of Electrical and Electronics Engineers
 IF Intermediate Frequency
 IFU Integral Field Unit
 IGM Intergalactic Medium
 I/O Input/Output

IQ. In-phase Quadrature
 IR. Infrared
 IRAS. Infrared Astronomical Satellite
 ISM. Interstellar Medium
 IV. Current-Voltage

J

JATIS Journal of Astronomical Telescopes, Instruments, and Systems
 JAXA. Japanese Aerospace eXploration Agency
 JCMT James Clerk Maxwell Telescope
 JHU Johns Hopkins University
 JPL Jet Propulsion Laboratory
 JVSTA. Journal of Vacuum Science and Technology
 JWST. James Webb Space Telescope

K

KID Kinetic Inductance Detector (or Device)
 KISS Keck Institute for Space Studies

L

LBNL Lawrence Berkeley National Lab
 LDR Large Deployable Reflector
 LIDAR. Light Detection and Ranging
 LISM. Local Interstellar Medium
 LLLCCD. Low-Light-Level Charge-Coupled Device
 LN Liquid Nitrogen
 LNA Low-Noise Amplifier
 LO Local Oscillator
 LSST. Large Synoptic Survey Telescope
 LTF. Low-Temperature Fusing
 LTS. Low-Temperature Slumping
 LUVOIR Large UV/Optical/IR
 LVDS. Low-Voltage Differential Signaling

M

MAG. Magnitude
 MBE Molecular Beam Epitaxy
 MCP Micro-Channel Plate
 MEMS. Micro-Electro-Mechanical-System
 MIDEX Medium-Class Explorer
 MIRI Mid-IR Instrument
 MKID Microwave Kinetic Inductance Detector
 MMIC Microwave Monolithic Integrated Circuit
 MOR. Modulus of Rupture
 MOS. Multi-Object Slit Spectrograph
 MPixel Mega-Pixel (10^6 pixels)
 MSFC Marshall Space Flight Center
 MTF Modulation Transfer Function
 MTSSP Measurement Techniques in Solar and Space Physics

N

NASA National Aeronautics and Space Administration
 Near-IR. Near-Infrared
 NEP Noise-Equivalent Power
 NESSF. NASA Earth and Space Science Fellowship
 NI. National Instruments
 NIR. Near-Infrared

NIS Normal-Insulator-Superconductor
 NPP NASA Postdoctoral Program
 NPR NASA Procedural Requirements
 NRC National Research Council
 NSF National Science Foundation
 NSS Nuclear Science Symposium
 NSTR NASA Space Technology Research
 NUV Near-Ultraviolet
 NWNH New Worlds, New Horizons in Astronomy and Astrophysics (2010 Decadal Survey)

O

OAO-3 Orbiting Astronomical Observatory 3
 ORFEUS Orbiting Retrievable Far and Extreme Ultraviolet Spectrometer
 OTA Optical Telescope Assembly

P

PACS Photodetector Array Camera and Spectrometer
 PATR Program Annual Technology Report
 PCB Printed Circuit Board
 PCOS Physics of the Cosmos
 PDR Photo-Dissociation Region
 PDR Preliminary Design Review
 PEALD Plasma-Enhanced Atomic Layer Deposition
 PMA Primary Mirror Assembly
 PSF Point Spread Function
 PVD Physical Vapor Deposition
 PXS Parallel Cross Strip
 PZC Pole-Zero-Cancellation

Q

QCL Quantum-Cascade Laser
 QE Quantum Efficiency
 QSO Quasi-Stellar Object

R

R&D Research and Development
 RF Radio Frequency
 RFI Request for Information
 RIT Rochester Institute of Technology
 rms root mean square

S

SAG Science Analysis Group
 SAT Strategic Astrophysics Technology
 SCUBA-2 Submillimetre Common-User Bolometer Array-2
 SEE Single Event Effect
 SEU Single Event Upset
 SFO Star Formation Observatory
 SHARC II Submillimeter High-Angular Resolution Camera II
 SIG Science Interest Group
 SIOSS Science Instruments, Observatory, and Sensor Systems
 SMD Science Mission Directorate
 SMEX Small Explorer
 SMFL Semiconductor and Microsystems Fabrication Laboratory
 SNR Signal-to-Noise Ratio
 SoC System-on-Chip

SOFIA Stratospheric Observatory for Infrared Astronomy
 SPICA Space Infrared Telescope for Cosmology and Astrophysics
 SPIE Society of Photo-optical Instrumentation Engineers
 SPIRE Spectral and Photometric Imaging Receiver
 SPUD Solid-state Photon-counting Ultraviolet Detector
 SQUID Superconducting Quantum Interference Device
 SR&T Supporting Research and Technology
 SSL Space Sciences Laboratory
 ST2020 Space Telescope 2020 (mission concept)
 STIS Space-Telescope Imaging Spectrograph
 STJ Superconducting Tunnel Junction
 STM Science Traceability Matrix
 STO Stratospheric Terahertz Observatory
 STSci Space Telescope Science Institute
 SURP Strategic University Research Partnership

T

TARGET TeV Array Readout with GSa/s sampling and Event Trigger
 TCOR Technology development for Cosmic Origins
 TES Transition Edge Sensor
 TI Texas Instruments
 TMB Technology Management Board
 TRL Technology Readiness Level
 TSMC Taiwan Semiconductor Manufacturing Company

U

UA University of Alabama
 UA University of Arizona
 UC University of California
 UCLA University of California, Los Angeles
 UH University of Hawai'i at Manoa
 UHV Ultra-High Vacuum
 ULE Ultra-Low Expansion
 USB Universal Serial Bus
 USC University of Southern California
 UV Ultraviolet
 UVIS Ultraviolet/Visible
 UVOIR UV/Optical/IR

V

VLSI Very-Large-Scale Integration

W

WaSP Wafer-Scale Imager for Prime
 WFE Wavefront Error
 WFIRST Wide-Field Infrared Survey Telescope
 WFSC Wave Front Sensing and Control

X

XGA eXtended Graphics Array
 XPS X-ray Photoelectron Spectroscopy
 XRCF X-Ray and Cryogenic Facility
 XS Cross-Strip

